Department of Chemical Engineering

Development of Accurate and Reliable Correlations for Various Design Parameters in Oil and Gas Processing Industries

Alireza Bahadori

This thesis is presented for the Degree of

Doctor of Philosophy

of

Curtin University

August 2011

Declaration

To the best of my knowledge and brief this thesis contains no material previously published by any other person except where due acknowledgement has been made.

This thesis contains no material which has been accepted for the award of any other degrees or diploma in any university.

Signature: 

Date: 18 April 2011

Summary

The continuing growth in the importance of oil and gas production and processing overall the globe increase the need for accurate prediction of various parameters and their impact on unit operations, process simulation and design. Because of the particular nature of various parameters, sometimes existing methods encounter difficulties. Currently several models are available to predict various design parameters in the oil and gas processing industries. However, their calculations may require rigorous computer solutions. Therefore, developing the new predictive tools to which are easier than the existing methods, less complicated with fewer computations to minimize the complex and time-consuming calculation steps is an essential need. It is apparent that mathematically compact, simple, and reasonably accurate predictive tools, as proposed in this thesis, would be preferable for computationally intensive simulations. In fact, the development of engineering correlations by a modification to the well-known Vogel-Tammann-Fulcher (VTF) [1921-1926] equation and Arrhenius equation (1889) was the primary motivation of the present thesis, which, nevertheless, yielded predictive tools with accuracy comparable to that of the existing rigorous simulations. Hence, some existing approaches lead to complicated equations for the purposes of engineering importance. This problem has been circumvented conveniently by resorting to simpler approaches, as described in this thesis.

The purpose of the proposed Dissertation work is to develop and formulate accurate and reliable predictive tools to serve two purposes. First, being conversion of a set of highly correlated variables to a set of independent variables by using linear transformations. Second one is for variable reductions. When a dependent variable is specified, the method is very efficient for dimensional reduction due to the supervised nature of its methodology. The developed tools in this study can be immense engineering value to predict different process design parameters, including the prediction of hydrate forming conditions of natural gases, hydrate forming

pressure of pure alkanes in the presence of inhibitors, water-hydrocarbon systems mutual solubilities, water content of natural gas, density, thermal conductivity and viscosity of aqueous glycol solutions, optimum size of inlet scrubber and contactor in natural gas dehydration systems, estimation of water-adsorption isotherms, estimation of equilibrium water dew point of natural gas in triethylene glycol dehydration systems, true vapour pressure (TVP) of LPG and natural gasoline, hydrocarbon components solubilities in hydrate inhibitors, methanol vaporization loss and solubility in hydrocarbon liquid phase for gas hydrate inhibition, storage pressure of gasoline in uninsulated tanks, emissivity of combustion gases, filling losses from storage containers, bulk modulus and volumetric expansion coefficient of water for leak tightness test of pipelines, silica solubility and carry-over in steam, carbon dioxide equilibrium adsorption isotherms, estimation of packed column size, estimation of thermal insulation thickness, transport properties of carbon dioxide, aqueous solubility of light hydrocarbons, estimation of economic thermal insulation thickness, water content of air at elevated pressures, surface tension of paraffin hydrocarbons, aqueous solubility and density of carbon dioxide, aqueous solubility of light hydrocarbons, thermal conductivity of hydrocarbons, downcomer design velocity and vapour capacity correction factor in fractionators, estimation of convection heat transfer coefficients and efficiencies for finned tubular sections, estimation of heat losses from process piping and equipment surfaces, prediction of absorption/stripping factors, correlating theoretical stages and operating reflux in fractionators, design of radiant and convective sections of direct fired heaters and many other engineering parameters.

Following the development of predictive tools, experimental work was undertaken to measure the density and viscosity, of ethylene glycol + water, diethylene glycol + water, and triethylene glycol + water mixtures at temperatures ranging from 290 K to 440 K and concentrations ranging from 20 mol % glycol to 100 mol % glycol. Our data were correlated using a novel Arrhenius-type equation based predictive tool and a thermodynamical method (the generalized corresponding states principle (GCSP)). Both novel Arrhenius-type equation based predictive tool and GCSP

method, with two adjustable parameters for each property, offer the potential for judicious extrapolation of density and viscosity data for all glycol + water mixtures.

In addition, in this thesis, the PreTOG software package has been developed, which covers a wide range of parameters in oil, gas and chemical processing industries and is using PC-based Windows and Matlab graphical user interfaces and tool boxes. The PreTOG software is also available on an stand-alone CD. Finally the following typical case studies for potential benefits to various processing plants industries will be presented and the results of new proposed model are compared with partial least squares (PLS) and principal component analysis (PCA):

- Methanol vaporization loss during gas hydrate inhibition
- Methanol loss in condensate liquid phase during gas hydrate inhibition
- Estimation of potential savings from reducing unburned combustible losses in coal-fired systems
- Recoverable heat from blowdown systems during steam generation
- Energy conservation benefits in excess air controlled gas-fired systems
- Prediction of salinity of salty crude oil

Acknowledgements

Firstly, I wish to acknowledge A/Professor Hari B. Vuthaluru, my supervisor for giving me the opportunity to pursue my PhD in oil and gas research filed. His confidence in my ability and his continuous guidance throughout my PhD program is greatly appreciated. I am also hugely grateful to my co-supervisor Professor Moses O. Tade for his academic support and concern for the progress of my thesis.

This PhD would not have been possible without the Australian Government' Department of Education Science and Training (DEST), Endeavour International Postgraduate Research Scholarship (EIPRS), the office of Research and Development' Curtin University Postgraduate Scholarship (CUPS) and the State Government of Western Australia top up scholarship through Western Australian Energy Research Alliance (WA:ERA).

Finally, I am truly indebted to my family especially my father, Abdolkarim Bahadori and my mother Sakineh Behbahanian for their continuous encouragement inspiring words (through long distance conversation) and their faith in me throughout these years.

Table of Contents

Brief Biography of the Author

Alireza Bahadori received the Bachelor of Chemical Engineering with academic distinctions from the Petroleum University Technology, Abadan Iran in 1998 as well as an Msc degree in chemical engineering from Shiraz University, Iran. So far He has been the lead author of over 130 refereed journal articles and international conference papers. Alireza is the recipient of the top author award from *Elsevier publishing Co* for selection as the outstanding author of *Journal of Natural Gas Science and Engineering* (2008-2010). He is also the recipient of the highly competitive and prestigious Australian Government's Department of Education Science and Training, Endeavour International Postgraduate Research Scholarship (EIPRS) and Curtin University Postgraduate scholarship as well as the Western Australia State Government's top-up scholarship through the Western Australian Energy Research Alliance (WA:ERA). He also serves as the editor for chemical and petroleum engineering area and an editorial board member for *Central European Journal of Engineering* and a reviewer for several leading international journals such as *Applied Thermal Engineering, Korean Journal of Chemical Engineering, Chemical Engineering Journal, Chemical Engineering & Technology, Chemical Engineering Communications, Journal of Energy Sources* and etc. Previously he was a senior process engineer in the Petroleum Engineering Department of National Iranian Oil Company, Ahwaz, Iran for 10 years and involved in several large-scale oil and gas projects.

Published books:

1- **A. Bahadori** (2011), Novel Predictive Tools for Oil, Gas and Chemical Industries, VDM Verlag Publishing, Saarbrücken, **Germany** (***ISBN: 978-3-639-32019-0***)

2- **A. Bahadori** (2011), Key Technical Points for Process Design of Water Systems, VDM Verlag Publishing, Saarbrücken, **Germany** (***ISBN: 978-3-639-25605-5***)

List of refereed journal publications during PhD candidacy:

1. **A. Bahadori** and H. B. Vuthaluru, (2011), Estimation of air specific heat ratio at elevated pressures using simple predictive tool, *Energy Conversion and Management. 52, 1526-1532.*
2. **A. Bahadori**, and H. B. Vuthaluru, (2011) Estimation of saturated air water content at elevated pressures using simple predictive tool, *Chemical Engineering Research and Design, 89, pp. 179-186.*
3. **A. Bahadori**, (2011), Prediction of Moisture Content of Natural Gases Using Simple Arrhenius type function, *Central European Journal of Engineering,* 1(1), pp. 81-88.
4. **A. Bahadori**, (2011), Prediction of compressed air transport properties at elevated pressures and high temperatures using simple method" *Applied Energy.* 88(4), 1434-1440.
5. **A. Bahadori** (2011), Prediction of Saturated Air Dew Point at Elevated Pressures Using Simple Arrhenius-type Function, *Chemical Engineering & Technology 34,(2), pp. 257-264.*
6. **A. Bahadori** (2011), Estimation of Combustion Flue Gas Acid Dew Point During Heat Recovery and Efficiency Gain, *Applied Thermal Engineering* 31 , 1457-1462
7. **A. Bahadori**, (2010), Determination of well placement and breakthrough time in horizontal wells for homogeneous and anisotropic reservoirs, *Journal of Petroleum Science and Engineering,.* 75, 196-202.
8. **A. Bahadori** and H. B. Vuthaluru, (2010), Simple method for estimation of unsteady state conduction heat flow with variable surface temperature in slabs and spheres, *International Journal of Heat and Mass Transfer,* 53, 4536–4542*.*
9. **A. Bahadori**, and H. B. Vuthaluru, (2010), Estimation of potential savings from reducing unburned combustible losses in coal-fired systems, *Applied Energy*87 (12) 3792-3799.
10. **A. Bahadori**, and H. B. Vuthaluru, (2010), Estimation of steam losses using a predictive tool, *Petroleum Technology Quarterly*, 15 (Q3), pp. 133-136.

11. **A. Bahadori**, and H. B. Vuthaluru, (2010) Simple Arrhenius-type function accurately predicts dissolved oxygen saturation concentrations in aquatic systems, *Process Safety and Environmental Protection* 88(5), pp. 335-340
12. **A. Bahadori** and H. B. Vuthaluru (2010) Prediction of silica carry-over and solubility in steam of boilers using simple correlation, *Applied Thermal Engineering,* 30 (2010) 250–253.
13. **A. Bahadori**, and H. B. Vuthaluru, (2010) A method for estimation of recoverable heat from blowdown systems during steam generation" *Energy* 35, (8) pp. 3501-350.
14. **A. Bahadori**, and H. B. Vuthaluru, (2010) Estimation of performance of steam turbines using a simple predictive tool, *Applied Thermal Engineering* 30 (2010) 1832-1838.
15. **A. Bahadori**, and H. B. Vuthaluru, (2010)"predictive tool for the estimation of methanol loss in condensate phase during gas hydrate inhibition" *Energy & Fuels*, 24, 2999–3002.
16. **A. Bahadori**, and H. B. Vuthaluru, (2010) "Estimation of maximum shell-side vapour velocities through heat exchangers" *Chemical Engineering Research and Design.* 88,1589-1592
17. **A. Bahadori**, and H. B. Vuthaluru, (2010) "A method for prediction of scale formation in calcium carbonate aqueous phase for water treatment and distribution systems" accepted for publication in *Water Quality Research Journal of Canada.*
18. **A. Bahadori**, and H. B. Vuthaluru, (2010) "Estimation of energy conservation benefits in excess air controlled gas-fired systems" *Fuel Processing Technology*, 91 (10), 1198-1203
19. **A. Bahadori**, and H. B. Vuthaluru, (2010) "Estimation of steam losses in stream traps", *Chemical Processing,* 73(10), pp 30-32.
20. **A. Bahadori**, and H. B. Vuthaluru, (2010) "Simple method for prediction of densities and vapour pressures of aqueous methanol solutions", *OIL GAS European Magazine,* 36(2), pp. 84-88.
21. **A. Bahadori**, and H. B. Vuthaluru, (2010) "Predictive tool for estimation of convection heat transfer coefficients and efficiencies for finned tubular sections" *International Journal of Thermal Sciences. 49, 1477-1483.*
22. **A. Bahadori**, and H. B. Vuthaluru, (2010) "Estimation of heat losses from process piping and equipment, *Petroleum Technology Quarterly*, 15 (3), PP. 121-123.*(translated version published in PTQ's Chinese-language sister magazine, Hydrocarbon China)*

23. **A. Bahadori**, M. Al-Haddabi and H. B. Vuthaluru, (2010), Estimation of reservoir brine properties during crude oil production using simple predictive tool, accepted for publication in *Petroleum Science & Technology*
24. **A. Bahadori**, and H. B. Vuthaluru, (2010) "Predictive tools for the estimation of downcomer velocity and vapor capacity factor in fractionators, *Applied Energy 87, 2615-2620.*
25. **A. Bahadori**, and H. B. Vuthaluru, (2010) "Prediction of methanol loss in vapor phase during gas hydrate inhibition using arrhenius-type functions" *Journal of Loss Prevention in the Process Industries,* 23(3), pp. 379-384.
26. **A. Bahadori**, and H. B. Vuthaluru, (2010)" Predictive tool for an accurate estimation of carbon dioxide transport properties, *International Journal of Greenhouse Gas Control,* 4 (2010) 532–536.
27. **A. Bahadori**, and H. B. Vuthaluru, (2010)" A new method for prediction of absorption/stripping factors, *Computers & Chemical Engineering* 34 (2010) 1731–1736
28. **A. Bahadori**, and H. B. Vuthaluru, (2010), Simple equations to correlate theoretical stages and operating reflux in fractionators, *Energy,* 35 (2010) 1439–1446.
29. **A. Bahadori**, and H. B. Vuthaluru, (2010), Novel predictive tools for design of radiant and convective sections of direct fired heaters, *Applied Energy* 87 (2010) 2194–2202.
30. **A. Bahadori** and H. B. Vuthaluru (2010)" A simple method for the estimation of thermal insulation thickness" *Applied Energy* 87 (2010) pp.613–619.
31. **A. Bahadori** (2011) A simple method for the estimation of performance characteristics of cooling towers, accepted for publication in *Journal of the Energy Institute.*
32. **A. Bahadori**, and H. B. Vuthaluru (2010), Accurate prediction of molten sulfur viscosity" *Petroleum Technology Quarterly* 15(1) pp. 13-14.
33. **A. Bahadori**, and H. B. Vuthaluru, (2010)" Estimation of displacement losses from storage containers using a simple method *Journal of Loss Prevention in the Process Industries, 23* (2010) 367-372.
34. **A. Bahadori**, and H. B. Vuthaluru, (2010) "Novel predictive tool for accurate estimation of packed column size" *Journal of Natural Gas Chemistry*. 19(2), PP. 146-150.
35. **A. Bahadori** and H. B. Vuthaluru (2010)" A simple correlation for estimation of economic thickness of thermal insulation for process piping and equipment" *Applied Thermal Engineering*, 30, 254–259.
36. **A. Bahadori** and H. B. Vuthaluru, (2010), Prediction of temperature drop accompanying a given pressure drop for natural gas, NAFTA Journal, 61 (7-8) 347-351.

37. **A. Bahadori** and H. B. Vuthaluru, (2010), Estimating compressor power and condenser duty in a refrigerant system, *Petroleum Technology Quarterly,* 15, Q4, PP.139-143.
38. **A. Bahadori**, (2010), "Estimation of heat-capacity ratios of hydrocarbon gases using a simple predictive tool" accepted for publication in *Journal of Energy Sources, Part A: Recovery, Utilization, and Environmental Effects.*
39. **A. Bahadori**, (2010), Estimation of equilibrium adsorption behaviour at cryogenic temperatures of CO2 and N2 using a simple predictive tool, accepted for publication in *SPE Projects, Facilities & Construction Journal, SPE-132309-PA*, (accepted 24, October, 2010).
40. **A. Bahadori** and H. B. Vuthaluru, (2010), Estimation of theoretical flame temperatures for Claus sulfur recovery unit using simple method, accepted for publication in *Journal of Energy Sources, Part A: Recovery, Utilization, and Environmental Effects.*
41. **A. Bahadori** and H. B. Vuthaluru, (2010),Prediction of salinity of salty crude oil using arrhenius-type asymptotic exponential function and vandermonde matrix, *SPE Projects, Facilities & Construction Journal,* 6 (1): 27-32. *SPE-132324-PA*,.
42. **A. Bahadori** and H. B. Vuthaluru (2009)" Rapid estimation of equilibrium water dew point of natural gas in teg dehydration systems" *Journal of Natural Gas Science & Engineering*1(3)(2009), pp. 68-71.
43. **A. Bahadori** and H. B. Vuthaluru (2009)" Simple methodology for sizing of absorbers for teg gas dehydration systems", *Energy* 34 (2009) 1910–1916.
44. **A. Bahadori** and H. B. Vuthaluru (2009) " New method accurately predicts carbon dioxide equilibrium adsorption isotherms" *International Journal of Greenhouse Gas Control* 3 (2009) 768–772
45. **A. Bahadori** and H. B. Vuthaluru (2009)" A novel correlation for estimation of hydrate forming condition of natural gases" *Journal of Natural Gas Chemistry,* 18(4)(2009) pp. 453-457.
46. **A. Bahadori** and S. Mokhatab (2009) "Simple correlation accurately predicts densities of glycol solutions" *Petroleum Science and Technology,* 27(3) pp. 325 – 330.
47. **A. Bahadori** and H. B. Vuthaluru (2010)" Rapid prediction of carbon dioxide adsorption isotherms for molecular sieves using simple correlation" *SPE Projects, Facilities & Construction Journal,* 5(1)pp.17-21, SPE-122882-PA. doi: 10.2118/122882-PA .
48. **A. Bahadori**, H. B. Vuthaluru and S. Mokhatab (2009) "Rapid estimation of water content of sour natural gases" *Journal of the Japan Petroleum Institute*. 52(5) pp. 270-274.

49. **A. Bahadori**, H, B, Vuthaluru and S. Mokhatab (2009)"Simple correlation accurately predicts h2s solubility in aqueous solutions of methyldiethanolamine", *Gas International, Engineering & Management Journal* 49 (3) pp. 13-15
50. **A. Bahadori**, H. B. Vuthaluru (2009)" Explicit numerical method for prediction of transport properties of aqueous glycol solutions" *Journal of the Energy Institute* 82 (4), pp. 218-222.
51. **A. Bahadori**, H. B. Vuthaluru and S. Mokhatab (2009)" New correlations predict aqueous solubility and density of carbon dioxide" *International Journal of Greenhouse Gas Control* (3), pp. 474–480.
52. **A. Bahadori** and H. B. Vuthaluru(2009) " Prediction of bulk modulus and volumetric expansion coefficient of water for leak tightness test of pipelines" *International Journal of Pressure Vessels and Piping,* (86)pp. 550–554
53. **A. Bahadori** (2009)"New model predicts hc emissions from teg plants" *Petroleum Chemistry,* 49(2), pp. 171–179.
54. **A. Bahadori**, (2009)"Estimating water-adsorption isotherms" *Hydrocarbon Processing*, 88(1) pp. 55-56.
55. **A. Bahadori**, H.B. Vuthaluru and S. Mokhatab (2009) "Simple correlation accurately predicts aqueous solubility of light alkanes" *Journal of Energy Sources, Part A: Recovery, Utilization, and Environmental Effects,* 31 :(9), 761—766.
56. **A. Bahadori**, H.B. Vuthaluru and S. Mokhatab (2009) "Method accurately predicts water content of natural gases" *Journal of Energy Sources, Part A: Recovery, Utilization, and Environmental Effects*31 (9) 754 — 760.
57. **A. Bahadori** and S. Mokhatab (2009)" Correlation rapidly estimates pure hydrocarbons' surface tension" *Journal of the Energy Institute* 82 (2) pp. 118-119.
58. **A. Bahadori**, H. B. Vuthaluru, and S. Mokhatab (2009)" Determining appropriate size of inlet scrubber and contactor in teg gas dehydration systems", *Petroleum Science & Technology*27 (16) 1894 — 1904.
59. **A. Bahadori** and H. B. Vuthaluru (2009)" Predicting emissivity of combustion gases" *Chemical Engineering Progress,* 105, (6), 38-41.
60. **A. Bahadori** (2009)"Minimize vaporization and displacement losses from storage containers" *Hydrocarbon Processing* 88(6) pp. 83-84.
61. **A. Bahadori**, (2009)" Estimation of hydrate inhibitor loss in hydrocarbon liquid phase", *Petroleum Science & Technology* (27) pp. 943–951.

62. **A. Bahadori** (2009)"Predicting storage pressure of gasoline in uninsulated tanks" *Journal of the Energy Institute* 82 (1) p. 61.
63. **A. Bahadori** (2008) Processing trends: Estimating water adsorption isotherms for molecular sieves in contact with natural gas, *Petroleum Technology Quarterly* 13 (4) pp. 10-12.
64. **A. Bahadori** and H. B. Vuthaluru (2008)" Simplified method for calculating hydrocarbons solubilities in hydrate inhibitors", *Chemical Engineering and Technology*, 31 (9) pp. 1369-1375.
65. **A. Bahadori**, H. B. Vuthaluru, M. O. Tade and S. Mokhatab (2008)" Predicting water-hydrocarbon systems mutual solubility" *Chemical Engineering & Technology* 31, (12)pp. 1743-1747.
66. **A. Bahadori**, H. B. Vuthaluru and S. Mokhatab (2008)"Estimating methanol vaporization loss and its solubility in hydrocarbon liquid phase" *OIL GAS European Magazine* 34, (3) pp. 149-151.
67. **A. Bahadori**, H.B. Vuthaluru, S. Mokhatab and M. O. Tade (2008) "Predicting hydrate forming pressure of pure alkanes in the presence of inhibitors", *Journal of Natural Gas Chemistry* Vol.17, No.3, pp. 249-255.
68. **A. Bahadori**, H. B. Vuthaluru and S. Mokhatab (2008) "Optimizing separators pressures in the multistage crude oil production unit ", *Asia-Pacific Journal of Chemical Engineering* ,3, (4) pp. 380-386.
69. **A. Bahadori** and S. Mokhatab (2008) "Estimating thermal conductivity of hydrocarbons" *Chemical Engineering* 115, (13) pp. 52-54.
70. **A. Bahadori**, Y. Hajizadeh, H. B. Vuthaluru, M. O. Tade and S. Mokhatab (2008)" Novel approaches for the prediction of density of glycol solutions " *Journal of Natural Gas Chemistry,* 17, (3) pp. 298-302.
71. **A. Bahadori** K. Zeidani (2008) "New equations predicting the best performance of electrostatic desalter" *Petroleum Science and Technology,* 26 (1) pp. 40-49.
72. **A. Bahadori** and S. Mokhatab, (2008)"Predicting water content of compressed air" *Chemical Engineering* Vol. 115, (9), pp. 56-57.
73. **A. Bahadori** and S. Mokhatab (2008) "Sizing of trayed fractionators" *Gas International Engineering & Management Journal*48, (8), pp. 32-33.
74. **A. Bahadori** and S. Mokhatab (2008)" Predicting physical properties of hydrocarbon compounds" *Chemical Engineering* 115 (8) pp. 46-48.

75. **A. Bahadori**, H. B. Vuthaluru and S. Mokhatab (2008)" Rapid prediction of co2 solubility in aqueous solutions of DEA and MDEA" *Chemical Engineering & Technology,* 31, (2) pp. 245-248.
76. **A. Bahadori**, S. Mokhatab and B. F. Towler (2008)" Predicting hydrate forming conditions of light alkanes and sweet natural gases" , *Hydrocarbon Processing*, 87 (1) pp. 65-68.
77. **A. Bahadori**, (2008)" New Correlation accurately predicts thermal conductivity of liquid paraffin hydrocarbons" *Journal of the Energy Institute* 81 (1) pp. 59-61.
78. **A. Bahadori**, (2008)" Correlation accurately predicts hydrate forming pressure of pure components" *Journal of Canadian Petroleum Technology.* 47, No.2, pp.13-16.
79. **A. Bahadori**, H. B. Vuthaluru and S. Mokhatab (2008) "Analyzing solubility of acid gas and light alkanes in triethylene glycol" *Journal of Natural Gas Chemistry* 17 (1) pp. 51-58.
80. **A. Bahadori**, (2011), Estimation of Potential Precipitation from an Equilibrated Calcium Carbonate Aqueous Phase Using Simple Predictive Tool" accepted for publication in the *SPE Projects, Facilities & Construction*
81. **A. Bahadori**, (in press), Estimating hydrate inhibitir loss: A case study, accepted for publication in *Petroleum Technology Quarterly.*
82. **A. Bahadori** (2011) Prediction of Axial Dispersion in Plug-Flow Reactors Using a Simple Method, accepted for publication in *Journal of Dispersion Science & Technology* (Ms JDST2011 / 236) acceptance date 19/1/2011.
83. **A. Bahadori**, (2011), **A. Bahadori**, (2011), A simple predictive tool for estimating water removal rate in solid desiccant dehydrators, accepted for publication in *Petroleum Science & technology*

***International Conference Papers* during PhD candidacy**

84. **A. Bahadori**, M. Bahadori and H. B. Vuthaluru (2011) An easy-to-use matlab-based computer program for prediction of n-alkanes surface tension, SPE (*Society of Petroleum Engineers)* Middle East Oil and Gas Show and Conference held in Manama, Bahrain, 6–9 March 2011.
85. **A. Bahadori**, M. Al-Haddabi, H. B. Vuthaluru and M. Bahadori,(2011) A simple-to-use matlab-based computer program for prediction of formation water properties, SPE (*Society of Petroleum Engineers)* Projects and Facilities Challenges Conference at METS held in Doha, Qatar, 13–16 February 2011.
86. **A. Bahadori**, and H. B. Vuthaluru (2010) Rapid estimation of carbon dioxide compressibility factor using simple predictive tool (*Society of Petroleum Engineers)* SPE Asia Pacific Oil & Gas Conference and Exhibition Brisbane, Queensland, Australia, 18–20 October 2010, (SPE paper # 131715).
87. **A. Bahadori**, and H. B. Vuthaluru (2010) A simple decline-curve analysis approach for evaluating gas reserves and predicting future production in gas reservoirs, (*Society of Petroleum Engineers)* SPE Eastern Regional Meeting held in Morgantown, West Virginia, USA, 12–14 October 2010 (SPE paper # 139057).
88. **A. Bahadori**, and H. B. Vuthaluru (2010) Rapid prediction of carbon dioxide and nitrogen adsorption behaviour at cryogenic temperatures, (*Society of Petroleum Engineers)* SPE Asia Pacific Oil & Gas Conference and Exhibition Brisbane, Queensland, Australia, 18–20 October 2010 (SPE paper # 132309).
89. **A. Bahadori**, and H. B. Vuthaluru and H. M. Ang (2010), Predictive tool for estimation of potential precipitation from an equilibrated calcium carbonate aqueous phase, 2010 SPE, (*Society of Petroleum Engineers)* Trinidad and Tobago Energy Resources Conference, 27-30 June 2010 in Port of Spain, Trinidad (SPE paper # 132403).
90. **A. Bahadori**, and H. B. Vuthaluru, and H. M. Ang, (2010) Estimation of salinity of salty crude oil using Arrhenius-type asymptotic exponential function and vandermonde matrix, 2010 SPE, (*Society of Petroleum Engineers)* Trinidad and Tobago Energy Resources Conference, 27-30 June 2010 in Port of Spain, Trinidad(SPE paper # 132324).
91. **A. Bahadori**, and H. B. Vuthaluru, (2010), Prediction of vapor pressure of aqueous hydrate inhibitor solutions using Arrhenius-type asymptotic exponential function, (*Society of Petroleum Engineers)* Nigeria Annual International Conference and Exhibition, 31 July - 7 August 2010, Tinapa - Calabar, Nigeria (SPE paper # 140677)

92. **A. Bahadori**, M. Maddahi and H. B. Vuthaluru, (2010), Simple-to-use predictive tool for an accurate estimation of the water content of carbon dioxide" 2010 *Society of Petroleum Engineers* (SPE), SPE EUROPEC 2010, 14-17 June 2010, Barcelona, Spain(SPE paper # 130344).
93. **A. Bahadori**, and H. B. Vuthaluru, and J. Jalili (2010) Novel approach for an accurate estimation of the saturated water content of sour natural gases, 2010 *Society of Petroleum Engineers* (SPE) International Oil & Gas Conference & Exhibition in China, (IOGCEC) 8-10 June 2010, Beijing, China. (SPE paper # 130135).
94. **A. Bahadori**, A predictive tool for rapid estimation of components absorption in lean oil absorbers, 2010 SPE, (*Society of Petroleum Engineers)* Trinidad and Tobago Energy Resources Conference, 27-30 June 2010 in Port of Spain, Trinidad(SPE paper # 132311).
95. **A. Bahadori**, and H. B. Vuthaluru, (2009) "Prediction of optimum thermal insulation thickness for oil and gas process piping and equipments using simple method" accepted for presentation at the *International Petroleum Technology Conference* held in Doha, Qatar, 7–9 December 2009. Paper IPTC-13121
96. **A. Bahadori** and H. B. Vuthaluru" A simple method for accurate prediction of temperature drops in natural gas production systems" *Society of Petroleum Engineers*, 2009 SPE/EAGE Reservoir Characterization and Simulation Conference held in Abu Dhabi, UAE, 19–21 October 2009. (SPE paper # 125510).
97. **A. Bahadori** and H. B. Vuthaluru (2009)" A novel correlation for estimation of economic thickness of insulation for process piping and equipments" SPE Asia Pacific Health, Safety, Security and Environment Conference and Exhibition (APHSSEC) scheduled 4-6 August 2009 in Jakarta, Indonesia. *Society of Petroleum Engineers* paper # 124173.
98. **A. Bahadori** and H. B. Vuthaluru, (2009) "A numerical method for prediction of transport properties of carbon dioxide" SPE Asia Pacific Health, Safety, Security and Environment Conference and Exhibition (APHSSEC) scheduled 4-6 August 2009 in Jakarta, Indonesia. *Society of Petroleum Engineers* paper # 122859.
99. **A. Bahadori** and H. B. Vuthaluru (2009)"Rapid prediction of carbon dioxide adsorption isotherms for molecular sieves using simple correlation" SPE Asia Pacific Health, Safety, Security and Environment Conference and Exhibition (APHSSEC) scheduled 4-6 August 2009 in Jakarta, Indonesia, *Society of Petroleum Engineers* paper # 122882.
100. **A. Bahadori**, H.B. Vuthaluru, M.O. Tade and S. Mokhatab (2009) "Novel correlations for determining appropriate mono-ethylene glycol injection rate to avoid gas hydrate

formation" *Canadian International Petroleum Conference* (CIPC), Calgary, Alberta, Canada, 16-18 June 2009 (paper CIPC 2009-009).

101. **A. Bahadori**, H. B. Vuthaluru and M.O. Tade (2009) "A novel method for estimation of silica carry-over and solubility in steam of boilers" *Canadian International Petroleum Conf*erence (CIPC) 2009, Calgary, Alberta, Canada, 16-18 June 2009, (Paper CIPC 2009-010).
102. **A. Bahadori**, H. B. Vuthaluru (2009)" An accurate numerical approach for predicting solubilities of hydrocarbons in hydrate inhibitors", *Society of Petroleum Engineers*, 2009 (SPE Paper # 122772) Latin American & Caribbean Petroleum Engineering Conference 31-MAY-2009 to 03-JUN-2009, Cartagena, Colombia.
103. **A. Bahadori** and H. B. Vuthaluru, (2009)" Novel predictive tool for accurate estimation of bulk modulus and volumetric expansion coefficient of water for leak tightness test of pipelines" *6th International Chemical Engineering Congress & Exhibition* (IChEC 2009)", 16-18, November, 2009, Kish Island, Iran.
104. **A. Bahadori** and H. B. Vuthaluru, " A novel correlation for estimation of hydrate forming condition of natural gases", *6th International Chemical Engineering Congress & Exhibition (IChEC 2009)* "16-18 November 2009, Kish Isaland, Iran.
105. **A. Bahadori** and H. B. Vuthaluru, Prediction of convection heat transfer coefficients and efficiencies for finned tubular sections using simple correlations, *6th International Chemical Engineering Congress & Exhibition (IChEC 2009)".* 16-18 November 2009, Kish Island, Iran.

List of Figures

List of Tables

Nomenclature

A Tuned coefficient

A_i The inlet air in moles of air per mol of fuel

A_o The theoretical air requirement of an arbitrary carbon based fuel compound, in moles of air per mol of fuel

B Tuned coefficient

C Tuned coefficient

C_P Condensate percent

D Tuned coefficient

E The activation energy of the process causing parameter variation (J/kmol)

E' Natural gas combustion efficiency, fraction

f Properly defined temperature-dependent parameter, the units for which are determined individually for a certain property

f_c Pre-exponential coefficient, having the same unit of the property of interest

H *E*nthalpy, kJ/kg

F1 Unit heat output correction factor (F1)

F2 Fuel cost correction factor

H_{EX} Enthalpy of liquid leaving the heat exchanger, kJ/kg

H_{TK} Enthalpy of liquid leaving the flash tank, kJ/kg

L_M Methanol vaporization loss $((kg/m^3)/((Wt\%\ Methanol)(10^6\ m^3)$

M Molecular weight

P Pressure, Kpa

P_b Operating boiler drum pressure kPa(abs)

P_{FD} Flash drum pressure, kPa(abs)

Q Design unit heat output (MW)

Q' Total percent of heat recoverable

Q_C Percent of heat recoverable from the condensate

S The percent of blowdown that is flashed to steam

R	*T*he universal gas constant (R), 8.314 J/(kmol K))
T	Absolute temperature, K
T_c	Characteristic-limit temperature, K
V	Molar volume
u	Coefficient of polynomial
V	Vandermonde matrix
W	Water content, mg/ Sm^3
Z	Compressibility factor
x	Mole fraction
X	Percent combustible in ash (X)
X’	Fraction of excess Air
Y	Achievable percent combustible in ash (Y)
Y_o	Oxygen mole fraction in flue gas
α	Matrix element
η	Dynamic viscosity
Δ T	Stack temperature rise (°C)
ω	Acentric factor
ψ	Binary interaction coefficient
θ	Binary interaction coefficient
ϕ	Volume fraction

$\xi = V_c^{2/3} T_c^{-1/2} M^{-1/2}$

η	Annual fuel savings (1000 US $)
ε	Average fuel cost (US$ per GJ)
c	Critical value
i, j	Components i, j
m	Mixture (pseudocritical) value
r l , r2	Reference fluids 1, 2
o	Spherical reference fluid
R	Reduced

CHAPTER 1
Introduction and Objectives

During the next two decades, the world marketed energy consumption is projected to grow by 40% which is approximately similar to annual percentage increases over the last 20 years (Berends, 2007). In absolute terms, this means that the oil and gas processing capacity that has to be realised during the next 20 years is more than twice the amount realised during the last two decades (Berends, 2007).

The continuing growth in the importance of oil and gas processing increases the need for accurate prediction of several parameters and their impact on unit operations, process simulation and design. Because of the particular nature of various parameters, existing methods sometimes encounter difficulties. In large-scale data mining and predictive modelling, especially for multivariate systems, we often start with a large number of possible explanatory/predictive variables. Therefore, variable selection and dimension reduction is a major task for multivariate analysis. A well-known method in numerical analysis for dimension reduction is called stepwise algorithm, one of the major limitations of the algorithm is that when several of the predictive variables are highly correlated, the tests of statistical significance that the stepwise method is based on are not sound, as independence is one of the primary assumptions of these tests. Currently several models are available to predict various design parameters in the oil and gas processing industries. However, their calculations may require rigorous computer solutions for some particular applications. Therefore, developing novel easy-to-use methods to minimize the complex and time-consuming calculation steps is an essential requirement. Because most simulations require simultaneous iterative solutions of many nonlinear and highly coupled sets of equations, it is apparent that a mathematically compact, simple, and reasonably accurate equations, as proposed in this thesis, would be preferable for computationally intensive simulations. In fact, the development of practical correlations by a modification to the well-known (Vogel, 1921; Tammann and Hesse, 1926; Fulcher, 1925) equation was the primary motivation of this research, which, nevertheless, yielded correlations with accuracy comparable to that of the existing rigorous simulations. Hence, some existing approaches lead to complicated equations for the purposes of engineering importance. In the literature, this problem has been

circumvented conveniently by resorting to simpler approaches, as described in this thesis. The purpose of this dissertation is to develop and formulate accurate and reliable predictive tools to predict several oil, gas and process engineering parameters. Following the development of predictive tools, experimental works are undertaken to measure the density and viscosity, of ethylene glycol and water, diethylene glycol and water, and triethylene glycol and water mixtures at temperatures ranging from 290 K to 440 K and concentrations ranging from 20 mol % glycol to 100 mol % glycol. Our data were correlated using a novel Arrhenius-type equation based predictive tool and a thermodynamical method (the generalized corresponding states principle (GCSP)).

1.1 Rationale behind the proposed work

Frequently, correlation and prediction of various engineering parameters, process design variables or physical and transport properties of substances have been attempted by means of existing rigorous approaches. Such exercises, however, do not always yield effective results (Wang et al., 2000, Civan, 2005, Civan 2007, Civan 2008a, b). For example, using equations of state to predict properties is convenient and easy, but such methods do not apply equally well for all properties. Accurate and reliable values result for gas phase densities, volumes and Z-factors, while liquid volumes and densities are less accurate but still as reliable as predictions using other calculation methods. Equations of state are not so accurate to predict thermal conductivities, viscosities and surface tensions (Gas Processors and Suppliers Association Data-book, 2004). For instance, an equation of state approach taken by Wagner and Pruss (2002) required more than 56 constants model for representing the anomalous behaviour of the density of liquid water. The same could be achieved using only four empirical fitting constants based on the Vogel–Tammann–Fulcher–Hesse–Civan equation (VTFHC) (Civan, 2007a, 2008a). Sastri and Rao (1999) draw attention to the fact that some theoretical and semi-theoretical correlations of thermal conductivity include other parameters such as density and therefore data or correlations of such additional parameters are also required when using these correlations. Consequently, in addition to creating an inconvenience, accuracy of correlations of physical properties expressed in terms of other physical properties inherits errors associated with additional properties included in such correlations. Fortunately, however, these problems can be alleviated readily because dependent quantities such as density should not be included at all in correlations of

other dependent quantities such as viscosity or thermal conductivity which are both temperature dependent. The bottom-line is that correlations of physical properties and most of process engineering variables should be sought only in terms of independent variables such as temperature, pressure, molecular weight, and concentration (Civan, 2007, 2008a, b). Several examples of effective correlation of various physical and chemical parameters with temperature using simple correlation (Vogel, 1921; Tammann and Hesse, 1926; Fulcher, 1925) and its variations are provided elsewhere (Civan, 2005, 2006, 2007a, b, and 2008a, b).

1.2 Objectives

The purpose of the proposed dissertation work is to develop and formulate accurate and reliable predictive tools to predict different physical properties and process design parameters, including the prediction of hydrate forming conditions of natural gases and pure components, hydrate forming pressure of pure alkanes in the presence of inhibitors, water-hydrocarbon systems mutual solubilities, mono-ethylene glycol injection rate to avoid natural gas hydrate formation, water content of natural gas, density, thermal conductivity and viscosity of aqueous glycol solutions, optimum size of inlet scrubber and contactor in natural gas dehydration systems, solubility of carbon dioxide in aqueous solutions of amines, estimation of water-adsorption isotherms, estimation of equilibrium water dew point of natural gas in TEG dehydration systems, true vapour pressure (TVP) of LPG and natural gasoline, hydrocarbon components solubilities in hydrate inhibitors, methanol vaporization loss and solubility in hydrocarbon liquid phase for gas hydrate inhibition, storage pressure of gasoline in uninsulated tanks, emissivity of combustion gases, filling losses from storage containers, bulk modulus and volumetric expansion coefficient of water for leak tightness test of pipelines, prediction of LPG vapour pressure in above-ground storage tanks, silica solubility and carry-over in steam, carbon dioxide equilibrium adsorption isotherms, estimation of packed column size, estimation of thermal insulation thickness, transport properties of carbon dioxide, aqueous solubility of light hydrocarbons, estimation of economic thermal insulation thickness, water content of compressed air, surface tension of paraffin hydrocarbons, aqueous solubility and density of carbon dioxide, aqueous solubility of light hydrocarbons, thermal conductivity of hydrocarbons, downcomer design velocity and capacity correction factor in fractionators estimation of recoverable heat from blowdown systems, estimation of performance of steam turbines,

Estimation of maximum shell-side vapour velocities, estimation of energy conservation benefits in excess air controlled gas-fired systems, Estimation of steam losses in stream traps, estimation of heat Losses from process piping and equipment, estimation of carbon dioxide transport properties, design of radiant and convective sections of direct fired heaters, prediction of molten sulfur viscosity, Estimation of displacement losses from storage containers, estimation of packed column size and many other parameters. Figure 1.1 illustrates a typical flow diagram for natural gas treating including typical engineering parameters.

Following the development of predictive tools, experimental works are undertaken to measure the density and viscosity of ethylene glycol + water, diethylene glycol + water, and triathlons glycol + water mixtures at temperatures ranging from 290 K to 440 K and concentrations ranging from 20 mol % glycol to 100 mol % glycol. Our data were correlated using a novel Arrhenius-type predictive tool and a thermodynamical method (the generalized corresponding states principle (GCSP)). The results of new proposed model will be also compared with partial least squares (PLS) and principal component analysis (PCA).

1.3 Outline of thesis

The thesis commences with chapter two which is literature review. This chapter will address the current status of research in this field such as introduction to oil and gas industries, parameters of interest to oil and gas engineers, current remedial practices and existing gaps, possible improvement options, experimental and thermodynamical modelling for validation. Chapter 3 introduces the formulation of simple-to-use approach for parameter prediction, formulation of generic algorithm, selection of appropriate variables for developing the predictive tools and the Generalized Corresponding States Principle (GCSP) thermodynamical model applications for prediction of density and viscosity of aqueous glycol solutions. In chapter 4 measurement of density and viscosity of aqueous glycol solutions in a wide temperature range for validation of proposed predictive tool and the Generalized Corresponding States Principle (GCSP) thermodynamical model. Chapters 5 and 6 are main chapters of the thesis which present the developed predictive tools for various engineering applications. Chapter 7 covers the development of new PreTOG software combined with typical case studies for overall summary and potential

benefits to oil and gas processing industries using the typical developed predictive tools. The final chapter (chapter 8) provides conclusions and some recommendations for the future works.

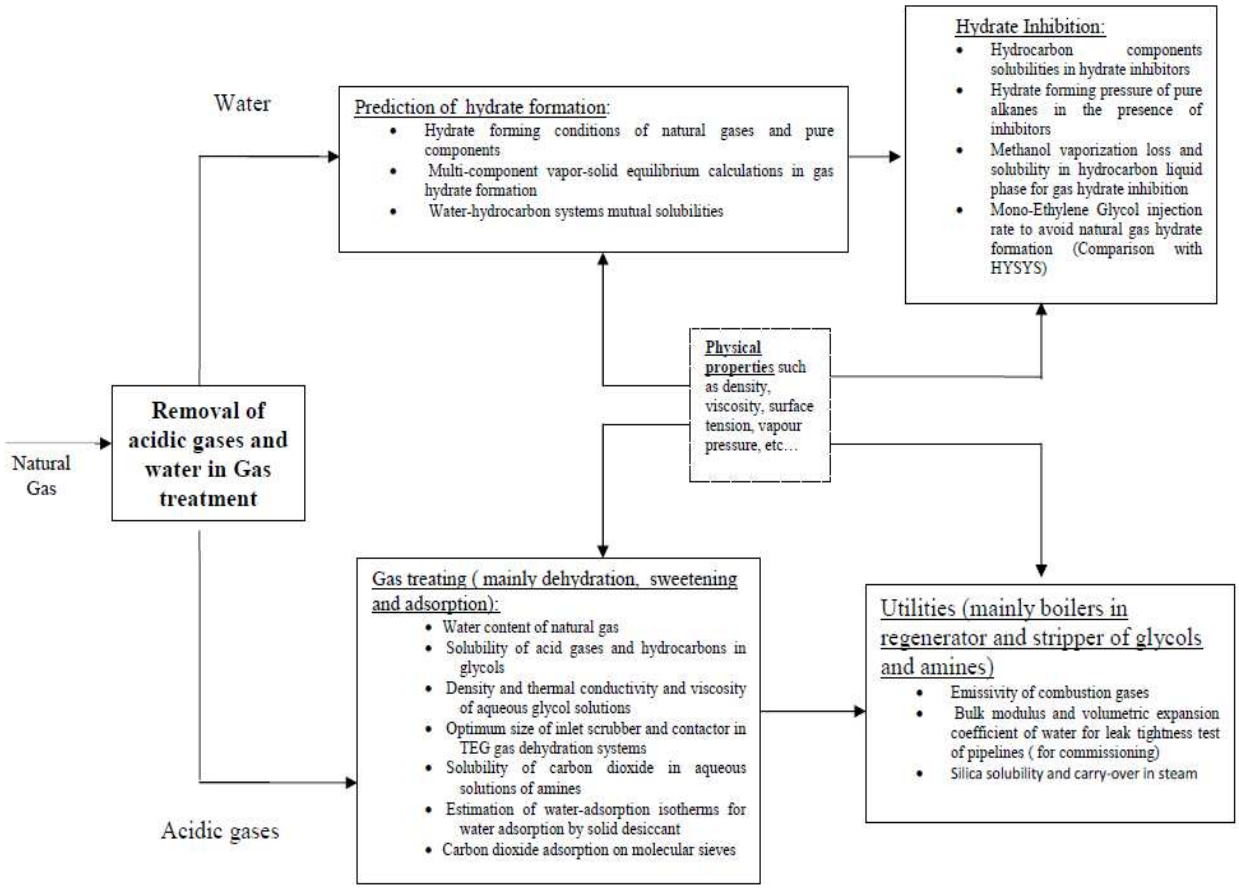

Figure 1.1: Flow chart for natural gas treatment including selected engineering parameters

1.4 Development of PreTOG software

In this thesis, the PreTOG software package has been developed, which covers a wide range of functions in oil, gas and chemical processing integration and is a PC-based using Windows and Matlab graphical user interfaces and tool boxes. Each predictive tool is self-contained and makes available all of the functionality required by chemical and petroleum engineers to carry out their engineering calculations tasks. This thesis provides sufficient information in the development of the software for professional engineers covering different topics in oil, gas and chemical industries. The PreTOG software allows users to use effectively the latest results from the

research outcomes from the developed predictive tools and taking a leading edge role in oil and gas production and processing industries. Figure 1.2 shows the vision for development of PreTOG software. The results of PreTOG software will be compared with partial least squares (PLS) and principal component analysis (PCA) in chapter 7.

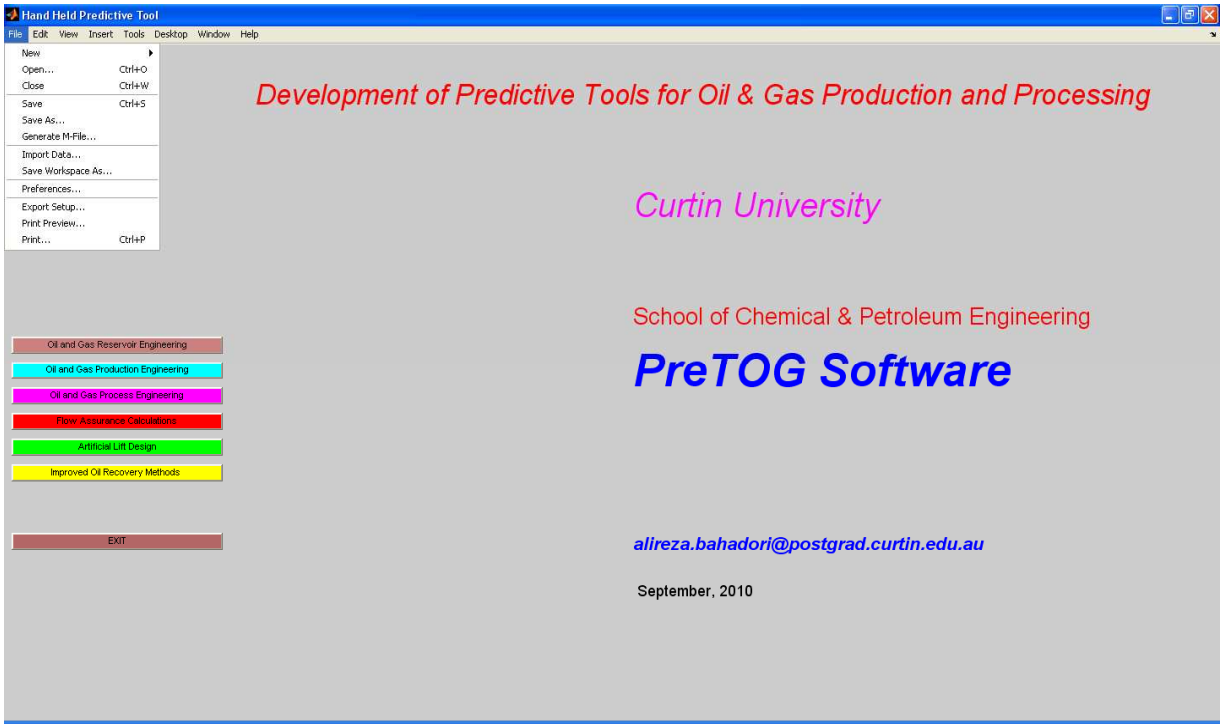

Figure 1:2 Development of PreTOG software

CHAPTER 2
Literature Review

The literature review provides insight into the background information and research that has been carried in relation to predicting various process engineering parameters mainly in oil and gas processing. The main objectives of this research are reviewed in this section and the literature survey is presented to set the context for the proposed research. In this chapter, first, selected outstanding research works undertaken in this area are reviewed, justifying the motivation for the present research.

2.1 Parameters of interest to oil and gas engineers

The water content of natural gas is an important parameter in the design of facilities for the production, transmission, and processing of natural gas. It is important for natural gas engineers to accurately predict aqueous dew points because natural gas reservoirs always have water associated with them (Carroll 2002, Carroll and Mather, 1989). Other water produced with the gas is water of condensation formed because of the changes in pressure and temperature during production. In the transmission of natural gas further condensation of water is problematic. It can increase pressure drop in the line and often leads to corrosion problems and gas hydrate formation. For these reasons, the water content of natural gas and acid gas is an important engineering consideration (Carroll 2002, Makogon, 1997 and Makogon, 2010).

However, if the gas composition is not known, even the previous methods cannot be used to predict the hydrate formation conditions and the reliable correlations can be used to predict the approximate pressure and temperature for hydrate formation. Therefore, there is an essential need to develop a simple-to-use predictive tool for appropriate prediction of hydrate formation conditions of natural gases (Sloan, 1998, Ameripour and Barrufet, 2009, Sloan, 1998).

Methanol is the most commonly used hydrate inhibitor in subsea petroleum industries, gas treatment and processing, pipelines and wells (Elgibaly and Elkamel, 1999 and Lundstrøm et al., 2006) with worldwide usage several million dollars per year (Bruinsma, et al, 2004). Often when applying this inhibitor, there is a significant expense associated with the cost of "lost" methanol (GPSA Data book, 2004). Owing to lower surface tension and viscosity of methanol, however, it makes it possible to have an effective separation from the gas phase at cryogenic conditions and usually the most preferred inhibitor (Esteban, 2000).

Methanol and ethylene glycol (EG) are used to treat natural gas streams in a number of ways (Minkkinen 1992, Jou et al. 1994, Epps 1994, Bucklin and Schendel, 1985). Extensive studies have been carried out on aqueous methanol and EG solutions at various temperature and pressure conditions and wide range of gas processing applications (Yokoyama et al 1988, Zheng et al. 1999, and Wang et al 2003). However, the current models may not be simple and sufficient if rapid and accurate predictions are a requirement.

Extensive literature is available on common gas dehydration systems including solid and liquid desiccant and refrigeration-based systems (Gandhidasan et al., 2001, Karimi and Abdi, 2009). In view of the above, it is necessary to formulate simple predictive tools to correlate various design parameters for natural gas dehydration system, as well as hydrate formation and gas hydrate inhibition. Several equilibrium correlations for predicting water dew point of natural gas in equilibrium with a TEG dehydration system have been presented since 1950. However, all methods are limited by the ability to measure accurately the equilibrium concentration of water in the vapour phase above triethylene glycol (TEG) solutions (Twu et al., 2005). In the correlations developed by Parrish et al. (1986) and Won (1994), the equilibrium water concentrations in the vapour phase were determined at infinite dilution (essentially 100% TEG). The other correlations use extrapolations of data at lower concentrations to estimate equilibrium in the infinite dilution region (Parrish et al., 1986 and Won, 1994).

Herskowitz and Gottlieb (1984) measured the activity coefficients of water in TEG at two temperatures, 297.60 and 332.60 K. The lowest mole fraction of water for which measured activities was 0.1938 and 0.2961 at 297.60 K and 332.60 K, respectively. These fit the measured activity coefficients to the van Laar equation. They did not measure data in the infinite dilution region. In order to predict the equilibrium behaviour in the infinite dilution region, most

researchers extrapolated the measured data at low water concentrations to infinite dilution using an activity coefficient model such as van Laar. However, extrapolating the van Laar or any other activity coefficient model will yield erroneous results for the infinite dilution activity coefficients. The GPSA data book (2004) presents an equilibrium correlation based on the work of Worley (1967). In general, the correlations of Worley, (1967), (Roman, 1973) and Parrish et al. (1986) agree reasonably well and are adequate for most TEG system designs. All are limited by the ability to measure accurately the equilibrium concentration of water in the vapour phase above TEG solutions.

In view of the above mentioned parameters, there is an essential need to develop easy-to-use predictive tools for rapid and accurate prediction of various process design parameters in oil and gas industries. **Fractionation is one of the pivotal unit operations in the gas processing and other industries utilized to separate mixtures into individual products. The primary parameters involved in the design of fractionators are the number of stages and the reflux ratio. Distillation is one of the single largest energy-degrading unit operations [Diwekar et al, 1989), (Miladi and Mujtaba, 2004) and [Tomazi,1997) . Several research papers have analyzed the influence of the various design parameters on the distillation and fractionation columns [Salomone et al 1997), and [Gadalla et al, 2006). In the past, the design and operation optimization of conventional and unconventional distillation columns have received significant attention [Farhat et al 1990), [Kerkhof and Vissers, 1978), [Logsdon and Biegler, 1993) and [Pommier et al, 2008). The difficulty of a separation in fractionators is directly related to the relative volatility of the components and the required purity of the product streams [Pommier et al, 2008) and [Logsdon et al 1990).**

It is necessary is to develop easy-to-use predictive tools, which are simpler than current available models involving fewer parameters, requiring less complicated and shorter computations, for an appropriate prediction operating reflux ratio for a given number of stages. Alternatively, for a given reflux ratio, the number of stages can be determined for accurately for the downcomer velocity and vapor capacity factor which also have to take into account to size fractionators without foaming formation.

Absorption is one of the unit operations which is widely used in the gas processing industry (Pyrenean & Rochelle, 2007). In an absorption column, rich gas enters the bottom of the absorber and flows upward contacting the counter-current lean oil stream. The lean oil preferentially absorbs the heavier components from the gas known as "rich oil" (GPSA, 2004). The rich oil is sent to a stripper (or still) where the absorbed components are removed by heating and/or stripping with steam. The lean oil is recycled to the absorber to complete the process loop (GPSA Engineering Data-book, 2004). For a given gas, the fraction of each component within the gas which is absorbed by the oil is a function of the equilibrium phase relationship of the components and lean oil, the relative flow rates, and the contact stages (GPSA, 2004). The phase relation is a function of pressure, temperature and the composition of the lean oil. In dynamic simulators, mathematical models are applied in order to study the time-dependent behaviour of a system, consisting of the system process units and the corresponding control units. With currently available computing power, the process unit models in a dynamic simulator still has to be simplified in comparison to steady-state models (Kvamsdal, et al, 2009). The challenge is to model the complex phenomena associated with the absorber unit without losing important information.

Another challenge is the validation of a dynamic model, because the relevant dynamic data from existing plants are not available. However, steady-state performance can be validated since there are more adequate data and advanced models available (Kvamsdal et al., 2009). Dynamic modelling and simulation has been a very time consuming and labour intensive activity, requiring highly skilled systems engineers and computer applications specialists (Tu and Rinard, 2006).

In view of the above-mentioned parameters, it is necessary to develop an accurate and simple method which will be easier than existing approaches, to be less complicated with fewer computations that can accurately predict the absorption efficiency as a function of absorption factor and number of stages.

2.2 Parameters of interest to other process applications

This research also covers developing and formulating accurate and reliable predictive tools to forecast many other engineering parameters in various process engineering systems. For instance, over the years, considerable research efforts have been expended in investigating the heat exchanger design details, specify heat exchanger performance, and determine the feasibility of using heat exchangers in new services (Butterworth, 2002), (Andrews and Master, 2005), (Master et al., 2006) and (Kapale and Chand, 2006). (Smith, 2005 and Ponce-Ortega et al., 2006). (Wang et al., 2009), (Li and Kottke, 1998a) and (Li and Kottke, 1998b) and (Rodriguez and Smith, 2007). However, to date, there is no simple-to-use predictive tool for an accurate and rapid estimation of maximum shell-side vapour velocities through heat exchangers. In view of this necessity, our efforts have been directed at formulating a simple-to-use tool to assist engineers and researchers for the other design parameters, These days about 90% of the total energy output worldwide is from the combustion of fossil fuels (Xu et al, 2005, Kaewboonsonga et al, 2006 and Fang et al, 2010). Hydrocarbon combustion has a major impact on the global environment due to the emission of CO_2, a greenhouse gas, which results in temperature increasing, drought, flood, hunger, and eventually economic chaos (Jou et al 2008). Furthermore, the emission of NO_x, SO_x, polycyclic aromatic hydrocarbons (PAHs), CO and particles leads to air pollution, acid rain, and health hazards (Barroso et al, 2004) and (Miller and Srivastava, 2000).

Nevertheless, the demand for fossil fuel continues to rise globally (Barroso et al, 2004). Therefore, techniques to achieve better combustion efficiency with the least amount of pollutant emissions are necessary, and this goal can be reached through the control of combustion processes or adjustment of the fuels applied (Jou et al 2008). It is an assertion well established by researchers and engineers related to the industrial boiler field that excess air is a control variable affecting thermal efficiency and the operating reliability of boilers (Jou et al 2008). The increase in the value of the excess of air in the furnace leads to a reduction in the adiabatic flame

temperature, and probably will prompt an increase in the heat transfer coefficients for all the convective equipments, causing a reduction in the flue gas temperature. As the excess air ratio goes up, the O_2 concentration in the main combustion area also increases, resulting in the rise of the flame temperature in the boiler. This leads to a decrease in temperature in the boiler radiation area, and eventually affects the boiler efficiency (Bebar et al, 2002) and (Yang and Blasiak, 2005). A boiler should always be supplied with more combustion air than is theoretically required, in order to ensure complete combustion and safe operation. If the air rate is too low, there will be a rapid build-up of carbon monoxide in the flue gas and, in extreme cases, smoke will be produced (i.e. unburned carbon particles) (Ozdemir, 2004) At the same time, boiler efficiency is very dependent on the excess air rate. Excess air should be kept at the lowest practical level to reduce the quantity of unneeded air that is heated and exhausted at the stack temperature (Ozdemir, 2004). Taplin (1991) presents more information on combustion efficiency including combustion efficiencies data for natural gas or other fuels.

In view of the above, it is necessary to develop an accurate and simple method which is easier than the existing approaches to be less complicated with fewer computations for predicting the natural gas combustion efficiency as a function of excess air fraction and stack temperature rise. The results of the proposed predictive tool can be used in follow-up calculations to determine relative operating efficiency and to establish energy conservation benefits for an excess air control program. Part of this thesis discusses the formulation of such a predictive tool in a systematic manner.

2.3 Current remedial practices and existing gaps

The basic Arrhenius (1889) equation and its modified asymptotic exponential forms have been successfully applied for the correlation of temperature dependence of parameters of various processes. For example, such functions have been proven to perform very well for correlation of diffusion coefficient (Callister, 2000), fluid viscosity (Civan, 2008a), and (Zhang et al 2003), emulsion stability (Civan and Weers, 2001), water flow capability of variably saturated soils, wettability related properties of porous rocks, and the frequency dispersion of dielectric relaxation (Nino et al 2001).

Many correlations such as the Vogel-Tammann-Fulcher (VTF) (1921-1926) equation has been applied successfully for correlating various parameters of engineering importance (Civan 2005, 2008a,b,c). Numerous applications reported in the literature indicate that the Vogel-Tammann-Fulcher (VTF) (1921-1926) equation performs well, in comparison to other approaches and rigorous methods. However, developed correlations such as Vogel-Tammann-Fulcher (VTF) (1921-1926) equation are not a panacea for all problems.

Presently some existing approaches sometimes lead to complicated equations for the purposes of engineering importance due to the particular nature of various parameters. sometimes the existing methods encounter difficulties. Currently several models are available to predict various design parameters in the oil and gas processing and production industries. However, their calculations can require rigorous computer solutions. Therefore, developing the new predictive tools to minimize the complex and time-consuming calculation steps is an essential need because most simulations require simultaneous iterative solutions of many nonlinear and highly coupled sets of equations. It is apparent that a mathematically compact, simple, and reasonably accurate equations that contained a fewer coefficients, as proposed in this thesis, would be preferable for computationally intensive simulations. This problem could be circumvented conveniently by resorting to simpler approaches as described in this thesis.

2.4 Possible improvement options

The purpose of the proposed dissertation work is to develop and formulate accurate and reliable predictive tools to predict different engineering parameters mainly in the oil and gas production and processing industries as indicated in the objective section in chapter 1. In this thesis, also the PreTOG software package has been developed, which covers a wide range of functions in oil, gas and chemical processing industries. Each predictive tool is self-contained and makes available all of the functionality required by chemical and petroleum engineers to carry out their engineering calculations tasks. Following the development of predictive tools, experimental works are undertaken to measure the density and viscosity, of ethylene glycol + water, diethylene glycol + water, and triethylene glycol + water mixtures are measured at temperatures ranging from 290 K to 440 K and concentrations ranging from 20 mol % glycol to 100 mol % glycol. Our data were correlated using a novel Arrhenius-type equation based predictive tool and a thermodynamical

method (the generalized corresponding states principle (GCSP)). Both novel Arrhenius-type equation based predictive tool and GCSP method, with adjustable parameters for each property, offer the potential for judicious extrapolation of density and viscosity data for all glycol + water mixtures.

2.5 Experimental and thermodynamical modelling for validation

Aqueous glycol solutions have widespread application in the manufacture of solvents, hygroscopic agents, lubricants and conditioning agents. Accurate knowledge of these solution's thermophysical properties is therefore essential in process calculations involving these mixtures. In order to validate the proposed predictive tools new experimental data were correlated using proposed Arrhenius based predictive tool and a thermodynamic model (the generalized corresponding states principle (GCSP)). In addition to the Arrhenius based predictive tool, the two-reference-fluid generalized corresponding states principle (GCSP) of Teja and Rice, (1981a, b, c) and Teja 1982 et al. was also used to correlate the data. The GCSP method relates the quantities *of* the mixture to the properties of two reference fluids at the same reduced temperature and reduced pressure.

Both Arrhenius based predictive tool and the GCSP method, with two adjustable parameters for each property, offer the potential for judicious extrapolation of density and transport property data for all glycol + water mixtures.

CHAPTER 3

Formulation of predictive tool approach for parameter prediction

In large-scale data mining and predictive modelling, especially for multivariate numerical exercises, we often start with a large number of possible explanatory/predictive variables. Therefore, variable selection and dimension reduction is a major task for multivariate numerical analysis. Statistically, correlation is a measure of linear dependence among variables and presence of highly correlated variables which indicate a linear dependence among the variables. The basic Arrhenius (1889) equation and its modified asymptotic exponential forms have been successfully applied for correlation of the temperature dependence of the parameters of various processes. For example, such functions have been proven to perform miraculously well for correlation of diffusion coefficient (Callister, 2000) , fluid viscosity (Civan 2008a), (Gilmont, 2002) and (Zhang et al 2003), emulsion stability (Civan and Weers, 2001), water flow capability of variably saturated soils, wettability related properties of porous rocks, and frequency dispersion of dielectric relaxation (Nino et al 2001). This research demonstrates that the experimental measurements and reported data of various design parameters can also be correlated accurately using the Arrhenius-type functions. The parameters of these equations are determined by means of the new experimental data generated in this research for the density and viscosity of aqueous ethylene glycol (EG), diethylene glycol (DEG) and triethylene glycol (TEG) and wide range of other data accessible in the literature. It is shown that such functions yield accurate correlations of these experimental data, proving the applicability of this equation to various cases.

3.1 Existing multivariate statistical methods

Two existing rigorous methodologies are principal component analysis (PCA) and partial least square (PLS), which are currently used in regression analysis when some of the independent variables are correlated. Bair at al, (2006) describe the algorithm used in each methodology. Other popular techniques exist which have been reviewed by Kadleca, et al (2009). These are the Artificial Neural Networks, Neuro-Fuzzy Systems and Support Vector Machines.

3.1.1 Principal component analysis

The principal component analysis algorithm is a traditional multivariate statistical method commonly used to reduce the number of predictive variables and solve the multi-colinearity problem (Bair et al., 2006). The principal component analysis involves a mathematical procedure that transforms a number of possibly correlated variables into a number of uncorrelated variables called principal components, related to the original variables by an orthogonal transformation. This transformation is defined in such a way that the first principal component has as high a variance as possible (that is, accounts for as much of the variability in the data as possible), and each succeeding component in turn has the highest variance possible under the constraint that it be orthogonal to the preceding components. Principal component analysis is sensitive to the relative scaling of the original variables and looks for a few linear combinations of the variables that can then be used to summarize the data without losing too much information in the process (Shaw, 2003).

The PCA algorithm reduces the number of variables by building linear combinations of those variables. This is done in such a way where these combinations cover the highest possible variance in the input space and are additionally orthogonal to each other (Kadleca et al., 2009). In this way the colinearity can be handled and the dimensionality of the input space can be decreased at the same time (Kadleca et al., 2009). It is mostly used as a tool in exploratory data analysis and for making predictive models. PCA can be done by eigenvalue decomposition of a data covariance matrix or singular value decomposition of a data matrix, usually after mean centering the data for each attribute.

The results of a PCA are usually discussed in terms of component scores (the transformed variable values corresponding to a particular case in the data) and loadings (the variance each original variable would have if the data were projected onto a given PCA axis) (Shaw, 2003). Application possibilities of the PCA in the process industry are reviewed in Warne, Prasad, Rezvani, and Maguire (2004).

PCA is mathematically defined as an orthogonal linear transformation that transforms the data to a new coordinate system such that the greatest variance by any projection of the data comes to lie on the first coordinate (called the first principal component), the second greatest variance on the second coordinate, and so on.

Define a data matrix, X^T, with zero empirical mean (the empirical (sample) mean of the distribution has been subtracted from the data set), where each of the *n* rows represents a different repetition of the experiment, and each of the *m* columns gives a particular kind of datum (say, the results from a particular probe). The singular value decomposition of X is, $X = W \sum V^T$,where, the $m \times m$ matrix 'W' is the matrix of eigenvectors of XX^T, the matrix $\sum$ is an $m \times n$ rectangular diagonal matrix with nonnegative real numbers on the diagonal, and the matrix V is $n \times n$. The PCA transformation that preserves dimensionality (that is, gives the same number of principal components as original variables) is then given by:

$$Y^T = X^T W = V \sum^T \qquad (3.1)$$

V is not uniquely defined in the usual case when $m < n - 1$, but Y will usually still be uniquely defined. Since W (by definition of the SVD of a real matrix) is an orthogonal matrix, each row of Y^T is simply a rotation of the corresponding row of X^T. The first column of Y^T is made up of the "scores" of the cases with respect to the "principal" component, the next column has the scores with respect to the "second principal" component, and so on (Shaw, 2003).

If we want a reduced-dimensionality representation, we can project X down into the reduced space defined by only the first *L* singular vectors, W_L : (Shaw, 2003).

$$Y = W_L^T X = \sum\nolimits_L V_L^T \qquad (3.2)$$

The matrix W of singular vectors of **X** is equivalently the matrix **W** of eigenvectors of the matrix of observed covariances C= XX^T , (Shaw, 2003)

$$XX^T = W \sum \sum {}^T W^T \qquad (3.3)$$

Given a set of points in Euclidean space, the first principal component corresponds to a line that passes through the multidimensional mean and minimizes the sum of squares of the distances of the points from the line. The second principal component corresponds to the same concept after all correlation with the first principal component has been subtracted out from the points. The singular values (in $\sum$) are the square roots of the eigenvalues of the matrix XX^T. Each eigenvalue is proportional to the portion of the "variance" (more correctly of the sum of the squared distances of the points from their multidimensional mean) that is correlated with each eigenvector. The sum of all the eigenvalues is equal to the sum of the squared distances of the points from their multidimensional mean. PCA essentially rotates the set of points around their mean in order to align with the principal components. This moves as much of the variance as possible (using an orthogonal transformation) into the first few dimensions. The values in the remaining dimensions, therefore, tend to be small and may be dropped with minimal loss of information. PCA is often used in this manner for dimensionality reduction. PCA has the distinction of being the optimal orthogonal transformation for keeping the subspace that has largest "variance" (as defined above). This advantage, however, comes at the price of greater computational requirements if compared, for example and when applicable, to the discrete cosine transform. Nonlinear dimensionality reduction techniques tend to be more computationally demanding than PCA.

PCA is sensitive to the scaling of the variables. If we have just two variables and they have the same sample variance and are positively correlated, then the PCA will entail a rotation by 45° and the "loadings" for the two variables with respect to the principal component will be equal. But if we multiply all values of the first variable by 100, then the principal component will be almost the same as that variable, with a small contribution from the other variable, whereas the second component will be almost aligned with the second original variable. This means that whenever the different variables have different units (like temperature and mass), PCA is a somewhat arbitrary method of analysis. (Different results would be obtained if one used Fahrenheit rather than Celsius for example.) One way of making the PCA less arbitrary is to use variables scaled so as to have unit variance.

3.1.2 Partial least squares

Partial least squares is a mathematical method that bears some relation to principal components analysis. Instead of finding hyper planes of maximum variance between the response and independent variables, it finds a linear model by projecting the predicted variables and the observable variables to a new space. Because both the X and Y data are projected to new spaces, the Partial least squares family of methods are known as bilinear factor models. Partial least squares Discriminant Analysis (PLS-DA) is a variant used when the Y is binary. PLS is used to find the fundamental relations between two matrices (X and Y), i.e. a latent variable approach to modeling the covariance structures in these two spaces (Chin, 1998; Fornell and Bookstein, 1982).

A Partial least square (PLS) model will try to find the multidimensional direction in the X space that explains the maximum multidimensional variance direction in the Y space. This method is particularly suited when the matrix of predictors has more variables than observations and when there is multicollinearity among X values. By contrast, standard regression will fail in these cases (Chin, 1998; Fornell and Bookstein, 1982). PLS-regression is an important step in the PLS path analysis, a multivariate data analysis technique that employs latent variables. This technique is often referred to as a form of variance-based or component-based structural equation modeling. An alternative term for PLS is the projection to latent structures, but the term partial least squares is still dominant in many areas (Chin, 1998; Fornell and Bookstein, 1982).

This rigorous algorithm, instead of focusing on the covering of the input space variance, pays attention to the covariance matrix that brings together the input and the output data space (Kadleca et al., 2009). The algorithm decomposes the input and output space simultaneously while keeping the orthogonally constraint (Kadleca et al., 2009). In this way it is assured that the model focuses on the relation between the input and output variables. A general description of the PLS technique is provided in Geladi and Esbensen (1991). As PLS is a very popular technique in chemical engineering and in chemometrics, there are several publications dealing with the application aspects of PLS to these domains (Kaspar and Ray, 1993 and Kourti, 2002).

PLS is used to find the fundamental relations between two matrices (X and Y), i.e. a latent variable approach to modeling the covariance structures in these two spaces. A PLS model will try to find the multidimensional direction in the X space that explains the maximum

multidimensional variance direction in the *Y* space. PLS-regression is particularly suited when the matrix of predictors has more variables than observations, and when there is multicollinearity among *X* values. By contrast, standard regression will fail in these cases.

PLS-regression is an important step in PLS path analysis, a multivariate data analysis technique that employs latent variables. This technique is often referred to as a form of variance-based or component-based structural equation modeling (Kaspar and Ray, 1993 and Kourti, 2002).

An alternative term for PLS is *projection to latent structures*, but the term *partial least squares* is still dominant in many areas. It is widely applied in the field of chemometrics, in sensory evaluation, and more recently, in the analysis of functional brain imaging data. (Kaspar and Ray, 1993 and Kourti, 2002).

The general underlying model of multivariate PLS is:

$$X = TP^T + E \qquad (3.4)$$

$$Y = TQ^T + F \qquad (3.5)$$

Where *X* is an $n \times m$ matrix of predictors, *Y* is an $n \times p$ matrix of responses, *T* is an $n \times l$ matrix (the *score*, *component* or *factor* matrix), *P* and *Q* are, respectively, $m \times l$ and $p \times l$ *loading* matrices, and matrices *E* and *F* are the error terms(Kaspar and Ray, 1993 and Kourti, 2002). Number of variants of PLS exist for estimating the factor and loading matrices *T, P* and *Q*. Most of them construct estimates of the linear regression between *X* and *Y* as

$$Y = X\ B + XB_0 \quad . \qquad (3.6)$$

Some PLS algorithms are only appropriate for the case where *Y* is a column vector, while others deal with the general case of a matrix *Y*. Algorithms also differ on whether they estimate the factor matrix *T* as an orthogonal, an orthonormal matrix or not. The final prediction will be the same for all these varieties of PLS, but the components will differ (Wold, 1984).

3.2 Formulation of Generic Algorithm

A well-known method in numerical analysis for dimension reduction is called stepwise analysis algorithm, which is covered by many statistical softwares. One of the major limitations of the algorithm is that when several of the predictive variables are highly correlated, the tests of statistical significance that the stepwise method is based on are not sound, as independence is one of the primary assumptions of these tests. The primary purpose of the present study is to accurately correlate various process engineering parameters for wide range of applications. This is accomplished by an improvement to the Arrhenius type equation. This is important, because such an accurate and mathematically simple correlation of various process design parameters are required frequently for the modelling and simulation of many processes, using computationally intensive computer simulation to avoid the additional computational burden of complicated calculations.

The Vogel-Tammann-Fulcher (VTF) (1921-1926) equation has been applied successfully for correlating various parameters of engineering importance (Civan 2005, 2008a, b, c). Numerous applications reported in the literature indicate that the Vogel-Tammann-Fulcher (VTF) (1921-1926) equation performs well, in comparison to other approaches and rigorous methods. For example, a critical modification may be required for applications that involve liquid water, as demonstrated by Civan (2007). The primary purpose of the present study is to accurately correlate various process parameters:
The Vogel-Tammann-Fulcher (VTF) (1921-1926) equation is an asymptotic exponential function that is given in the following general form:

$$\ln f = \ln f_c - \frac{E}{R(T - T_c)} \tag{3.7}$$

In equation 3.7, f is a properly defined temperature-dependent parameter, the units for which are determined individually for a certain property; fc is a pre-exponential coefficient, having the same unit of the property of interest; T and T_c are the actual temperature and the characteristic-limit temperature, respectively (both given in degrees Kelvin); E is referenced as the activation energy of the process causing parameter variation (given in units of J/kmol); and R is the

universal gas constant (R) 8.314 J/(kmol K). A special case of the Vogel-Tammann-Fulcher (VTF) (1921-1926) equation for T_c =0 is the well-known Arrhenius (1889) equation:

$$\ln f = \ln f_c - \frac{E}{RT} \tag{3.8}$$

By examination of the most of available experimental data for temperature-dependent parameter, it is obvious that such nonlinear data cannot possibly be represented by the conventional Arrhenius equation given by equation (3.8), because this equation can only represent a straight-line behaviour with a slope of -E/R. and intercept of ln fc, when plotted in the form of ln f vs 1/(T). Therefore, no attempt has been made to correlate various available data using the original Arrhenius (1889) equation: Instead, for the purposes of various applications:

$$\ln f = a + \frac{b}{T} + \frac{c}{T^2} + \frac{d}{T^3} \tag{3.9}$$

Where a is ln(fc) and b, c and d are adjusted parameters. The term f is defined as the relative deviation of a value from the characteristic-limit value. Equation 3.9 is recommended for temperature-dependent parameters, however for non-temperature dependent parameter, the same mathematical method and equation form with empirical parameters can be applied and validated for the recommended range. As previously mentioned, some theoretical and semi-theoretical models include other parameters such as density and therefore data or correlations of such additional parameters are also required when using these rigorous models. Consequently, in addition to creating an inconvenience, accuracy of correlations of physical properties expressed in terms of other physical properties inherits errors associated with additional properties included in such correlations. Fortunately, however, these problems can be alleviated readily because dependent quantities such as density should not be included at all in correlations of other dependent quantities such as viscosity or thermal conductivity which are both temperature dependent.

The Arrhenius (1889) equation was intended to describe the rate constants of chemical reactions, but similar equations have also been used frequently for correlation of other temperature-dependent physical properties, such as Beggs and Robinson (1975) and Glasø (1980).

Originally, one of the Arrhenius-based equations (Vogel–Tammann–Fulcher) (1921-1925) has been proposed for representation of the liquid viscosity was based on the free-volume theory, where the free volume is equal to the apparent liquid specific volume minus the total specific volume of all the molecules forming the liquid. Limited attempts have been made to justify for such equations theoretically. However, for all engineering purposes, these equations still remain essentially an empirical expression. Nevertheless, it has performed miraculously well for various applications, including the new applications presented in this research.

The research outcomes will demonstrate that the Arrhenius-type asymptotic exponential functions can provide simple and accurate tools for various properties of fluids, oil and gas engineering as well as process design parameters. The approach for developing predictive tools is verified by numerous data including new experimental data reported in this research. It is demonstrated that the present approach yields a mathematically simple predictive tool.

The following methodology has been applied to develop this tool for various process design parameters and physical properties. In this research, Vandemonde matrix is utilized to tune the coefficients of equations. Vandermonde matrix is a matrix with the terms of a geometric progression in each row, i.e., an $m \times n$ matrix (Horn and Johnson, 1991).

$$V = \begin{bmatrix} 1 & \alpha_1 & \alpha_1^2 & \cdots & \alpha_1^{n-1} \\ 1 & \alpha_2 & \alpha_2^2 & \cdots & \alpha_2^{n-1} \\ 1 & \alpha_3 & \alpha_3^2 & \cdots & \alpha_3^{n-1} \\ \vdots & \vdots & \vdots & \ddots & \vdots \\ 1 & \alpha_m & \alpha_m^2 & \cdots & \alpha_m^{n-1} \end{bmatrix} \tag{3.10}$$

Or

$$V_{i,j} = \alpha_i^{j-1} \tag{3.11}$$

For all indices i and j, the determinant of a square Vandermonde matrix (where m=n) can be expressed as (Horn and Johnson, 1991):

$$\det(V)=\prod_{1\le i<j\le n}(\alpha_j-\alpha_i) \qquad (3.12)$$

The Vandermonde matrix evaluates a polynomial at a set of points; formally, it transforms coefficients of a polynomial $a_0+a_1x+a_2x^2+\ldots+a_{n-1}x^{n-1}$ to the values the polynomial takes at the point's α_i. The non-vanishing of the Vandermonde determinant for the distinct points α_i shows that, for distinct points, the map from coefficients to values at those points is a one-to-one correspondence, thus the polynomial interpolation problem is solvable with an unique solution; this result is called the unisolvence theorem (Fulton and Harris 1991). These are thus useful in polynomial interpolation, since solving the system of linear equations Vu = y for u with V, an m × n Vandermonde matrix is equivalent to finding the coefficients u_j of the polynomial(s) (Fulton and Harris 1991):

$$q(x)=\sum_{j=0}^{n-1}u_j x'^{j} \qquad (3.13)$$

$$q(\alpha_i)=y_i \quad \text{For i=1,..., m.} \qquad (3.14)$$

The Vandermonde matrix can easily be inverted in terms of the Lagrange basis polynomials. Each column is the coefficients of the Lagrange basis polynomial, with terms in increasing order going down.

Polynomial interpolation is also essential to perform sub-quadratic multiplication and squaring, where an interpolation through points on a polynomial which defines the product yields the product itself. For example, given $a = f(x) = a_0x^0 + a_1x^1 + \ldots$ and $b = g(x) = b_0x^0 + b_1x^1 + \ldots$ then the product ab is equivalent to $W(x) = f(x)g(x)$. Finding points along $W(x)$ by substituting x for small values in $f(x)$ and $g(x)$ yields points on the curve. Interpolation based on those points will yield the terms of $W(x)$ and subsequently the product ab. In the case of Karatsuba multiplication this technique is substantially faster than quadratic multiplication, even for modest-sized inputs. This is especially true when implemented in parallel hardware.

Given a set of n+1 data points (x_i,y_i) where no two x_i are the same, one is looking for a polynomial p of degree at most n with the property (Chin, 1998)

$$p(x_i)=y_i,\ i=0,\ldots,n. \qquad (3.15)$$

The unisolvence theorem states that such a polynomial *p* exists and is unique, and can be proved by the Vandermonde matrix, as described below.

The theorem states that for *n*+1 interpolation nodes (x_i), polynomial interpolation defines a linear bijection (Bair et al., 2006).

$$L_n : \mathbb{K}^{n+1} \to \Pi_n \tag{3.16}$$

where Π_n is the vector space of polynomials (defined on any interval containing the nodes) of degree at most *n*

Suppose that the interpolation polynomial is in the form:

$$P(x) = a_n x^n + a_{n-1} x^{n-1} + \ldots + a_2 x^2 + a_1 x + a_0 \tag{3.17}$$

The statement that *p* interpolates the data points means that

$$p(x_i) = y_i \qquad \text{for all } i \in \{0, 1, \ldots, n\}.$$

If we substitute equation (3.11) in here, we get a system of linear equations in the coefficients a_k. The system in matrix-vector form reads (Bair et al., 2006):

$$\begin{bmatrix} x_0^n & x_0^{n-1} & x_0^{n-2} & \ldots & x_0 & 1 \\ x_1^n & x_1^{n-1} & x_1^{n-2} & \ldots & x_1 & 1 \\ \vdots & \vdots & \vdots & & \vdots & \vdots \\ x_n^n & x_n^{n-1} & x_n^{n-2} & \ldots & x_n & 1 \end{bmatrix} \begin{bmatrix} a_n \\ a_{n-1} \\ \vdots \\ a_0 \end{bmatrix} = \begin{bmatrix} y_0 \\ y_1 \\ \vdots \\ y_n \end{bmatrix}. \tag{3.18}$$

We have to solve this system for a_k to construct the interpolant $p(x)$. The matrix on the left is commonly referred to as a Vandermonde matrix (Bair et al., 2006).

The condition number of the Vandermonde matrix may be large, causing large errors when computing the coefficients a_i if the system of equations is solved using Gaussian elimination(Bair et al., 2006).

Suppose we interpolate through *n+1* data points with an at-most *n* degree polynomial $p(x)$ (we need at least *n+1* datapoints or else the polynomial can't be fully solved for). Suppose also another polynomial exists also of degree at most *n* that also interpolates the *n+1* points; call it $q(x)$ (Kaspar and Ray, 1993).

Consider $r(x) = p(x) - q(x)$. We know,

$r(x)$ is a polynomial

$r(x)$ has degree at most *n*, since $p(x)$ and $q(x)$ are no higher than this and we are just subtracting them.

At the $n + 1$ data points, $r(x_i) = p(x_i) - q(x_i) = y_i - y_i = 0$. Therefore $r(x)$ has *n+1* roots.

But $r(x)$ is an n degree polynomial (or less). It has one root too many. Formally, if $r(x)$ is any non-zero polynomial, it must be writable as $r(x) = (x - x_0)(x - x_1)...(x - x_n)$. By distributivity the $n+1$ x's multiply together to make x^{n+1}, i.e. one degree higher than the maximum we set. So the only way $r(x)$ can exist is if $r(x) = 0$ (Kaspar and Ray, 1993).

$$r(x) = 0 = p(x) - q(x) \implies p(x) = q(x) \tag{3.19}$$

So $q(x)$ (which could be any polynomial, so long as it interpolates the points) is identical with $p(x)$, and $p(x)$ is unique.

Given the Vandermonde matrix used above to construct the interpolant, we can set up the system (Kaspar and Ray, 1993).

$Va = y$

We want to show that V is nonsingular. Given

$$\det(V) = \prod_{i,j=0, i<j}^{n} (x_i - x_j) \tag{3.20}$$

since the $n+1$ points are distinct, the determinant can't be zero as $x_i - x_j$ is never zero, therefore V is nonsingular and the system has a unique solution.

Either way this means that no matter what method we use to do our interpolation: direct, spline, lagrange etc., (assuming we can do all our calculations perfectly) we will always get the same polynomial.

When interpolating a given function f by a polynomial of degree n at the nodes $x_0,...,x_n$ we get the error:

$$f(x) - p_n(x) = f[x_0, \ldots, x_n, x] \prod_{i=0}^{n} (x - x_i) \tag{3.21}$$

Where $f[x_0, \ldots, x_n, x]$ is the notation for divided differences. When f is $n+1$ times continuously differentiable on the smallest interval I which contains the nodes x_i and x then we can write the error in the Lagrange form as:

$$f(x) - p_n(x) = \frac{f^{(n+1)}(\xi)}{(n+1)!} \prod_{i=0}^{n} (x - x_i) \tag{3.22}$$

for some ξ in *I*. Thus the remainder term in the Lagrange form of the Taylor theorem is a special case of interpolation error when all interpolation nodes x_i are identical.

Lagrange Polynomial:

In numerical analysis, Lagrange polynomials are used for polynomial interpolation. For a given set of distinct points x_j and numbers y_j, the Lagrange polynomial is the polynomial of the least degree that at each point x_j assumes the corresponding value y_j (i.e. the functions coincide at each point). The interpolating polynomial of the least degree is unique, however, and it is therefore more appropriate to discuss of "the Lagrange form" of that unique polynomial rather than "the Lagrange interpolation polynomial," since the same polynomial can be arrived at through multiple methods.

Lagrange interpolation is susceptible to Runge's phenomenon, and the fact that changing the interpolation points requires recalculating the entire interpolant can make Newton polynomials easier to use. Lagrange polynomials are used in the Newton-Cotes method of numerical integration and in Shamir's secret sharing scheme in Cryptography.

Given a set of $k + 1$ data points $(x_0, y_0),\ldots,(x_j, y_j),\ldots(x_k, y_k)$,where no two x_j are the same, **the** interpolation polynomial in the Lagrange form is a linear combination

$$L(x) = \sum_{j=0}^{k} y_j \ell_j(x) \qquad (3.23)$$

of Lagrange basis polynomials:

$$\ell_j(x) = \prod_{0 \le m \le k} \frac{x - x_m}{x_j - x_m} = \frac{(x - x_0)}{(x_j - x_0)} \cdots \frac{(x - x_{j-1})}{(x_j - x_{j-1})} \frac{(x - x_{j+1})}{(x_j - x_{j+1})} \cdots \frac{(x - x_k)}{(x_j - x_k)} \qquad (3.24)$$

Note how, assuming no two x_i are the same (and they can't be, or the data set doesn't make sense), $x_j - x_m \neq 0$, so this expression is always well-defined (Kaspar and Ray, 1993 and Kourti, 2002).

Because $\ell_j(x)$ includes the term ($x - x_i$) in the numerator, it will be zero in the case that $x = x_i$. This ensures that the only basis polynomial which is non-zero at the point $x = x_i$ is $\ell_i(x)$ since only $\ell_i(x)$ will lack the ($x - x_i$) clause. $\ell_i(x)$=1 and hence $y_i \ell_i(x_i) = y_i$ by definition, so at each point x_i, $\ell(x_i) = y_i + 0 + 0 + 0 + \ldots + 0 = y_i$, showing that ℓ interpolates the function exactly.

Function $L(x)$ being sought is a polynomial in x of the least degree that interpolates the given data set; that is, assumes value y_j at the corresponding x_j for all data points j:

$$L(x_j) = y_j \qquad j = 0,\ldots,k \tag{3.25}$$

Observe that:

In $\ell_i(x)$ there are k terms in the product and each term contains one x, so $L(x)$ (which is a sum of these k-degree polynomials) must also be a k-degree polynomial.

$$\ell_j(x_i) = \prod_{m=0, m\neq j}^{k} \frac{x_i - x_m}{x_j - x_m} \tag{3.26}$$

Watch what happens if we expand this product. Because the product skips $m = j$, If $i = j$ then all terms are (Kaspar and Ray, 1993).

$$\frac{x_j - x_m}{x_j - x_m} = 1 \tag{3.27}$$

(Except where $x_j = x_m$ but that case is impossible as pointed out in the definition section---if you tried to write out that term you'd find that $m = j$ and since $m \neq j$, $i \neq j$, contrary to $i = j$). Also if $i \neq j$ then since $m \neq j$ doesn't preclude it, one term in the product **will** be for $m = i$, i.e.

$$\frac{x_i - x_i}{x_j - x_i} = 0 \tag{3.28}$$

, zeroing the entire product. So

$$\ell_j(x_i) = \delta_{ji} = \begin{cases} 1, & if \quad j = i \\ 0, & if \quad j \neq i \end{cases} \tag{3.29}$$

Where δ_{ij} is the Kronecker delta. So:

$$L(x_i) = \sum_{j=0}^{k} y_j \ell_j(x_i) = \sum_{j=0}^{k} y_j \delta_{ji} = y_i. \tag{3.30}$$

Thus the function $L(x)$ is a polynomial with degree at most k and where $L(x_i) = y_i$. Additionally, the interpolating polynomial is unique, as shown by the unisolvence theorem at Polynomial interpolation (Kaspar and Ray, 1993).

Since, there is no simple-to-use predictive tools exist in the literature for rapid estimation of some particular engineering parameters, our efforts directed at formulating novel predictive tools which can be expected to assist engineers for rapid and accurate calculation of these parameters using a novel methodology developed in this work. The proposed novel tools in the present work are simple and unique formulations non-existent in the literature. Furthermore, the selected exponential function to develop the tool leads to well-behaved (i.e. smooth and non-oscillatory) equations enabling fast and more accurate predictions. The developed predictive tools serve two purposes in numerical analysis. First, both to convert a set of highly correlated variables to a set of independent variables by using linear transformations. Secondly, for variable reductions. When a dependent variable for an analysis is specified, this method is very efficient for dimension reduction due to the supervised nature of its methodology. If proposed tool is not as a function of temperature, then the developed tool is an empirical correlation and it is recommended just for a specific range.

3.3 Selection of appropriate variables

As we have indicated in previous sections, presently, some theoretical and semi-theoretical correlations of some properties such as thermal conductivity include other parameters such as density therefore data or correlations of such additional parameters are also required when using these correlations. The bottom-line is that correlations of parameters and in particular

properties should be sought in terms of independent variables such as temperature, pressure, molecular weight, concentration and so on.

3.4 Generalized corresponding states principle (GCSP)

A pure fluid (with critical parameters T_c, P_c, V_c, and molecular weight M) is defined to be in corresponding states with a reference fluid,o, if the compressibility ,Z, and the reduced viscosity ($\eta\xi$) of the two substances at the same reduced temperature T_R and reduced pressure P_R are given by:

$$Z = Z^{(o)} \tag{3.31}$$

$$(\eta\xi) = (\eta\xi)^{(o)} \tag{3.32}$$

Where:

$$\xi = V_c^{2/3} T_c^{-1/2} M^{-1/2} \tag{3.33}$$

Equations 3.31 and 3.32 are strictly valid only for pairs of substances (such as the noble gases) in which the molecules interact with spherically symmetric two-parameter potentials. The resulting statements then describe the two-parameter corresponding states principle and the superscript (o) denotes the properties of a spherical reference substance. In the more general case of nonspherical molecules, Pitzer et al (1955) showed that equation 3.31 can be written as a Taylor series expansion in the acentric factor:

$$Z = Z^{(0)} + \omega Z^{(1)} \tag{3.34}$$

Where $Z^{(o)}$ is the compressibility of a simple fluid with zero acentric factor (i.e., a spherical reference substance) and $Z^{(1)}$ is a complicated deviation function. Letsou and Stiel (1973) later extended this approach to viscosities of liquids by rewriting equation 3.32 in the form:

$$\ln(\eta\xi) = \ln(\eta\xi)^{(0)} + \omega \ln(\eta\xi)^{(1)} \tag{3.35}$$

Lee and Kesler (1975) provided an analytical framework for the three-parameter corresponding states principle by writing equation as:

$$Z = Z^{(0)} + \frac{\omega}{\omega^{(r)}}\left[Z^{(r)} - Z^{(o)}\right] \tag{3.36}$$

Where the compressibility of any fluid of acentric factor ω is expressed in terms of a simple fluid (analytical) equation of state, $Z^{(0)}$ and a (heavy) reference fluid equation of state $Z^{(r)}$. Lee and Kesler (1975), however, retained Pitzer's original proposal of a Taylor series expansion of a thermodynamic property about that property of a simple spherical reference fluid. Then Teja and Rice (1981a, b) have proposed a generalized corresponding states principle (GCSP) for thermodynamic properties which no longer retains the simple spherical fluid as one of the references. Equation 3.36 is written as:

$$Z = Z^{(r1)} + \frac{\omega - \omega}{\omega^{(r2)} - \omega^{(r1)}}\left[Z^{(r2)} - Z^{(r1)}\right] \tag{3.37}$$

Where the superscripts r_1 and r_2 refer to two (nonspherical) reference fluids which are chosen so that they are similar to the pure component of interest or, in the case of mixtures, to the key components of interest. Equation 3.37 provides a method for generalizing equations of state using the known equations of two pure components. Thermodynamic properties can then be predicted with considerable success, as has been shown elsewhere (Teja, 1980; Teja and Sandler, 1980). In an analogous manner, Teja, and Rice, (1981) extended equation 3.18 to viscosities in the work as follows:

$$\ln(\eta\xi) = \ln(\eta\xi)^{(r1)} + \frac{\omega - \omega^{(r1)}}{\omega^{(r2)} - \omega^{(r1)}}\left[\ln(\eta\xi)^{(r2)} - \ln(\eta\xi)^{(r1)}\right] \tag{3.38}$$

Where the superscripts r_1 and r_2 again refer to two (nonspherical) reference fluids.

If one of the references chosen is a simple fluid of zero acentric factor, Eqn. (3.38) reduces to:

$$\ln(\eta\xi) = \ln(\eta\xi)^{(0)} + \frac{\omega}{\omega^{(r)}}\left[\ln(\eta\xi)^{(r)} - \ln(\eta\xi)^{(0)}\right] \tag{3.39}$$

3.4.1 Viscosity of aqueous glycol solutions

Equation 3.20 can be extended to mixtures using the van der Waals one-fluid model to replace T_c, V_c, ω and M of a pure fluid by the pseudocritical properties T_c, V_c, ω *and* M *of* a hypothetical equivalent substance for aqueous glycol solutions. The GCSP method relates the quantities $Z_C V_R$, $\ln(\eta\xi)$,of the mixture to the properties of two reference fluids r_1 and r_2 at the same reduced temperature T_R and reduced pressure P_R as follows:

$$\ln(\eta\xi) = x_1 \ln(\eta\xi)^{(r1)} + x_2 \ln(\eta\xi)^{(r2)} \tag{3.40}$$

In which:

$$\xi = V_C^{2/3} T_C^{-1/2} M^{1/2} \tag{3.41}$$

In the above equations, *Z* is the compressibility and *V* is the volume. The subscript C denotes the critical point, and superscripts r_1 and r_2 denote the properties of two reference fluids. These equations can be extended to mixtures using:

$$V_C = \sum\sum x_i x_j V_{Cij} \tag{3.42}$$

$$T_c V_c = \sum_{ij} \sum x_i x_j T_{cij} V_{cij} \tag{3.43}$$

$$Z_C = \sum x_i Z_{Ci} \tag{3.44}$$

Where subscripts *i* or *ii* denote pure component properties. When ($i \neq j$):

$$V_{Cij} = \left(\frac{1}{8}\right)\left(V_{Ci}^{1/3} + V_{Cj}^{1/3}\right)^3 \theta_{ij} \tag{3.45}$$

$$T_{Cij} V_{Cij} = \left(T_{Cii} T_{Cjj} V_{Ci} V_{Cj}\right)^{1/2} \psi_{ij} \tag{3.46}$$

θ_{ij} and ψ_{ij} are binary interaction parameters which must be obtained by fitting experimental data. Critical properties (experimental or estimated values) of pure glycols and water required in the calculations were obtained from the literature (Rowley, et al 2002).

3.4.2 Density of aqueous glycol solutions

The principle which is extended in this study was originally proposed by Pitzer et al. (1955) who showed that the compressibility factor (expressed as a function of reduced temperature and reduced pressure) can be written as a linear function of the acentric factor as:

$$Z = Z^{(0)} + \omega Z^{(1)} \tag{3.47}$$

Where $Z^{(0)}$ is the compressibility factor of a simple fluid with zero acentric factor at the same reduced conditions and $Z^{(1)}$ is a complicated deviation function. Other thermodynamic properties can be written in a similar way. Lee and Kesler (1975) showed that Equationn (3.47) can also be written as:

$$Z = Z^{(0)} + \frac{\omega}{\omega^{(r)}}\left(Z^{(r)} - Z^{(0)}\right) \tag{3.48}$$

Where the compressibility of any fluid of acentric factor ω is expressed in terms of a simple fluid contribution $Z^{(0)}$ and a reference fluid contribution Z^{r}. Lee and Kesler used the properties of (mainly) argon to obtain an analytic equation for the simple fluid and the properties of (mainly) n-octane to obtain an equation for the reference fluid. The Lee-Kesler (1975) correlation is accurate for the estimation of the thermodynamic properties of nonpolar fluids (Reid et al. 1977) and has been expressed in terms of saturated volumes by Lin and Daubert (1979) as follows:

$$\frac{V}{\left(\frac{RT_c}{P_c}\right)} = V_R^{(0)} + \frac{\omega}{\omega^{(r)}}\left(V_R^{(r)} - V_R^{(0)}\right) \tag{3.49}$$

Both Equations (3.48) and (3.49) retain Pitzer's original proposal of a Taylor series expansion of *a* thermodynamic function about the properties of a simple reference fluid of zero acentric factor. The new equation proposed here no longer retains the simple fluid as one of the references. Equation (3.49) is rewritten as:

$$\frac{V}{\left(\frac{RT_c}{P_c}\right)} = \frac{V^{(r1)}}{\frac{RT_c^{r1}}{P_c^{r1}}} + \frac{\omega - \omega^{(r1)}}{\omega^{(r2)} - \omega^{(r1)}}\left[\frac{V^{(r2)}}{\frac{RT_c^{(r2)}}{P_c^{(r2)}}} - \frac{V^{(r1)}}{\frac{RT_c^{(r1)}}{P_c^{(r1)}}}\right] \tag{3.50}$$

Where the superscripts r_1 and r_2 refer to two reference fluids which are chosen so that they are similar to the pure component of interest or, in the case of mixtures, to the key components of interest. If one of the references chosen is a simple fluid of zero acentric factor, Equation. (3.50) reduces to:

$$\frac{V}{\left(\frac{RT_c}{P_c}\right)} = \frac{V^{(0)}}{\frac{RT_c^{(0)}}{P_c^{(0)}}} + \frac{\omega}{\omega^{(r)}}\left[\frac{V^{(r)}}{\frac{RT_c^{(r)}}{P_c^{(r)}}} - \frac{V^{(0)}}{\frac{RT_c^{(0)}}{P_c^{(0)}}}\right] \tag{3.51}$$

Or

$$Z_c V_R = Z_C^{(0)} V_R^{(0)} + \frac{\omega}{\omega^{(r)}}\left(Z_c^{(r)} V_R^{(r)} - Z_c^{0} V_R^{0}\right) \tag{3.52}$$

Equation 3.52 can be extended to mixtures using the van der Waals one-fluid model to replace T_c, V_c ω and M of a pure fluid by the pseudocritical properties T_c, V_c, ω *and* M *of* a hypothetical equivalent substance for aqueous glycol solutions. The GCSP method relates the quantity $Z_C V_R$, of the mixture to the properties of two reference fluids r_1 and r_2 at the same reduced temperature T_R and reduced pressure P_R as follows:

$$Z_C V_R = x_1 \left(Z_c V_R\right)^{(r1)} + x_2 \left(Z_c V_R\right)^{(r2)} \tag{3.53}$$

In the above equations, *Z* is the compressibility and *V* is the volume. The subscript C denotes the critical point, and superscripts r_1 and r_2 denote the properties of two reference fluids. These equations can be extended to mixtures using:

$$V_C = \sum\sum x_i x_j V_{Cij} \tag{3.54}$$

$$T_c V_c = \sum_{ij} \sum x_i x_j T_{cij} V_{cij} \tag{3.55}$$

$$Z_C = \sum x_i Z_{Ci} \tag{3.56}$$

Where subscripts *i* or *ii* denote pure component properties. When ($i \neq j$):

$$V_{Cij} = \left(\frac{1}{8}\right)\left(V_{Ci}^{1/3} + V_{Cj}^{1/3}\right)^3 \theta_{ij} \tag{3.57}$$

$$T_{Cij} V_{Cij} = \left(T_{Cii} T_{Cjj} V_{Ci} V_{Cj}\right)^{1/2} \psi_{ij} \tag{3.58}$$

θ_{ij} and ψ_{ij} are binary interaction parameters which must be obtained by fitting experimental data. Critical properties (experimental or estimated values) of pure glycols and water required in the calculations were obtained from the literature (Rowley, et al 2002).

CHAPTER 4

Experimental validation of modeling and predictive tools

In order to validate the proposed Arrhenius-type predictive tool with an available rigorous thermodynamic model, the density and viscosity of aqueous ethylene glycol, aqueous diethylene glycol, and aqueous triethylene glycol mixtures are measured at temperatures ranging from 290 K to 380 K with concentrations ranging from 25 mol % glycol to 100 mol % glycol. Aqueous glycol solutions have widespread applications in the manufacture of solvents, natural gas industries, hygroscopic agents, lubricants, and conditioning agents. Accurate knowledge of their properties is therefore essential in process calculations involving these mixtures.

Despite this need, literature data on density, viscosity, glycol and water mixtures are generally limited and have to be verified before using models. (Tsierkezos, and Molinou, 1998, Lee and Hong 1990, Bohne et al 1984, Obermeier et al 1985 and Riddick et al 1986). The density and viscosity of aqueous ethylene glycol, aqueous diethylene and aqueous triethylene glycol mixtures were measured at temperatures ranging from 290 K to 450 K with concentrations ranging from 25 mol % glycol to 100 mol % glycol. Our new experimental data were correlated using proposed Arrhenius based predictive tool and a rigorous thermodynamical model (the generalized corresponding states principle (GCSP)).

4.1. Measurement of density and viscosity of aqueous glycol solutions in a wide temperature range.

Reagent grade ethylene glycol (EG), diethylene glycol (DEG), and triethylene glycol (TEG) were purchased from Sigma-Aldrich Pty. Ltd, Australia (12 Anella Avenue Castle Hill NSW 2154, Australia) and used in the experiments without further purification. The stated minimum purity of these reagents was 99.9 mol %, 99.1 mol %, and 99.2 mol %, respectively. Glycol and water mixtures were prepared gravimetrically using double distilled water. Densities and viscosities of the mixtures were measured using a densitometer and viscometer.

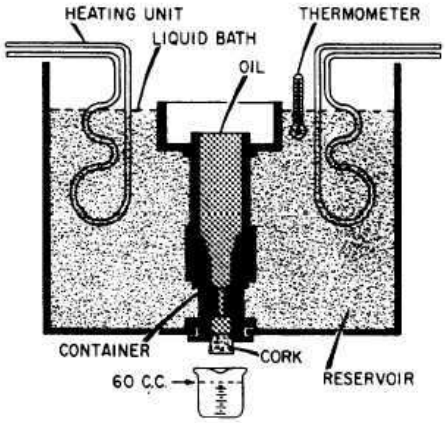

Figure 4.1: Schematic of viscometer

Figure 4.1 shows the viscometer which was used to measure the fluid's kinematic viscosity. The Saybolt viscometer measures the time in seconds required for the tested fluid to flow through the capillary. The time is then multiplied by the temperature constant of the viscometer in use to provide the viscosity expressed in centistokes.

The viscometer calibration was validated by measurement of the viscosity of some liquids. Measured viscosities were reproducible to 1%, and the uncertainty was estimated to be 2% as well as its uncertainty was estimated to be 0.1 K.

The densitometer provides unparalleled ease of use and state-of-the-art digital density measurement. Among the DMA 4100 M density meter's numerous applications are used in industrial quality control, in research, at authorities and at standards organizations. The density check function allows the user either to check the validity of the factory adjustment after transport or the validity of user adjustments. To check the factory adjustment, pure water is used as calibration fluid. To check our own adjustments, either degasses bi-distilled water or different density calibration fluids or standardized samples can be used. The density check should be performed once every day before doing the experiment. The reproducibility of the density measurements was (0.1%). In order to measure the density, the following flow-chart has been applied:

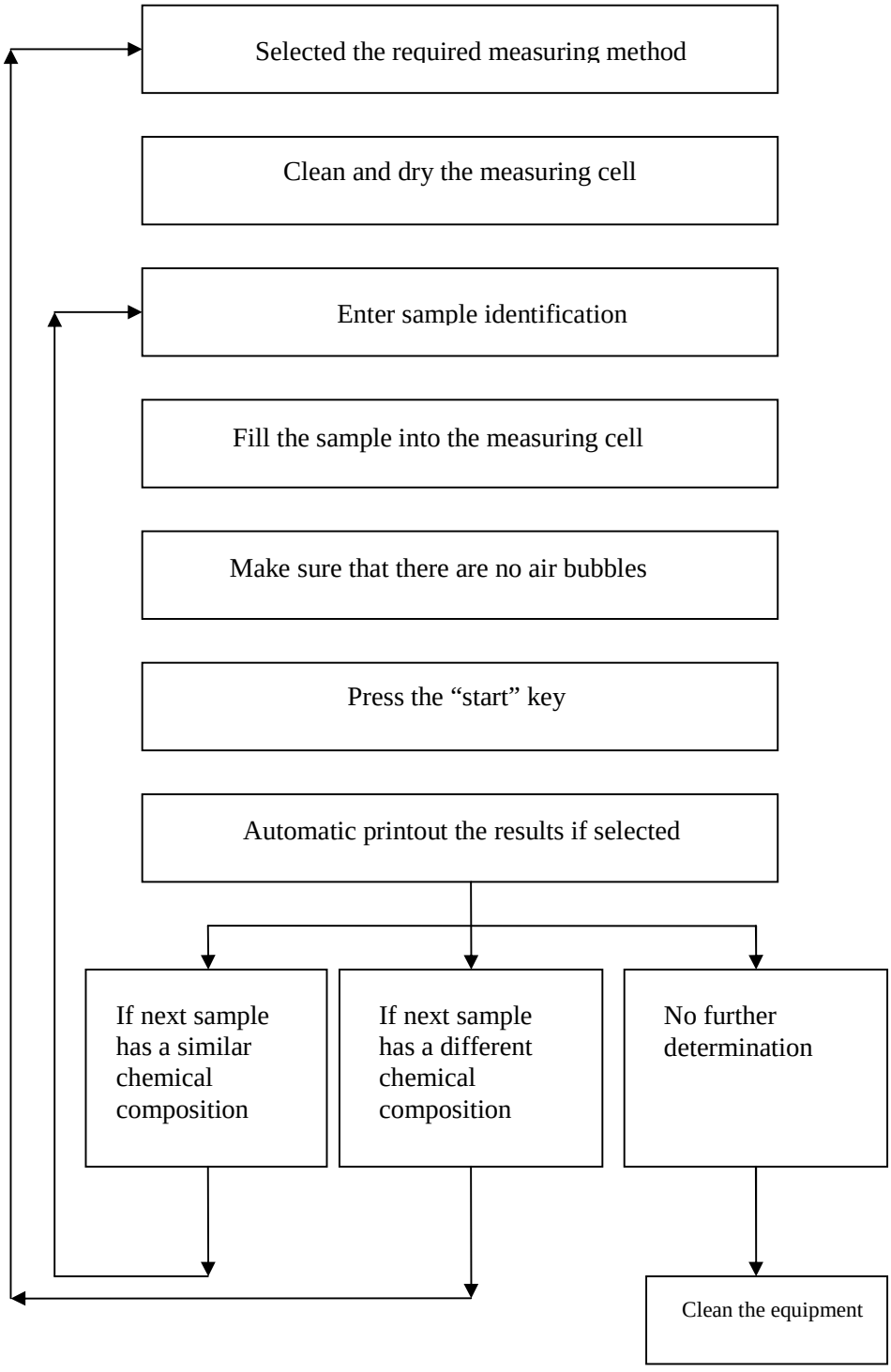

Figure 4.2: Measurement procedure

4.2 Viscosity and Density of Aqueous Glycol solutions

As previously mentioned in chapter 3, equation 4.1 can be extended to mixtures using the van der Waals one-fluid model to replace T_c, V_c , ω and M of a pure fluid by the pseudocritical properties T_c, V_c, ω *and* M *of* a hypothetical equivalent substance for aqueous glycol solutions. The GCSP method relates the quantities $Z_C V_R$, ln($\eta\xi$),of the mixture to the properties of two reference fluids r1 and r2 at the same reduced temperature T_R and reduced pressure P_R as follows:

$$Z = Z^{(r1)} + \frac{\omega - \omega}{\omega^{(r2)} - \omega^{(r1)}}\left[Z^{(r2)} - Z^{(r1)}\right] \tag{4.1}$$

$$\ln(\eta\xi) = x_1 \ln(\eta\xi)^{(r1)} + x_2 \ln(\eta\xi)^{(r2)} \tag{4.2}$$

$$Z_C V_R = x_1 (Z_c V_R)^{(r1)} + x_2 (Z_c V_R)^{(r2)} \tag{4.3}$$

In which:

$$\xi = V_C^{2/3} T_C^{-1/2} M^{1/2} \tag{4.4}$$

In the above equations, *Z* is the compressibility and *V* is the volume. The subscript C denotes the critical point, and superscripts r1 and r2 denote the properties of two reference fluids. These equations can be extended to mixtures using:

$$V_C = \sum\sum x_i x_j V_{Cij} \tag{4.5}$$

$$T_c V_c = \sum_{ij}\sum x_i x_j T_{cij} V_{cij} \tag{4.6}$$

$$Z_C = \sum x_i Z_{Ci} \tag{4.7}$$

Where subscripts *i* or *ii* denote pure component properties. When ($i \neq j$):

$$V_{Cij} = \left(\frac{1}{8}\right)\left(V_{Ci}^{1/3} + V_{Cj}^{1/3}\right)^3 \theta_{ij} \tag{4.8}$$

$$T_{Cij}V_{Cij} = \left(T_{Cii}T_{Cjj}V_{Ci}V_{Cj}\right)^{1/2}\psi_{ij} \tag{4.9}$$

θ_{ij} and ψ_{ij} are binary interaction parameters which must be obtained by fitting experimental data. Critical properties (experimental or estimated values) of pure glycols and water required in the calculations were obtained from the literature (Rowley, et al 2002). Binary interaction coefficients were determined using the Generalized Corresponding States Principle (GCSP). The results demonstrate that it is possible to correlate all data within experimental uncertainty using adjustable parameters per binary system for each property.

4.3 Arrhenius-type exponential functions

The Arrhenius-type exponential functions can provide simple and accurate correlations for various properties of fluids; this approach for developing correlations is verified by numerous new experimental data reported in this research. It is demonstrated that the present approach yields a mathematically simple correlation.

In brief, equations 4-10 to 4-13 present the new developed correlation for $\ln f$ (density and viscosity, of aqueous ethylene glycol, aqueous diethylene glycol, and aqueous triethylene glycol mixtures) as a function of temperature (T) and glycol fraction in liquid phase (x).

$$\ln f = \mathrm{a} + \frac{b}{T} + \frac{c}{T^2} \tag{4.10}$$

Where:

$$a = A_1 + \frac{B_1}{x} + \frac{C_1}{x^2} + \frac{D_1}{x^3} \quad (4.11)$$

$$b = A_2 + \frac{B_2}{x} + \frac{C_2}{x^2} + \frac{D_2}{x^3} \quad (4.12)$$

$$c = A_3 + \frac{B_3}{x} + \frac{C_3}{x^2} + \frac{D_3}{x^3} \quad (4.13)$$

The unknown coefficients "a", "b" and "c" can be obtained by solving the above equations 4.11 to 4.13.

In brief, the following steps are repeated to tune the correlation's coefficients using Vandermonde matrix:

1. Correlate "$\ln f$ "as a function of temperature (T) for a given glycol fraction in aqueous liquid phase (x).
2. Repeat step 1 for other glycol fractions in aqueous liquid phase (x).
3. Correlate corresponding polynomial coefficients, which were obtained for different temperature versus glycol fractions in aqueous liquid phase (x), a = f (x), b = f (x), c = f (x), d = f (x) [see equations (4.11)-(4.13)].

Equation 4.10 represents the proposed governing equation in which four equations [equations (4.11)-(4.13)] are used to correlate $\ln f$ as a function of temperature and pressure wherein the relevant coefficients have been reported in tables 4.1 and 4.2 for viscosity and density of aqueous glycol solutions respectively. Figures 4.2, 4.3 and 4.4 show the calculated densities of aqueous ethylene glycol, diethylene glycol and triethylene glycol mixture using Arrhenius-type predictive tool respectively. Figures 4.5, 4.6 and 4.7 illustrate the results for the prediction of the viscosity of the same aqueous glycol solutions.

Figures 4.8 and 4.9 illustrate the accuracy of proposed Arrhenius-type predictive tool for prediction of density and viscosity of aqueous glycol solutions in comparison with Generalized Corresponding States Principle (GCSP) respectively. Tables 4-3 to 4-8 illustrate the experimental data and the accuracy of Arrhenius based predictive tool.

Table 4.9 and 4.10 show GCSP correlations' accuracy for prediction of density and viscosity for glycol and water mixtures.

Table 4.1: Tuned coefficients used in Equations 4.11 to 4.13 for viscosity of aqueous glycol solutions

Symbol	Ethylene Glycol	Diethylene Glycol	Triethylene Glycol
A_1	-1.2569	7.7265×10^{-2}	-8.2290×10^{-1}
B_1	-2.8422×10^{-1}	-2.5049×10^{-1}	7.6427×10^{-1}
C_1	1.5372×10^{-2}	5.5911×10^{-2}	-1.3363×10^{-1}
D_1	-1.2874×10^{-4}	-5.3131×10^{-4}	1.2566×10^{-3}
A_2	-1.1935×10^{3}	-2.0143×10^{3}	-1.2178×10^{3}
B_2	1.9189×10^{2}	1.9112×10^{1}	-7.7256×10^{2}
C_2	-1.1723×10^{1}	-8.2201	1.2884×10^{2}
D_2	1.0013×10^{-1}	7.8363×10^{-2}	-1.2097
A_3	8.2430×10^{5}	9.4439×10^{5}	7.7644×10^{5}
B_3	-1.5307×10^{5}	-3.7994×10^{4}	1.4667×10^{5}
C_3	1.7625×10^{4}	1.0671×10^{3}	-2.8649×10^{4}
D_3	-1.6164×10^{2}	-6.8869	2.7137×10^{2}

Table 4.2: Tuned coefficients used in Equations 4.11 to 4.13 for density of aqueous glycol solutions

Symbol	Ethylene Glycol	Diethylene Glycol	Triethylene Glycol
A_1	6.3636	6.3867	6.3391
B_1	-5.2894×10^{-2}	-4.9003×10^{-2}	-2.7353×10^{-2}
C_1	2.3957×10^{-3}	2.0356×10^{-3}	2.7412×10^{-4}
D_1	-1.9112×10^{-5}	-1.5917×10^{-5}	-4.0472×10^{-7}
A_2	3.4637×10^{2}	3.3051×10^{2}	3.6600×10^{2}
B_2	2.6284×10^{1}	2.719×10^{1}	1.2583×10^{1}
C_2	-1.2789	-1.4166	-2.0580×10^{-1}
D_2	1.0342×10^{-2}	1.1642×10^{-2}	9.5432×10^{-4}
A_3	-4.4175×10^{4}	-4.2127×10^{4}	-4.8130×10^{4}
B_3	-4.6056×10^{3}	-4.1037×10^{3}	-1.3937×10^{3}
C_3	2.2008×10^{2}	1.7799×10^{2}	-5.7512×10^{1}
D_3	-1.7712	-1.4022	6.8829×10^{-1}

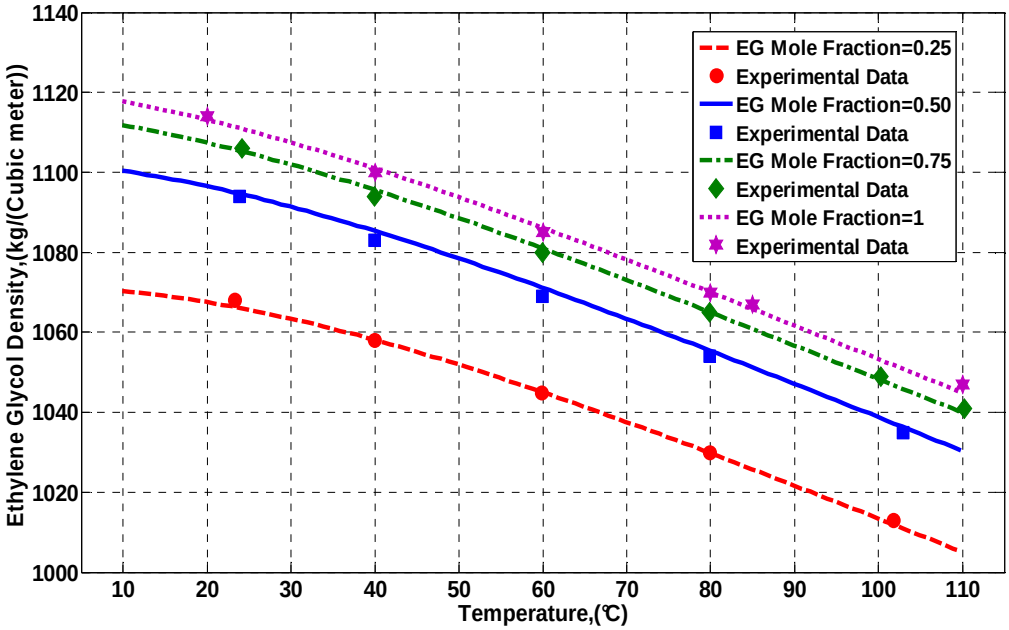

Figure 4.3: Prediction of density of aqueous ethylene glycol mixture using Arrhenius-type predictive tool (Bahadori, A. and Vuthaluru H. B. (2009i) *Journal of the Energy Institute* 82 (4), pp. 218-222)

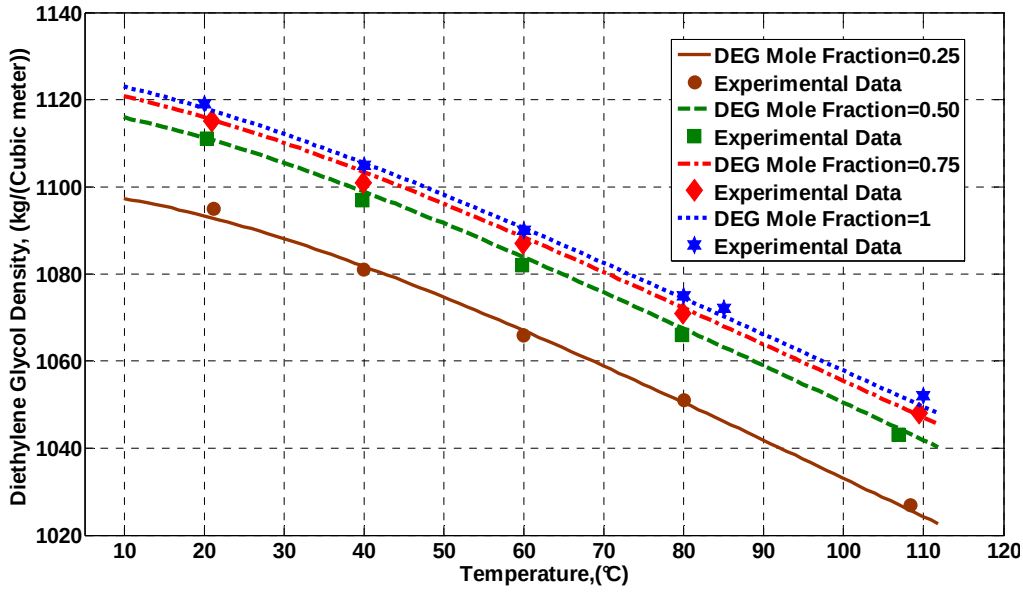

Figure 4.4: Prediction of density of aqueous diethylene glycol mixture using Arrhenius-type predictive tool (Bahadori, A. and Vuthaluru H. B. (2009i) *Journal of the Energy Institute* 82 (4), pp. 218-222)

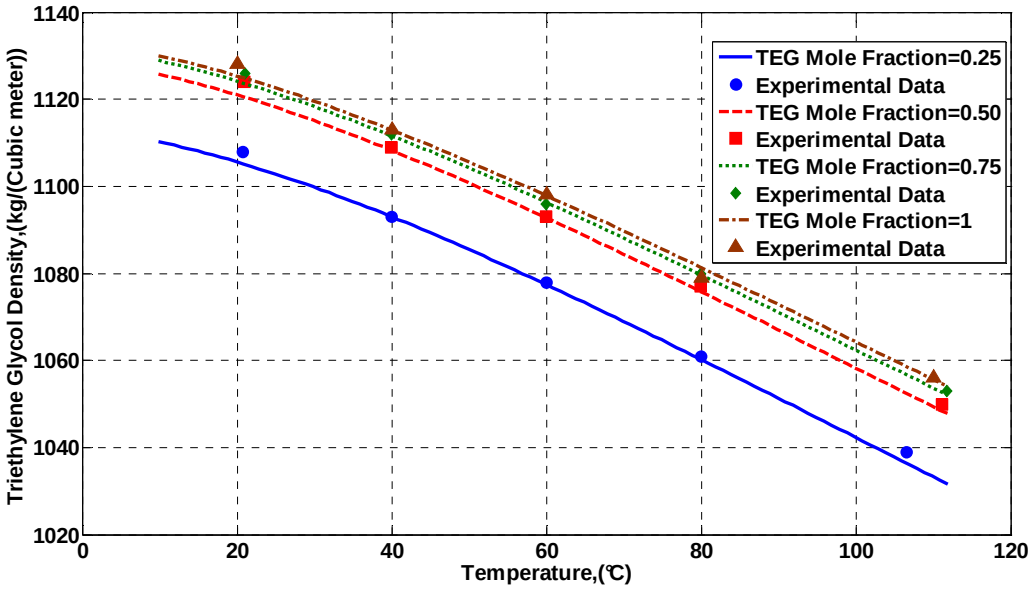

Figure 4.5: Prediction of density of aqueous triethylene glycol mixture using Arrhenius-type predictive tool (Bahadori, A. and Vuthaluru H. B. (2009i) *Journal of the Energy Institute* 82 (4), pp. 218-222)

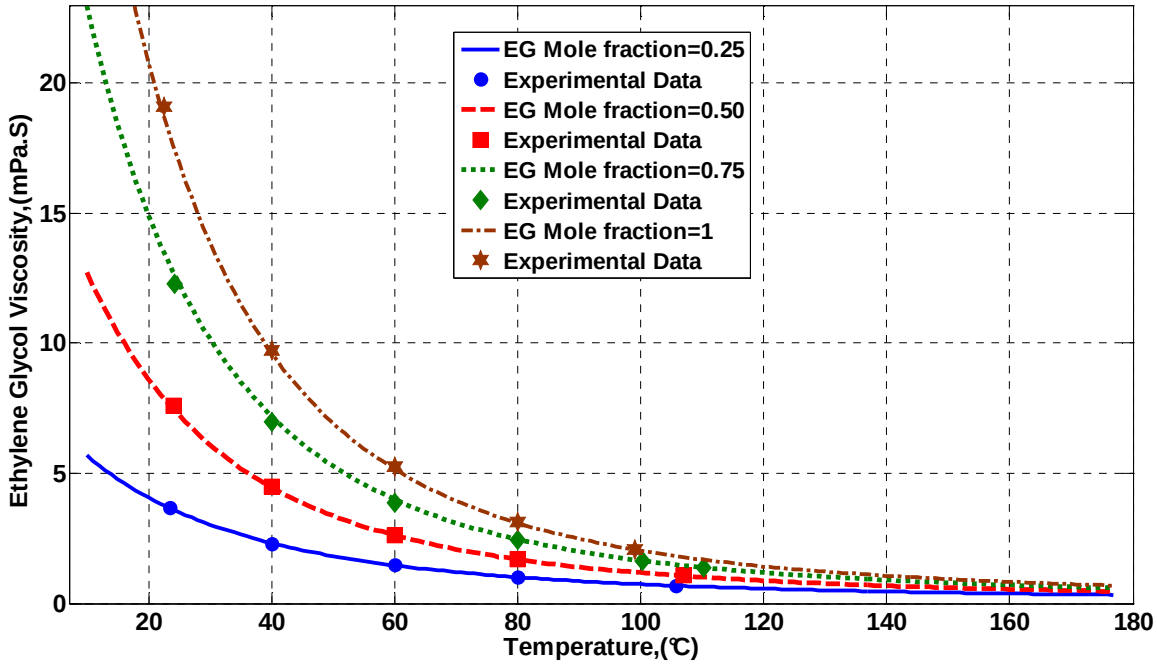

Figure 4.6: Prediction of viscosity of aqueous ethylene glycol mixture using Arrhenius-type predictive tool (Bahadori, A. and Vuthaluru H. B. (2009i) *Journal of the Energy Institute* 82 (4), pp. 218-222)

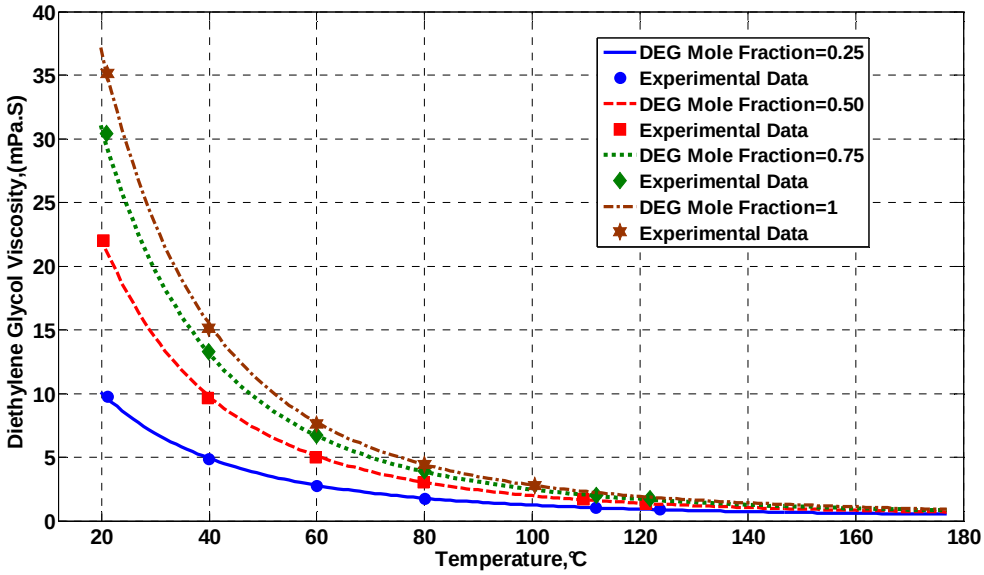

Figure 4.7: Prediction of viscosity of aqueous diethylene glycol mixture using Arrhenius-type predictive tool (Bahadori, A. and Vuthaluru H. B. (2009i) *Journal of the Energy Institute* 82 (4), pp. 218-222)

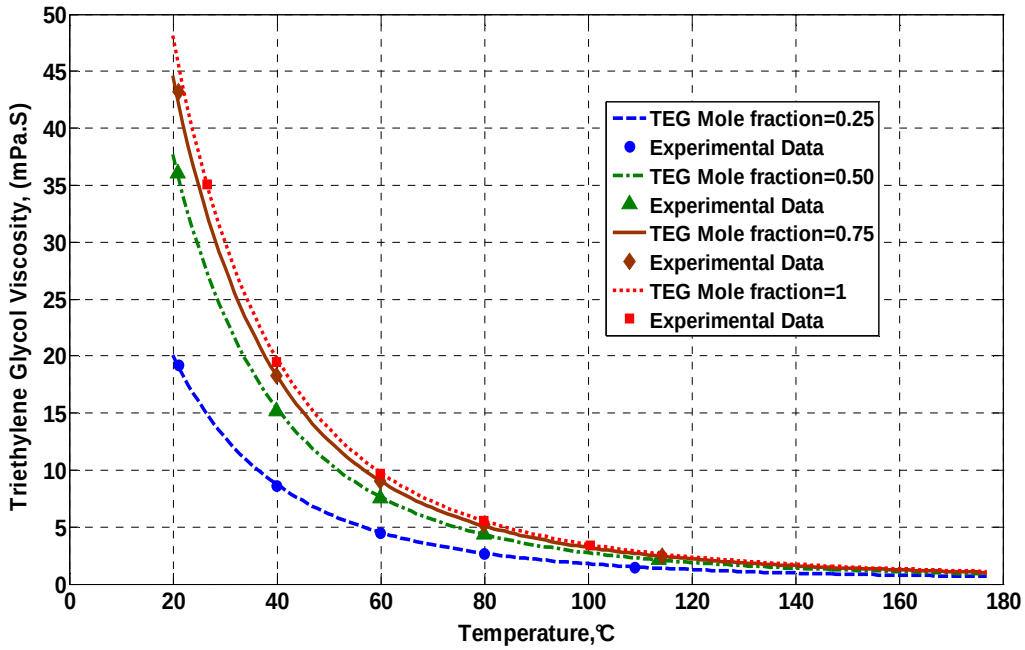

Figure 4.8: Prediction of viscosity of aqueous trirthylene glycol mixture using Arrhenius-type predictive tool (Bahadori, A. and Vuthaluru H. B. (2009i) *Journal of the Energy Institute* 82 (4), pp. 218-222)

Table 4.3: Experiment results for density of ethylene glycol

Mole Fraction of ethylene glycol	Temperature, K	Experimental Density, $\frac{kg}{m^3}$	Calculated Density, $\frac{kg}{m^3}$	Absolute Deviation Percent
0.25	296.4	1067	1066	0.06
0.25	313.05	1058	1058	0.01
0.25	333.05	1045	1045	0.004
0.25	353.05	1030	1029	0.02
0.25	374.85	1012	1011	0.004
0.50	297.05	1095	1094	0.03
0.50	313.05	1084	1085	0.12
0.50	333.1	1070	1071	0.11
0.50	353.05	1055	1055	0.03
0.50	376.05	1036	1036	0.03
0.75	297.35	1105	1105	0.02
0.75	313.05	1095	1095	0.06
0.75	333.1	1081	1081	0.003
0.75	353.05	1065	1065	0.003
0.75	373.45	1048	1048	0.003
1	293.15	1113	1113	0.01
1	313.15	1101	1100	0.006
1	333.15	1086	1086	0.01
1	353.15	1070	1069	0.0009
1	358.15	1066	1065	0.01
Average Absolute Deviation Percent				0.027

Table 4.4: Experiment results for density of diethylene glycol

Mole fraction of diethylene glycol	Temperature, K	Experimental Density, $\frac{kg}{m^3}$	Calculated Density, $\frac{kg}{m^3}$	Absolute Deviation Percent
0.25	294.25	1093	1092	0.02
0.25	313.05	1082	1081	0.02
0.25	333.05	1067	1067	0
0.25	353.15	1050	1050	0.03
0.25	381.45	1026	1025	0.03
0.50	293.45	1111	1111	0.005
0.50	312.95	1098	1098	0.087
0.50	332.95	1083	1083	0.087
0.50	352.95	1067	1067	0.05
0.50	380.05	1044	1044	0.045
0.75	294.05	1115	1115	0.039
0.75	313.05	1102	1103	0.13
0.75	333.05	1088	1088	0.04
0.75	353.05	1072	1072	0.02
0.75	382.55	1047	1047	0.048
1	293.15	1118	1118	0.002
1	313.15	1105	1105	0.036
1	333.15	1090	1090	0.04
1	353.15	1074	1074	0.031
1	358.15	1071	1070	0.07
1	383.15	1051	1049	0.15
Average Absolute Deviation Percent				0.046

Table 4.5: Experiment results for density of Triethylene glycol

Mole Fraction of triethylene glycol	Temperature, K	Experimental Density, $\frac{kg}{m^3}$	Calculated Density, $\frac{kg}{m^3}$	Absolute Deviation Percent
0.25	293.85	1107	1105	0.16
0.25	313.05	1093	1093	0.006
0.25	333.05	1079	1080	0.118
0.25	353.05	1061	1060	0.067
0.25	379.65	1038	1036	0.15
0.50	294.05	1122	1120	0.13
0.50	313.05	1109	1108	0.06
0.50	333.05	1093	1092	0.016
0.50	353.05	1076	1075	0.013
0.50	384.25	1049	1048	0.057
0.75	294.15	1125	1123	0.12
0.75	313.05	1112	1111	0.029
0.75	333.05	1096	1096	0.038
0.75	353.05	1080	1079	0.025
0.75	384.95	1052	1052	0.01
1	293.15	1126	1125	0.059
1	313.25	1113	1112	0.01
1	333.15	1098	1097	0.014
1	353.15	1080	1081	0.12
1	383.15	1056	1055	0.03
Average Absolute Deviation Percent				0.06

Table 4.6: Experiment results for viscosity of ethylene glycol

Mole Fraction of ethylene glycol	Temperature, K	Experimental Viscosity, mPa.S	Calculated Viscosity, mPa.S	Absolute Deviation Percent
0.25	296.45	3.67	3.66	0.27
0.25	313.05	2.30	2.31	0.43
0.25	333.05	1.47	1.46	0.68
0.25	353.05	0.99	1.00	1.01
0.25	378.85	0.68	0.67	1.47
0.50	297.05	7.51	7.46	0.66
0.50	313.05	4.46	4.45	0.22
0.50	333.1	2.62	2.61	0.38
0.50	353.05	1.69	1.68	0.59
0.50	380.05	1.07	1.05	1.86
0.75	297.35	12.3	12.5	1.62
0.75	313.05	6.99	7.20	3
0.75	333.1	3.89	3.98	2.26
0.75	353.05	2.43	2.46	1.23
0.75	373.45	1.62	1.63	0.61
1	295.55	19.0	18.7	1.57
1	313.05	9.70	9.62	0.82
1	333.1	5.22	5.15	1.34
1	353.05	3.11	3.09	0.64
1	372.15	2.06	2.06	0
Average Absolute Deviation Percent				1.03

Table 4.7: Experiment results for viscosity of diethylene glycol

Mole Fraction of diethylene glycol	Temperature, K	Experimental Viscosity, mPa.S	Calculated Viscosity, mPa.S	Absolute Deviation Percent
0.25	294.25	9.69	9.62	0.72
0.25	313.05	4.89	4.93	0.81
0.25	333.05	2.78	2.80	0.71
0.25	353.15	1.76	1.78	1.13
0.25	384.95	1.03	1.03	0
0.50	293.45	22	21.8	0.9
0.50	312.95	9.74	9.85	1.12
0.50	332.95	5.07	5.13	1.18
0.50	352.95	3.02	3.03	0.33
0.50	382.55	1.66	1.66	0
0.75	294.05	30.3	29.56	2.44
0.75	313.05	13.3	13.20	0.75
0.75	333.05	6.70	6.68	0.29
0.75	353.05	3.9	3.86	1.02
0.75	385.05	2	1.97	1.5
1	294.2	35.1	35.05	0.14
1	313.05	15.2	15.52	2.10
1	333.05	7.64	7.75	1.43
1	353.05	4.41	4.42	0.22
1	373.6	2.76	2.77	0.36
Average Absolute Deviation Percent				0.86

Table 4.8: Experiment results for viscosity of triethylene glycol

Mole Fraction of triethylene glycol	Temperature, K	Experimental Viscosity, mPa.S	Calculated Viscosity, mPa.S	Absolute Deviation Percent
0.25	294.25	19.05	18.95	0.52
0.25	313.05	8.68	8.74	0.69
0.25	333.05	4.53	4.54	0.22
0.25	353.05	2.7	2.69	0.37
0.25	382.15	1.5	1.50	0
0.50	294.05	36	35.76	0.66
0.50	313.05	15.2	15.47	1.77
0.50	333.05	7.58	7.64	0.79
0.50	353.05	4.33	4.34	0.23
0.50	386.75	2.09	2.10	0.47
0.75	294.15	43.2	42.1	2.54
0.75	313.05	18.3	18.3	0
0.75	333.05	9.04	9.03	0.11
0.75	353.05	5.19	5.10	1.76
0.75	387.45	2.41	2.41	0
1	299.65	35.1	35.0	0.28
1	313.05	19.5	19.8	1.53
1	333.1	9.66	9.78	1.24
1	353.05	5.55	5.53	0.36
1	373.5	3.41	3.43	0.58
Average Absolute Deviation Percent				0.706

Table 4.9: GCSP correlations of density for glycol + water mixtures

System	Number of data points	Average Absolute Deviation Percent
Ethylene Glycol + Water	20	0.08
Diethylene Glycol + Water	21	0.11
Triethylene Glycol + Water	20	0.11

Table 4.10: GCSP correlations accuracy for prediction of viscosity for glycol + water mixtures

System	Number of data points	Average Absolute Deviation Percent
Ethylene Glycol + Water	20	2.07
Diethylene Glycol + Water	20	1.86
Triethylene Glycol + Water	20	3.16

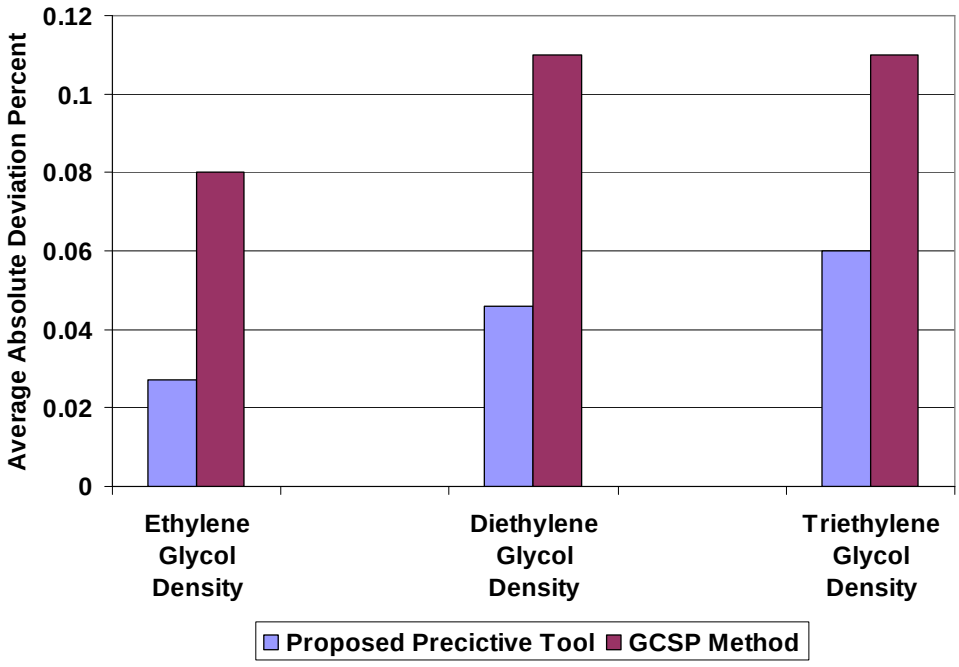

Figure 4.9: Accuracy of proposed Arrhenius-type predictive tool for prediction of density of aqueous glycol solutions in comparison with Generalized Corresponding States Principle (GCSP)

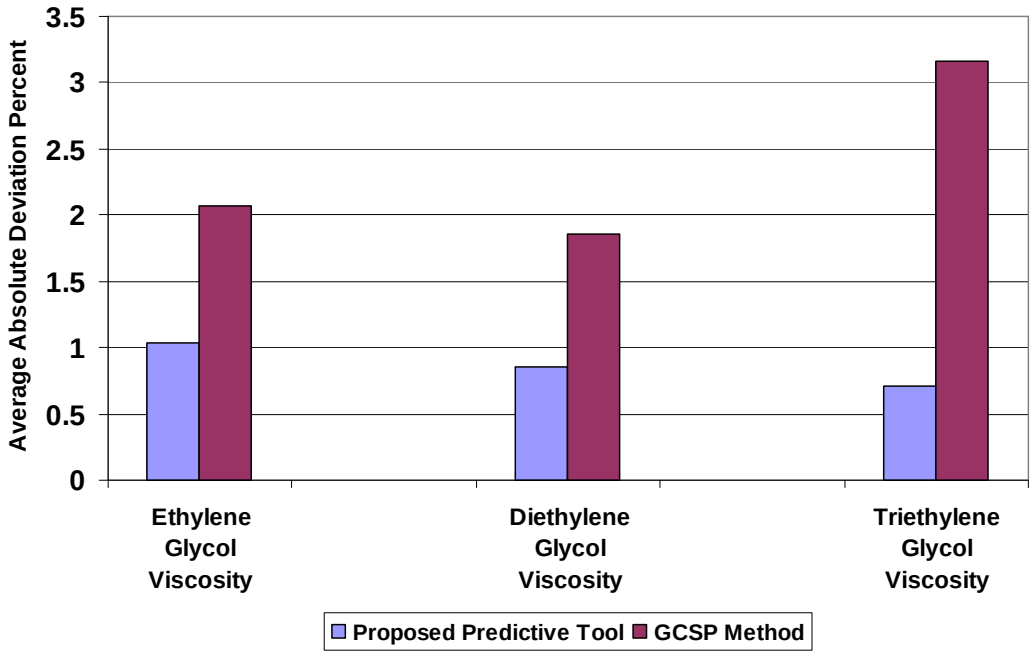

Figure 4.10: Accuracy of proposed Arrhenius-type predictive tool for prediction of viscosity of aqueous glycol solutions in comparison with Generalized Corresponding States Principle (GCSP)

CHAPTER 5

Development of Predictive Tools, Testing and Validation for Oil and Gas Industries Applications

In this chapter accurate and reliable predictive tools are developed and formulated to predict the following selected oil and gas engineering parameters.

- Methanol loss in condensate phase during gas hydrate inhibition
- Physical properties of aqueous methanol solutions
- Hydrate forming condition of natural gases
- Hydrocarbons solubilities in hydrate inhibitors
- Methanol vaporization loss during gas hydrate inhibition
- Aqueous solubility of light alkanes in water
- Water content of sour natural gases
- Natural gases water content
- Sizing of absorbers for TEG gas dehydration systems
- Water-adsorption isotherms for molecular sieves
- Equilibrium water dew point of natural gas in TEG dehydration systems
- Displacement losses from storage containers
- Storage pressure of volatile hydrocarbons
- Molten sulfur viscosity
- Correlating theoretical stages and operating reflux in fractionators
- Surface tension of paraffin hydrocarbons
- Thermal conductivity of liquid paraffin hydrocarbons
- Downcomer velocity and vapour capacity factor in fractionators
- Estimation of packed column size
- Determination of well placement and breakthrough time in horizontal wells
- Determination of the time to water cone breakthrough in horizontal oil wells

Table 5.1 summarizes the list of selected engineering parameters, independent variables and the accuracy of the developed predictive tools in terms of average absolute deviation percent.

Table 5.1: List of selected parameters, independent variables and the accuracy of method

Engineering Parameter (f)	Independent variable (X)	Independent variable (Y)	Accuracy in terms of Average absolute deviation percent
Methanol loss in hydrocarbon liquid phase, mole fraction in condensate phase	Temperature, K	Methanol mass fraction in aqueous phase	2.2
Density of aqueous methanol solution, kg/m^3	Temperature, K	Methanol mass fraction in aqueous phase	1.4
Vapour pressure of aqueous methanol solution, kPa	Temperature, K	Methanol mass fraction in aqueous phase	2.8
Hydrate formation pressure, kPa	Temperature, K	Molecular weight	1.6
Hydrate formation temperature, K	Pressure, kPa	Molecular weight	2.3
Solubility of light alkanes in hydrate inhibitors, mole fraction	Reduced pressure	Reduced temperature	2.7
The ratio of methanol vapour composition to methanol liquid composition	Pressure, kPa	Temperature, K	2.9
Aqueous solubility of light alkanes	Reduced pressure	Reduced temperature	2.2
Water content, mg/m^3 (First method)	Pressure, kPa	Temperature, K	0.8
Water content, mg/m^3 (second method)	Pressure, kPa	Temperature, K	1.8
water removal efficiency	TEG circulation rate, $\frac{TEG, m^3}{kg\,Water}$	Triethylene glycol purity, Mass fraction	0.9
Water adsorbed on activated adsorbent	Partial pressure of water in kPa	Temperature, K	1.9
water dew point (Td) of natural gas stream, K	Temperature, K	TEG purity (weight percent)	2.3
True vapour pressure, kPa (abs	Temperature, K (263 K - 373 K)	Reid vapour pressure, kPa up to 400 kPa (g)	2.8
LPG Vapour pressure, kPa	Temperature, (K) (240K	Propane volume percent	2.9

(abs)	-315 K)	up to 100%	
Filling losses from storage containers in percent of liquid pumped	working pressure in KPa (abs) up to 250 kPa(abs)	vapour pressure at liquid temperature less than 100 kPa (abs).	2.2
Prediction of Storage Pressure of volatile hydrocarbons	True vapour pressure, kPa	Liquid temperature, K	1.3
Viscosity of liquid sulfur	Pressure, kPa	Temperature, K	1.1
operating reflux ratio	ratio of minimum stages to theoretical stages	minimum reflux ratio	1.5
Surface tension, mN/m	Temperature, K	Molecular weight	1.8
Thermal conductivity in W/(m.°C)	Temperature, K	Molecular weight	1.9
Vapor capacity factor, corrected, m/s	Vapor density, kg/ m^3	Tray spacing, m	2.1
Downcomer velocity (uncorrected), $m^3/hr/m^2$	Liquid and vapour density difference, kg/ m^3	Tray spacing, m	2.2
"Y" dimensionless parameter	"X" dimensionless parameter	Pressure drop in packed column, mmH_2O /(meter of packing)	2.9
B_{opt} : Optimum fractional well placement	Density difference ratio	flow rate	2.2
t_{DBT} : Dimensionless breakthrough time	Density difference ratio	flow rate	1.8
Time to water cone breakthrough in horizontal oil wells	Flow rate	Sweep efficiency	2.6

Chapters 1 and 2 discuss several models that are currently available to predict various design parameters in the oil and gas processing industries. However, sometimes their calculations may require rigorous computer solutions. Therefore, developing new predictive tools to minimize the complex and time-consuming calculation steps is an essential requirement. Because some simulations require simultaneous iterative solutions of many nonlinear and highly coupled sets of equations, it is obvious that a mathematically compact, simple, and reasonably accurate predictive tools are required with few tuned coefficients, as proposed in this dissertation work, would be preferable for computationally intensive simulations. In fact, the development of practical correlations by a small modification to the well-known Vogel-Tammann-Fulcher (VTF) equation [1921-1926] and Arrhenius equation (1889) was the primary motivation of this

research, which, nevertheless, yielded correlations with accuracy comparable to the existing rigorous simulations.
The details of the developments and validation of the proposed predictive tools have been previously presented in chapters 3 and 4.

5.1 Methanol loss in condensate phase during gas hydrate inhibition

An inherent problem with natural gas production or transmission is the formation of gas hydrates, which can lead to safety hazards to production/transportation systems and substantial economic risks. Therefore, an understanding of conditions where hydrates form is necessary to overcome hydrate related issues (Bahadori 2007c; Bahadori 2008a; Bahadori and Vuthaluru, 2009g). In this section, a simple Arrhenius-type function, which is easier than existing approaches, less complicated with fewer computations and is suitable for process engineers, is presented for the estimation of methanol loss in paraffinic hydrocarbons as a function of temperatures and methanol concentrations in water phase. Often when applying methanol as a hydrate inhibitor, there is a significant expense associated with the cost of lost methanol, so it is important to know how much methanol is lost to the hydrocarbon liquid phase in the pipeline. Prediction of inhibitor losses to the hydrocarbon liquid phase requires rigorous calculations.

The solubility of methanol in paraffin hydrocarbons is calculated for temperatures in the range of -30°C to 50°C and methanol concentrations up to 0.70 mass fraction in the water phase (Bahadori and Vuthaluru 2010f). Estimations are found to be in excellent agreement with the reliable data in the literature. The tool developed in this study can be of immense practical value for the engineers and scientists to quickly check on the loss of methanol in paraffinic hydrocarbons phase at various conditions without opting for any experimental measurements (Bahadori and Vuthaluru 2010f).

In view of the above mentioned issues, it is necessary to develop an accurate and simple predictive tool which is easier than existing approaches, less complicated with fewer computations for predicting the loss of methanol in paraffinic hydrocarbons as a function of temperatures and methanol concentrations in the water phase. The proposed novel tool developed is simple and it has unique expression which is non-existent in current literature. Furthermore, the selected exponential function to develop the tool leads to well-behaved (i.e. smooth and non-oscillatory) equations enabling fast and more accurate predictions. Figure 5.1

illustrates the solubility of methanol in paraffinic hydrocarbons for temperatures ranging between -30 to 50°C and methanol mass percent in hydrocarbons up to 0.70 mass fraction (Bahadori and Vuthaluru 2010f).

Figure 5.2 shows the proposed numerical method results which show excellent performance in the prediction of methanol solubility in hydrocarbon liquid phase in gas hydrate inhibition for wide range of conditions (Bahadori and Vuthaluru 2010f). It displays high temperatures and more injected methanol in the water phase caused more solubility of methanol in liquid phase. In this research, a predictive tool is presented for the estimation of methanol loss in liquid paraffinic hydrocarbon phase as a function of temperatures and methanol concentrations in water phase.

Unlike complex mathematical approaches for estimation of methanol loss in liquid paraffinic hydrocarbon phase, the proposed predictive tool would be of immense assistance for process engineers especially those dealing with natural gas transmission and processing. Additionally, the level of mathematical formulations associated with the estimation of methanol loss in condensate phase can be easily handled by an oil and gas practitioner.

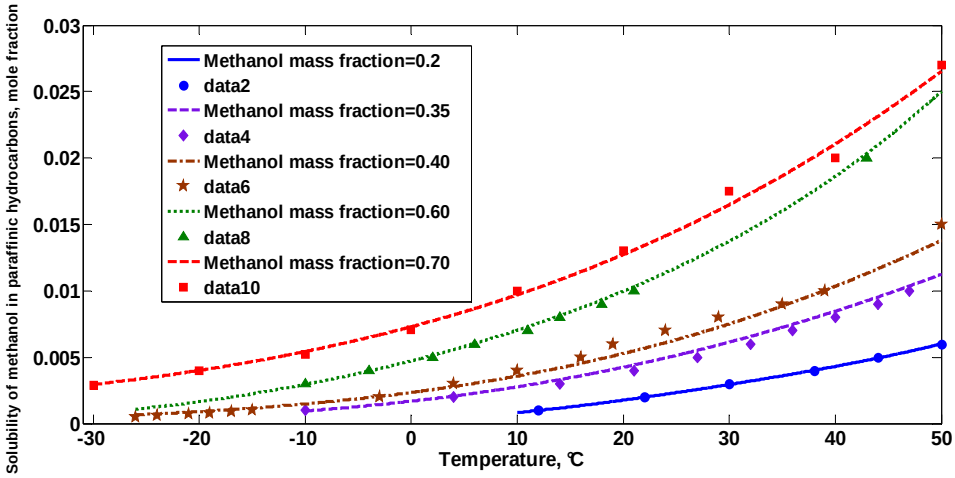

Figure 5.1: Prediction of solubility of methanol in paraffinic hydrocarbon liquid phase using new proposed correlation in comparison with data (Bahadori A. and Vuthaluru H. B. (2010f), *Energy & Fuels,* 24, 2999-3002)

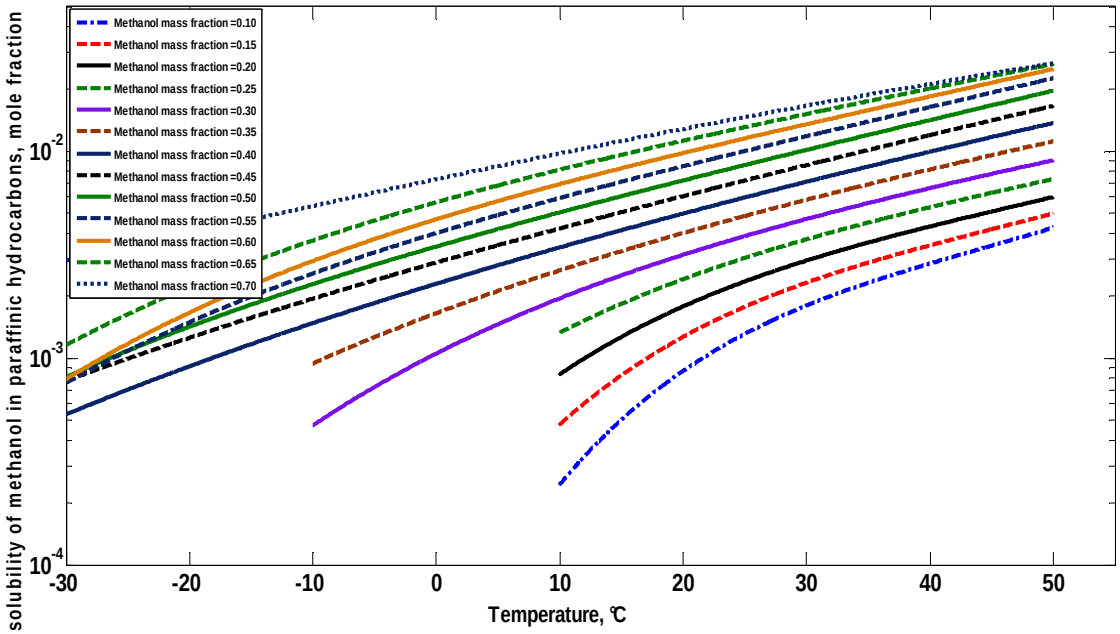

Figure 5.2: Performance of proposed predictive tool for prediction of solubility of methanol in hydrocarbon condensate phase (Bahadori A. and Vuthaluru H. B. (2010f), *Energy & Fuels,* 24, 2999-3002)

5.2 Densities and vapor pressures of aqueous methanol solutions using simple method

Inhibition utilizes injection of one of the glycols or methanol into a process stream where it can combine with the condensed aqueous phase to lower the hydrate formation temperature at a given pressure. The vapor pressure of methanol must be high enough so that significant quantities to vaporize. In this part of research, a simple method, which is easier than existing approaches, less complicated with fewer computations is formulated to accurately predict the densities and vapor pressures of aqueous methanol solutions as a function of temperature and methanol mass fraction using a novel and theoretically meaningful Arrhenius-type asymptotic exponential function combined with the Vandermonde matrix (Bahadori and Vuthaluru, 2010g).

The proposed correlation predicts the densities of aqueous methanol solutions for temperatures between -30 and 20°C and vapor pressures of aqueous methanol solutions for

temperatures up to 100°C. From an engineering view point, methanol aqueous solution vapour pressure changes with both temperature and mass fraction of methanol in aqueous phase. If the need for a methanol injection for hydrate inhibition is established, the unit design will depend on other factors including the density of aqueous methanol solution, which will be used to determine the methanol circulation flow rate and sizing of relevant equipments (Bahadori and Vuthaluru, 2010g).

Methanol aqueous solution density also changes with both temperature and mass fraction of methanol in aqueous phase. However, according to the authors' knowledge, there is no predictive tool for an accurate estimation of density and vapor pressure of aqueous methanol solutions as a function of temperature and methanol mass fraction. Considering this, there is an essential need for developing an accurate correlation to represent some properties of aqueous methanol solution such as vapor pressure and density. In addition developing the new predictive tools to minimize the complex and time-consuming calculation steps are an essential requirement.

The present study discusses the formulation of such a novel predictive tool which can be of significant importance for the process engineers. The predictive tool has practical value for engineers in terms of assessing densities and vapor pressures of aqueous methanol solutions by providing an advance indication of process variables which can assist practice engineers to take appropriate remedial measures to monitor the quality of aqueous methanol solutions at various conditions (Bahadori and Vuthaluru, 2010g). These optimum tuned coefficients(Tables A2 and A3 in appendix A) help to cover the vapor pressure and density of aqueous methanol solutions for temperatures up to 100 °C and temperature range between -30 and 20°C respectively. The optimum tuned coefficients given in Tables A2 and A3 can be further retuned quickly according to the proposed approach if more data are available in the future.

Figure 5.3 shows the predicted results from the proposed predictive tool for the vapour pressure of aqueous methanol solution as a function of methanol mass fraction in aqueous phase and temperature (Bahadori and Vuthaluru, 2010g) with the reported data (GPSA, Gas Processors and Suppliers Association,2004) It is evident from the results that there is a good agreement between predicted values for temperatures up to 373 K (Bahadori and Vuthaluru, 2010g) and the reliable data (Perry and Green, 1997). Figure 5.4 shows the performance of

the proposed predictive tool to predict the vapour pressure of aqueous methanol solution (Bahadori and Vuthaluru, 2010g). Figure 5.5 illustrates the predicted results from the proposed predictive tool for the density of aqueous methanol solution as a function of methanol mass fraction in aqueous phase and temperature (Bahadori and Vuthaluru, 2010g) with the reported data (Perry and Green 1997 and GPSA, Gas Processors and Suppliers Association 2004).

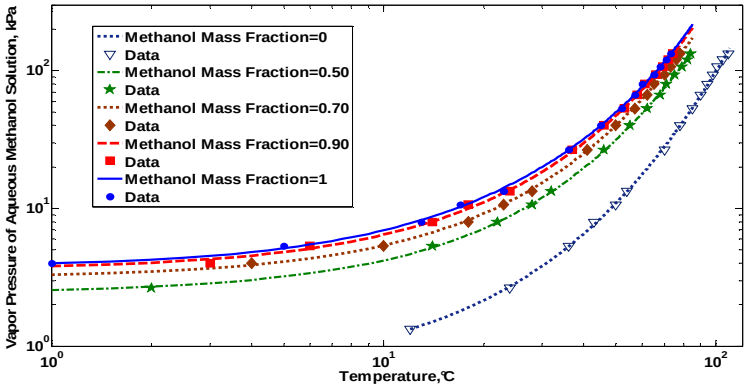

Figure 5.3: Vapor pressure of aqueous methanol solution as a function of temperature and methanol mass fraction in aqueous phase (Bahadori A. and Vuthaluru H. B. (2010g), *Oil Gas European Magazine*, 36(2), pp.84-88)

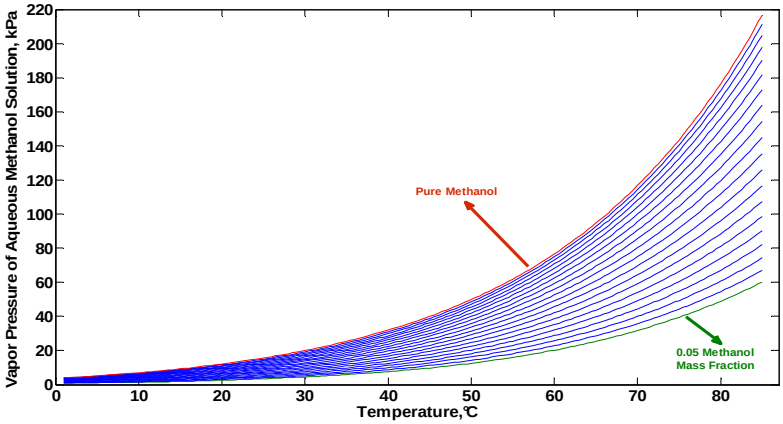

Figure 5.4: Vapor pressure of aqueous methanol solution as a function of temperature and methanol mass fraction in aqueous phase (Bahadori A. and Vuthaluru H. B. (2010g), *Oil Gas European Magazine*, 36(2), pp.84-88)

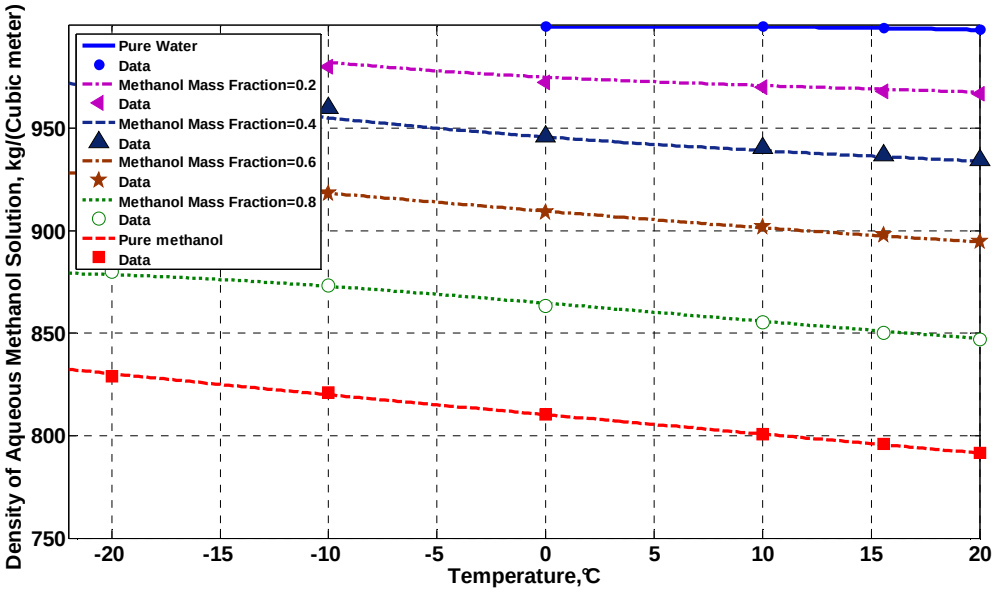

Figure 5.5: Density of aqueous methanol solution as a function of temperature and methanol mass fraction in aqueous phase (Bahadori A. and Vuthaluru H. B. (2010g), *Oil Gas European Magazine*, 36(2), pp.84-88)

5.3 Hydrate forming condition of natural gases

An inherent problem with natural gas production or transmission is the formation of gas hydrates, which can lead to safety hazards to production/transportation systems and to substantial economic risks (Bahadori and Vuthaluru, 2009g). Therefore, an understanding of conditions where hydrates form is necessary to overcoming hydrate related issues. Over the years, several models requiring more complicated and longer computations have been proposed for the prediction of hydrate formation conditions of natural gases. For these reasons, it is essential to develop a reliable predictive tool for oil and gas practitioners. The purpose of this study is to formulate a novel predictive tool for rapid estimation of the hydrate formation condition of natural gases. The developed correlation holds for wide range of temperatures (265 - 298 K), pressures (1200 to 40,000 kPa) and molecular weights (16-29) (Bahadori and Vuthaluru, 2009g). New proposed correlation shows consistently accurate results across proposed pressure, temperature and molecular weight ranges. This consistency can not be matched by any of the widely accepted existing correlations within the investigated range.

Figures 5.6 to 5.10 illustrate the performance of new developed predictive tools against the data from Katz (1945). These graphs show the excellent performance of proposed correlation for both hydrate formation pressure and temperature. (Bahadori and Vuthaluru, 2009g) These correlations cover molecular weight between 16 to 29 and temperatures between 265 to 298 K as well as pressures between 1200 to 40000 kPa.

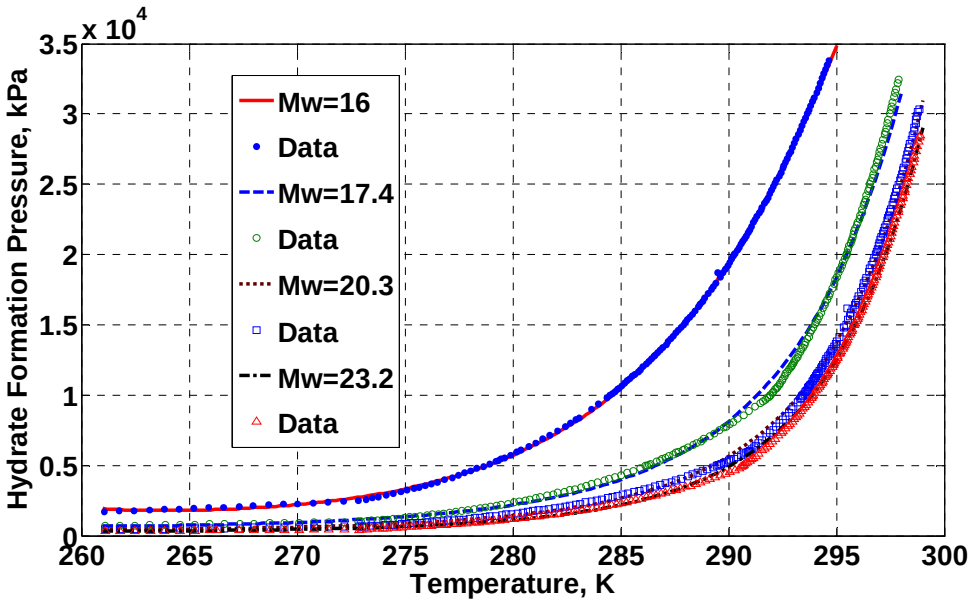

Figure 5.6: Comparison of obtained results of the new developed method for predicting hydrate formation pressure with data derived from Katz (1945) data for natural gases with molecular weight less than 23 (Bahadori A and Vuthaluru, H. B. 2009g, *Journal of Natural Gas Chemistry* 18(4), 453-457)

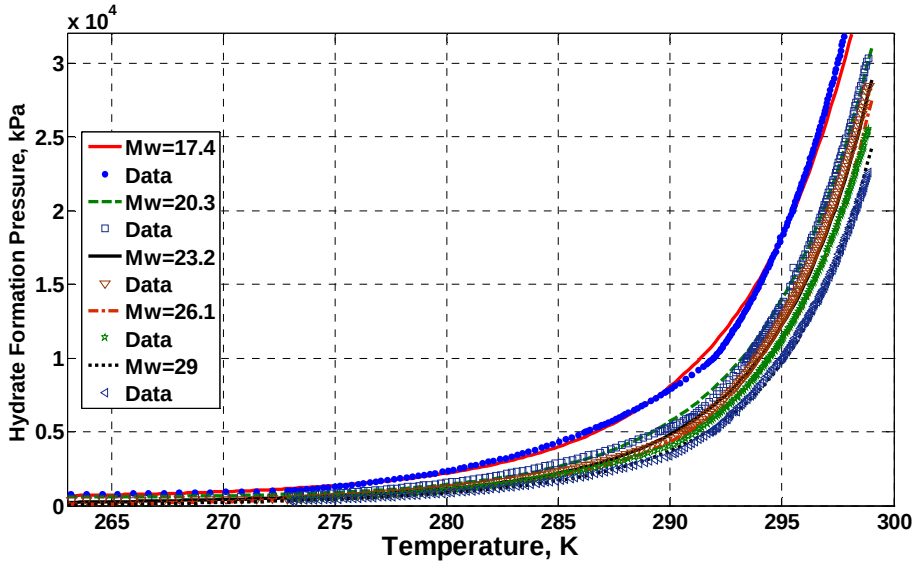

Figure 5.7: Comparison of obtained results of new developed method for predicting hydrate formation pressure with data derived from Katz (1945) data for natural gases with molecular weight more than 23, (Bahadori Aand Vuthaluru, H. B. 2009g, *Journal of Natural Gas Chemistry* 18(4), 453-457)

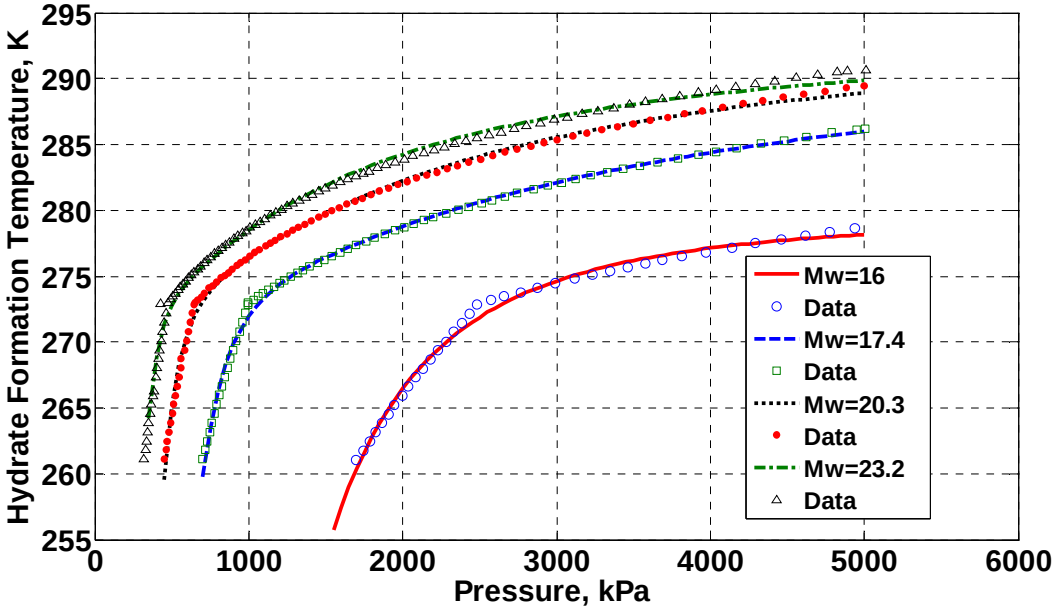

Figure 5.8: Comparison of obtained results of the new developed method for predicting hydrate formation temperature with data derived from Katz data(1945) for natural gases with molecular weight less than 23 and pressure less than 5000 kPa, (Bahadori A and Vuthaluru, H. B. 2009g, *Journal of Natural Gas Chemistry* 18(4), 453-457)

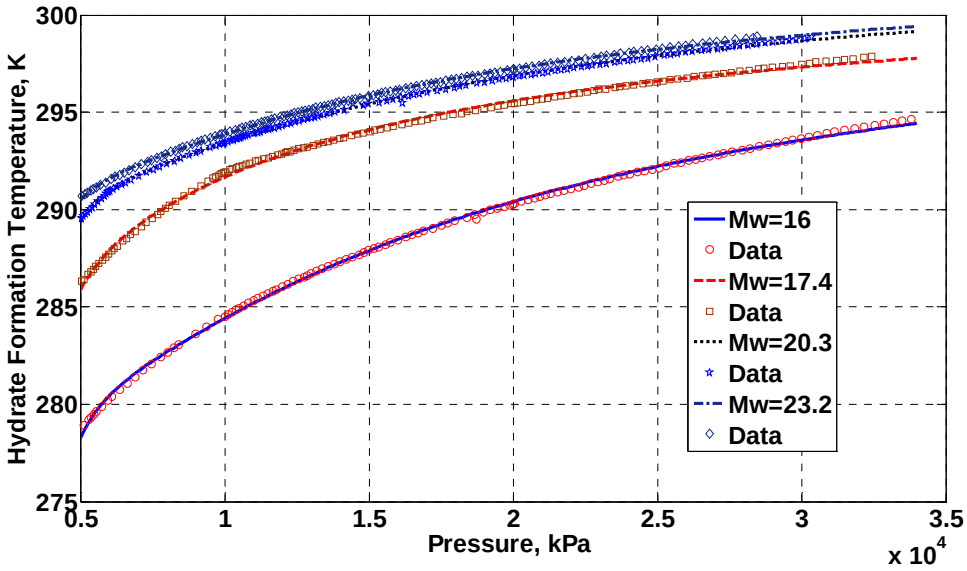

Figure 5.9: Comparison of obtained results of the new developed method for predicting hydrate formation temperature with data derived from Katz data(1945) for natural gases with molecular weight less than 23 and pressure more than 5000 kPa, (Bahadori Aand Vuthaluru, H. B. 2009g, *Journal of Natural Gas Chemistry* 18(4), 453-457)

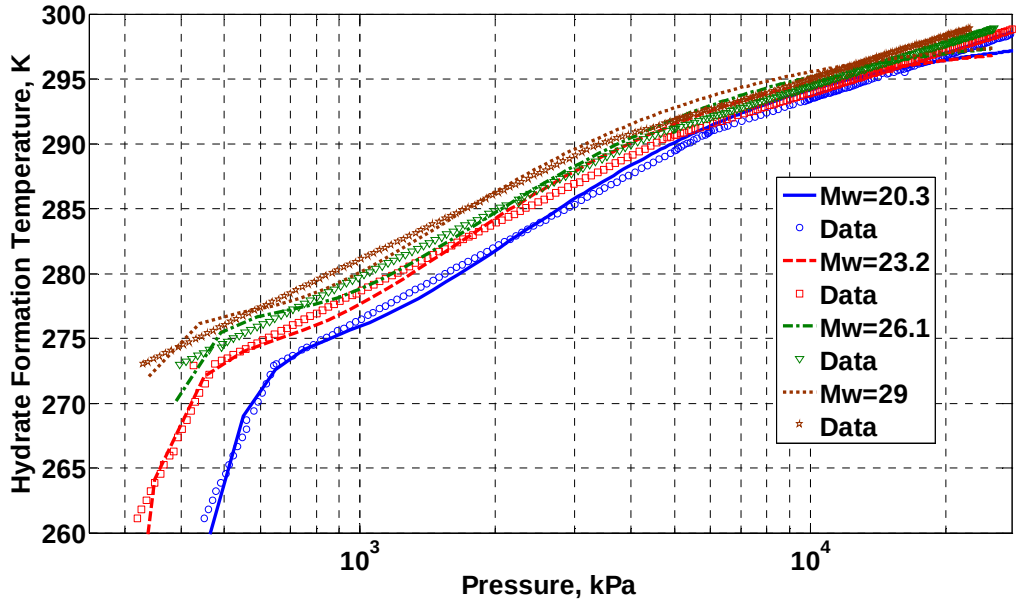

Figure 5.10 Comparison of obtained results of the new developed method for predicting hydrate formation temperature with data from Katz (1945) data for natural gases with molecular weight more than 23, (Bahadori A and Vuthaluru, H. B. 2009g, *Journal of Natural Gas Chemistry* 18(4), 453-457)

In brief, novel predictive tools were developed for accurate prediction of hydrate forming conditions of natural gases based on the extracted data from Katz (1945). The new proposed tool provided reliable results in comparison with other existing correlations for pressures between 1200 to 40000 kPa and temperatures between 265 K and 298 K, as well as the gas molecular weight within the range 16 to 29. The New proposed correlation shows accurate results consistently across all pressure ranges and gas molecular weights.

5.4 Simplified method for calculating hydrocarbons solubilities in hydrate inhibitors

Physical solvents are used to treat natural gas streams in a number of ways. Methanol and ethylene glycol (EG) are commonly used in wet gas dehydration processes. Acid gas removal can be accomplished by the methanol and physical solvent DEPG, which is a mixture of dimethyl-ethers of polyethylene glycols. Methanol and EG are also injected into wet gas to act as hydrate inhibitors (Bahadori and Vuthaluru 2008a). Methanol and ethylene glycol have a tendency to remove the hydrocarbon product. When methanol and ethylene glycol are injected into gas streams to inhibit hydrate formation these always absorb some hydrocarbons. After chilling and separation from the hydrocarbon phases, the aqueous EG or methanol phase is usually stored in atmospheric pressure tanks for disposal. Since the atmospheric storage tanks are below the separator pressure, hydrocarbons absorbed by the injected methanol or EG may flash. Therefore, quantifying this amount of absorption is critical to minimize hydrocarbon losses or to optimize hydrocarbon recovery depending on the objective of the process (Bahadori and Vuthaluru 2008a).

A great amount of research works have been performed in order to determine the solubility of light hydrocarbons (methane and ethane) in commonly used hydrate inhibitors (methanol and ethylene glycol) at various temperatures and pressures. These solubility data have been compiled and correlated. In most cases, however, the current models may not be sufficient if accurate predictions are needed. The aim of this research section is to present a predictive tool for accurate predictions of light hydrocarbons solubilities in methanol and ethylene glycol (at different weight percent in water) as a function of reduced partial pressure and reduced temperature. (Bahadori and Vuthaluru 2008a)The results show the proposed method have

been compared with reported experimental data and found that there is good agreement between observed data and the obtained values (Bahadori and Vuthaluru 2008a). Extensive experimental works have been done to measure the solubility of natural gas components in aqueous methanol and EG solutions at various temperature and pressure conditions (Wang et al, 2003).

The principle of the proposed method is based on thermodynamic properties including reduced temperature, and reduced pressure for individual components and some experimental data (Bahadori and Vuthaluru 2008a). The required data to develop this simplified method are experimental solubilities as a function of temperature and partial pressure. At first, solute mole fractions in liquid phase are correlated as a function of reduced partial pressure at different constant temperatures, and then the calculated coefficients for these polynomials are correlated for different reduced temperatures (Bahadori and Vuthaluru 2008a).

The method used in this study is to predict the solubility of methane and ethane components in the methanol and followed by EG. For weight percents, which have not been mentioned in the tables A5 and A6 in appendix A, an interpolation formula to extend the calculated solubility of light alkanes in methanol or EG (Bahadori and Vuthaluru 2008a).Figures 5.11 to 5.14 show typical solubility of methane and ethane in methanol and ethylene glycol at different temperatures, pressures and wt % by applying the proposed correlation. In brief, in this section illustrates a method which has been developed for accurate predictions of light alkanes solubilities in methanol and ethylene glycol (at different weight percent in water) as a function of reduced partial pressure and reduced temperature. The results for the proposed method have been compared with reported experimental data and found that there is good matching between observed data and the obtained values.

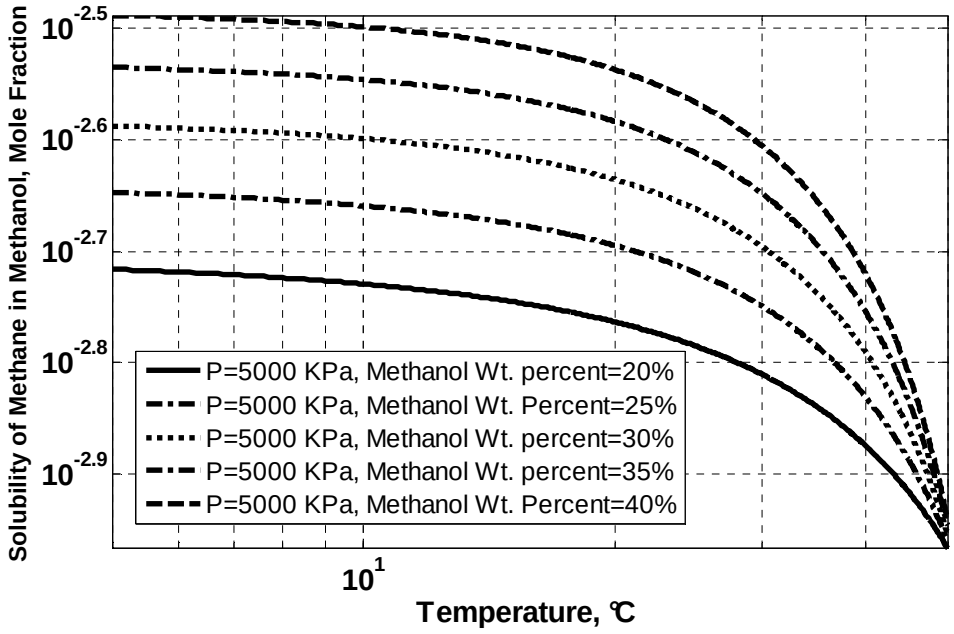

.

Figure 5.11: Predicting the solubility of methane in methanol based on the proposed correlation (20-40% wt. methanol) (Bahadori A. and Vuthaluru H. B.2008a, *Chemical Engineering and Technology* 31 (9), pp. 1369-1375)

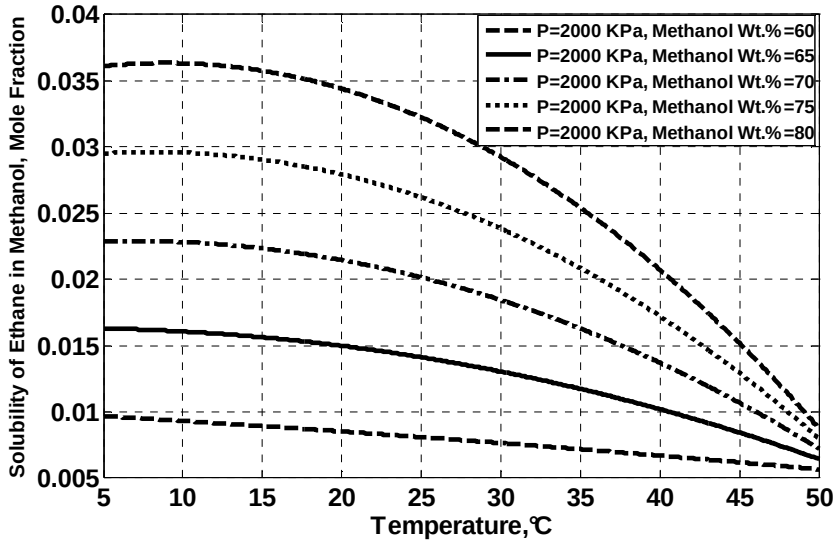

Figure 5.12: Predicting the solubility of ethane in methanol based on the proposed correlation (60-80% wt. methanol) (Bahadori A. and Vuthaluru H. B. 2008a, *Chemical Engineering and Technology* 31 (9), pp. 1369-1375).

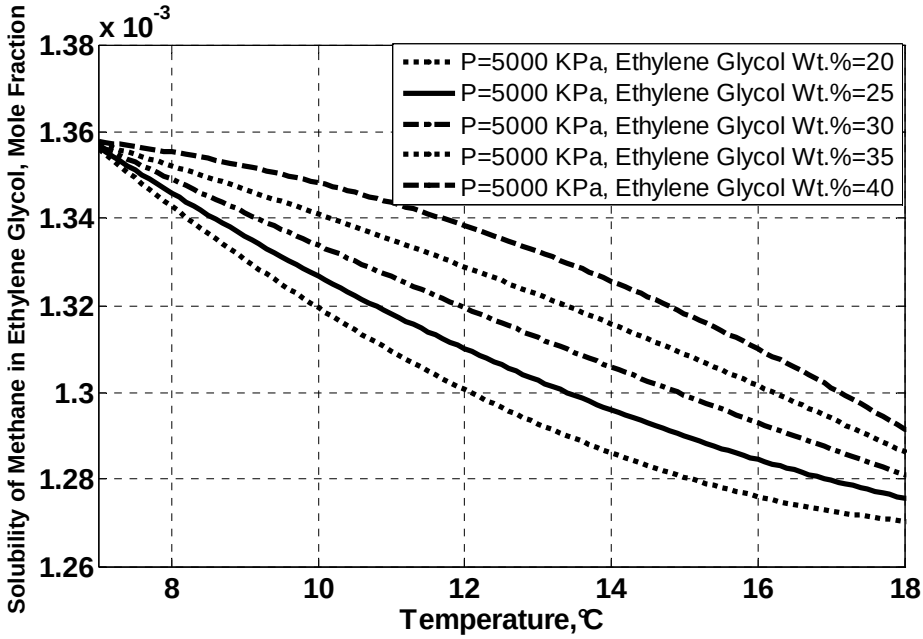

Figure 5.13: Predicting the solubility of methane in ethylene glycol based on the proposed correlation (20-40% wt. ethylene glycol) (Bahadori A. and Vuthaluru H. B. 2008a, *Chemical Engineering and Technology* 31 (9), pp. 1369-1375).

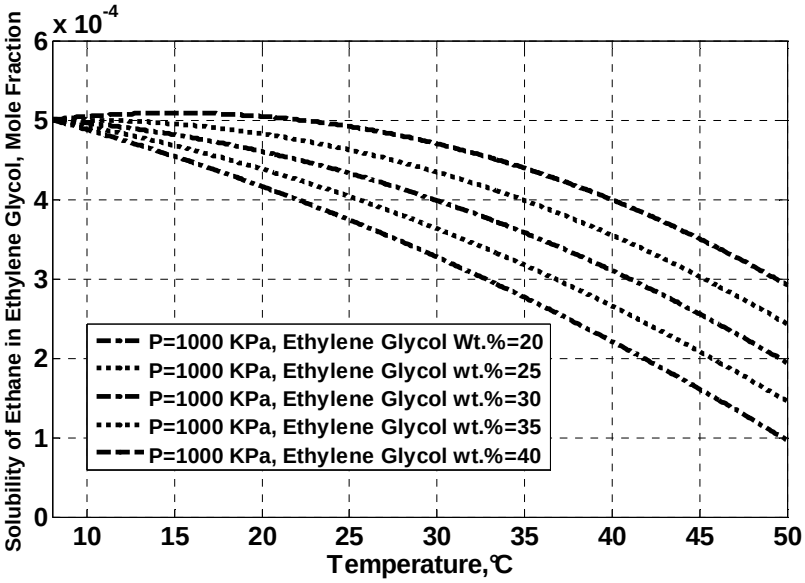

Figure 5.14: Predicting the solubility of ethane in ethylene glycol based on the proposed correlation (20-40% wt. ethylene glycol) (Bahadori A. and Vuthaluru H. B. 2008a *Chemical Engineering and Technology* 31 (9), pp.1369-1375).

5.5 Methanol vaporization loss during gas hydrate inhibition

Gas hydrate formation in natural gas and NGL systems can block pipelines, equipment, and instruments, restricting or interrupting flow leading to safety hazards to production/transportation systems. The amount of hydrate inhibitor to be injected not only must be sufficient to prevent freezing of the inhibitor water phase, but must also be sufficient to provide for the equilibrium vapor phase content of the inhibitor. The vapor pressure of methanol must be high enough for significant quantities will vaporize (Bahadori et al, 2008b).

Therefore to estimate methanol vaporization losses, it is necessary to develop a new predictive tool. In this research, a simple correlation, which is a mathematically compact and accurate equation containing few tuned coefficients, is presented for the prediction of methanol vaporization loss and vapour pressures of aqueous methanol solutions as a function of temperature and methanol mass fraction in aqueous solutions utilising a novel and simple Arrhenius-type asymptotic exponential function. The proposed correlation predicts the vapour pressures of aqueous methanol solutions for temperatures up to 100°C and methanol vaporization loss for temperature between -16 and 16°C. (Bahadori and Vuthaluru 2010h) The predictive tool developed in this study can be useful for the engineers and scientists to have a quick check on the methanol vaporization loss and vapor pressures of aqueous methanol solutions at various conditions without opting for any experimental measurements. In particular, chemical and process engineers would find the approach to be user-friendly with transparent calculations involving no complex expressions. The amount of inhibitor required to treat the water phase including the amount of inhibitor lost to the vapour phase and the amount that is soluble in the hydrocarbon liquid, equals the total amount required. Considering the above issues, there is an essential requirement for developing an accurate and simple predictive tool to represent the aqueous methanol solution vapour pressure and methanol vaporization loss. The new predictive tools development minimizes the complex and time-consuming calculation steps which are an essential requirement in the engineering calculations.

It is apparent that a mathematically compact, simple, and reasonably accurate equations which contains a fewer tuned coefficients, would be preferable for computationally intensive simulations In fact, the development of practical correlations by a small modification to the well-

known Vogel-Tammann-Fulcher (VTF) (Vogel, 1921, Tammann, G., Hesse, 1926, Flucher, 1926) and Arrhenius (1889) equations was the primary motivation of this research, which, nevertheless, yielded correlations with accuracy comparable to that of the existing rigorous simulations (Bahadori and Vuthaluru 2010h).

Currently, there are no predictive tools available in the literature for rapid estimation of methanol vaporization loss and the vapor pressure of aqueous methanol solutions. Our efforts directed at formulating predictive tools to assist engineers for the rapid calculation of the methanol vaporization loss and vapor pressure of aqueous methanol solutions using an Arrhenius-type asymptotic exponential function which is theoretically acceptable and meaningful. The proposed novel tools in the present work are simple and unique formulations which is non-existent in the literature. Furthermore, the selected exponential function to develop the tool, leads to well-behaved (i.e. smooth and non-oscillatory) equations enabling fast and more accurate predictions (Bahadori and Vuthaluru 2010h).

Figure 5.15 shows the performance of proposed predictive tool to predict the vapour pressure of aqueous methanol solution. Figures 5.16 and 5.17 show the methanol vapor composition to the methanol liquid composition using the new proposed correlation as a function of pressure and temperature for pressure less than 6000 kPa and pressure between 6000 and 20000 kPa respectively in comparison with data (Gas Processors and Suppliers Association, 2004).

Simple predictive tools are developed for the prediction of methanol vaporization loss and vapour pressures of aqueous methanol solutions as a function of temperature and methanol mass fraction in aqueous solutions using a novel and theoretically acceptable Arrhenius-type asymptotic exponential function. The proposed correlation predicts the vapour pressures of aqueous methanol solutions for temperatures up to 100°C and methanol vaporization loss for temperature between -16 and 16 °C.

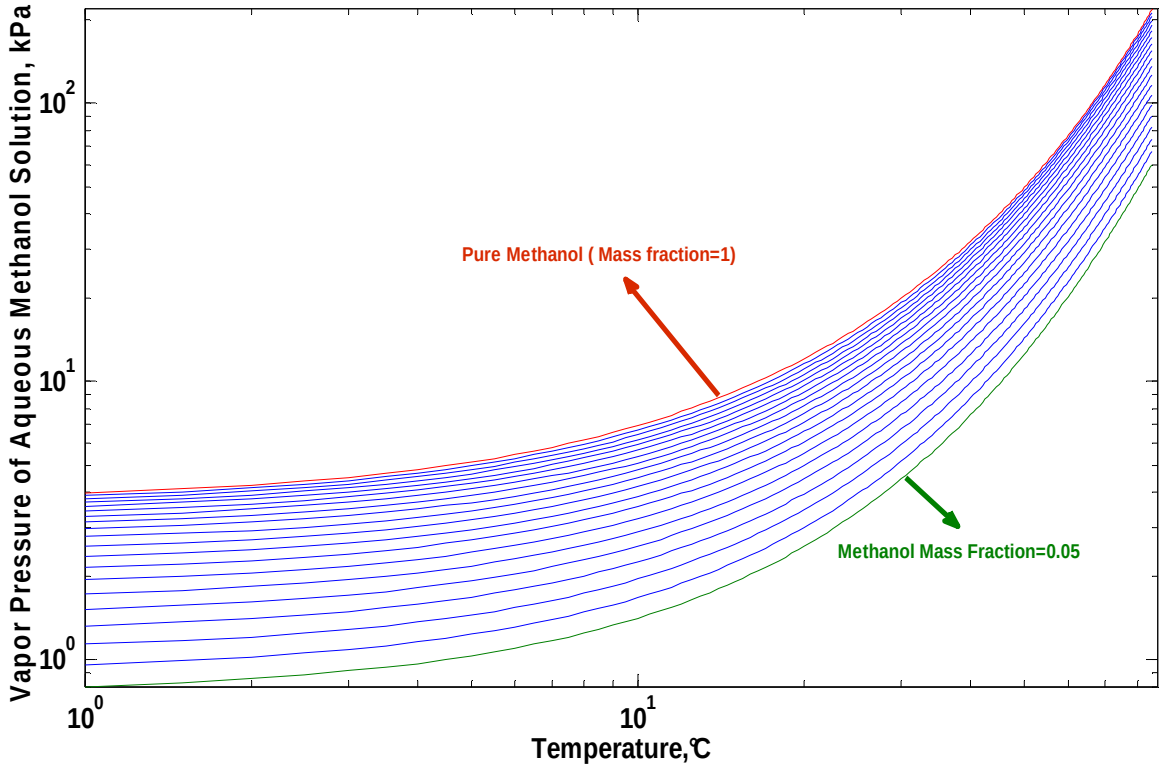

Figure 5.15: Vapor pressure of aqueous methanol solution as a function of temperature and methanol mass fraction in aqueous phase (Bahadori A and Vuthaluru H. B. (2010h) *Journal of Loss Prevention in the Process Industries*, 23(3), pp. 379-384)

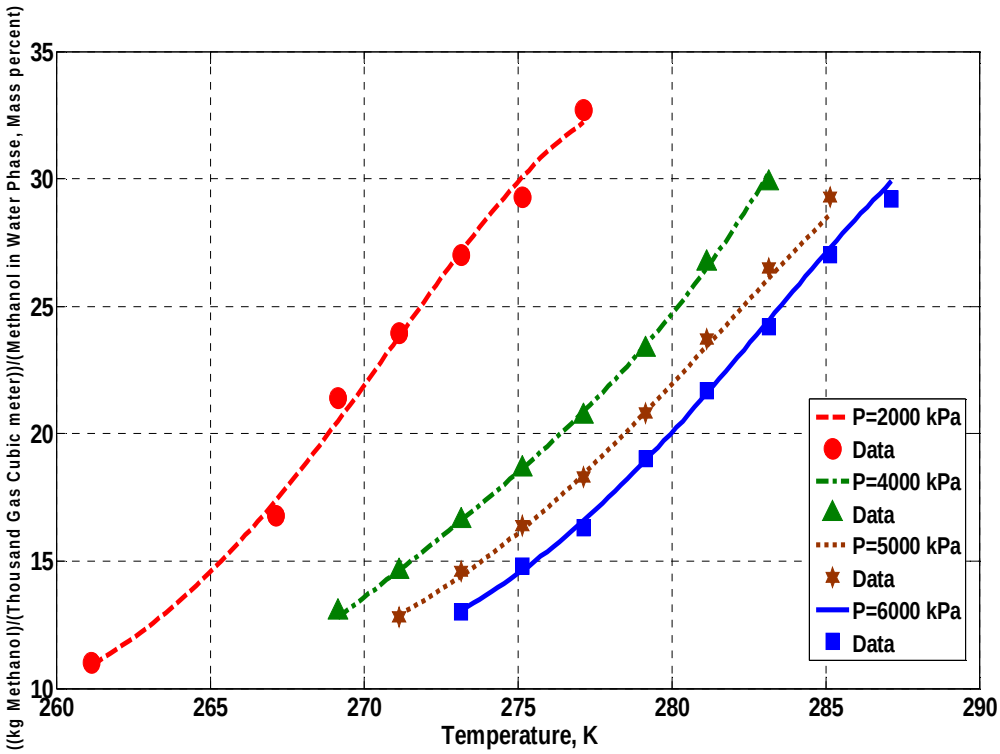

Figure 5.16: Prediction of methanol vapor composition to the methanol liquid composition using the new proposed correlation as a function of pressure and temperature for pressure less than 6000 kPa in comparison with data (Bahadori A and Vuthaluru H. B. (2010h) *Journal of Loss Prevention in the Process Industries*, 23(3), pp. 379-384)

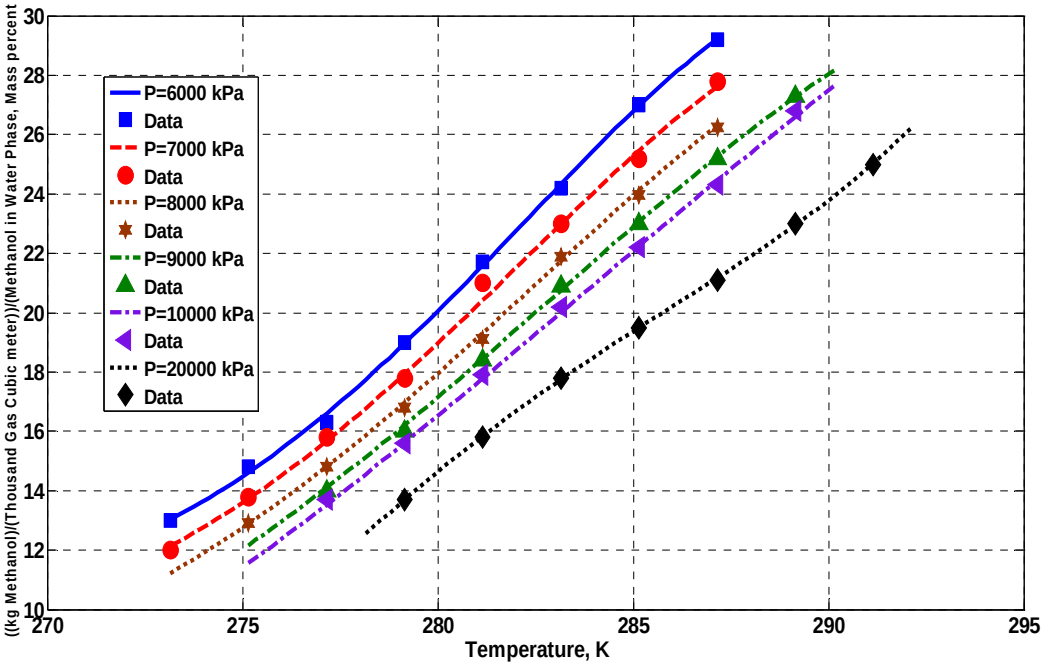

Figure 5.17: Prediction of methanol vapor composition to the methanol liquid composition using the new proposed correlation as a function of pressure and temperature for pressure between 6000 kPa and 20000 kPa (Bahadori A and Vuthaluru H. B. (2010h) *Journal of Loss Prevention in the Process Industries*, 23(3), pp. 379-384)

5.6 Aqueous solubility of light alkanes in water

The solubility of hydrocarbon components in water is of great importance for the environmental sciences. Its prediction is usually based on using the pure component solubilities and the mole fraction of the components in the mixture. The solubility of light alkanes (methane and ethane) in pure water have been studied extensively in the past decades. However, due to the extremely low solubilities, it is necessary to predict the aqueous solubility of those components using an accurate method (Bahadori et al 2009d).

In this section, a predictive tool is presented for the prediction of aqueous solubility of light alkanes, where the obtained results of the proposed method illustrated excellent and reliable observed values. Soluble organics in produced water and refinery effluents are treatment

problems for the petroleum industry. Production facilities and refineries have to meet regulatory discharge requirements for dissolved organics (Bahadori et al 2009d). This is expected to become more difficult as environmental regulations become stricter and production from deepwater operations increases. However, offshore analysis and remediation of produced water is expensive, and the relatively high polar content of deepwater crude oil also has a higher solubility of organic components in the aqueous phase. Neither of the identities of the water-soluble components are well known, nor are their concentrations in the produced water brines. Hence, quantitative characterization data are needed as the first step in understanding the dissolution of water-soluble organic compounds in produced water (Bahadori et al 2009d).

Largely for environmental reasons, research lab heavily undertaken in order to determine the solubility of hydrocarbons in water at various temperatures. These solubility data were compiled and correlated. In most cases, however, the thermodynamics models were insufficient for accurate predictions. On the contrary, the use of an accurate activity coefficient model was required for that purpose. The goal of this research is to contribute to the modelling and the understanding of the water solubility behaviour of light alkanes. Using a predictive tool, it will explain the observed solubility behaviour (Bahadori et al 2009d).

An easy-to-use predictive tool is proposed in this study to predict the aqueous solubility of methane and ethane components. The tuned constants are also given in the appendix A.

Figures 5.18 and 5.19 illustrate the solubility trends of methane and ethane components in water at different temperatures and pressures, applying the new developed method. As can be seen from those figures, the aqueous solubility of methane and ethane components are almost independent of temperature at high pressures, while at low pressures the solubility decreases with rising temperature (Bahadori et al 2009d).

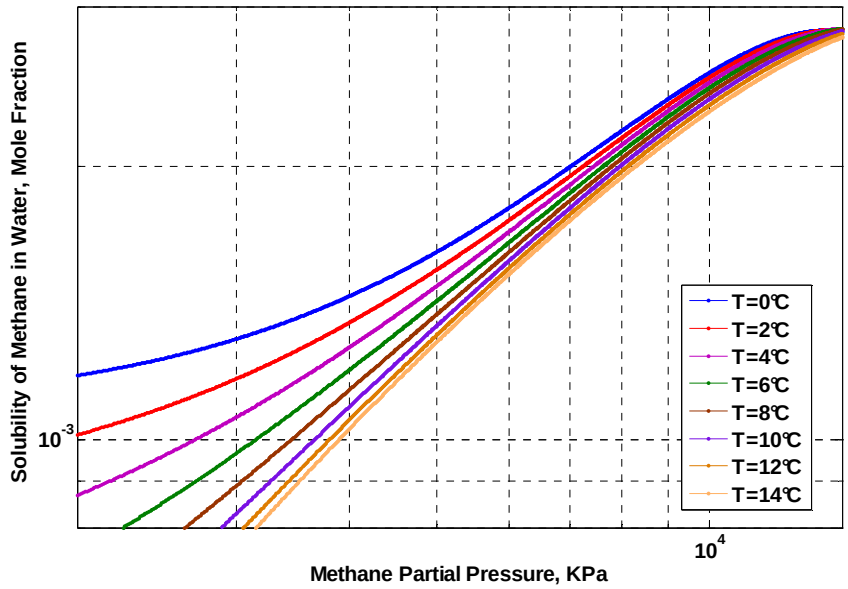

Figure 5.18: Predicting the aqueous solubility of methane based on the new developed correlation (Bahadori A., Vuthaluru H. B. and Mokhatab S. (2009d) *Journal of Energy Sources, Part A: Recovery, Utilization, and Environmental Effects*, 31 (9), 761-766)

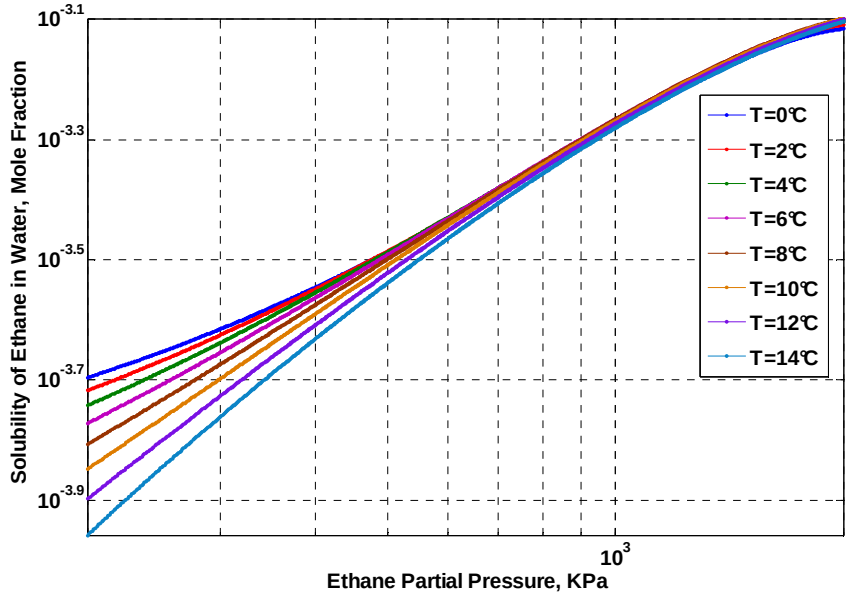

Figure 5.19: Predicting the aqueous solubility of ethane based on the new developed correlation (Bahadori A., Vuthaluru H. B. and Mokhatab S. (2009d) *Journal of Energy Sources, Part A: Recovery, Utilization, and Environmental Effects*, 31 (9), 761-766)

5.7 Water content of sour natural gases (first method)

Natural gas reservoirs always have water associated with them and hence the gas in the reservoir is water saturated. When gas is produced there is a simultaneous production of water as well (Bahadori and Vuthaluru 2009a). Some of this water is produced water from the reservoir directly. Other water produced with the gas is a result of water condensation due to the variations in pressure and temperature during production. Accurate determination of water content of sour natural gases therefore requires a careful study of the existing literature information and available experimental data.

Operating experience and thorough engineering have proved that it is necessary to reduce and control the water content of gas to ensure safe processing and transmission (Bahadori et al 2010i). Water is associated with natural gas from the reservoir through the production and processing and is a concern in transmission. Also the water content of sour natural gases is an important parameter in the design of facilities for the natural gas production, transmission, and processing (Bahadori and Vuthaluru 2009b). The aim in this section is to describe a predictive tool which is simpler than current available models involving a fewer number of parameters and requiring less complicated and shorter computations, for an appropriate estimation of water content of sour natural gas mixtures containing up to 40% acid gas components (CO_2 and H_2S). The new developed method works for pressures ranging from 1000 to 15000 KPa and temperatures from 15 to 120°C (Bahadori and Vuthaluru 2009b).

A new approach can be of immense practical value for engineers and scientists to enable them a quickly calculate the water content of sour natural gases at various temperatures and pressures without performing any experimental measurements. The proposed approach consists of two main sets of equations and a table containing tuned coefficients based on the data reported in the Gas Processor and Suppliers Association (Gas Processors and Suppliers Association) Engineering Data Book (GPSA 2004) (Bahadori and Vuthaluru 2009b). Figure 5.20 illustrates the obtained results for the prediction of water content of sweet natural gases (Bahadori and Vuthaluru 2009b). Figures 5.21 and 5.22 show the obtained results of new proposed correlations for predicting the effective water contents of CO_2 and H_2S components in natural gas mixtures, respectively (Bahadori and Vuthaluru 2009b). As can be seen, the obtained results show good matching with the reported data. In this section of thesis, a new predictive tool for an accurate

estimation of water content of sour natural gas mixtures containing up to 40% acid gas components has been developed. The obtained results show good agreement with the reported data, where the new developed method works for pressures ranging from 1000 to 15000 KPa and temperatures from 15 to 120 °C(Bahadori and Vuthaluru 2009b). New approach can be of immense practical value for the engineers and scientists to have a quick check on the water content of sour natural gases at various temperatures and pressures without performing any experimental measurements.

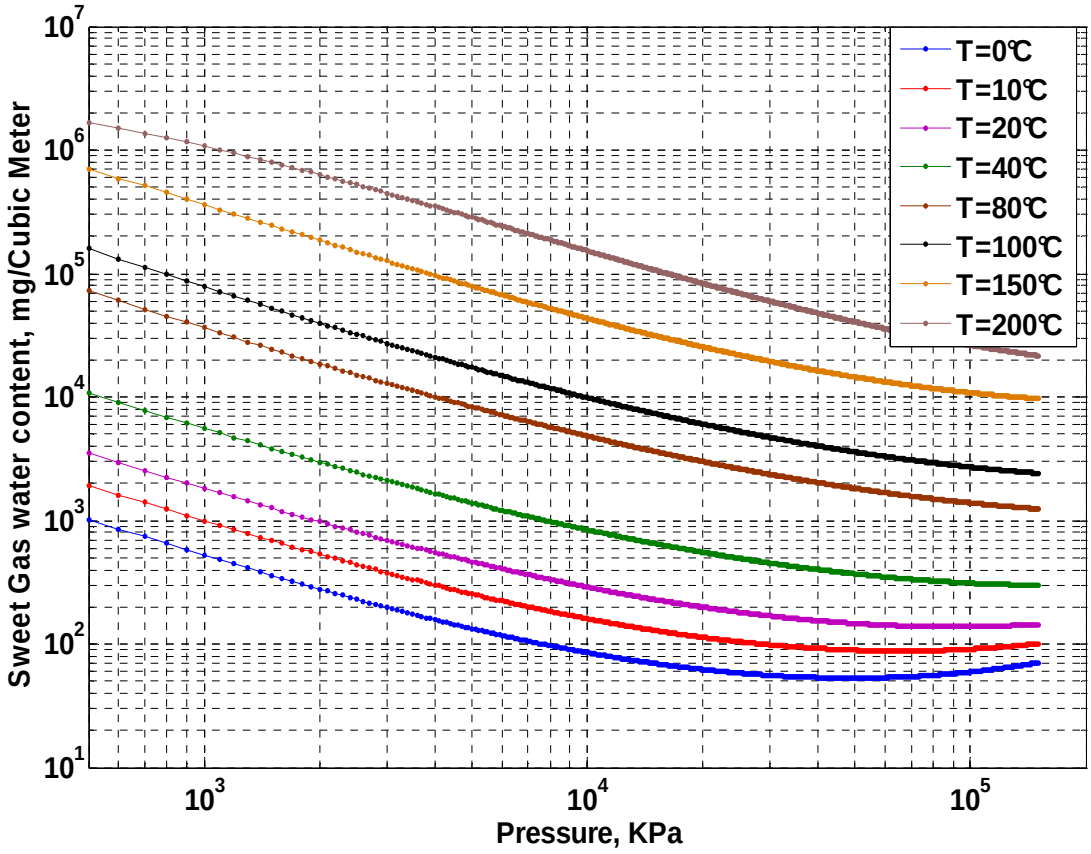

Figure 5.20: Determination of water content of sweet natural gases, (Bahadori A., Vuthaluru H. B. and Mokhatab S. (2009b) *Journal of the Japan Petroleum Institute*, 42(5) pp. 270-274)

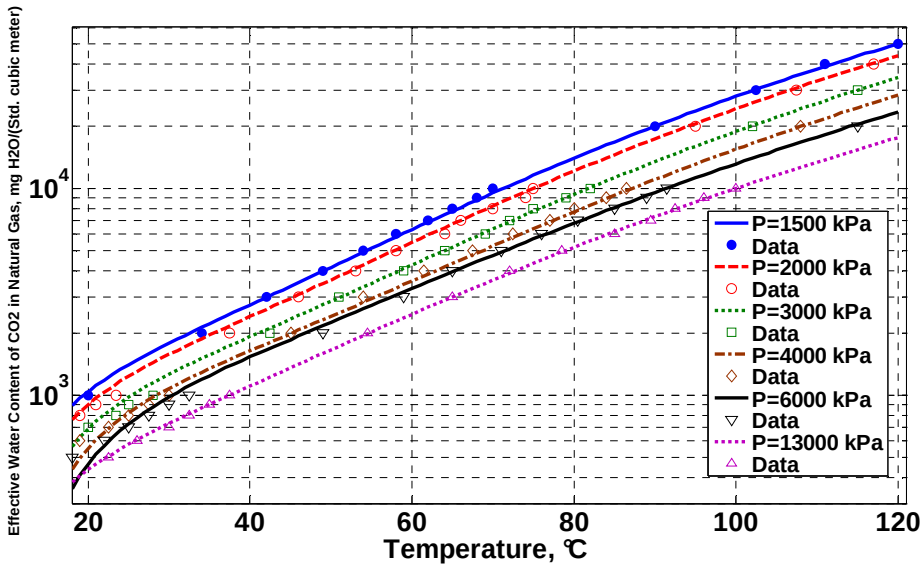

Figure 5.21: Determination of CO_2 effective water content in natural gas mixtures based on the new proposed method (Bahadori A., Vuthaluru H. B. and Mokhatab S. (2009b) *Journal of the Japan Petroleum Institute*, 42(5) pp.270-274)

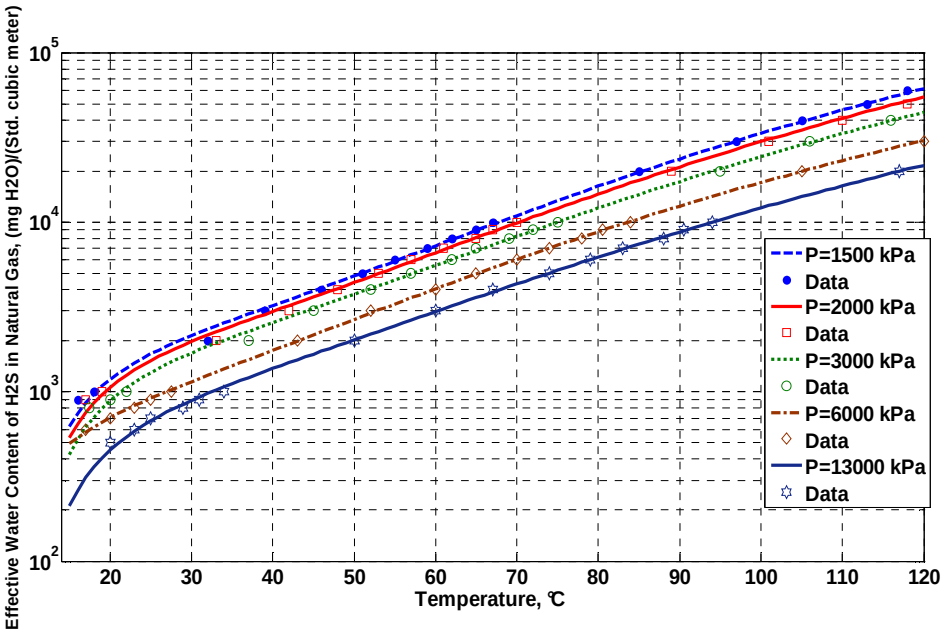

Figure 5.22: Determination of H_2S effective water content in natural gas mixtures based on the new proposed method and reported data (Bahadori A., Vuthaluru H. B. and Mokhatab S. (2009b) *Journal of the Japan Petroleum Institute*, 42(5) pp.270-274)

5.8 Water content of natural gases (second method)

An accurate prediction of natural gas water content is an important parameter in the proper designing of natural gas production, transmission and processing facilities (Bahadori and Vuthaluru 2009a). The aim of this part of thesis is to describe an accurate method for predicting water content of sweet and sour natural gases, where the obtained results by the proposed method show good matching with the data. The proposed method provides reliable estimates of the equilibrium water vapor content of sour natural gas for a range of conditions, including H2S contents of 0-50 mole % with CO2 contents of 0-40 mole %, pressures from atmospheric to 100000 KPa for sweet gas and 70000 KPa for sour gas, and temperatures from 10 to 150 °C for sour gases and 10-200°C for sweet gases (Bahadori and Vuthaluru 2009a). Figures 5.23 illustrates the obtained results of new method for predicting water content of sweet natural gas, where Figures 5.24 and 5.25 are used to determine the water content of sour natural gases as a function of temperature and pressure based on the proposed method.

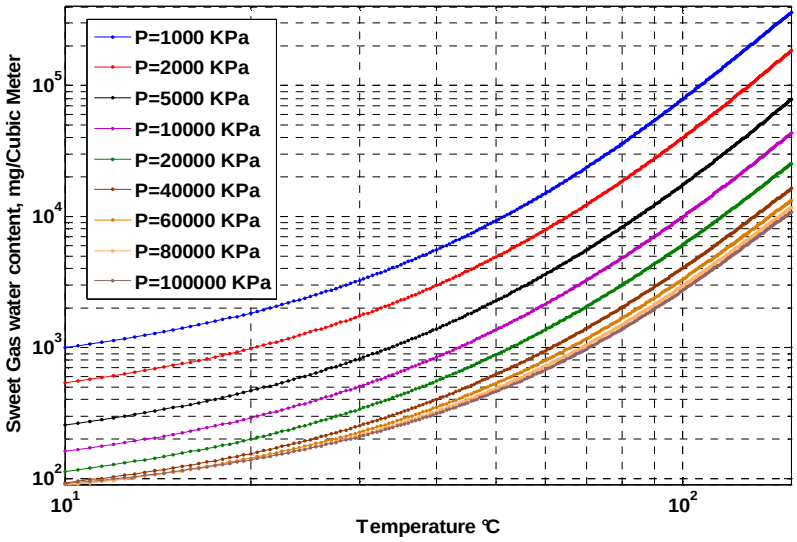

Figure 5.23: Determining water content of sweet natural gas based on the new proposed method (Bahadori et al (2009a) *Journal of Energy Sources, Part A: Recovery, Utilization, and Environmental Effects*,31:(9) pp. 754 - 760).

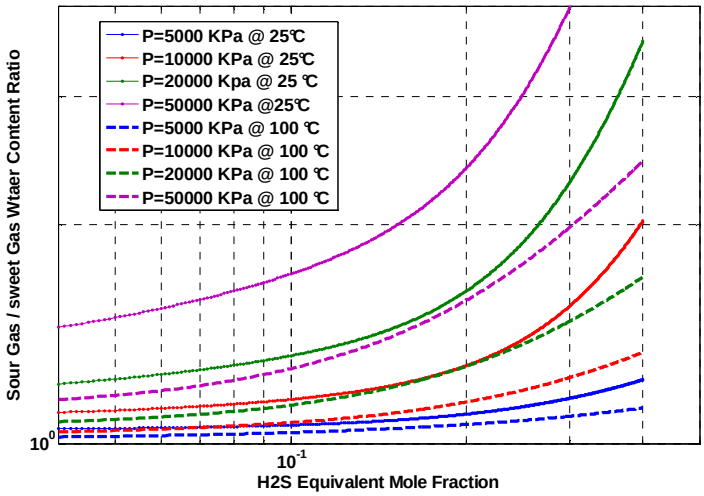

Figure 5.24: Determining sour gas water content over sweet gas water content ratio based on the new proposed method at different temperatures and pressures (Bahadori et al (2009a) *Journal of Energy Sources, Part A: Recovery, Utilization, and Environmental Effects,*31:(9) pp. 754 -760).

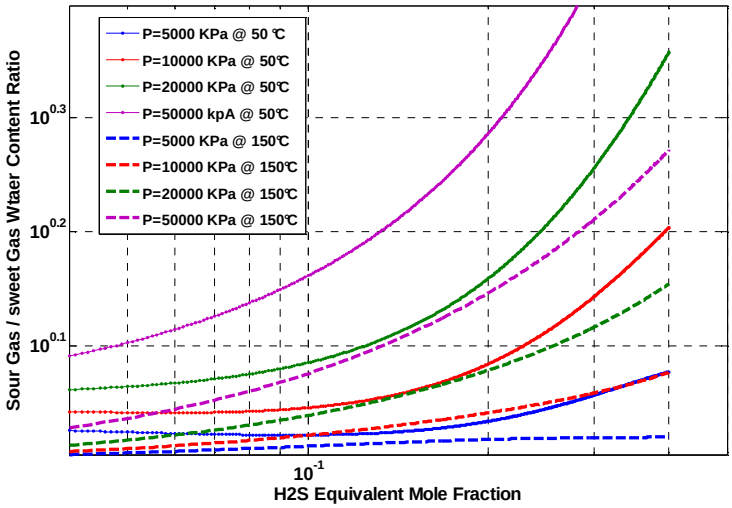

Figure 5.25: Determining sour gas water content over sweet gas water content ratio based on the new proposed method at different temperatures and pressures. (Bahadori et al, (2009a) *Journal of Energy Sources, Part A: Recovery, Utilization, and Environmental Effects,31:(9) pp. 754 – 760)*

5.9 Simple Methodology for Sizing of Absorbers for TEG Gas Dehydration Systems

Natural gas is saturated with water vapor under normal production conditions. In the design of natural gas dehydration systems, correct estimation of absorption column size is crucial (Bahadori and Vuthaluru 2009h). Once the lean triethylene glycol (TEG) concentration has been established, the circulation rate of triethylene glycol (TEG) and number of trays (height of packing) must be determined. The current methods to correlate the triethylene glycol (TEG) circulation rate, triethylene glycol (TEG) purity, water removal efficiency, number of equilibrium stages (or height of packing) and the diameter of contactor employs rigorous calculation techniques involving more complicated and longer computations (Bahadori and Vuthaluru 2009h). The aim of this study is to develop a technique, by employing basic algebraic equations to correlate water removal efficiency as a function of triethylene glycol (TEG) circulation rate and triethylene glycol (TEG) purity for appropriate sizing of the absorber at wide range of operating conditions of triethylene glycol (TEG) dehydration systems. Conversion from equilibrium stages to actual trays can be made assuming an overall tray efficiency of 25-30% (Bahadori and Vuthaluru 2009h).

The proposed simple approach, correlates the triethylene glycol (TEG) circulation rate, triethylene glycol (TEG) purity, water removal efficiency, number of equilibrium stages (or height of packing) and the diameter of contactor with ease and computationally less time consuming unlike conventional simulation approaches involving of rigorous and time consuming calculations and plotting of graphs etc. A number of commercial simulation softwares and mathematical models have been reported in the literature. However, to date, no simplified approach exists in the literature for correlating the triethylene glycol (TEG) circulation rate, triethylene glycol (TEG) purity, water removal efficiency, number of equilibrium stages (or height of packing) and the diameter of contactor (Bahadori and Vuthaluru 2009h). In view of this necessity, our efforts have been directed at formulating a method which will assist to rapidly estimate the water removal efficiency as a function of TEG circulation rate and TEG concentrations.

The required data to develop this correlation includes the reported data (Gas Processors and Suppliers Association, 2004) for the water removal efficiency as a function of TEG circulation rate and TEG concentrations (X). In this work, the water removal efficiency is predicted rapidly by proposing a simple correlation. The following methodology has been applied to develop this correlation (Bahadori and Vuthaluru 2009h).

Figures 5.26 to 5.31 compared the results of new proposed correlation for predicting the water removal efficiency vs. TEG circulation rate at various TEG concentrations and number of theoretical stages with some of the reported data (Gas Processors and Suppliers Association 2004). As illustrated, there is a good matching between predicted and reported values. The results demonstrate that a process engineer may consider this correlation as an appropriate estimation tool during the design of a gas dehydration system utilizing triethylene glycol (TEG) solvent (Bahadori and Vuthaluru 2009h).

The proposed correlation is novel and contains a unique expression which is non-existent in the literature and is recommended for appropriate sizing of the absorber at wide range of conditions of TEG dehydration systems. Results show that a designer may consider this correlation as appropriate estimation tool during the design of a gas dehydration system utilizing TEG solvent. This approach can be useful in the design of absorbers at wide range of conditions of TEG dehydration systems. In particular, process and chemical engineers would find the proposed method to be of practical value and user friendly involving no complex expressions with transparent calculations (Bahadori and Vuthaluru 2009h)

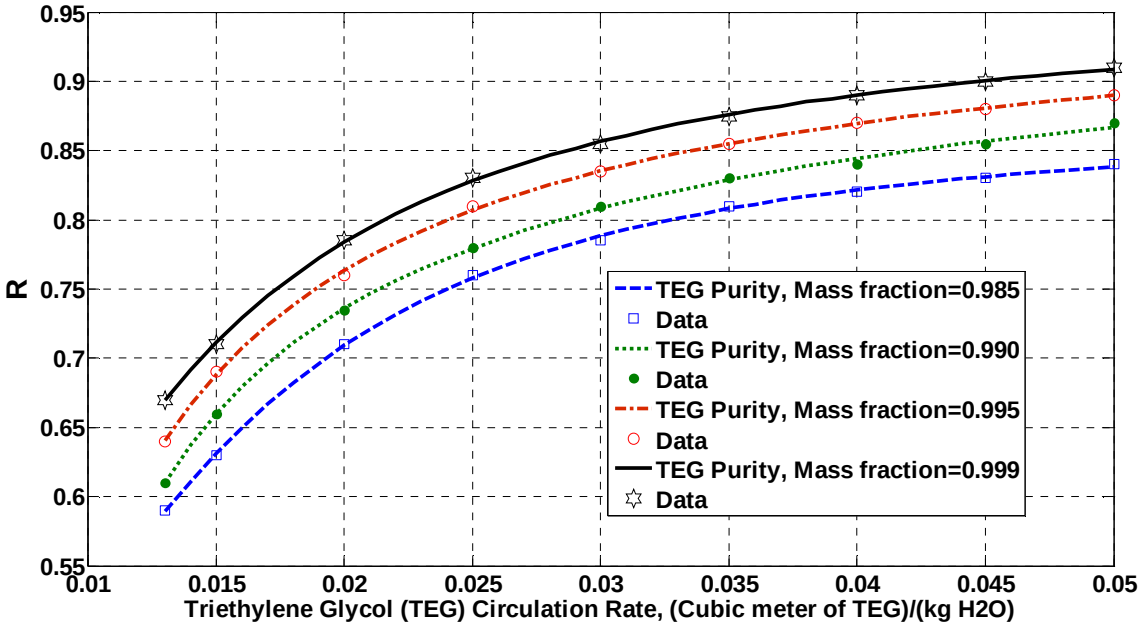

Figure 5.26: Water Removal Efficiency vs. TEG Circulation Rate at Various TEG Concentrations (Number of theoretical stages, N = 1) (Bahadori, A. and Vuthaluru H. B. (2009h) *Energy* 34, 1910–1916)

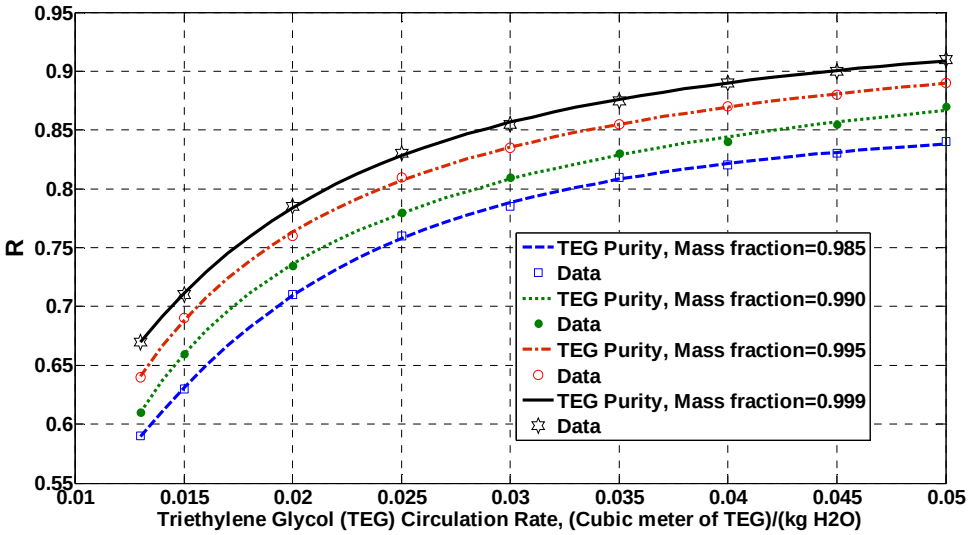

Figure 5.27: Water Removal Efficiency vs. TEG Circulation Rate at Various TEG Concentrations (Number of theoretical stages, N = 1.5) (Bahadori, A. and Vuthaluru H. B. (2009h) *Energy* 34, 1910–1916)

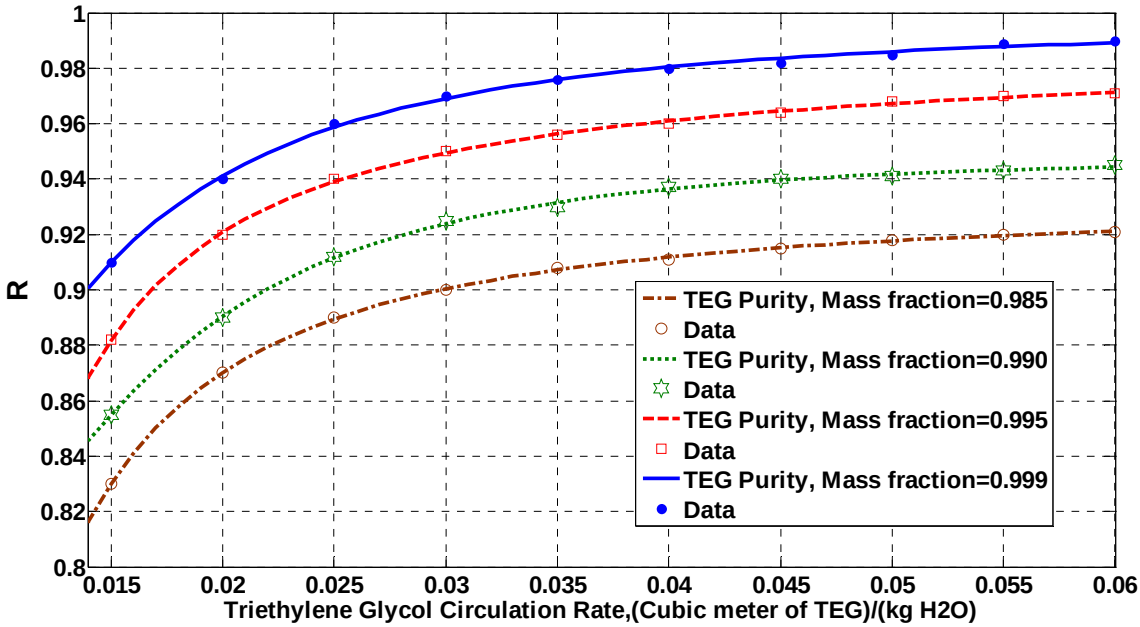

Figure 5.28: Water Removal Efficiency vs. TEG Circulation Rate at Various TEG Concentrations (Number of theoretical stages, N = 2 Bahadori, A. and Vuthaluru H. B. (2009h) *Energy* 34, 1910–1916)

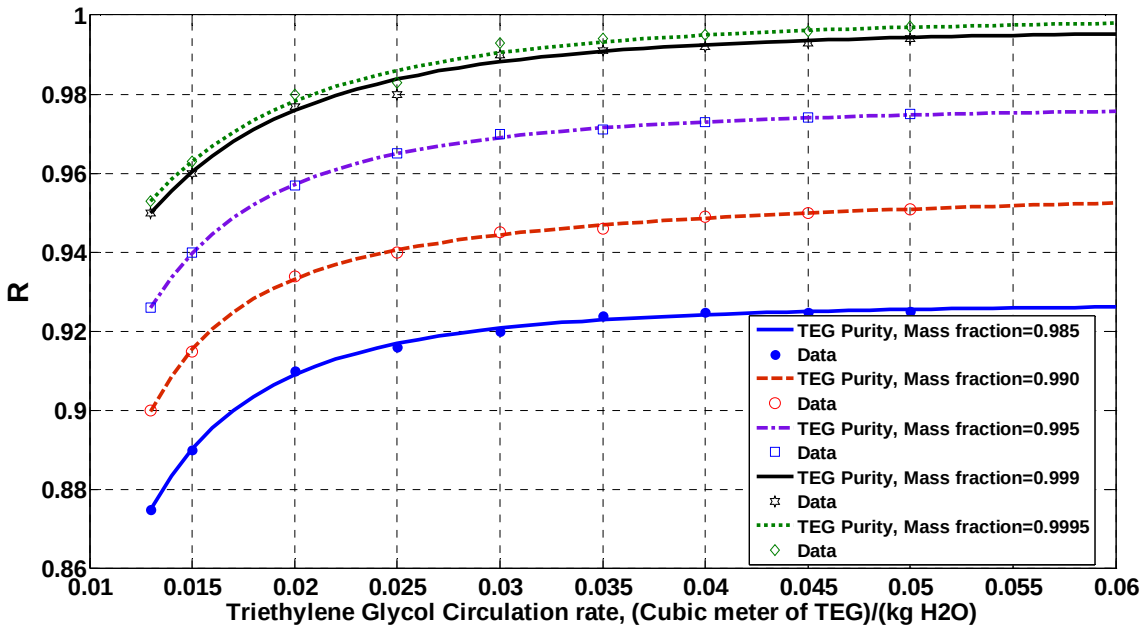

Figure 5.29: Water Removal Efficiency vs. TEG Circulation Rate at Various TEG Concentrations (Number of theoretical stages, N = 2.5) (Bahadori, A. and Vuthaluru H. B. (2009h) *Energy* 34, 1910–1916)

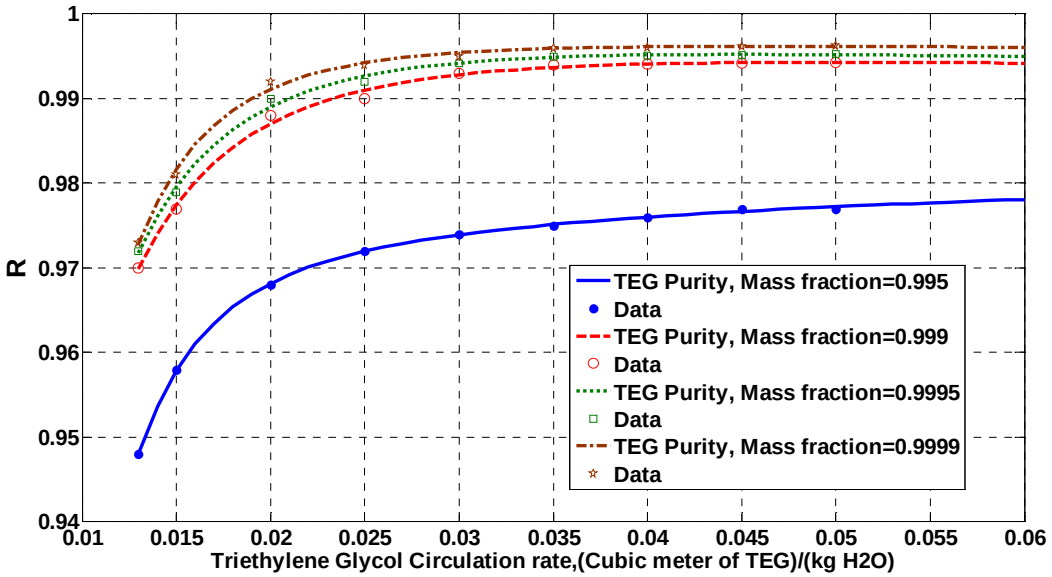

Figure 5.30: Water Removal Efficiency vs. TEG Circulation Rate at Various TEG Concentrations (Number of theoretical stages, N = 3) (Bahadori, A. and Vuthaluru H. B. (2009h) *Energy* 34, 1910–1916)

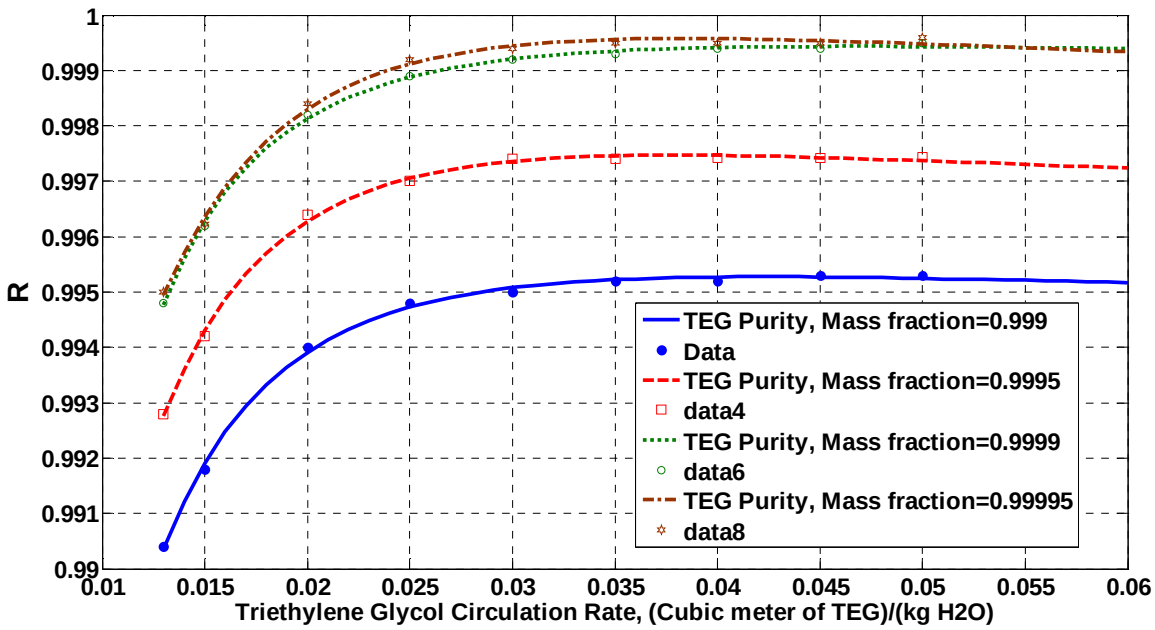

Figure 5.31: Water Removal Efficiency vs. TEG Circulation Rate at Various TEG Concentrations (Number of theoretical stages, N= 4) (Bahadori, A. and Vuthaluru H. B. (2009h) *Energy* 34, 1910–1916)

5.10 Water-Adsorption isotherms for molecular sieve in contact with natural gas

In this section, a new predictive tool is developed to estimate water-adsorption isotherms for molecular sieve in contact with natural gas. This gives the relationship of static-equilibrium water capacity to the operating temperature and water partial pressure which are important parameters has to be considered while designing any refrigeration system (Bahadori 2009d). The new correlation is suitable for the range of evaporator temperatures between 0°C and 65°C and the partial pressures of water in range between 0.0001 kPa to 5 kPa. There are several solid desiccants which possess the physical characteristic to adsorb water from natural gas. These desiccants are generally used in dehydration systems consisting of two or more towers and associated regeneration equipment. Molecular sieve dehydrators are commonly used ahead of NGL recovery plants designed to recover ethane (Bahadori 2009d). These plants operate at very cold temperatures and require very dry feed gas to prevent formation of hydrates. Dehydration to a –100°C dewpoint is possible with molecular sieves. Water dewpoints less than –100°C can

be accomplished with special design and strict operating parameters (Gas Processors and Suppliers Association, 2004).
Other streams may be used if they are dry enough, such as part of the residue gas.

The tuned coefficients are given in appendix A for different water partial pressure ranges. These tuned coefficients can be retuned quickly if more accurate data are available in future.

Figures 5.32 and 5.33 illustrate the obtained results of the new developed correlation comparing with data from **Gas Processors and Suppliers Association** 2004. As can be seen, there is a good agreement between the predicted and reported values (Bahadori 2009d). It is therefore recommended to use this predictive tool for estimating water-adsorption isotherms for molecular sieve in contact with natural gas system within the proposed ranges (Bahadori 2009d). In this study, a simple predictive tool has been developed to estimate water-adsorption isotherms for 4A molecular sieve in contact with gas. This gives the relationship of static-equilibrium water capacity to the operating temperature and gas dew point temperature which are important parameters that should be considered while designing any refrigeration system. The new correlation is suitable for the range of evaporator temperatures between 0°C and 65°C and the partial pressures of water in range between 0.0001 kPa to 5 kpa (Bahadori 2009d).

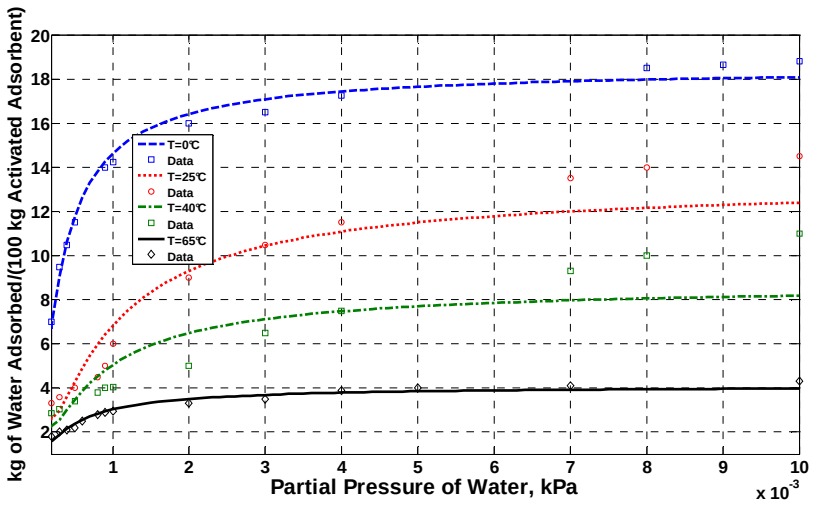

Figure 5.32: Comparing predicted values of new developed correlation for estimating water-adsorption isotherms for molecular sieve in contact with natural gas system within the proposed ranges for water partial pressure between 0.0001<p<0.01 kpa. Bahadori A., (2009d), *Hydrocarbon Processing*, 88(1) pp. 55-56

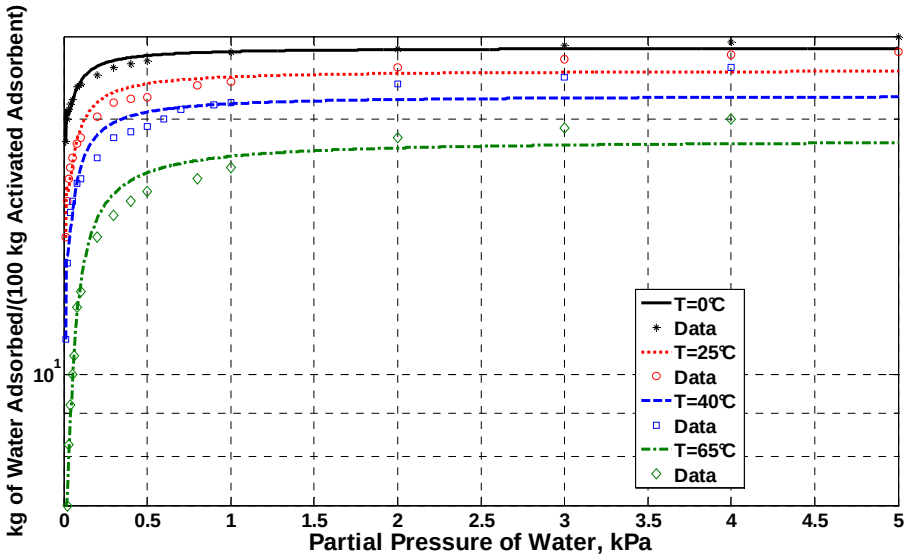

Figure 5.33: Comparing predicted values of new developed correlation for estimating water-adsorption isotherms for molecular sieve in contact with natural gas system within the proposed ranges for water partial pressure between 0.01<P<5 kpa. Bahadori A., (2009d), *Hydrocarbon Processing*, 88(1) pp. 55-56.

5.11 Equilibrium water dew point of natural gas in TEG dehydration systems

Evaluation of a triethylene glycol (TEG) system involves establishing the minimum triethylene glycol (TEG) concentration required to meet the outlet gas water dewpoint specification. In this study, predictive tool is utilised for the rapid estimation of the water dewpoint of a natural gas stream in equilibrium with a TEG solution at various temperatures and TEG concentrations.

This correlation can be used to estimate the required TEG concentration for a particular application or the theoretical dewpoint depression for a given TEG concentration and contactor temperature. Actual outlet dewpoints depend on the TEG circulation rate and number of equilibrium stages, but typical approaches to equilibrium is 6–11°C. Equilibrium dewpoints are relatively insensitive to pressure and this correlation may be used up to 10300 kPa (abs) with little error. The proposed correlation covers VLE data for TEG–water system for contactor temperatures between 10°C to 80°C and TEG concentrations ranging from 90.00 to 99.999 wt%.

Figure 5.34 to 5.36 show the water dew point of a natural gas stream in equilibrium with a TEG solution at various TEG concentrations and contactor temperature between 10°C and 80°C. As can be seen, there is a good agreement between predicted results and the reported values. Since the TEG dehydrators usually operate at temperatures of less than 70 °C, there was no practical need to include temperatures higher than 70 °C in the graphs of this work. The equilibrium water dewpoints calculated by this correlation are based on the fact that the condensed water phase is considered as a metastable liquid.

At low dewpoints the true condensed phase will be a hydrate. The equilibrium dewpoint temperature above a hydrate is higher than that above a metastable liquid. Therefore, this correlation predicts dewpoints which are colder than those which can actually be achieved. The difference is a function of temperature, pressure and gas composition but can be as much as 8–11°C. When dehydrating to very low dewpoints, such as those required upstream of a refrigeration process, the TEG concentration must be sufficient to dry the gas to the hydrate dewpoint. This correlation can be used to estimate the required TEG concentration for a particular application or theoretical dewpoint depression for a given TEG concentration and contactor temperature. Actual outlet dewpoints depend on the TEG circulation rate and the number of equilibrium stages, but typical approaches to equilibrium are 6–11°C.

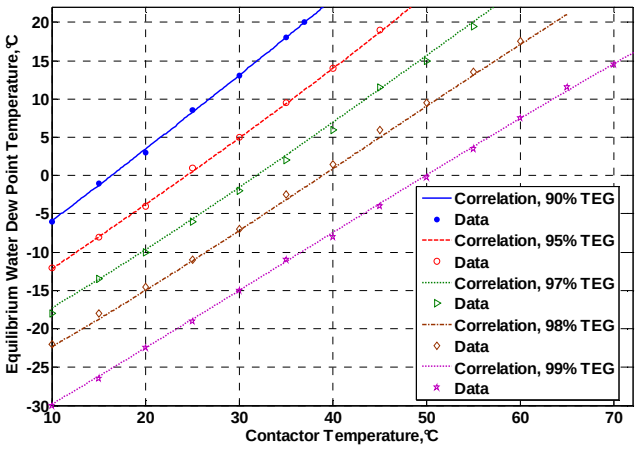

Figure 5.34: Water dewpoint of a natural gas stream in equilibrium with a TEG solution at various contactor temperatures and TEG concentrations ranging from 90% to 99% (Bahadori A. and Vuthaluru H. B. (2009a) *Journal of Natural Gas Science & Engineering*. 1(3) (2009), pp. 68-71)

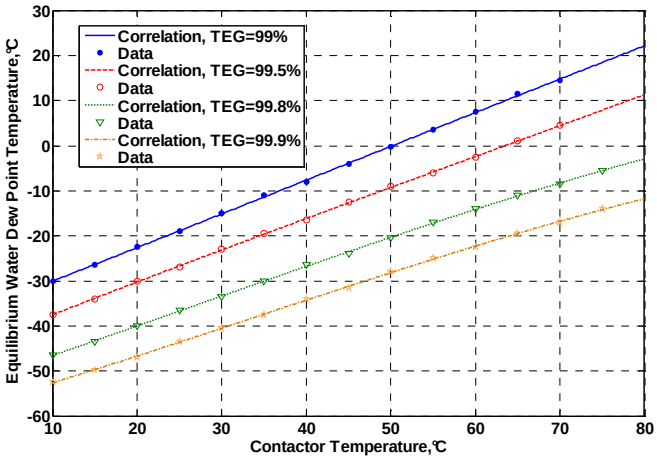

Figure 5.35: Water dewpoint of a natural gas stream in equilibrium with a TEG solution at various contactor temperatures and TEG concentrations ranging from 99% to 99.9% (Bahadori A. and Vuthaluru H. B. (2009a) *Journal of Natural Gas Science & Engineering*. 1(3) (2009), pp. 68-71).

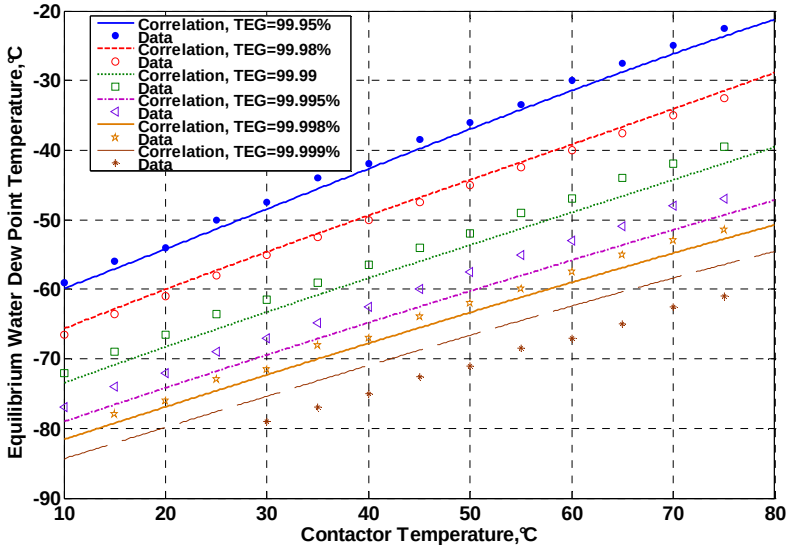

Figure 5.36: Water dewpoint of a natural gas stream in equilibrium with a TEG solution at various contactor temperatures and TEG concentrations ranging from 99.9 % to 99.999% (Bahadori A. and Vuthaluru H. B. (2009a) *Journal of Natural Gas Science & Engineering*. 1(3) (2009), pp. 68-71)

The correlation proposed in this study is a novel and unique expression which is non-existent in the literature. It is a approach designed to be of immense practical value for gas engineers to have a rapid check on water dew point of natural gas at various temperatures and TEG weight percents without performing any experimental measurements. In particular, personnel dealing with natural gas dehydration and processing would find the proposed approach to be user friendly involving no complex expressions with transparent calculations.

5.12 Displacement losses from storage containers

Filling losses in tanks due to the expansion of the liquid into the tank and the vapors that are forced out of the tank are generally called displacement losses. Restrictions on vaporization loss of petroleum products give added emphasis to the accurate prediction of vapor pressure and hydrocarbon losses for petroleum products. In this study, a correlation was developed to estimate the true vapor pressure of liquefied petroleum gas (LPG) and natural gasoline as a function of Reid Vapor pressure (RVP), and temperature as well as the vapor pressure of different mixtures of propane and butane were correlated as a function of ambient air temperature and propane volume percent. Also, the filling losses from storage containers were estimated in percentage of liquid pumped in tanks as a function of working pressure and vapor pressure at liquid temperature (Bahadori and Vuthaluru 2010j).

According to the authors' knowledge, there is no transparent and simplified approach exists in the current literature for the rapid estimation of filling losses associated with the liquid expansion into the storage tank. In view of this necessity, our efforts have been directed at formulating correlation which can assist engineers for rapid estimation of vapor pressure of LPG and natural gasoline as well as filling losses associated with the liquid expansion into the storage tank. The correlation proposed in this study is simple and has an unique expression which is non-existent in the literature. The proposed approach can be of significant practical value for the process engineers and scientists to have a quick check on the prediction of the displacement losses from storage containers as well as for rapid estimation of vapor pressure of LPG and natural gasoline (Bahadori and Vuthaluru 2010j).

Figure 5.37 illustrates the results of proposed correlation for the prediction of true vapor pressure of LPG and natural gasoline as a function of temperature and Reid vapor pressure. The figure also compares the obtained results of the new developed correlation with some available reported data (Gas Processors and Suppliers Association 2004). As can be seen, there is a good agreement between predicted and reported values. This correlation covers LPG and natural gasoline for Reid vapor pressure up to 400 kPa (gauge) and temperature range between -10°C to 100°C. Figure 5-38 presents the results of the proposed correlation for predicting the vapor pressure of propane and butane mixtures as a function of propane volume percent and ambient outside temperature comparing with some typical data from Frankel (2000). The results of the proposed correlation were accurate and acceptable, where the deviation from the typical reported data was very low (Bahadori and Vuthaluru 2010j).

Figure 5-39 compares the new proposed correlation results for predicting the filling losses from storage containers in percent of liquid pumped in to available reported data (Gas Processors and Suppliers Association, 2004). As shown, there is a good matching between predicted and reported values. This correlation covers the reported data for working pressure less than 250 kPa (abs) and for vapor pressure at liquid temperature in kPa (abs) for less than 100 kPa (abs) (Bahadori and Vuthaluru 2010j).

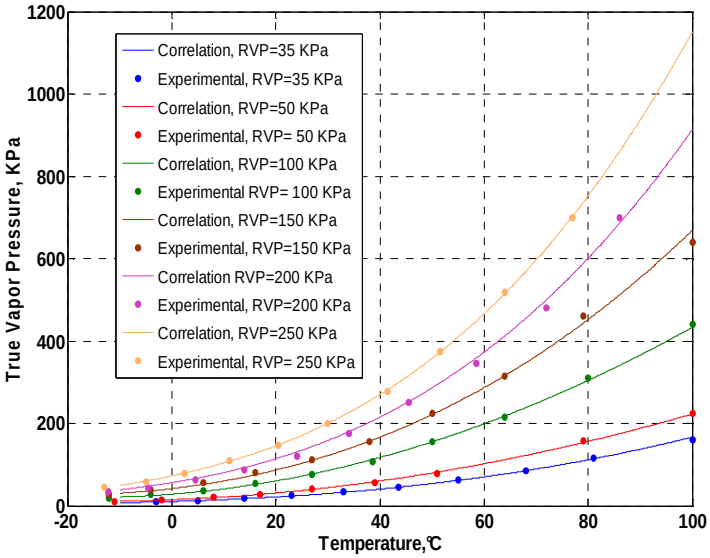

Figure 5.37: Comparison of predicted values of new developed correlation with some experimental data (Gas Processors and Suppliers Association 2004) for true vapor pressure of LPG and natural gasoline (Bahadori A. and Vuthaluru H. B, (2010j) *Journal of Loss Prevention in the Process Industries*, 23 (2010) 367-372)

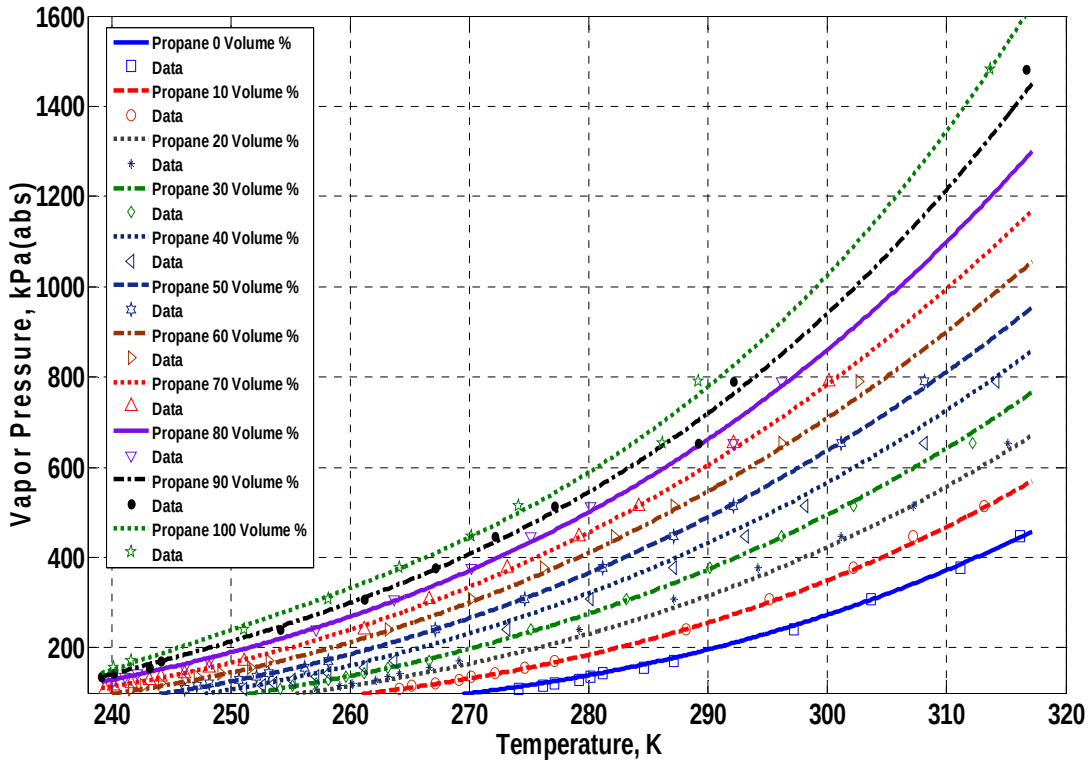

Figure 5.38: Proposed correlation's results in predicting the vapor pressure of propane and butane mixtures as a function of propane volume percent and ambient out side temperature comparing with some typical data (Bahadori A. and Vuthaluru H. B, (2010j) *Journal of Loss Prevention in the Process Industries*, 23 (2010) 367-372)

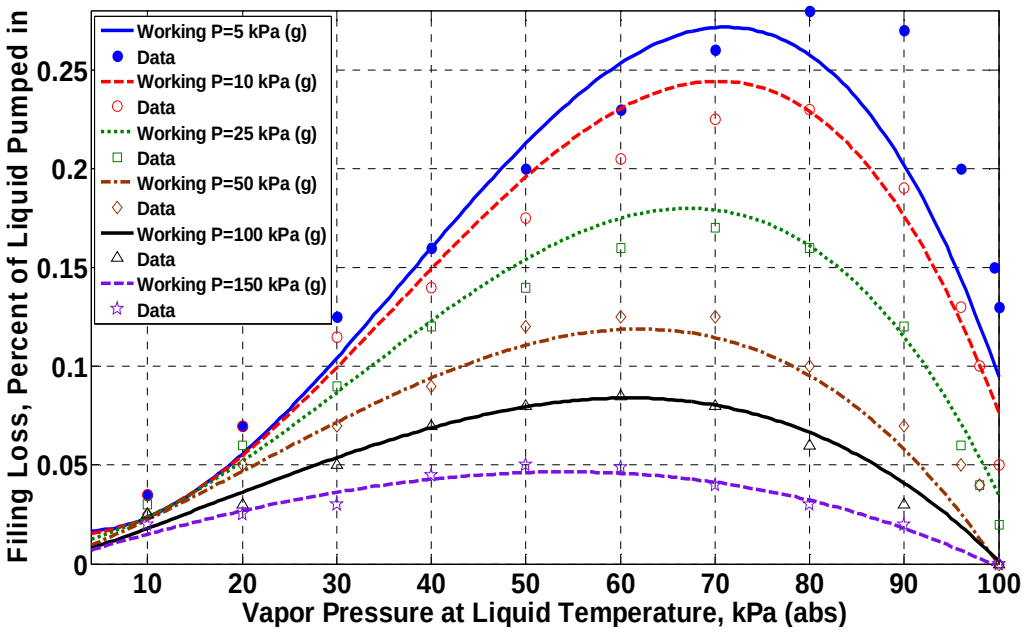

Figure 5.39: Comparison of predicted and reported data (Gas Processors and Suppliers Association 2004) of the displacement losses from storage containers (Bahadori A. and Vuthaluru H. B, (2010j), Journal of Loss Prevention in the Process Industries, 23 (2010) 367-372)

5.13 Storage pressure of volatile hydrocarbons

A design working pressure of any storage tank can be determined to prevent breathing, and thereby save standing storage losses. However, this should not be used in lieu of any environmental regulatory requirements regarding the design of storage tanks. The environmental regulatory requirements for the specific location should be consulted prior to the design of storage facilities. Generally there are regulatory requirements specifying the type of storage tank to be used, based on the storage tank capacity and the vapor pressure of the product being stored. In addition, there are usually specific design requirements, for example in the type of seals to be used in a floating roof tank. The working pressure required to prevent breathing losses depends upon the vapor pressure of the product, the temperature variations of the liquid surface and the vapor space, and the setting of the vacuum vent. Figure 5.40 compares the results of new proposed correlation for predicting the storage pressure of gasoline of various volatilities in uninsulated tanks with some available reported experimental data (Gas Processors and Suppliers Association 2004). This correlation covers gasoline of various volatilities in uninsulated tanks for temperature variations between 20-50°C and true vapor pressure up to 250 KPa (abs).

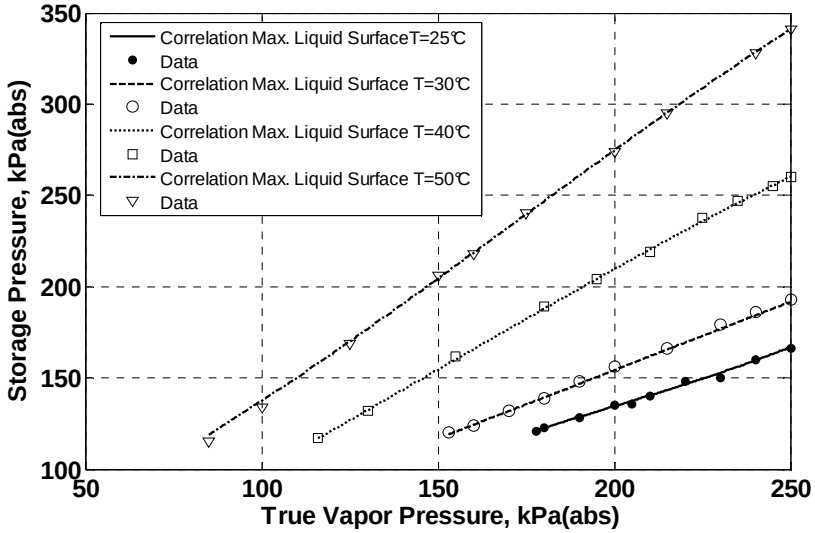

Figure 5.40: Comparison of predicted and reported experimental values of storage pressure for gasolines Bahadori A. (2009c), *Journal of the Energy Institute* 82(1), p. 61

5.14 Molten sulfur viscosity

Improved molten and final formed solid product quality can be greatly enhanced by degassing the molten sulfur produced from Claus sulfur recovery units. Controlling molten sulfur viscosity is a critical operating and engineering parameter in appropriate designing a molten sulfur supply pipeline and downstream handling facilities (Bahadori and Vuthaluru 2010k). In this section of thesis, a simple predictive tool is presented here for the prediction of the viscosity of liquid sulfur as a function of temperature and hydrogen sulfide content of liquid sulfur, using an Arrhenius-type asymptotic exponential function where the values predicted by the proposed predictive tool are a near perfect match with the experimental data (Bahadori and Vuthaluru 2010k).

The proposed method is superior due to its accuracy and clear numerical background, wherein the relevant coefficients can be retuned quickly for various cases. Degassed sulfur will become highly viscous and difficult to pump above 157- 160°C. As the H_2S is removed by degassing, viscosity will approach the viscosity of pure sulfur. Therefore, molten sulfur temperature should be monitored at key points in the process and maintained below the viscous transition, which is dependent upon H_2S content of the molten sulfur, and at the same time safely above the solidification temperature (Bahadori and Vuthaluru 2010k). In lights of the above, there is an essential need to develop a new correlation for predicting the viscosity of pure liquid sulfur as a function of temperature and partial pressure of hydrogen sulfide. Figure 5.41 illustrates the comparison results of the new developed correlation for predicting the viscosity of liquid sulfur with the reported data (GPSA Engineering Data Book, 2004). As can be seen, the proposed method returned results in excellent accuracy.

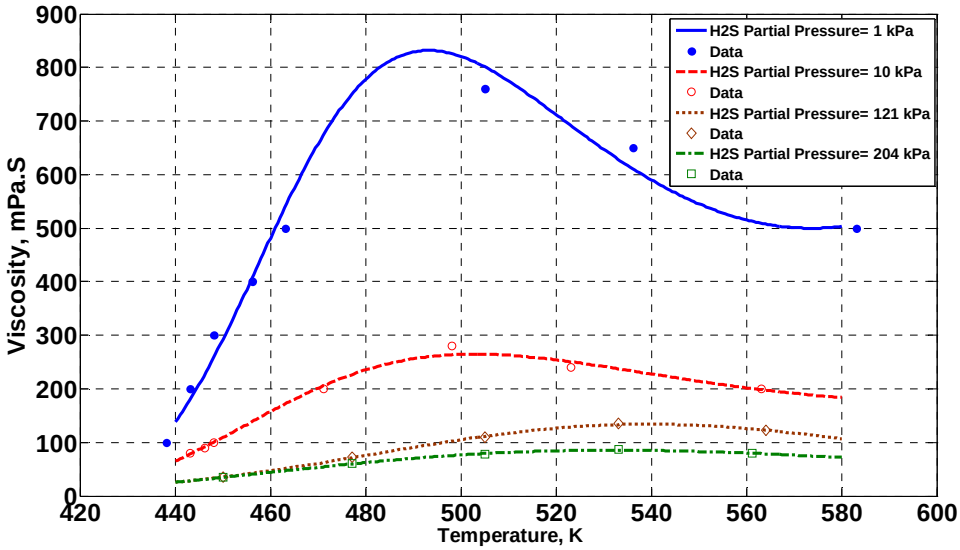

Figure 5.41: Comparing the obtained results of the new correlation for predicting the viscosity of liquid sulfur (Bahadori A. and Vuthaluru H. B, (2010k), *Petroleum Technology Quarterly* 15(1) pp.13-14).

5.15 Simple equations to correlate theoretical stages and operating reflux in fractionators

Virtually all gas processing plants producing natural gas liquids require at least one fractionator to produce a liquid product which can meet sales specifications. Fractionation is one of the pivotal unit operations in refineries, gas processing and other industries utilized to separate mixtures into individual products (Bahadori and Vuthaluru, 2010 L). However, it is capital and energy intensive and, with decreasing relative volatility, the size and energy requirements of a column tend to increase.

The primary parameters involved in the design of fractionators are the number of stages and the reflux ratio. The aim of this study is to develop easy-to-use equations, which are simpler than current available models involving a large number of parameters and requiring more complicated and longer computations, for an appropriate prediction the operating reflux ratio for a given number of stages. Alternatively, for a given reflux ratio, the number of stages can be determined (Bahadori and Vuthaluru, 2010 L). These equations can be of immense practical use for the engineers.

In particular, process engineers would find the proposed approach to be user friendly involving no complex expressions with transparent calculations (Bahadori and Vuthaluru, 2010 L). All process engineers develop a reflux-stage plot and extrapolate it to determine the minimum reflux ratio and minimum number of stages. To develop this plot, simulation runs are performed at different number of stages while keeping the mass balance, product compositions, and the ratio of the feed stage to the number of stages constant. The reflux ratio is then allowed to vary follow by creating a plot of the number of stages versus reflux or reflux ratio is plotted. The curve is extrapolated asymptotically to an infinite reflux ratio to an infinite number of stages to obtain the minimum reflux ratio and asymptotically to an infinite reflux ratio to obtain the minimum number of stages (Bahadori and Vuthaluru, 2010 L).

This is a complicated and time consuming approach. Therefore there is a need to develop a simple approach which enables the determination the above-mentioned parameters with ease and computationally less time consuming unlike conventional simulation approaches involving the plotting of graphs with a large number of parameters, requiring more complicated and longer computations. Figures 5.42 and 5.43 illustrate the results of proposed simple equations for predicting the operating reflux as a function of ratio of minimum stages to theoretical stages and minimum reflux ratio. This correlation can useful for the process engineers enabling them to quickly estimate the ratio of minimum stages to theoretical stages to the minimum reflux ratio and the operating reflux ratio (Bahadori and Vuthaluru, 2010 L).

All process engineers develop a reflux-stage plot and extrapolate it to determine the minimum reflux ratio and minimum number of stages. To develop this plot, simulation runs are performed at different number of stages while keeping the mass balance, product compositions, and the ratio of the feed stage to the number of stages constant. The reflux ratio is then allowed to vary. The number of stages versus reflux or reflux ratio is plotted. The curve is extrapolated asymptotically to an infinite reflux ratio to an infinite number of stages to obtain the minimum reflux ratio.

The proposed novel approach, however, enables the determination of the above-mentioned parameters with ease and computationally less time consuming unlike conventional simulation approaches involving of plotting of graphs etc. As the economic optimization of a distillation column involves the selection of the number of trays and feed location, as well as the operating conditions to minimize the total investment and operation cost, the proposed approach for an accurate and fast estimation of operating conditions will lead to the reduction in the costs associated with not only designing the fractionation columns but can also provide the optimum

operating reflux conditions for the separation of any multi-component mixture (Bahadori and Vuthaluru, 2010 L).

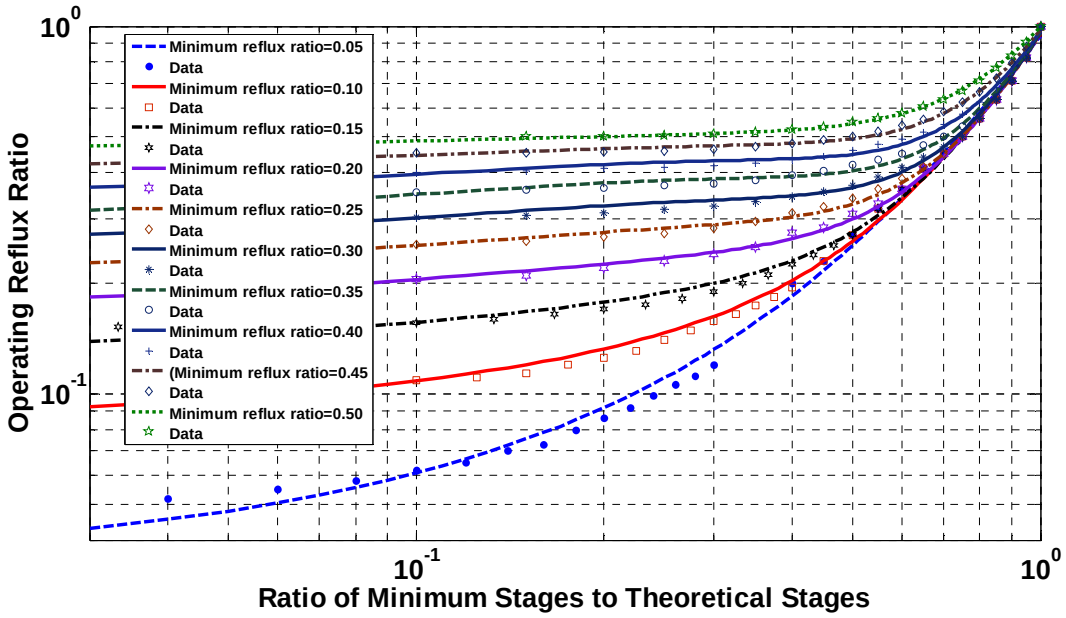

Figure 5.42: Proposed equations performance in comparison with literature data for minimum reflux ratio less than 0.5, (Bahadori A. and Vuthaluru H. B, *Energy*, 35 (2010L) 1439–1446)

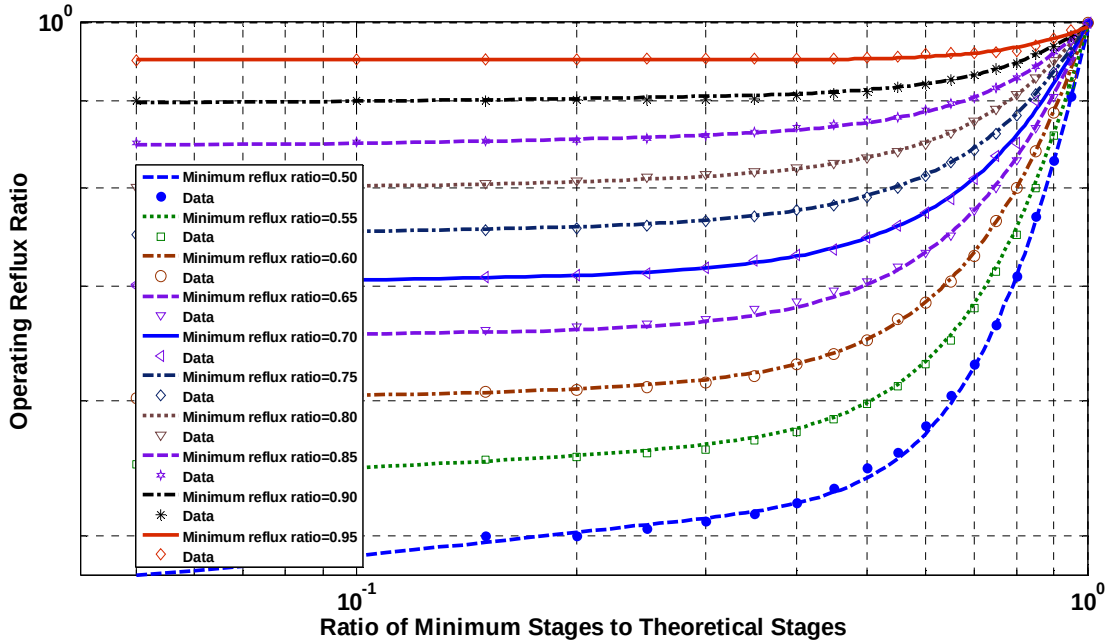

Figure 5.43: Proposed equations performance in comparison with literature data [17, 23] for minimum reflux ratio more than 0.5, (Bahadori A. and Vuthaluru H. B, *Energy*, 35 (2010L) 1439–1446)

5.16 Surface tension of paraffin hydrocarbons

Surface tension, an important property where wetting, foaming, emulsification, and droplet formation are encountered, is used in the design of fractionators, absorbers, two-phase pipelines, and in reservoir calculations. In this study, a simple correlation is developed to predict paraffin hydrocarbon surface tension as a function of molecular weight and temperature. The new correlation is suitable for the range of temperatures between -30°C and 150°C and the paraffin hydrocarbon molecular weights between the range of 30 and 240 (Bahadori and Mokhatab 2009b).

These tuned coefficients help to cover experimental data in temperature variation of -30°C to 150°C; however, the coefficients can be changed if more accurate experimental data are available. Figure 5.44 compares the obtained results of the new developed correlation with some reported data (Gas Processors and Suppliers Association, 2004).

It is therefore recommended to use this correlation for predicting the surface tension of paraffin hydrocarbons within the proposed ranges. In brief, a new correlation was developed to predict paraffin hydrocarbons surface tension as a function of molecular weight and temperature. The new correlation is suitable for the range of temperatures between -30°C and 150°C and the paraffin hydrocarbon molecular weights between the range of 30 and 240.

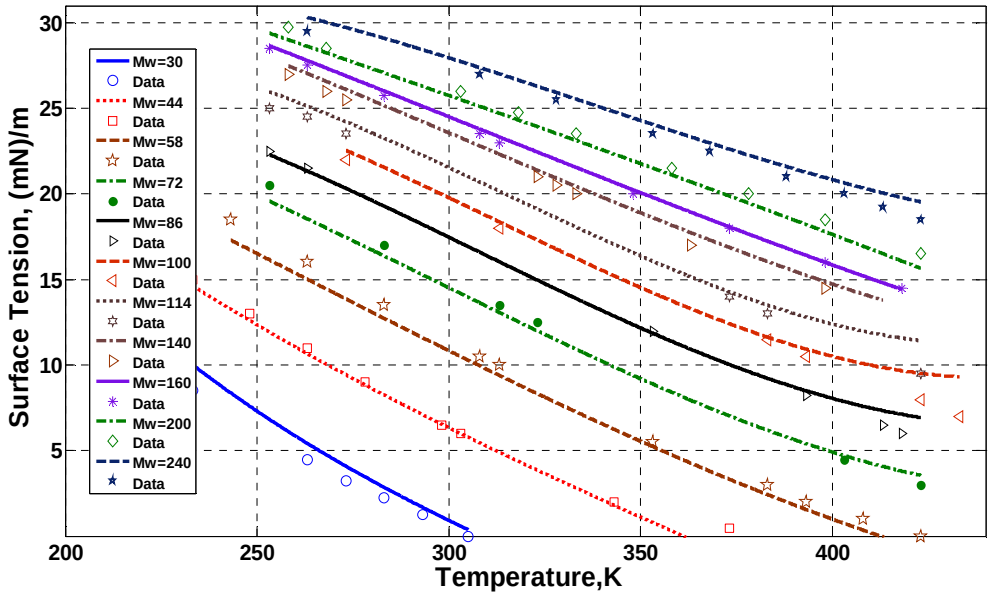

Figure 5.44: Comparing predicted values of new developed correlation for predicting surface tension of paraffin hydrocarbons with some reported data Bahadori A. and Mokhatab S. (2009b) Correlation rapidly estimates pure hydrocarbons' surface tension", *Journal of the Energy Institute* 82 (2), pp.118-119

5.17 Thermal conductivity of liquid paraffin hydrocarbons

Knowledge of the thermal conductivity of the fluids involved is an essential for the prediction of the rate of heat transfer in all heat exchangers. Therefore in this work a correlation was developed to accurately predict the thermal conductivity of liquid paraffin hydrocarbons as a function of temperature and molecular weight (Bahadori, 2008b).

Thermal conductivity data is extremely important in designing heat exchangers. Heat transfer coefficients in these components are usually computed using correlations which require thermal conductivity data. Due to the importance of two-phase heat transfer processes in many processes, thermal conductivity of the saturated liquid and vapor are crucial in the processes. It is difficult to measure the thermal conductivity at saturation and thus single-phase measurements will be extrapolated to saturation conditions (Bahadori, 2008b). The higher thermal conductivities and larger temperature gradients cause a greater heat flux in a one-dimensional system with correspondingly larger responses to changes in gas thermal conductivity. The physical mechanism of thermal-energy conduction in liquids is qualitatively the same as in gases, however, the situation is highly more complex because the molecules are more closely spaced and molecular force field exert a strong influence on the energy exchange in the collision process (Bahadori, 2008b).

Figures 5.45 and 5.46 show new proposed correlation results for the thermal conductivity of liquid paraffin hydrocarbons as a function of temperature and molecular weight in two different view points.

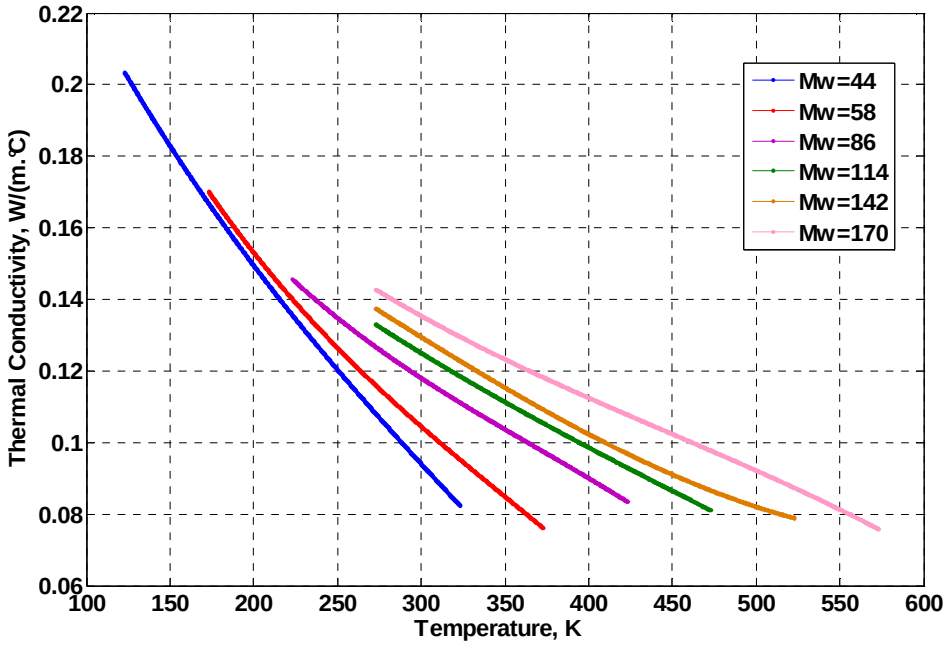

Figure 5.45: Prediction of the thermal conductivity of different liquid paraffin hydrocarbons as a function of temperature using the proposed correlation Bahadori A. (2008b) *Journal of the Energy Institute* 81 (1) 59-61

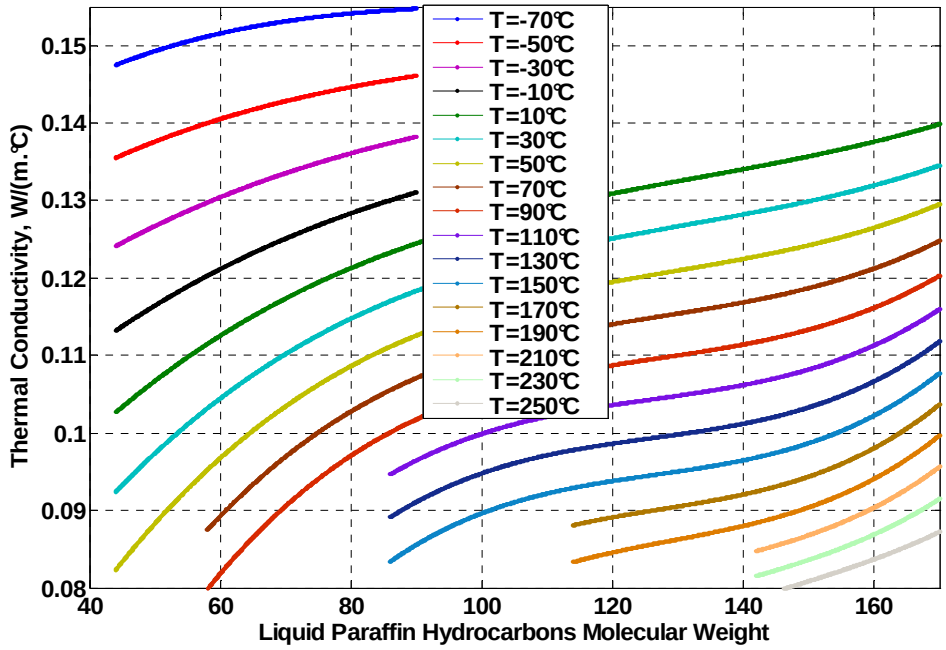

Figure 5.46: Prediction of the thermal conductivity of liquid paraffin hydrocarbons using the proposed correlation from another view point Bahadori A. (2008b) Journal of the Energy Institute 81(1) 59-61

5.18 Downcomer velocity and vapour capacity factor in fractionators

Fractionation is one of the pivotal unit operations in refineries and gas processing industries which is the single largest energy-degrading processing unit utilized to separate mixtures into individual products (Bahadori and Vuthaluru 2010m). A reliable design method for sizing tray fractionators must be taken into account for foaming which is also a major consideration in many process systems.

The aim of section is to develop a simple predictive tool, which is easier to use than current available techniques by avoiding large number of parameters where requires less complicated and shorter computations, for the accurate determination of downcomer velocity and vapor capacity factor as a function of tray spacing and density (Bahadori and Vuthaluru 2010m). The results can be used in follow-up design calculations to size fractionators without foaming formation for tray spacing up to 1.2 m, vapor densities up to 100 kg/m^3 and liquid and vapor density differences up to 950 kg/m^3 (Bahadori and Vuthaluru 2010m). The present study discusses the formulation of a simple predictive tool which can be of significant importance for the engineers associated with the design of fractionators. The approach is of practical significance for petroleum and chemical industries in terms of assessing operational issues. In particular the proposed correlation gives an advance indication of key parameters which could potentially enable practice engineers to take appropriate remedial measures to avoid foaming which is a major consideration in many process separations systems (Bahadori and Vuthaluru 2010m).

Figures 5.47 and 5.48 illustrate the results of proposed simple correlation for predicting the vapor capacity factor, as a function of vapor density and tray spacing (Bahadori and Vuthaluru 2010m). Figure 5.49 illustrates the results of proposed simple correlation for predicting the downcomer velocity (uncorrected), $m^3/h/m^2$ as a function of ratio of difference between density of liquid and vapor and tray spacing (Bahadori and Vuthaluru 2010m).

Furthermore, the model enables the determination the above-mentioned parameters with ease with less computational time unlike conventional rigorous simulation methods. The proposed tool appears to be superior owing to its accuracy and simple background, wherein the relevant coefficients can be retuned if new and more accurate data become available in the future. Our efforts in this investigation pave the way for alleviating the problems associated with the fractionator sizing due to foaming formation and fractionator inefficiencies by arriving at an

accurate estimation of downcomer design velocity and vapor capacity factor which can be used by process engineers for rapid monitoring the operational parameters (Bahadori and Vuthaluru 2010m).

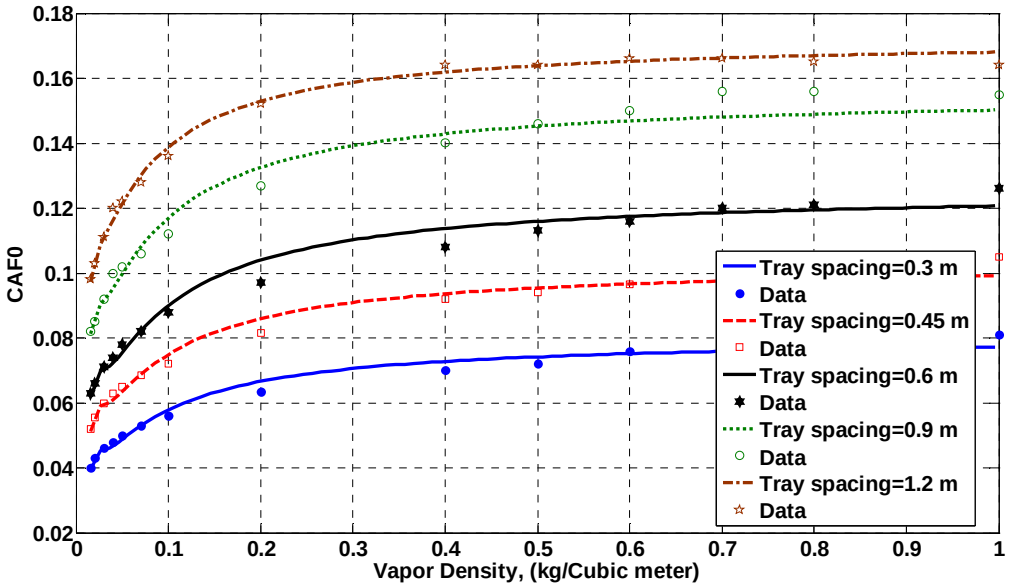

Figure 5.47: Proposed correlation performance in comparison with data for vapor density less than 1, Bahadori A. and Vuthaluru H. B, (2010m) *Applied Energy* 87, 2615-2620

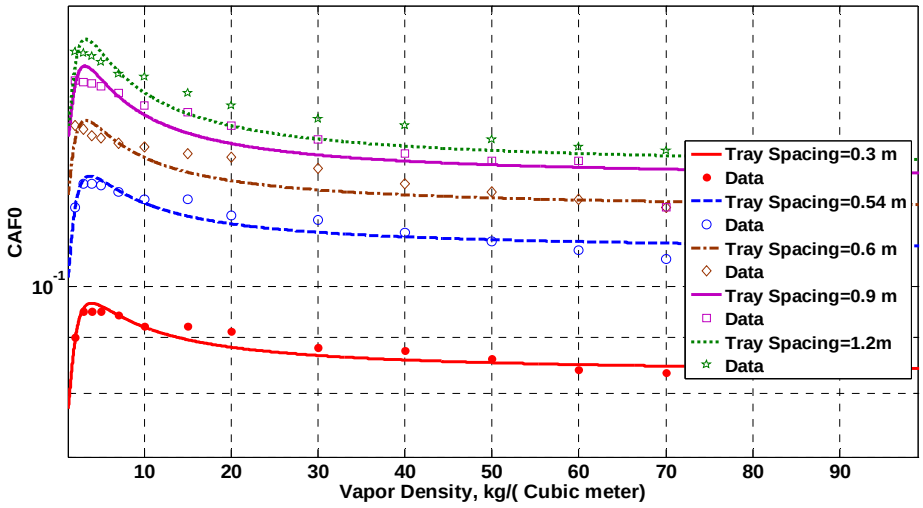

Figure 5.48: Proposed correlation performance in comparison with data for vapor density more than 1, Bahadori A. and Vuthaluru H. B, (2010m) *Applied Energy* 87, 2615-2620

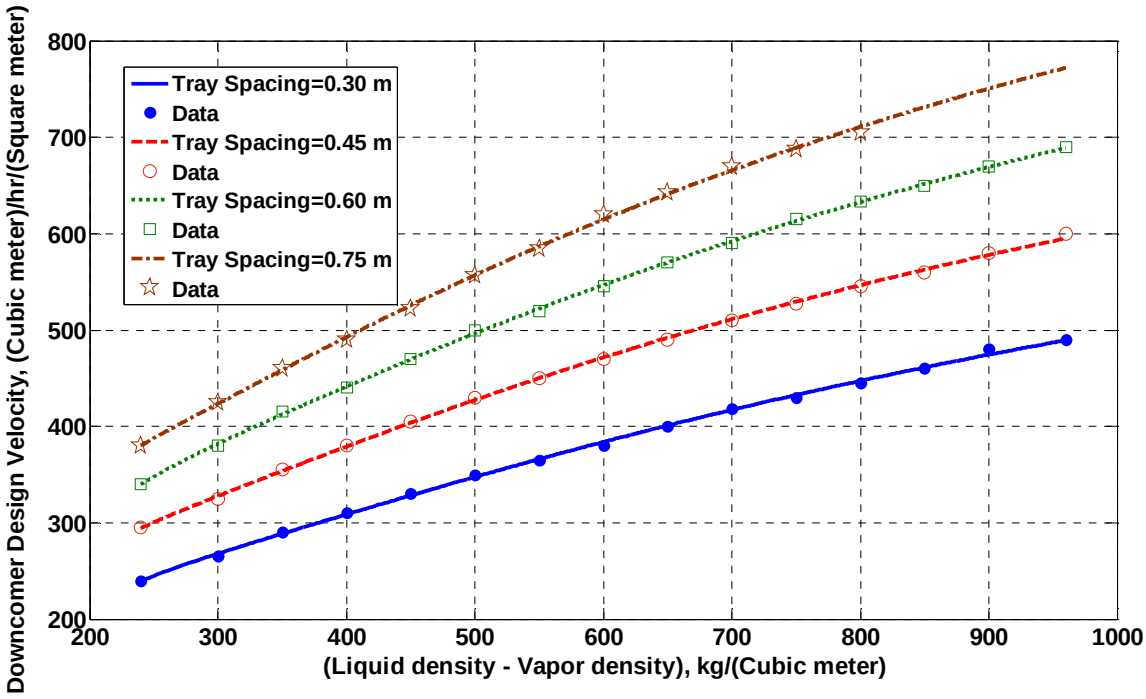

Figure 5.49: Proposed correlation performance in comparison with data for predicting downcomer design velocity Bahadori A. and Vuthaluru H. B, (2010m), *Applied Energy* 87, 2615-2620

5.19 Packed column sizing

Traditionally the majority of fractionation columns in natural gas processing plants were equipped with trays. Another option is to use packing. Packed columns offer a larger surface area per unit volume for mass transfer and the continuous gas to liquid contact throughout the column rather than at specific levels (such as in tray columns). For process design purposes, it is essential to estimate the pressure drop for enabling the proper operation of packed columns (Bahadori and Vuthaluru 2010c).

In this study, a simple generalized pressure drop correlation (GPDC) which is easier than existing approaches requiring more complicated and longer computations was developed for sizing randomly packed fractionation columns for pressure drops up to 150 mm water per meter of packing(Bahadori and Vuthaluru 2010c). This correlation can be used to estimate pressure drop for a given loading and column diameter. Alternatively, for a given pressure drop the diameter can be determined. Figures 5.50 and 5.51 illustrate the results of proposed predictive tool for predicting design dimensionless variables and the pressure drop in mm H_2O per meter of packing. The proposed correlation is simple to use, employing basic algebraic

equations that can easily and quickly be solved by a spreadsheet. In addition, the estimates are quite accurate, as evidenced by the comparisons with literature data. The proposed simple method works for sizing randomly packed columns for pressure drops up to 150 mm water per meter of packing. This approach is of significant practical value for practice engineers in terms of assessing operational issues. In particular, the proposed predictive tool gives an advance indication of key parameters which could potentially enable practice engineers to take appropriate remedial measures in the design of facilities for the natural gas production, transmission, and processing.

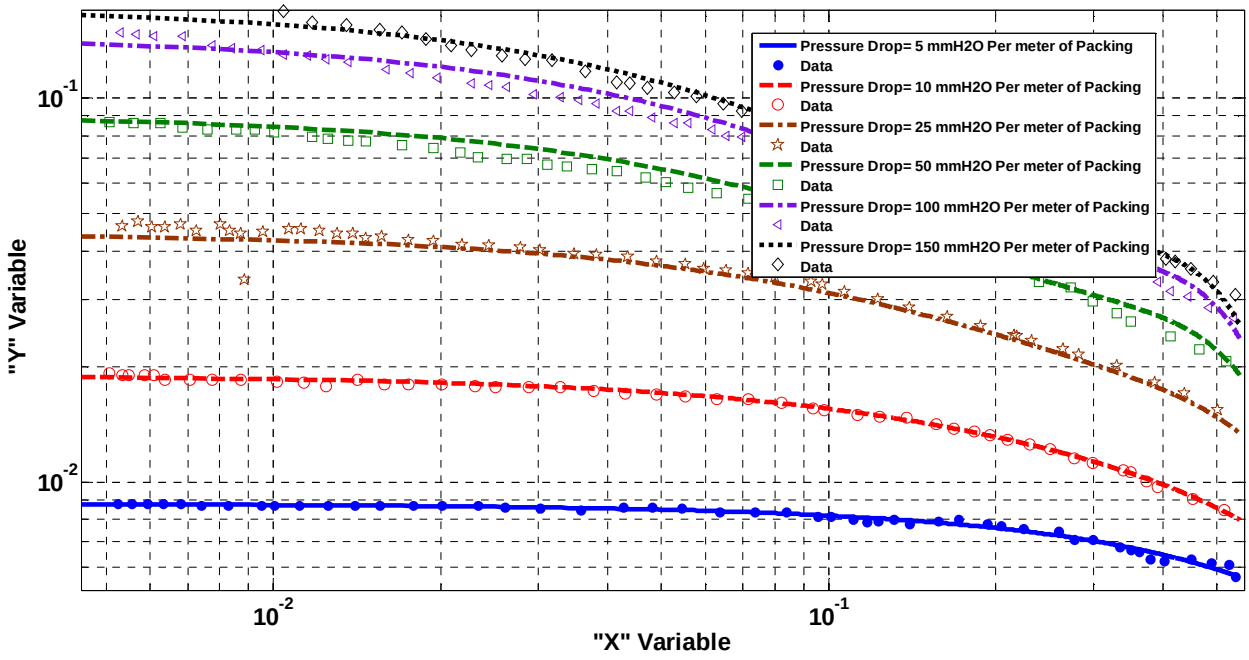

Figure 5.50: Comparison of correlation results with reported data from literature (GPSA, 2004) for "X" variable less than 0.5, Bahadori A. and Vuthaluru H. B. (2010c) *Journal of Natural Gas Chemistry*, 19(2), pp. 146-150

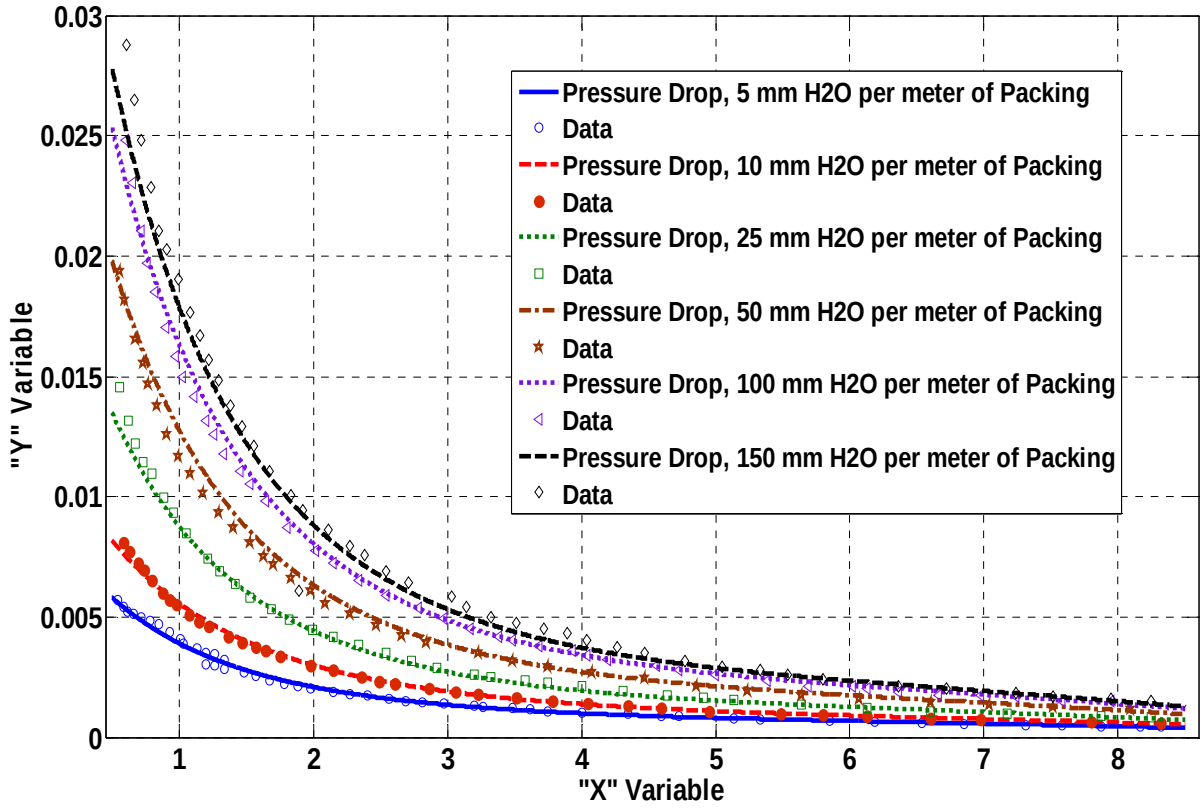

Figure 5.51: Comparison of correlation results with reported data from literature (GPSA, 2004) for "X" variable more than 0.5 (Bahadori A. and Vuthaluru H. B. (2010c) *Journal of Natural Gas Chemistry*, 19(2), pp. 146-150).

5.20 Determination of well placement and breakthrough time in horizontal wells

Gas and/or water coning encountered in many oil wells is a serious problem which results in lower oil production rates, lower oil recovery and increased lifting cost. In the present section, a predictive tool was developed to arrive at an appropriate prediction of dimensionless breakthrough times as well as optimum horizontal well placement in homogeneous and anisotropic reservoirs as a function of dimensionless rate and density difference ratio. The proposed approach can be of immense practical value for petroleum engineers to have a quick check on estimating the simultaneous water and gas breakthrough time and the optimum location of horizontal well in the presence of both gas cap and aquifer for wide range of conditions without the necessity of any field test trials. In particular, petroleum engineers would find the proposed approach to be user friendly involving transparent calculations with no complex expressions for their applications.

Figure 5.52 shows the performance of proposed predictive tool for the prediction of dimensionless breakthrough times (t_{DBT}) as a function of dimensionless rate (q_D) and density difference ratios (ψ) in comparison with model data (Papatzacos et al. 1989, 1991 and Ahmed 2006). Figure 5.53 illustrates the performance of predictive tool for estimation of dimensionless breakthrough times (t_{DBT}).

Figures 5.54 and 5.55 show the optimum horizontal well placement (B_{opt}) for two-cone case as a function of dimensionless rate (q_D) and density difference ratios (ψ) in comparison with model data (Papatzacos et al., 1989, 1991 and Ahmed 2006). Figures 5.56 and 5.57 show the performance of predictive tool for estimation of optimum well placement above the water oil contact (WOC). In this study, our efforts were directed at formulating a method that can assist engineers and researchers immensely for the estimation of simultaneous water and gas breakthrough time and the optimum horizontal well location in order to maximize the pre-breakthrough cumulative oil production.

It is expected that our efforts in this investigation will pave the way for arriving at an accurate prediction of the above-cited parameters which can be used by petroleum engineers for follow up calculations for estimating the simultaneous water and gas breakthrough time and the optimum horizontal well location.

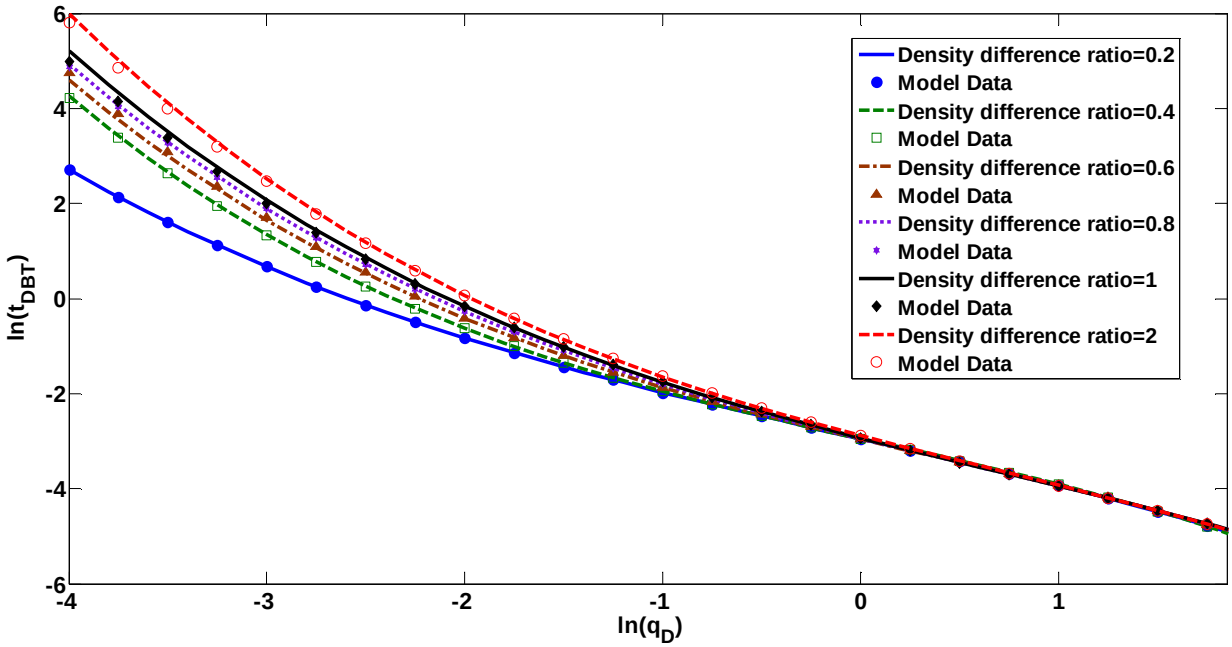

Figure 5.52: Prediction of dimensionless breakthrough times (t_{DBT}) in comparison with model data (Papatzacos et al. 1989, 1991 and Ahmed 2006) (Bahadori A(2011), Determination, *Journal of Petroleum Science and Engineering*, in press, 10.1016/j.petrol.2010.11.007)

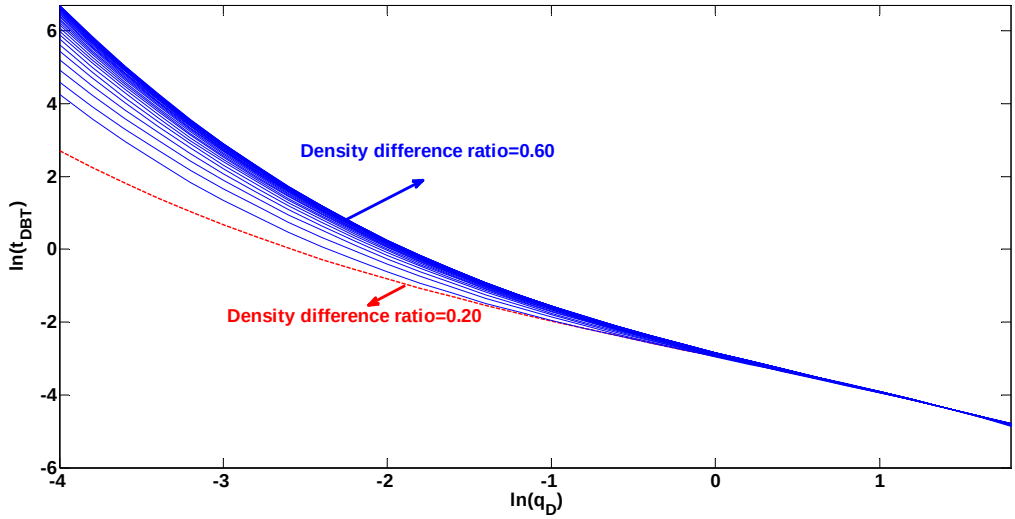

Figure 5.53: Performance of predictive tool for estimation of dimensionless breakthrough times (t_{DBT})(Bahadori A, (2011) *Journal of Petroleum Science and Engineering*, in press, 10.1016/j.petrol.2010.11.007)

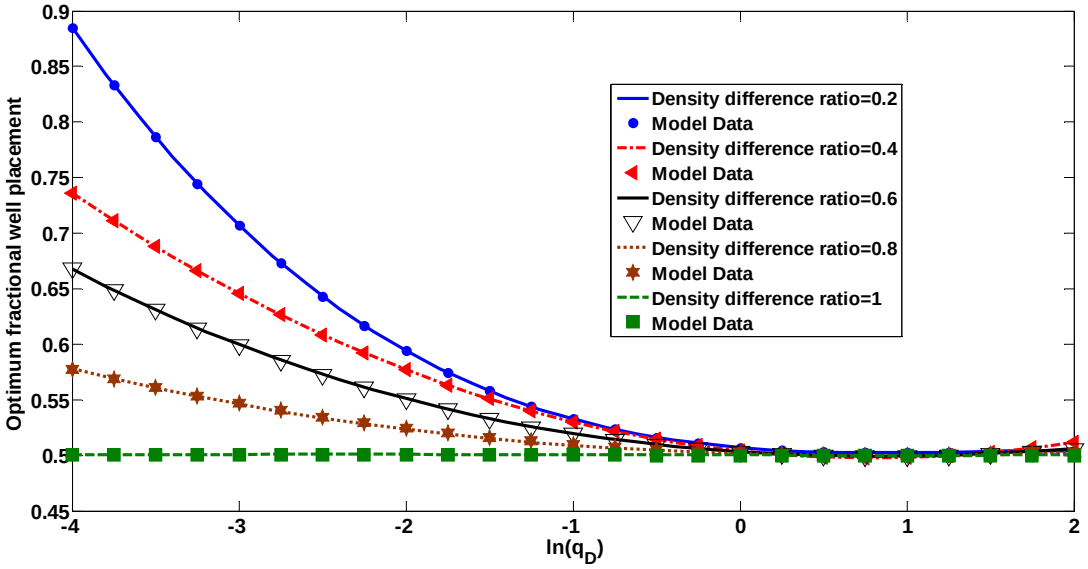

Figure 5.54: Prediction of optimum well placement above the WOC for density difference ratio (ψ) less than 1in comparison with model data (Papatzacos et al. 1989, 1991 and Ahmed 2006) (Bahadori A, (2011) *Journal of Petroleum Science and Engineering*, in press, 10.1016/j.petrol.2010.11.007)

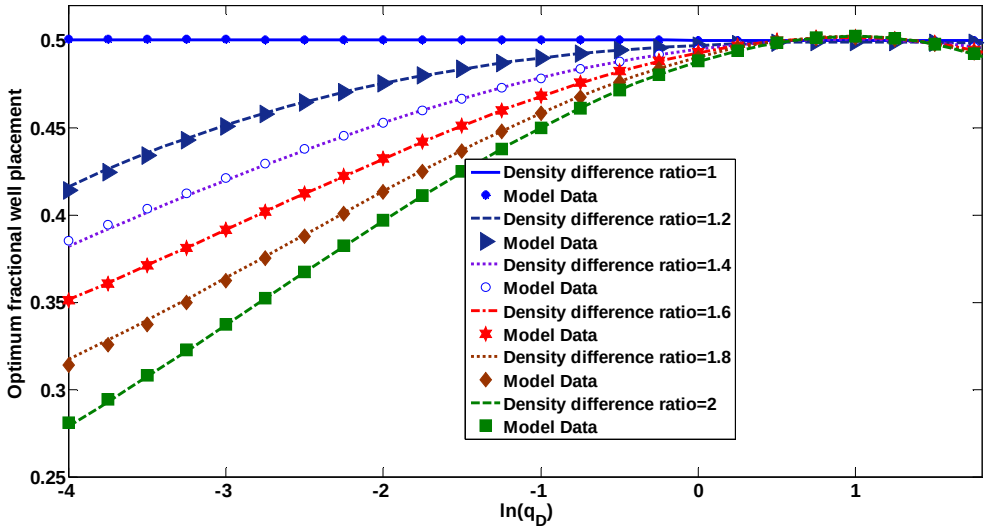

Figure 5.55: Prediction of optimum well placement above the WOC for density difference ratio (ψ) greater than 1 in comparison with model data (Papatzacos et al. 1989, 1991 and Ahmed 2006) (Bahadori A, (2011) *Journal of Petroleum Science and Engineering*, in press, 10.1016/j.petrol.2010.11.007)

.

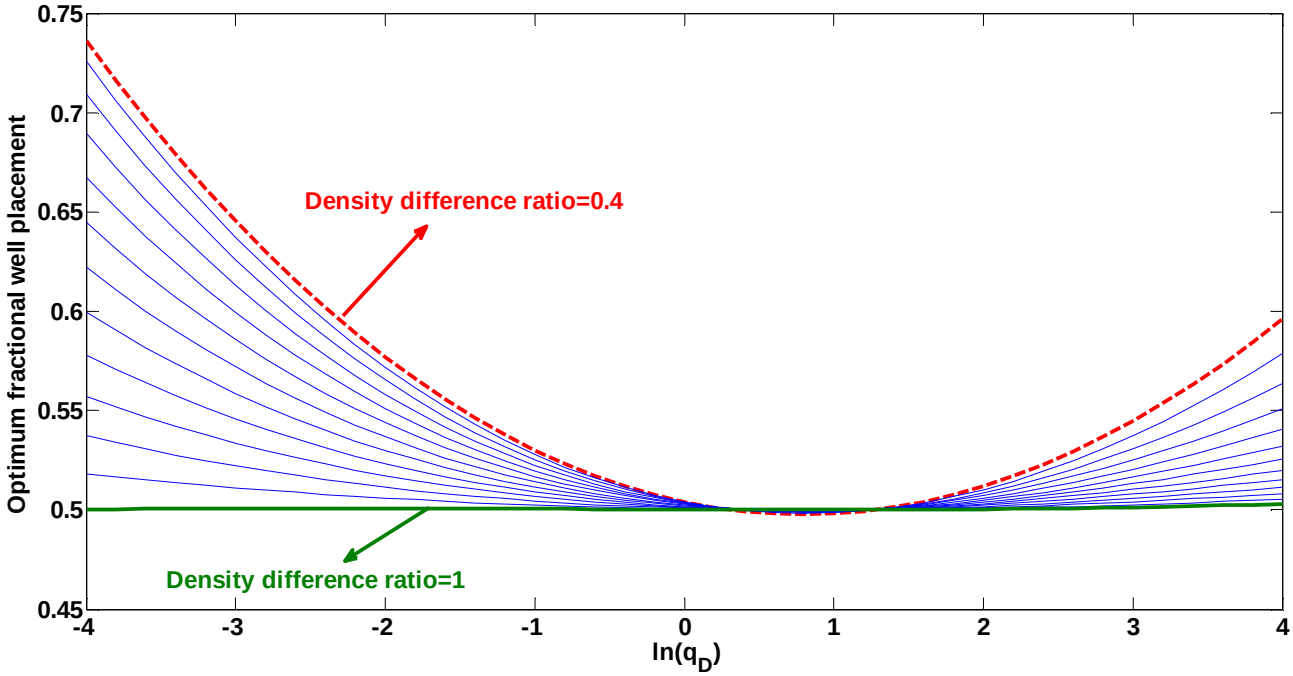

Figure 5.56: Performance of predictive tool for estimation of optimum well placement above the WOC for density difference ratio (ψ) less than 1(Bahadori A, (2011) *Journal of Petroleum Science and Engineering*, in press, 10.1016/j.petrol.2010.11.007)

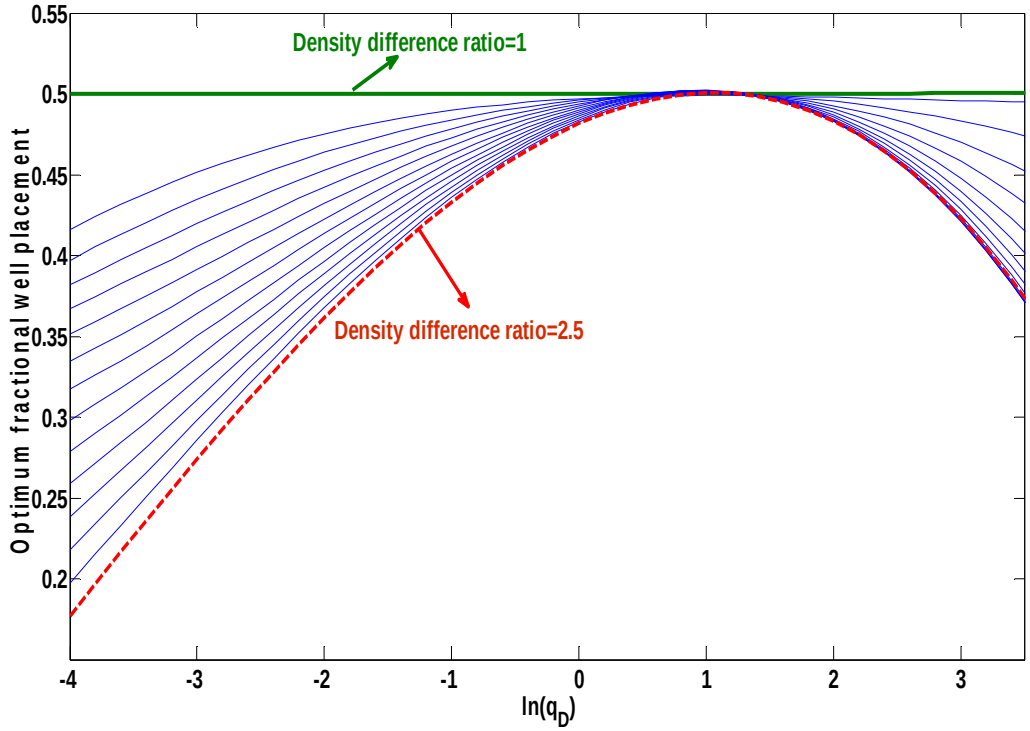

Figure 5.57: Performance of predictive tool for estimation of optimum well placement above the WOC for density difference ratio (ψ) greater than 1. (Bahadori A, (2011) *Journal of Petroleum Science and Engineering*, in press, 10.1016/j.petrol.2010.11.007)

5.21 Determination of the time to water cone breakthrough in horizontal oil wells

Production of associated water from the oil wells is a common but undesirable occurrence when the reservoir is underlain by a water layer. If the drawdown exerted on the reservoir exceeds a limiting value, the water cone can become unstable and water can start replacing the oil in the production stream. During past decades, several methods have been proposed in the form of mathematical expressions in determining the time to water cone breakthrough in horizontal wells. In the present work, new predictive tool, which is easier than existing approaches, less complicated with fewer calculations, is formulated to arrive at an appropriate estimation of the sweep efficiency as a function of the dimensionless well length and dimensionless vertical distance parameters to investigate the water cone breakthrough in horizontal wells. The results can be used in follow-up calculations for calculating time to breakthrough in a bottom-water-drive reservoir. Results show that the proposed predictive tool has a good agreement with the reported data. The proposed new approach can be of immense practical value for engineers and scientists to have a quick check on the time to water breakthrough in a bottom-water-drive reservoir for wide range of operating conditions without the necessity of any field test trials. In particular, petroleum engineers would find the proposed approach to be user friendly involving transparent calculations with no complex expressions for their applications.

Figures 5.58 and 5.59 shows the results of proposed predictive tool for the estimation of sweep efficiency as a function of dimensionless well lengths and dimensionless vertical distance in comparison with literature reported data (Ozkan and Raghavan 1988, 1990 and Ahmed 2006). As can be seen, the results show good agreement with the reported data and the proposed new correlation is accurate, reliable and acceptable. Figure 5.60 shows the performance of proposed predictive tool for wide range of conditions. To date, there is no new predictive tool for an accurate estimation of sweep efficiency as a function of dimensionless well lengths and dimensionless vertical distance. In view of this necessity, our efforts directed at formulating a new method that can help engineers and researchers immensely.

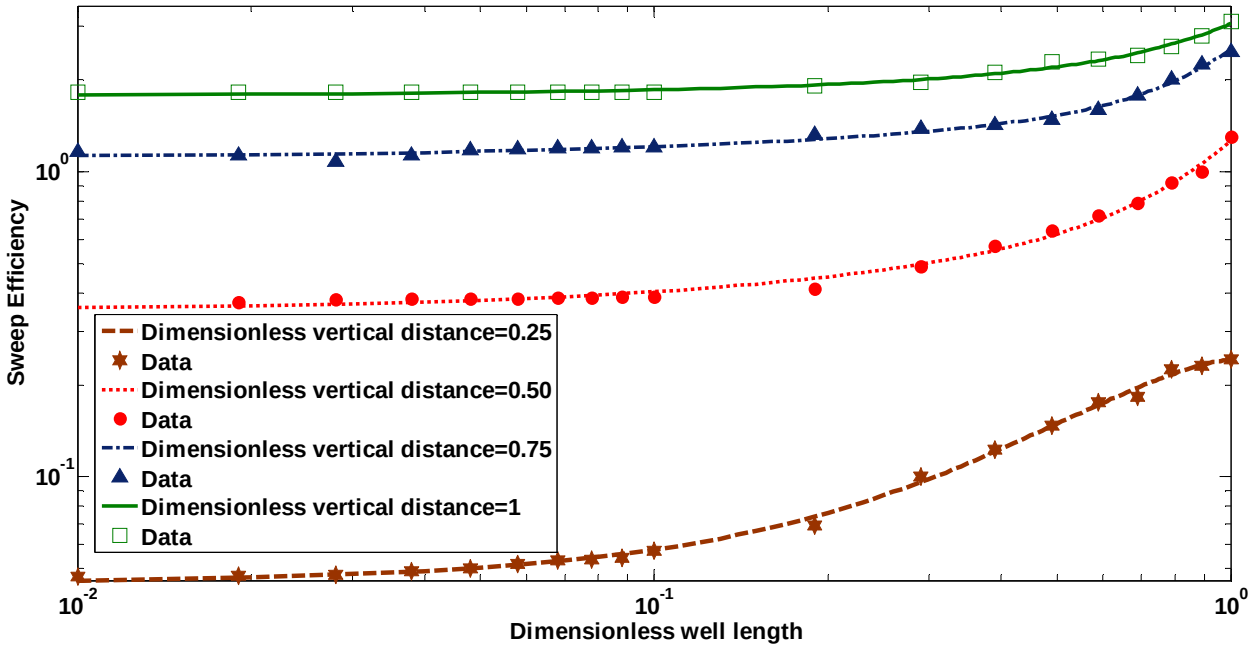

Figure 5.58: Prediction of sweep efficiency as a function of dimensionless well length and dimensionless vertical distance for dimensionless well length less than 1 in comparison with data (Ozkan and Raghavan 1988, 1990 and Ahmed 2006)

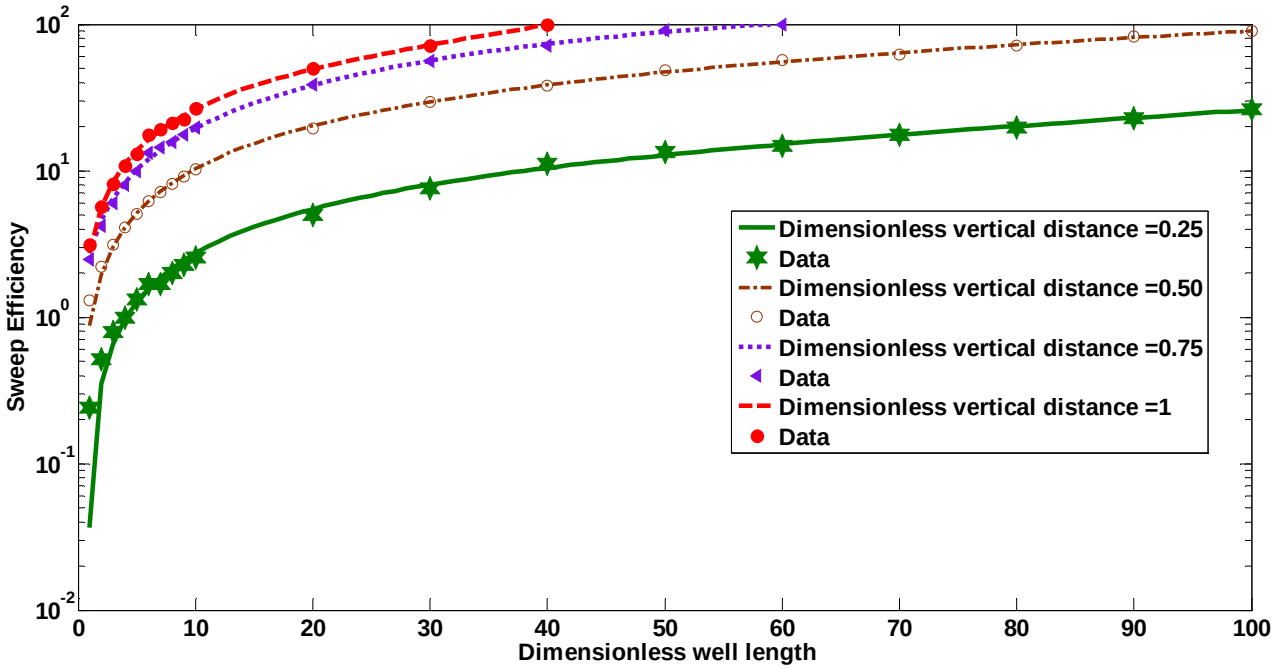

Figure 5.59: Prediction of sweep efficiency as a function of dimensionless well length and dimensionless vertical distance for dimensionless well length more than 1 in comparison with data (Ozkan and Raghavan 1988, 1990 and Ahmed 2006)

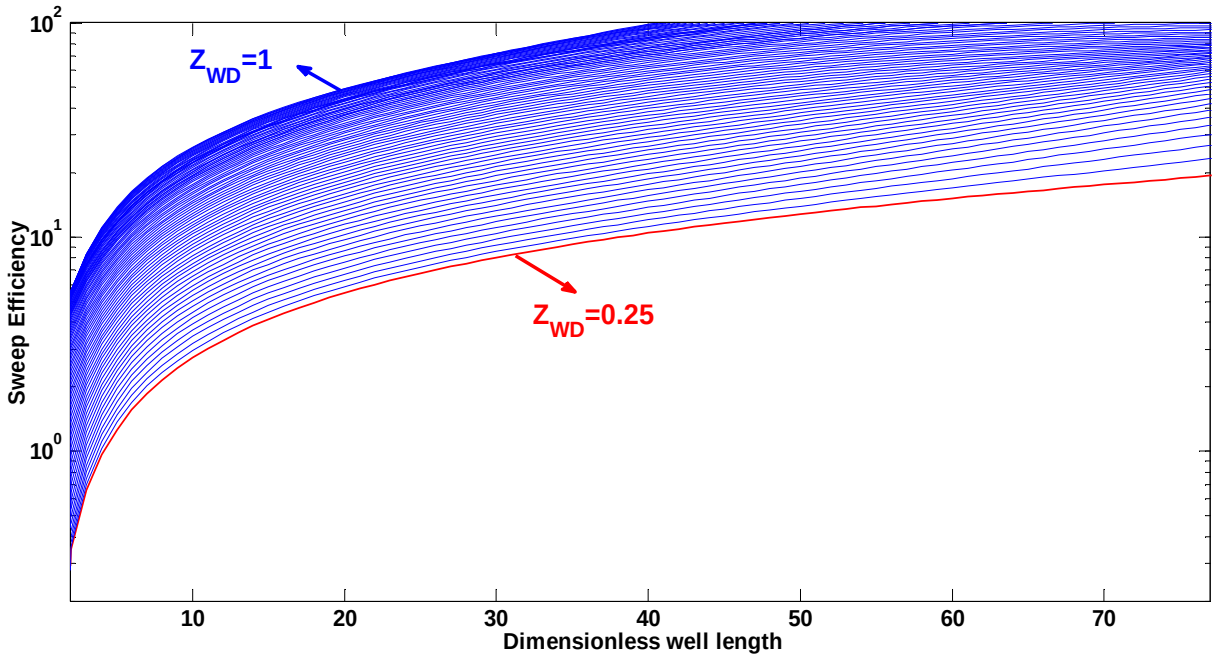

Figure 5.60: Proposed predictive tool' performance for Prediction of sweep efficiency as a function of dimensionless well length and dimensionless vertical distance.

CHAPTER 6

Development of predictive tools, testing and validation for typical process applications

In this chapter, accurate and reliable predictive tools are developed and formulated to predict the following process engineering design parameters.

- Emissivity of combustion gases
- Bulk modulus and volumetric expansion coefficient of water for leak tightness test of pipelines
- Silica carry-over and solubility in steam of boilers using simple correlation
- Carbon dioxide equilibrium adsorption isotherms
- Economic thickness of thermal insulation for process piping and equipment
- Estimation of thermal insulation thickness
- Transport properties of carbon Dioxide
- Estimation of saturated air water content at elevated pressures
- Aqueous solubility and density of carbon dioxide
- Thermal conductivity of hydrocarbons
- Water-hydrocarbon systems mutual solubility
- Design of radiant and convective sections of direct fired heaters
- Estimation of absorption/stripping factors
- Estimation of maximum shell-side vapour velocities through heat exchangers
- Prediction of dissolved oxygen saturation concentrations in aquatic systems
- Simple method for estimation of unsteady state conduction heat flow in slabs and spheres
- Estimation of performance of steam turbines using a simple predictive tool
- Compressed air transport properties
- Compressed air specific heat ratio at elevated pressures
- Prediction of saturated air dew point at elevated pressures
- Performance characteristics of cooling towers

Table 6.1: List of selected parameters, independent variables and the accuracy of methods

Engineering Parameter	Independent variable	Independent variable	Average absolute deviation percent
Emissivities of Combustion Gases	sum of partial pressures of CO_2 and H_2O, multiply by beam length, m	Temperature, K	2.2
bulk modulus of water	Temperature, K	Pressure, kPa	2.3
volumetric expansion coefficient water	Temperature, K	Pressure, kPa	2
Silica concentration in steam, mg/kg	Pressure, kPa	Boiler water silica, mg/kg	1.8
adsorption values (mmol/g)	Pressure, kPa	Temperature, K	1.7
Y variable from equation 6.2 estimate packed column size	Pressure drop, mmH_2O /(meter of packing)	X variable from equation 6.1	1.6
optimum economic thickness of insulation	diameter	Thermal conductivity	1.4
Estimation of Thermal Insulation Thickness for flat surfaces	Thermal Resistance	Temperature drop °C	1.2
The actual thickness for tubing and ducts	required insulation thickness (mm) for flat surfaces	outside diameter of tubing or duct. mm	1.5
CO_2 viscosity and thermal conductivity in W/(m.K) and (mPa.S)	Pressure, MPa	Temperature, K	1.4
The water content of air in milli litre of water per cubic meter of air (ml/m^3)	The Relative Humidity (RH) in percent at the atmospheric pressure or pressure for compressed air	T, Temperature in K	1.6
CO_2 solubility in aqueous	CO_2 Reduced partial pressure	Reduced	1.7

solutions		Temperature	
Density of CO_2	Pressure, kPa	Temperature	1.9
Liquid paraffin hydrocarbon thermal conductivity, *W/(m.°C)*	Molecular Weight	Temperature (K)	2.1
Hydrocarbon gases (at atmospheric pressure) *W/(m.°C)*	Temperature (K)	Molecular Weight	2.2
Liquid Petroleum Fractions, thermal conductivity, *W/(m.°C)*	Temperature (K)	Relative Density (Sp.Gr.)	2.3
Hydrocarbon solubility in water	Reduced temperature	Normal boiling point	2.4
the vapor pressure of LPG in *kPa*	Temperature (K)	Propane volume percent	0.9
absorbed heat fraction in the radiant section of a fired heater	Air to fuel mass ratio	the average heat flux to the tubes	0.6
Gross thermal efficiency	Percent excess air	Stack gas temperature	0.8
Absorption/stripping efficiency	Absorption/stripping factor	Number of stages	1.2
maximum shell-side vapour velocities through heat exchangers, m/s	Pressure, kPa(abs)	Molecular weight	1
dissolve oxygen saturation concentrations in aquatic systems, mg/litre	Temperature (K)	Chloride concentration, g/litre	0.8
average temperature change	Biot number	Fourier number	1
Efficiency correction factor in steam turbines	Percent Power Multi-Valve Steam Turbines	Number of stages	1.2
Efficiency Percent	Turbine rating, kW	Inlet stream pressure, kPa(abs)	1.4

Speed efficiency correction factor	Rated Speed, (RPM/1000)	Turbine rating, kW	1.6
Approximate steam rate, kg/(kW.h)	Pressure ratio, (Exhaust pressure, kPa(abs))/(Inlet pressure, kPa(abs))	Speed (RPM)	1.8
Air thermal conductivity, W/(m.K)	Pressure, kPa	Temperature, K	1.1
Viscosity, Pa.s$\times 10^{-4}$	Pressure, kPa	Temperature, K	0.90
Specific heat ratio	Pressure, kPa	Temperature, K	1.2
Dewpoint temperature at elevated pressure, K	Relative humidity, percent	Temperature, K	0.8
Cooling tower performance actor	Wet bulb temperature, K	Cooling water temperature, K	2.8

Currently several models available to predict design parameters in various industries. However, the calculations may require rigorous computer solutions. Therefore, developing the new predictive tools to minimize the complex and time-consuming calculation steps is needed to be simplified. Because most simulations require simultaneous iterative solutions of many nonlinear and highly coupled sets of equations, it is apparent that a mathematically compact, simple, and reasonably accurate equations that contained less tuned coefficients, as proposed in this research, would be preferable for computationally intensive simulations. In fact, the development of novel predictive tools by a small modification to the well-known Vogel-Tammann-Fulcher (VTF) (1921-1926) and Arrhenius equation (1889) equation was the primary motivation of this research, which, nevertheless, yielded correlations with accuracy comparable to that of the existing rigorous simulations. The details of proposed predictive tools are given in chapters 3 and 4 Table 6.1 summarises the selected parameters and relevant independent variables.

6.1 The emissivity of combustion gases

The main mode of heat transfer of combustion gases at high temperatures is via thermal radiation of the participating gases, consisting of mainly carbon dioxide and water vapor. Therefore, the information on the emissivities of carbon dioxide and water vapor would be crucial in analyzing thermal performance of a furnace or a boiler (Bahadori and Vuthaluru, 2009b). The aim of this study is to develop a correlation suitable for combustion engineers for predicting the emissivities of carbon dioxide and water vapor as a function of combustion gas temperature and the product of the partial pressure of carbon dioxide and water times the beam length (PL product).

Results indicate that the proposed tool has are nearly perfectly matched with the reported data and will be of particular interest to combustion engineers for their applications to the design and operation of gas-fired furnaces and boilers (Bahadori and Vuthaluru, 2009b). It should be noted that these calculations are based on an arbitrary gaseous fuel (mainly comprising of natural gas) assuming complete combustion at atmospheric pressure. The effects of C to H ratios are not expected to influence the emissivity predictions as other forms of hydrocarbons present in the selected arbitrary fuels will be in minor proportions; however the relevant calculations for natural gas will be presented in this article (Bahadori and Vuthaluru, 2009b). Charts developed by Hottel (1954) enable the calculation of total emissivity of the gas as a function of gas temperature and of the product of partial pressure and path length of the optical beam.

The application of theoretical and experimental data of infrared-band spectra to the calculation of radioactive performance of combustion chambers is complicated by the contributions of different bands to the gas emissivity varies differently with the path length L (Bahadori and Vuthaluru, 2009b). In reality, gases such as air, oxygen (O_2), hydrogen (H_2), and nitrogen (N_2) have a symmetrical molecular structure and neither emit nor absorb radiation at low to moderate temperatures. Hence, for most engineering applications, such non-participating gases can be ignored. However, polyatomic gases, such as water vapor (H_2O) and carbon dioxide (CO_2) emit and absorb significant amounts of radiation (Bahadori and Vuthaluru, 2009b).

These participating gases absorb and emit radiation in limited spectral ranges and are referred to as spectral bands. In calculating the emitted or absorbed radiation for a gas layer, the thickness, shape, surface area, pressure and temperature distribution must be considered. Although a precise method for calculating the effect of these participating media is quite

complex, the effective total emissivities of carbon dioxide and water vapor are a function of the temperature and the product of the partial pressure and the mean beam length of the substance (Bahadori and Vuthaluru, 2009b). The gas emissivity, however, can be calculated knowing the furnace dimensions and the mean beam length. It can be described by the curve presented by Lobo and Evans (1939).

The only constituents normally in the flue gas that contribute significantly to the radiant emission are the carbon dioxide and the water, the sum of these are all that are considered. The partial pressure of a gas component is the mole volume fraction percent of that component (Bahadori and Vuthaluru, 2009b). Over the last 40 years or so, several approximate models for total emissivity and absorptivity calculations of water vapor and carbon dioxide mixtures have been developed. However, these models are not easy to use for practitioners and detailed understanding of complex mathematical formulations and spectral information are required. In view of this, our efforts have been directed at formulating correlations which are suitable for combustion engineers to understand the thermal performance of an existing boiler or to make alterations to the boiler design (Bahadori and Vuthaluru, 2009b).

This part of research presents the results the proposed correlations and the usefulness is highlighted with a step-by-step approach along with a typical example to substantiate the practical application of empirical formulations. The tuned coefficients reported in Table B1 assists in covering the reported data for the temperatures ranging from 500°C to 1600°C. These coefficients can be retuned quickly if more accurate data are available in the future (Bahadori and Vuthaluru, 2009b).

Figure 6.1 shows the comparison of predicted emissivity of combustion gases as a function of temperature and product of the partial pressure of carbon dioxide and water times the beam length with some typical literature data (Lobo, and Evans, 1939). As can be seen, the results show good agreement with the reported data and the proposed correlation is accurate, reliable and acceptable. It also shows the emissivity of combustion gases decreases at higher temperatures, and increases with product of the partial pressure of the carbon dioxide and water times the beam length (P Lb) at constant temperature. Figure 6.2 shows the predicted partial pressure of water plus carbon dioxide as a function of percent excess air.

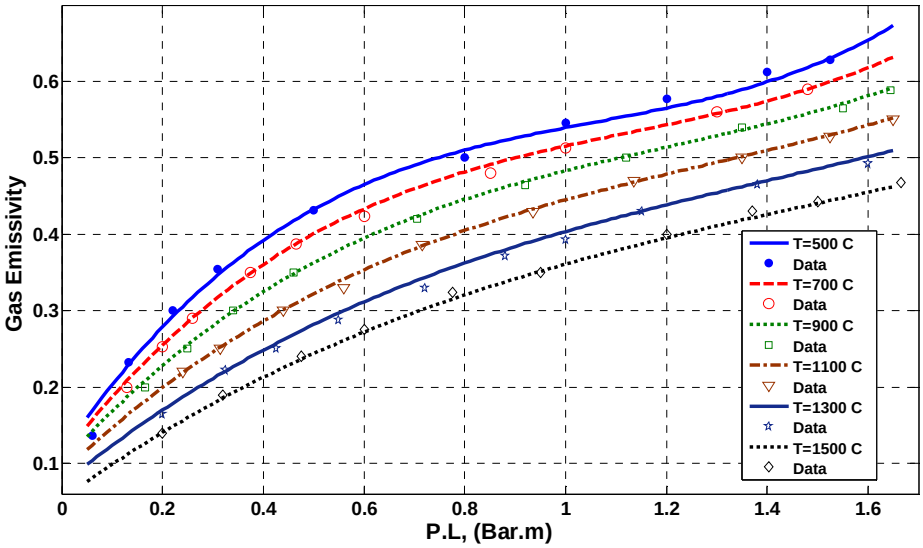

Figure 6.1: Comparison of predicted emissivity of combustion gases against typical literature data (Bahadori A. and Vuthaluru H. B. (2009b) *Chemical Engineering Progress*, 105 (6), pp. 38-41)

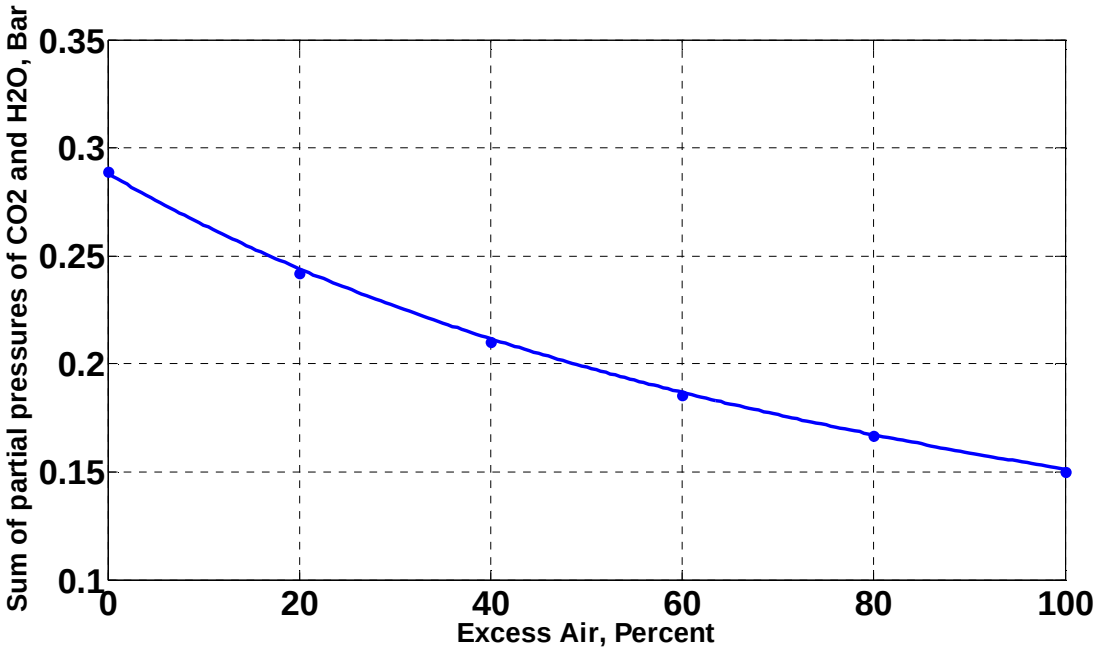

Figure 6.2: Prediction of sum of partial pressures of H_2O and CO_2 as a function of percent excess air (Bahadori A. and Vuthaluru H. B. (2009b) *Chemical Engineering Progress*, 105 (6), pp. 38-41)

Unlike complex mathematical approaches for estimating emissivities of combustion gases, the proposed correlation would be of immense help for combustion engineers especially those dealing with boiler design. Additionally, the understanding of thermal efficiency of natural gas fired furnaces is expected to address the environmental aspects (Bahadori and Vuthaluru, 2009b). By knowing the content of carbon dioxide and water vapor, one can easily deduce the emissivities without having any expertise in radiative heat transfer. The level of mathematical formulations associated with the estimation of emissivities can be easily handled by a combustion engineer without any in-depth mathematical abilities. Furthermore, the estimations are quite accurate as evidenced from the comparisons with literature data and would help in attempting design modifications with less time (Bahadori and Vuthaluru, 2009b).

6.2. Bulk modulus and volumetric expansion coefficient of water for leak tightness test of pipelines

To determine whether any pressure variation in pipeline hydrostatic test is a result of temperature changes or presence of leaks, the calculation of pressure/temperature changes are required for test sections. In these calculations, bulk modulus and volumetric expansion coefficient of fresh or sea water must be taken into account. In this section of thesis, a correlation is developed to predict the bulk modulus and volumetric expansion coefficient of both fresh and sea water as a function of temperature and pressure. The proposed correlation helps to cover the bulk modulus and volumetric expansion coefficient of both fresh and sea water for temperatures less than 50 °C (40°C for sea water) as well as pressure up to 55000 kPa (550 bar) (Bahadori and Vuthaluru 2009c).

The results can be used in follow-up calculations to determine whether any pressure variation in pipeline hydrostatic test is a result of temperature changes or presence of leak. The novel correlation is easy to use and will prove to be of immense value for project engineers to test the critical limits accurately (Bahadori and Vuthaluru 2009c). Both bulk modulus of water and the volumetric expansion coefficient of water are as a function of temperature and pressure where the relevant coefficients have been reported in tables B2 and B3. Figures 6.3-6.6 show the results of the proposed correlation for predicting the bulk modulus and volumetric expansion coefficient of both fresh and sea water as a function of temperature and pressure compared to the reported data (Bahadori and Vuthaluru 2009c). It is clear that the proposed method results in excellent accuracy.

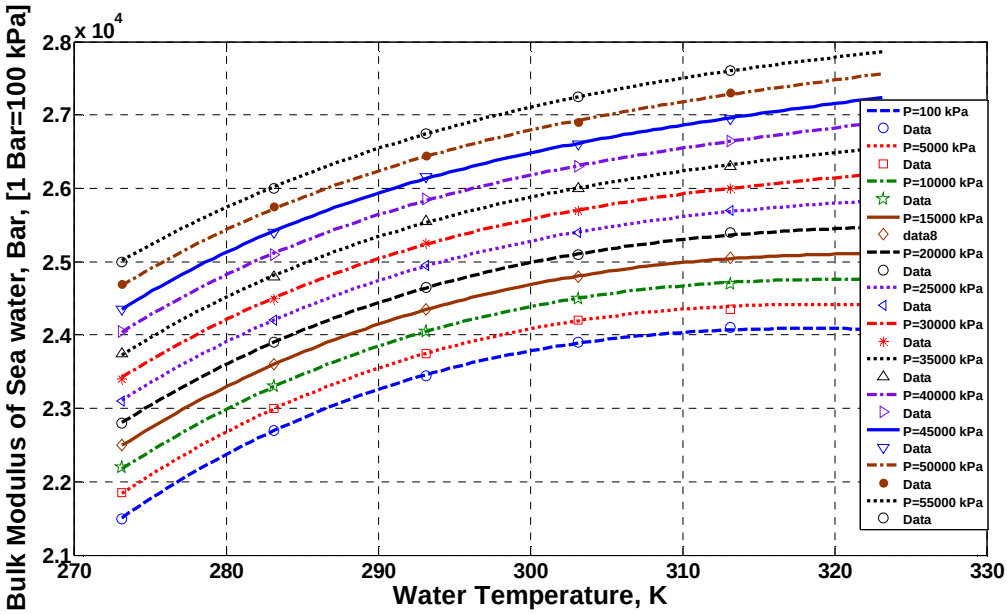

Figure 6.3: New correlation's results for prediction of bulk modulus of sea water in compare with the reported data (Bahadori A and Vuthaluru H. B *International Journal of Pressure Vessels and Piping*, (86) pp. 550–554)

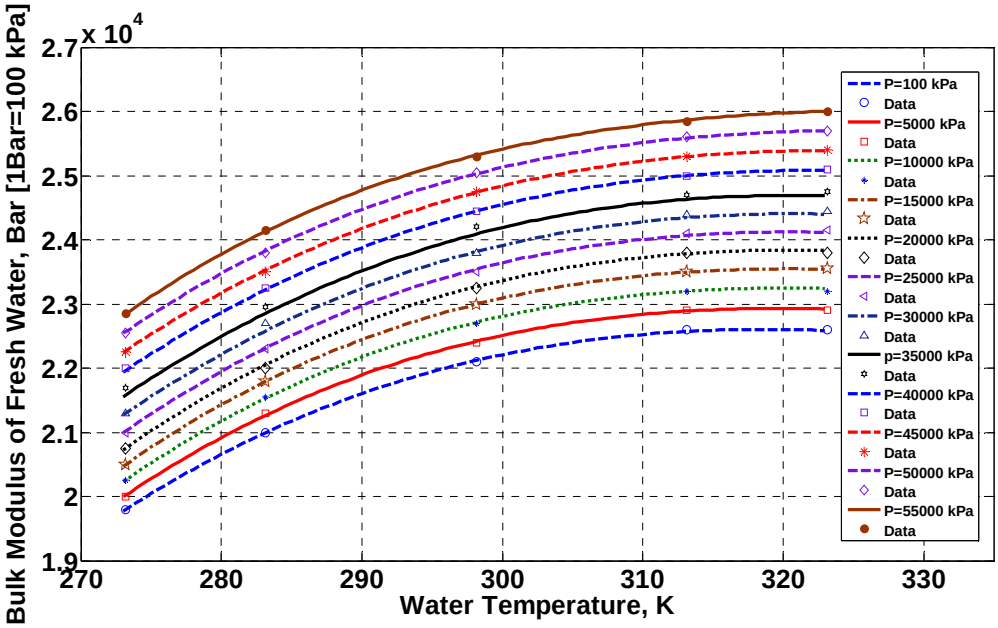

Figure 6.4: New correlation's model's results for prediction of bulk modulus of fresh water in comparison with the reported data (Bahadori A and Vuthaluru H. B 2009c *International Journal of Pressure Vessels and Piping*, (86)pp. 550–554)

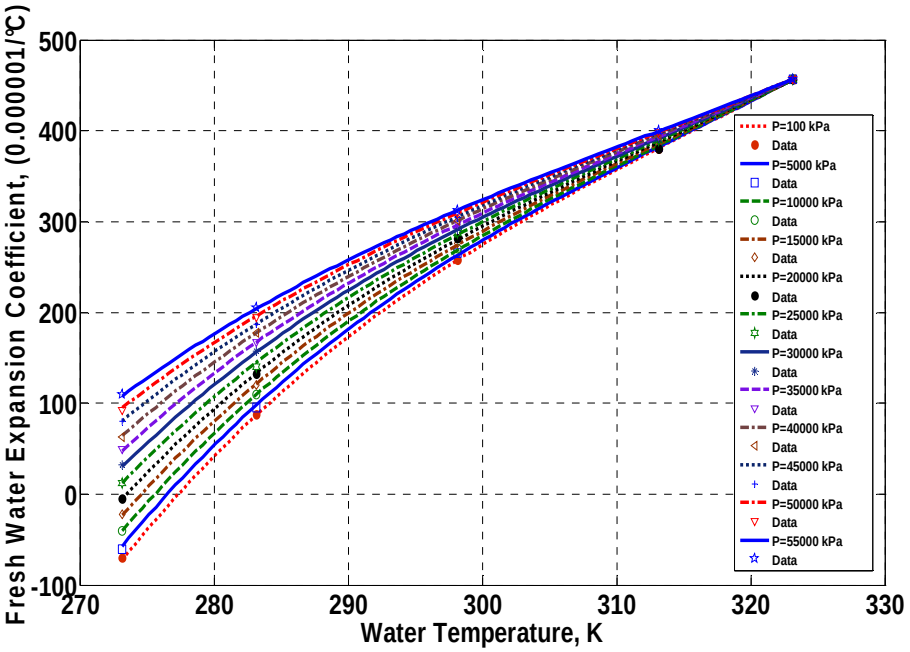

Figure 6.5: New correlation's results for prediction of volumetric expansion coefficient of fresh water in comparison with the reported data (Bahadori A and Vuthaluru H. B 2009c *International Journal of Pressure Vessels and Piping*, (86) pp. 550–554)

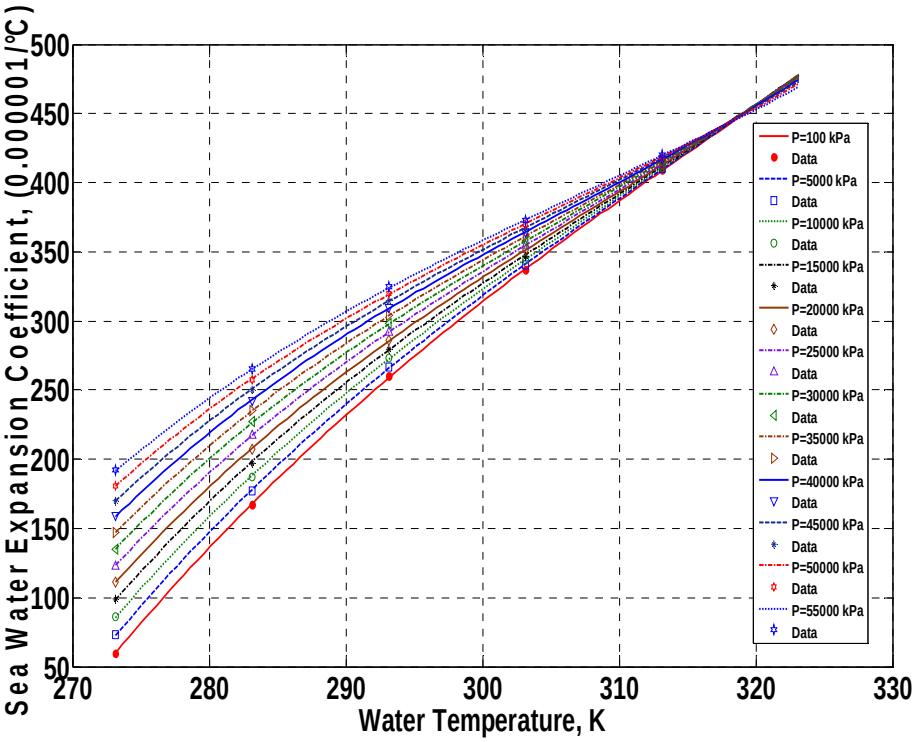

Figure 6.6: New correlation's results for prediction of volumetric expansion coefficient of sea water in comparison with the reported data (Bahadori A and Vuthaluru H. B.2009c *International Journal of Pressure Vessels and Piping*, (86) pp. 550–554)

New correlation was developed to predict the bulk modulus and volumetric expansion coefficient suitable for both fresh and sea water as a function of temperature and pressure (Bahadori and Vuthaluru 2009c). The obtained results show excellent agreement with the reliable data reported in the literature. The proposed correlation helps to cover the bulk modulus and volumetric expansion coefficient of both fresh and sea water as a function of temperature and pressure for temperatures less than 50 °C (40°C for sea water) and pressures up to 55000 kPa (550 bar). The results can be used in further calculations to determine whether any pressure variation in pipeline hydrostatic test is a result of temperature changes or due to the presence of leaks in the pipelines (Bahadori and Vuthaluru 2009c). The proposed correlation also has this advantage that the coefficients can be recalculated quickly if new data become available in the future.

6.3 Silica Carry-over and Solubility in Steam of Boilers

Silica content of the boiler water is critical for steam turbines and scaling of boiler heat transfer surfaces. Silica (SiO_2) can volatilize with the steam in sufficient concentrations to deposit in steam turbines leading to scale formation on boiler surfaces (Bahadori and Vuthaluru 2010b). Here, it will be shown how simple correlation is presented to predict silica (SiO_2) solubility in steam of boilers as a function of pressure and water silica content. The solubility of silica in steam directly depends on both the density and temperature of steam. With decreasing temperature and density, solubility of silica reduces. As the pressure affects steam density which has a strong bearing on steam temperature, it has an important effect on the solubility of silica in steam.

The proposed correlation predicts the solubility of silica (SiO2) in steam for pressure up to 22000 kPa and boiler water silica contents up to 500 mg/kg (Bahadori and Vuthaluru 2010b). The present study discusses the formulation of a simple correlation which can be of significant importance for the engineers associated with the utility boilers. The present approach is of practical significance for power generating industries in terms of assessing operational issues. In particular the proposed correlation gives an advance indication of key parameters which could potentially enable practice engineers to take appropriate measures to avoid and reduce the carry-over of silica in steam of boilers (Bahadori and Vuthaluru 2010b). The method presented in this work helps to predict the solubility of silica in steam of boilers for pressures up to 22000 kPa(g) as well as boiler water up to 500 mg/kg(Bahadori and Vuthaluru 2010b). The optimum tuned coefficients given in Table B4 can be retuned quickly according to proposed approach if

more data are available in the future. According to the authors' knowledge, there is correlation in literature for the rapid estimation of solubility of silica in steam (Bahadori and Vuthaluru 2010b).

In view of this, our efforts have been directed at formulating a correlation that can help engineers for rapid prediction of silica (SiO_2) solubility in steam of boilers as a function of pressure and water silica content (Bahadori and Vuthaluru 2010b). The method proposed in this section is simple and unique expression which is non-existent in the literature. In addition, we have selected exponential function to develop the correlation, as these functions are smooth and well-behaved (i.e. smooth and non-oscillatory) equations which should allow for more accurate predictions. Figures 6.7 and 6.8 show the results of the proposed correlation for predicting the silica solubility in steam of boilers as a function of pressure and water silica content in comparison with the reported data. The solubility of silica in steam directly depends on both the density and temperature of steam. With decreasing temperature and density, solubility of silica reduces. As the pressure affects steam density which has a strong bearing on steam temperature, it has an important effect on the solubility of silica in steam. These figures show the solubility of silica in steam increases at high pressures and high boiler water silica. If the proposed approach is adopted in utilities on a periodic basis, significant savings can be assured with reduced maintenance issues in terms of failure of boiler surfaces and scaling problems associated with the carry-over of silica in steam of boilers. Current efforts in this investigation pave the way for alleviating the problems associated with the overheating and failure of boiler sections due to scale formation and turbine inefficiencies by arriving at an accurate measure of silica solubility in steam which can be used by the utility personnel for monitoring the operational parameters.

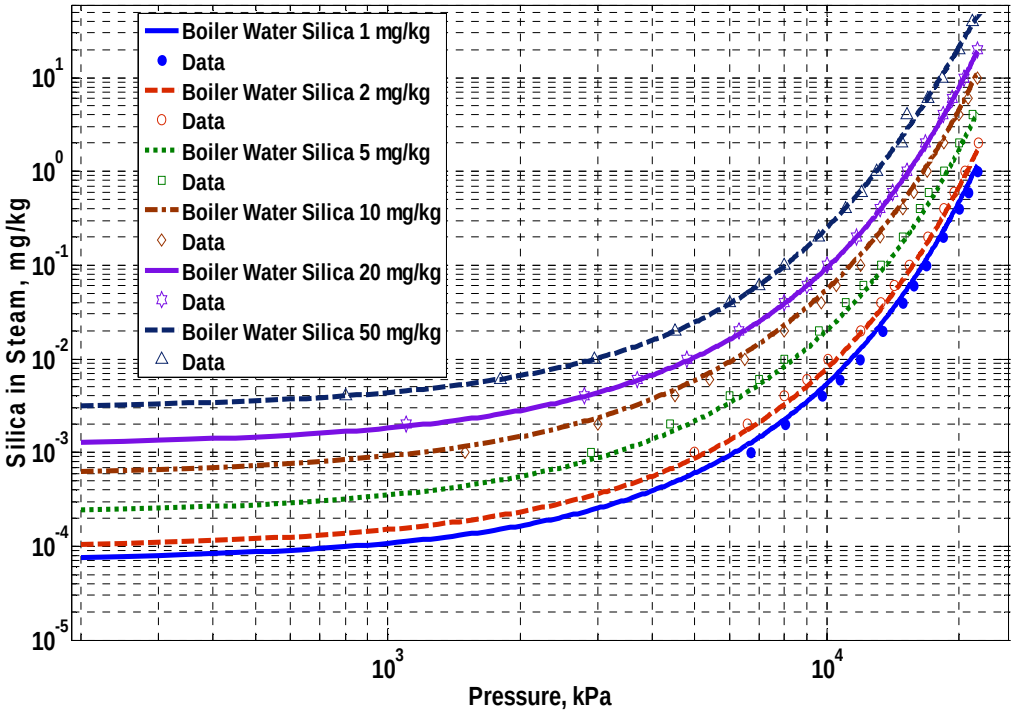

Figure 6.7: Comparison of predicted solubility of silica against literature reported data [4] for low concentration of boiler water silica (1-50 mg/kg) (Bahadori A. and Vuthaluru H. B. (2010b) *Applied Thermal Engineering* 30 (2010) 250-253)

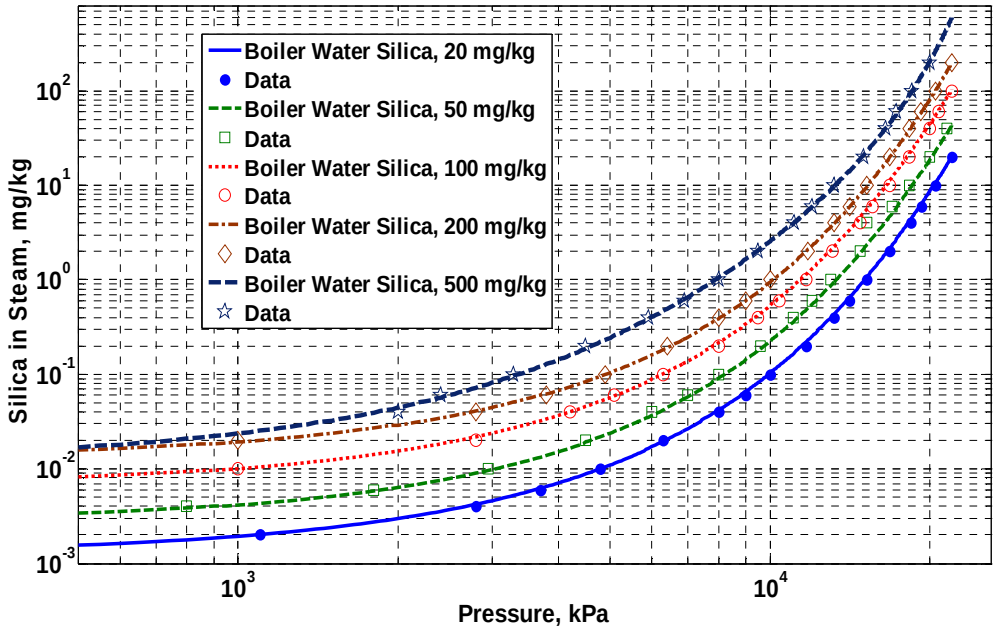

Figure 6.8: Comparison of predicted solubility of silica against literature reported data [4] for high concentration of boiler water silica (20-500 mg/kg) (Bahadori A. and Vuthaluru H. B. (2010b) *Applied Thermal Engineering* 30 (2010) 250-253)

6.4 Carbon dioxide equilibrium adsorption isotherms

Among the methods that are being developed to date for CO_2 capture and separation, carbon dioxide adsorption is of great interest due to its low energy consumption, low equipment cost and easiness for application. In this section, a simple method which is easier than existing approaches requiring more complicated and longer computations is presented to accurately predict the carbon dioxide adsorption isotherms for a microporous material as a function of temperature and partial pressure of carbon dioxide (Bahadori and Vuthaluru, 2009f). The method appears promising and can be extended for CO_2 capture as well as for separation of wide range of adsorbents and microporous materials including several molecular sieves merely by the quick readjustment of tuned coefficients. The proposed method showed consistently accurate results across the proposed pressure and temperature ranges (Bahadori and Vuthaluru, 2009f).

The proposed method is superior due to its accuracy and clear numerical background, wherein the relevant coefficients can be retuned quickly for various cases. This approach can be of immense practical value for the engineers and scientists to have a quick check on adsorption capacities of a given adsorbent at various temperatures and pressures without the necessity of any experimental measurements. In brief, adsorption is one of the promising methods applicable for the separation of CO2 from the gas mixtures (Bahadori and Vuthaluru, 2009f). Carbon dioxide is a non-ideal gas with high critical temperature which means it condenses easily, and it can be easily adsorbed where ideal gases (like N_2 for instance) will not adsorb,. In view of the above mentioned benefits of adsorption method, there is an essential need for developing an accurate and simple method in order to appropriately determine the carbon dioxide adsorption isotherms for molecular sieves as a function of temperature and carbon dioxide partial pressure(Bahadori and Vuthaluru, 2009f). These optimum tuned coefficients (A, B, C and D) in table B4 help to cover the carbon dioxide adsorption isotherms equilibrium data. The optimum tuned coefficients given in Table B5 (appendix B) have been adjusted for Davison 4A molecular sieve according to isotherms equilibrium data from Reynolds (2002). These tuned coefficients are recommended for carbon dioxide partial pressures and temperatures up to 120 kPa and 470 K respectively with Davison 4A molecular sieve.

These coefficients can be retuned quickly according to the proposed approach for CO_2 capture and separation for wide range of adsorbents including various molecular sieves just by readjusting the tuned coefficients (Bahadori and Vuthaluru, 2009f). Figures 6.9 and 6.10 show

the results of the proposed model in comparison with the reported data obtained with Davison 4A Molecular Sieve (Reynolds, 2002). It is clear that the proposed method yields results with good accuracy. Figure 6.11 illustrates the results of the proposed correlation for predicting the carbon dioxide adsorption isotherms as a function of temperature and carbon dioxide partial pressure. As can be seen from the figure, predicted values are reasonable for wide range of carbon dioxide partial pressures and temperatures. This shows that the adsorption of carbon dioxide decreases at high temperatures and low pressures.

In order to compare the proposed method's performance with other existing methods a case study according to Pakseresht et al., (2002) equilibrium isotherm data for CO_2 on the 5A molecular sieve pellets is presented here(Bahadori and Vuthaluru, 2009f). In brief, in the present study, a robust and simple method is developed for the prediction of carbon dioxide adsorption isotherms for a molecular sieve as a function of temperature and partial pressure of carbon dioxide. Predicted results are compared with the reliable data and shows good agreement.

The method can be extended for CO_2 capture and separation of wide range of adsorbents including several molecular sieves by readjusting the tuned coefficients. Results indicate that the proposed method appears to be superior owing to its accuracy (with much lower deviations compared to the existing correlations to date) and clear numerical background, wherein the relevant coefficients can be retuned quickly for new cases (Bahadori and Vuthaluru, 2009f). The correlation proposed in the present work is novel and unique expression which is non-existent in the literature. This is expected to benefit and making design decisions leading to informed decisions for the selection of adsorbents for a given application in any process industry. For every microporous material the basis will be experimental data (isotherms at different temperatures) to be able to use the method proposed for various cases (Bahadori and Vuthaluru, 2009f).

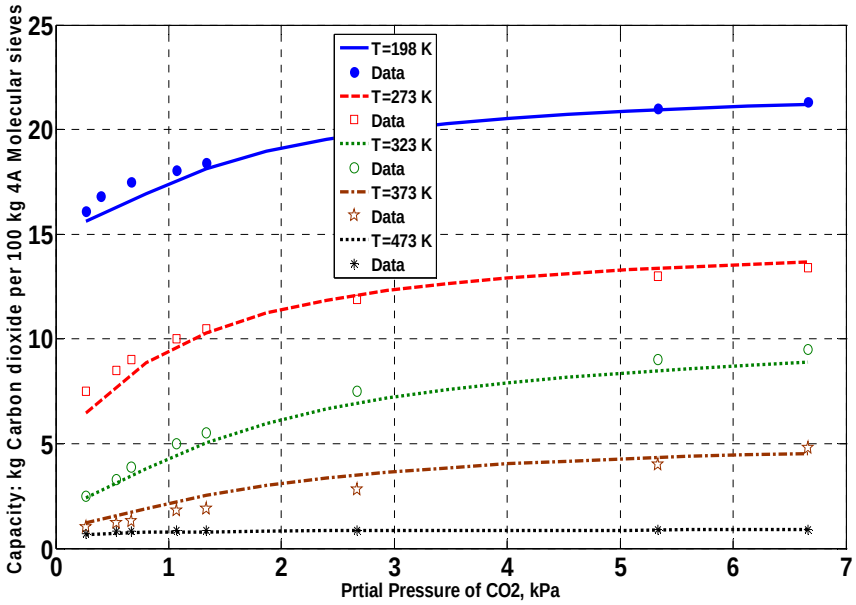

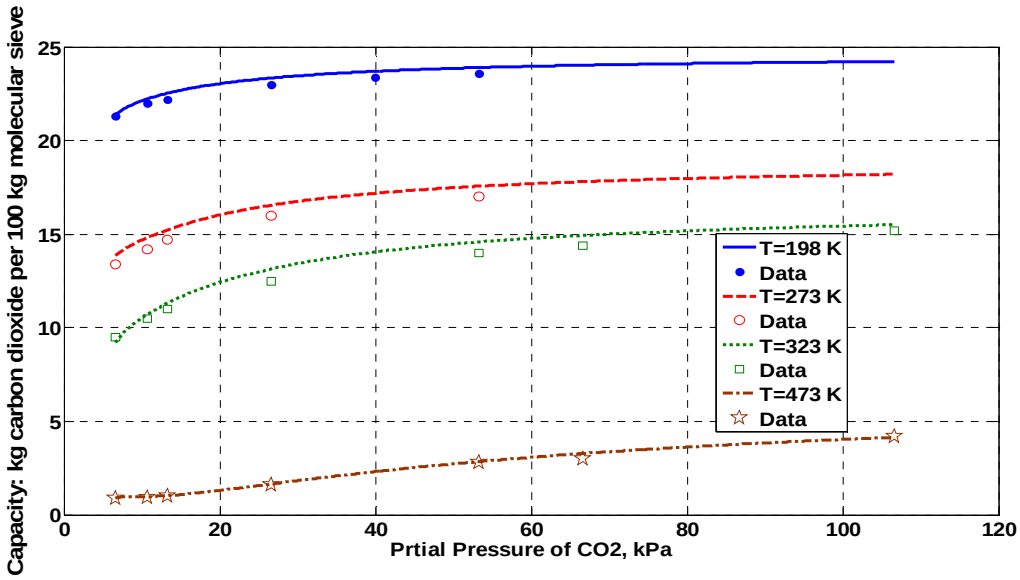

Figures 6.9-6.10: Prediction of adsorption of carbon dioxide using the proposed method in comparison with the literature reported data for low partial pressures of carbon dioxide (Bahadori, A. and Vuthaluru H. B. 2009f, *International Journal of Greenhouse Gas Control* (3), 768-772)Figure 6.10, Prediction of adsorption of carbon dioxide using the proposed method in comparison with the literature reported data for high partial pressures of carbon dioxide (Bahadori, A. and Vuthaluru H. B. 2009f, *International Journal of Greenhouse Gas Control* (3), 768-772)

6.5 Economic thickness of thermal insulation for process piping and equipment

Where the sole object of applying insulation to a portion of plant is to achieve the minimum total cost during a specific period (evaluation period), the appropriate thickness is usually termed as the economic thickness. The principle is to find the thickness further expenditure on insulation would not be justified by the additional financial saving on heat to be anticipated during the evaluation period. Although an increase in the amount of insulation applied will raise the initial installed cost, but it will reduce the rate of heat loss through the insulation (Bahadori and Vuthaluru, 2010e).

Therefore it is necessary to reduce the total cost during the evaluation period. In this work, a correlation employing basic algebraic equations which are simpler than current available models involving a large number of parameters, more complicated and longer computations, is formulated to arrive at the economic thickness of thermal insulation suitable for process piping and equipment. The correlation is a function of steel pipe diameter and thermal conductivity of insulation for surface temperatures at 100°C, 300°C, 500°C and 700°C (Bahadori and Vuthaluru, 2010e). A simple interpolation formula generalizes this correlation for wide range of surface temperatures. The proposed correlation covers pipeline diameter and surface temperature up to 0.5 m and 700°C respectively (Bahadori and Vuthaluru, 2010e).

Various thermal insulation systems taking advantages of different types of thermal insulation materials on both organic (expanded plastics, wood wool, cork, straw, technical hemp) and inorganic basis (foamed glass, glass and mineral fibres) are being designed and tested (Bahadori and Vuthaluru, 2010e) and new methods for analysing the properties of both insulation materials and insulation systems are currently being devised. Researchers in thermal science are attempting to minimize capital and operation costs as well as heat loss (Bahadori and Vuthaluru, 2010e).

In previous research, multiple objective functions were applied by researchers for the design analysis of a piping system to minimize the heat loss and the amount of insulation used. In these types of complicated methods, a common approach is to sum all objective functions with appropriate weighting factors, and minimize the resulting composite function (Kalyon and Sahin, 2002). However, the analytical solution should only be attempted if a very precise value of thickness is required as it takes into account the specific details and often it is not a requirement in a practical view point as many types of insulation are available only in certain specific sizes.

The required thickness of insulation for any specific application depends on the characteristics of the insulating material as well as the purpose of equipment. If a process is critical, the most important single consideration may be reliability. If heat or power conservation is the deciding factor, the savings per year as compared to the installed cost is the most important factor. In contrast, when insulation is to be used for a temporary function such as holding the heat in while a lining is being heat cured, then the lowest possible installed cost would be decisive. Thus, the conflicting requirements, there can be no multipurpose insulation. Nor there is a "perfect" insulation for each set of requirements (Bahadori and Vuthaluru, 2010e).

Over the past decades, several methods for determining the optimum thermal insulation thickness have been developed. However, in practice, these approaches are not easy to use, since they require a detailed understanding of complex mathematical formulations. According to the authors' knowledge, there is no correlation in the literature for rapid estimation of the economic thickness of thermal insulation. In view of this status, our efforts have been directed at formulating correlation that can help engineers for rapid estimation of the economic thickness of thermal insulation as a function of thermal conductivity, outside steel pipe diameter and surface temperatures (Bahadori and Vuthaluru, 2010e).

The required data to develop this method includes the reliable and widely accepted by industry data (IPS 1996) for various Optimum economic thickness of thermal insulation as a function of steel pipe and equipment diameter as well as thermal conductivity of insulation and surface temperature (Bahadori and Vuthaluru, 2010e).

The optimum economic thickness of thermal insulations are predicted rapidly as a function of steel pipe and equipment diameter and thermal conductivity of insulation by proposing simple correlation, where the relevant coefficients have been reported in appendix B.

Figures 6.11 to 6.14 show the thickness of insulation as a function of outside diameter of pipe and insulation of varying thermal conductivity at 100, 300, 500 and 700°C respectively(Bahadori and Vuthaluru, 2010e). The proposed correlation covers pipeline diameter and temperature up to 0.5 meter and 700°C respectively.

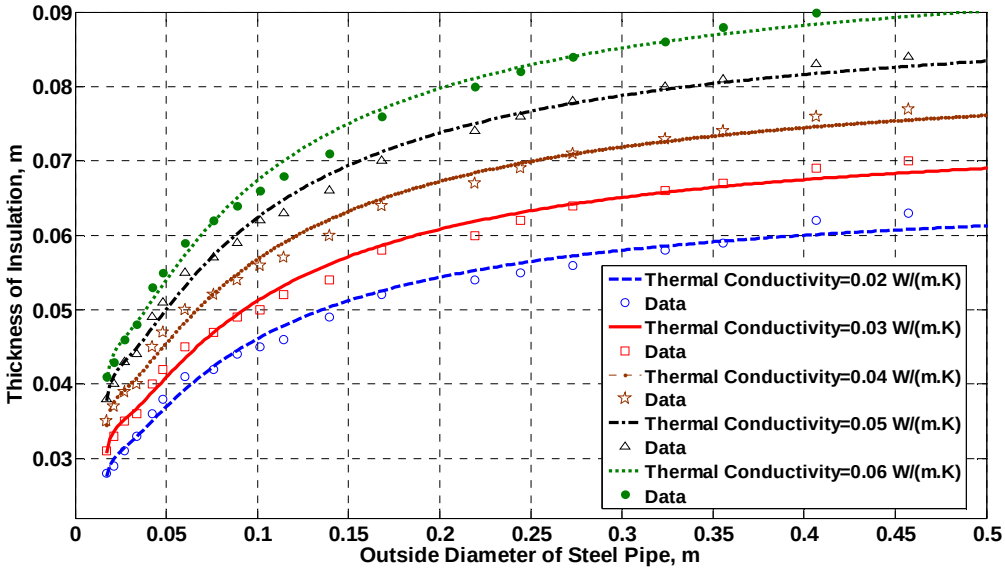

Figure 6.11: Comparison of predicted results from simple correlation with the reported data for surface temperature of 100°C (Bahadori A. and Vuthaluru H. B. *Applied Thermal Engineering*, 30 (2010e) 254–259)

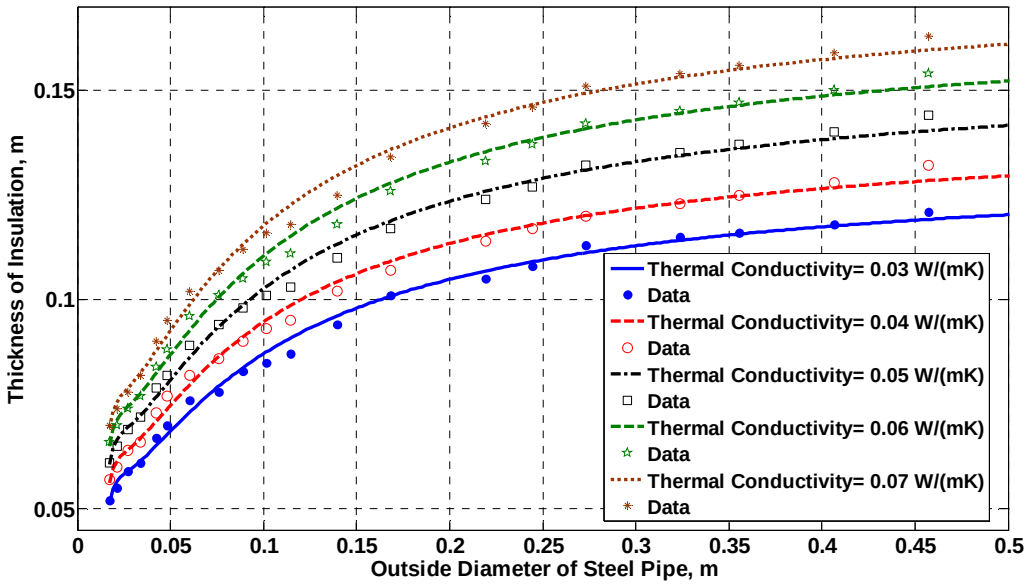

Figure 6.12: Comparison of predicted results from simple correlation with the reported data for surface temperature of 300°C, (Bahadori A. and Vuthaluru H. B *Applied Thermal Engineering*. 30 (2010e) 254–259)

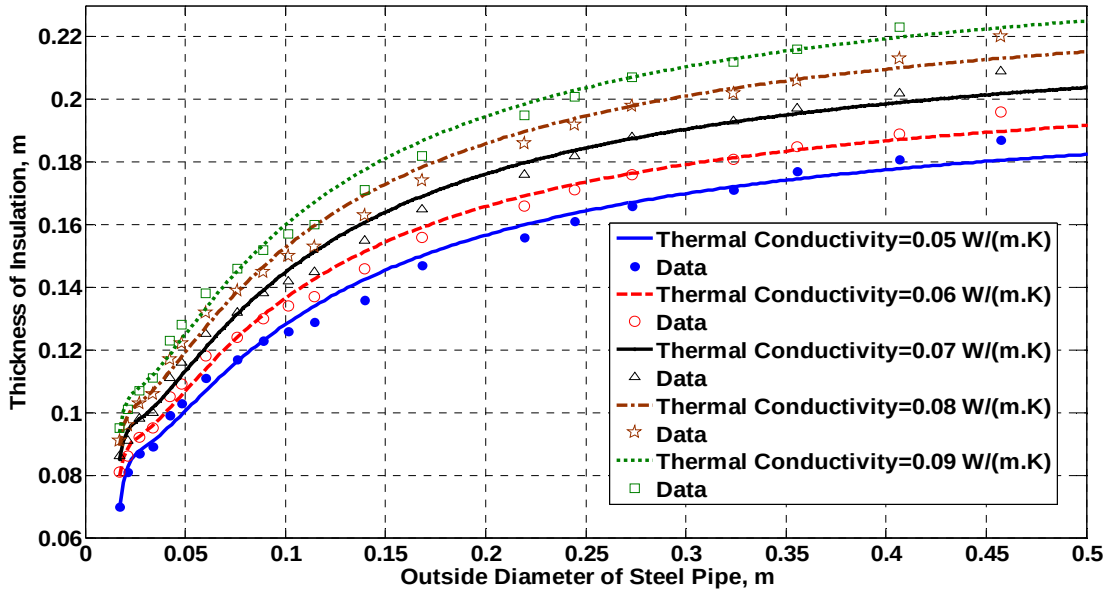

Figure 6.13: Comparison of predicted results from simple correlation with the reported data for surface temperature of 500°C Bahadori A. and Vuthaluru H. B *Applied Thermal Engineering*. 30 (2010e) 254–259

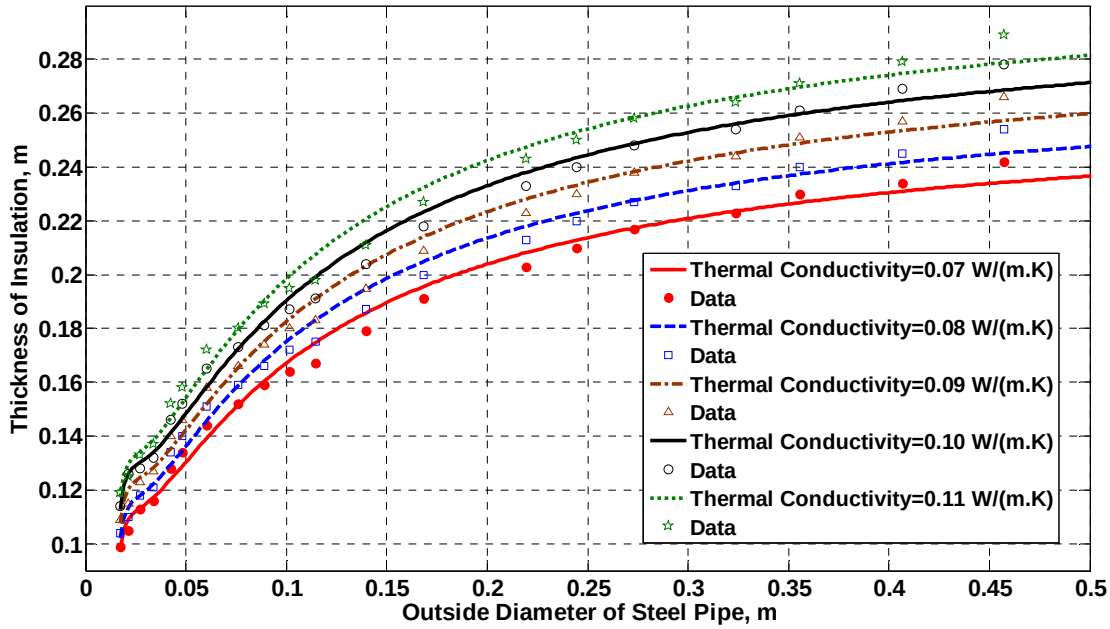

Figure 6.14: Comparison of predicted results from simple correlation with the reported data for surface temperature of 700°C Bahadori A. and Vuthaluru H. B, *Applied Thermal Engineering*. 30 (2010e) 254–259

6.6. Thermal insulation thickness

Researchers in thermal science are attempting to minimize capital and operation costs as well as heat loss. Selection and determination of optimum thickness of insulation is of prime interest for many engineering applications (Bahadori and Vuthaluru 2010d). In this study, a simple method is developed to estimate the thickness of thermal insulation required to arrive at a desired heat flow or surface temperature for flat surfaces, ducts and pipes. The proposed simple method covers the temperature difference between ambient and outside temperatures up to 250°C and the temperature drop through insulation up to 1000°C (Bahadori and Vuthaluru 2010d). The proposed correlation calculates the thermal thickness up to 250 mm for flat surfaces and estimates the thermal thickness for ducts and pipes with outside diameters up to 2400mm. The method is based on the basic fundamentals of heat transfer and reliable data. Therefore the formulated expression is justified and applicable to any industrial application (Bahadori and Vuthaluru 2010d).

Figure 6.15 illustrates the results of the proposed method capabilities in predicting the heat flow as a function of thermal resistance of insulation and temperature drop through insulation. Figures 6.16 and 6.17 show the results for predicting the actual insulation thickness for duct and tube as a function of outside diameter of pipe and ducts and required insulation thickness for flat surfaces (Bahadori and Vuthaluru 2010d). These graphs show good agreement between reported data and the estimated results from the proposed simple correlations. The correlations proposed in the present work are novel and unique and are non-existent in the literature. This is expected to benefit and making design decisions leading to informed decisions for the determination and selection of optimum thickness of insulation for a given application in any process industry (Bahadori and Vuthaluru 2010d).

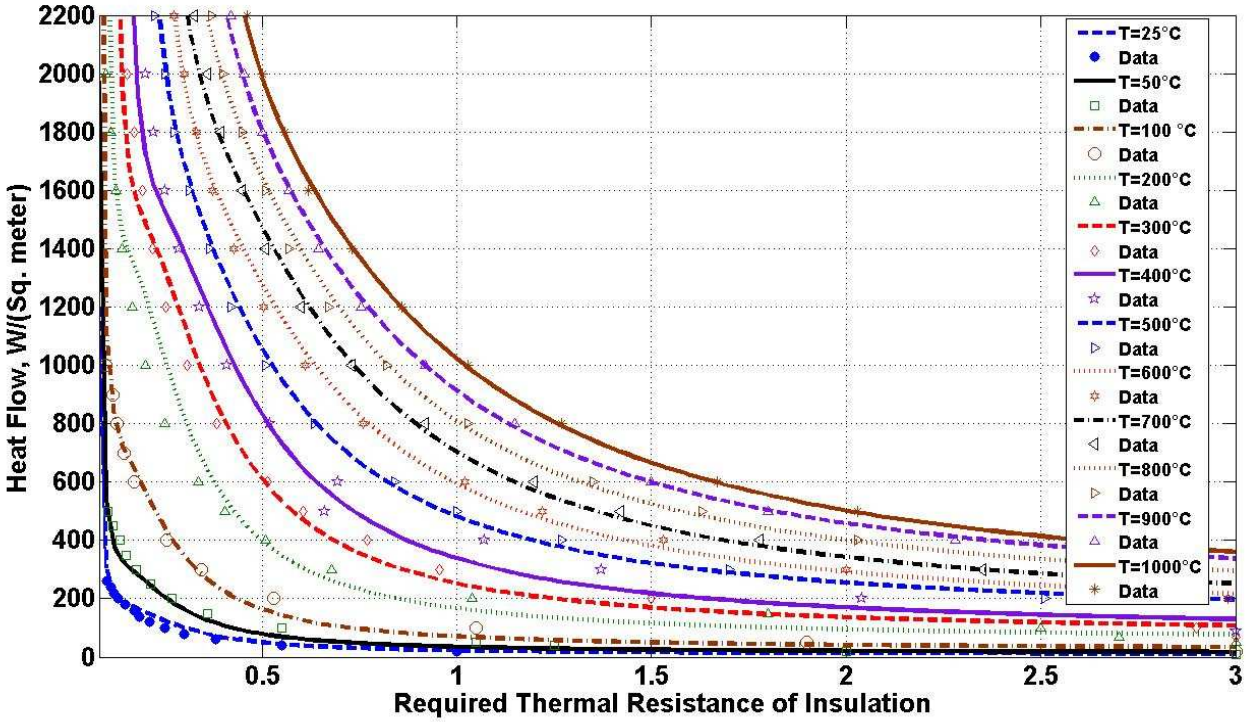

Figure 6.15: Prediction of heat flow as a function of thermal resistance of insulation and temperature drop through insulation in comparison with the data Bahadori A. and Vuthaluru H. B. (2010d) *Applied Energy*, 87, 613–619

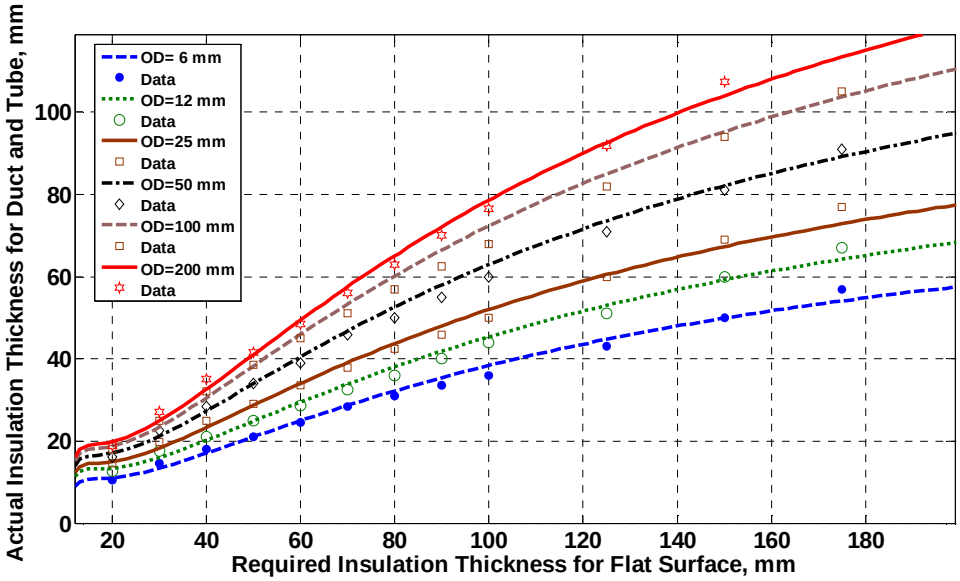

Figure 6.16: Actual insulation thickness for duct and tube a function of outside diameter (less than 200 mm) and required insulation thickness for flat surfaces in comparison with the data (Bahadori A. and Vuthaluru H. B. (2010d), *Applied Energy*, 87, 613–619)

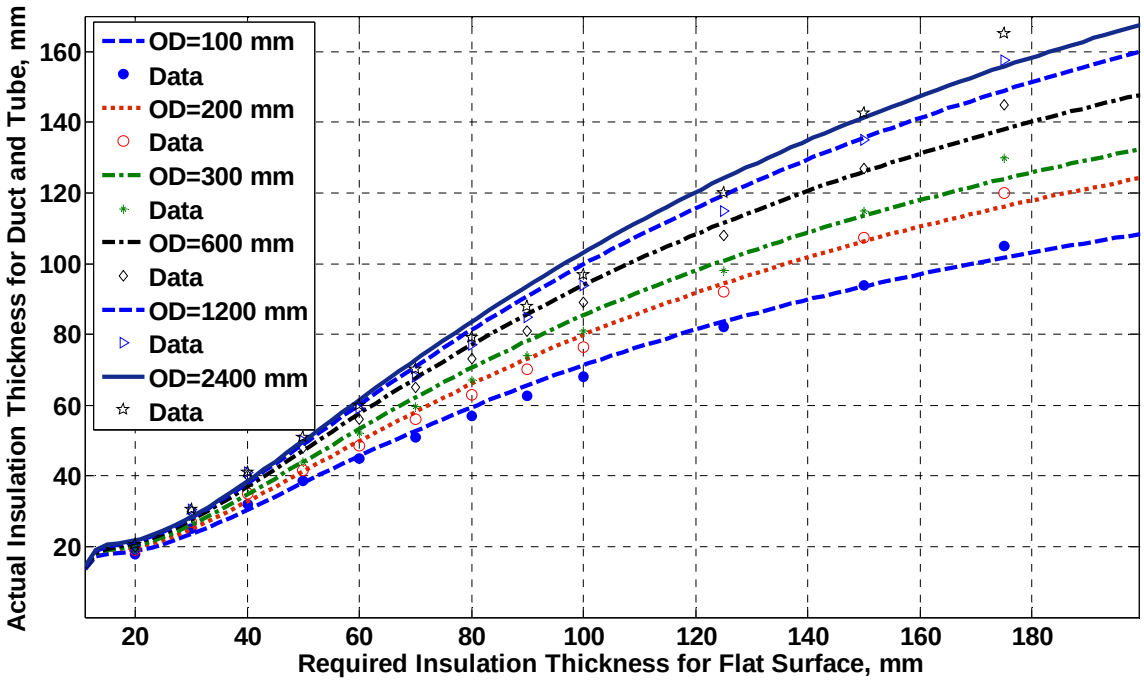

Figure 6.17: Actual insulation thickness for duct and tube a function of outside diameter (between 100mm and 2400 mm) and required insulation thickness for flat surfaces in comparison with the data. (Bahadori A. and Vuthaluru H. B. (2010d), *Applied Energy*, 87, 613–619)

In this section, simple correlations were formulated for the estimation of heat flow through insulation, thermal resistance and thermal insulation thickness for flat surfaces, ducts and pipes (Bahadori and Vuthaluru 2010d). The proposed correlation covers the temperature difference between ambient temperature and outside temperature up to 250°C and the temperature drop through insulation up to 1000°C. The proposed simple correlation calculates the thermal thickness for flat surfaces up to 200 mm and predicts the thermal thickness for ducts and pipes with outside diameters up to 2400 mm (Bahadori and Vuthaluru 2010d).

6.7 Transport properties of carbon dioxide

In this section, new correlation has been developed for the prediction of transport properties (namely viscosity and thermal conductivity) of carbon dioxide (CO_2) as a function of pressure and temperature. This correlation accurately predicates for temperature ranges between 260 K and 450 K as well as pressures between 10 and 70 MPa which is the range of pressure that is

widely considered in CO_2 sequestration. In the design for CO_2 capture and geological storage, many parameters including the pipeline diameter and appropriate sizing of other equipments have important roles.

Many technical factors play a role in the design and engineering calculations, namely flow rate, pressure drop per unit length, density, viscosity, thermal conductivity of CO_2, pipeline material roughness, topographic differences, amount and type of bends in pipe (Vandeginste and Piessens, 2008). The properties of CO_2 are considerably different from other fluids commonly transported by pipeline such as natural gas. Thus, it is necessary to use accurate representations of the phase behaviour, density, thermal conductivity and viscosity of CO_2 in the design of the pipeline. Reliable and reference data for CO_2 transport properties have been presented by Vesovic et al. (1990).

It is generally recommended that a CO_2 pipeline operates at pressures greater than 8.6 MPa where the sharp changes in compressibility of CO_2 can be avoided across a range of temperatures that may be encountered in the pipeline system (Farris, 1983). If the need for a CO_2 transport pipelines is established, the design of the unit will depend on many factors including the viscosity and thermal conductivity of CO_2 because of its influence on the hydraulic calculations and heat transfer capability. In view of the above, there is an essential need for developing an accurate method as a function of pressure and temperature in order to appropriately determine the transport properties of CO_2 especially in high pressures.

The optimum adjusted coefficients are given in appendix B. These optimum tuned coefficients help to cover the transport properties of CO_2 in temperature range of 260 K to 450 K and pressures the range of 10 to 70 MPa. The new predictive tool shows consistently accurate results across recommended pressure ranges and temperatures. Figure 6.18 compares results of the proposed correlation for predicting the thermal conductivity of CO_2 with the reported data from Vesovic et al. (1990). Figures 6.19 and 6.20 compare the results of proposed correlation for predicting the viscosity of CO_2 with the reported data from Vesovic et al. (1990). As can be seen, there is an excellent agreement between the reported data and the new correlation predictions. In brief an easy-to-use correlation has been developed to accurately predict the CO_2 thermal conductivity as well as the viscosity of carbon dioxide as a function of temperature and pressure in the present study.

These are simpler than currently available models which involve a large number of parameters and requiring more complicated and longer computations. The predictions showed excellent

agreement with those reported in the literature. This novel correlation predicts the transport properties of carbon dioxide for pressures and temperatures ranging between 10 and 70 MPa and 260 K and 450 K respectively. The proposed correlation is simple to use, employing basic algebraic equations that can easily and quickly be solved by spreadsheet. In addition, the estimates are quite accurate, as evidenced by the comparisons with the literature data.

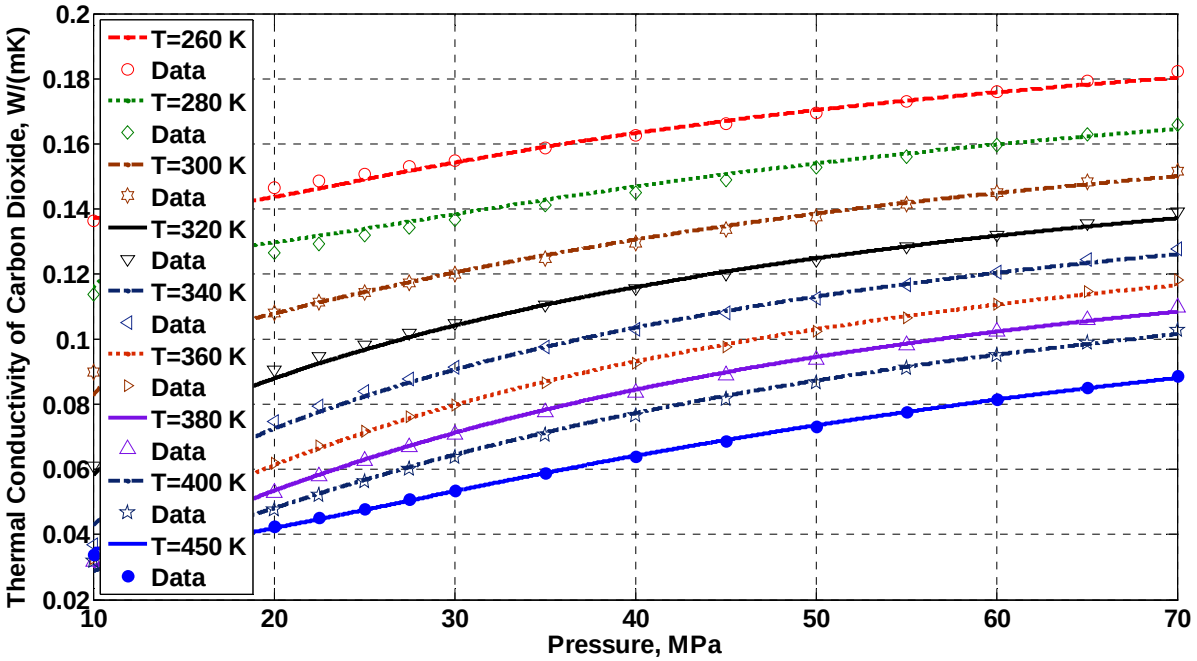

Figure 6.18: Comparison of correlation results with the data from Vesovic et al. (1990) for the prediction of CO_2 thermal conductivity

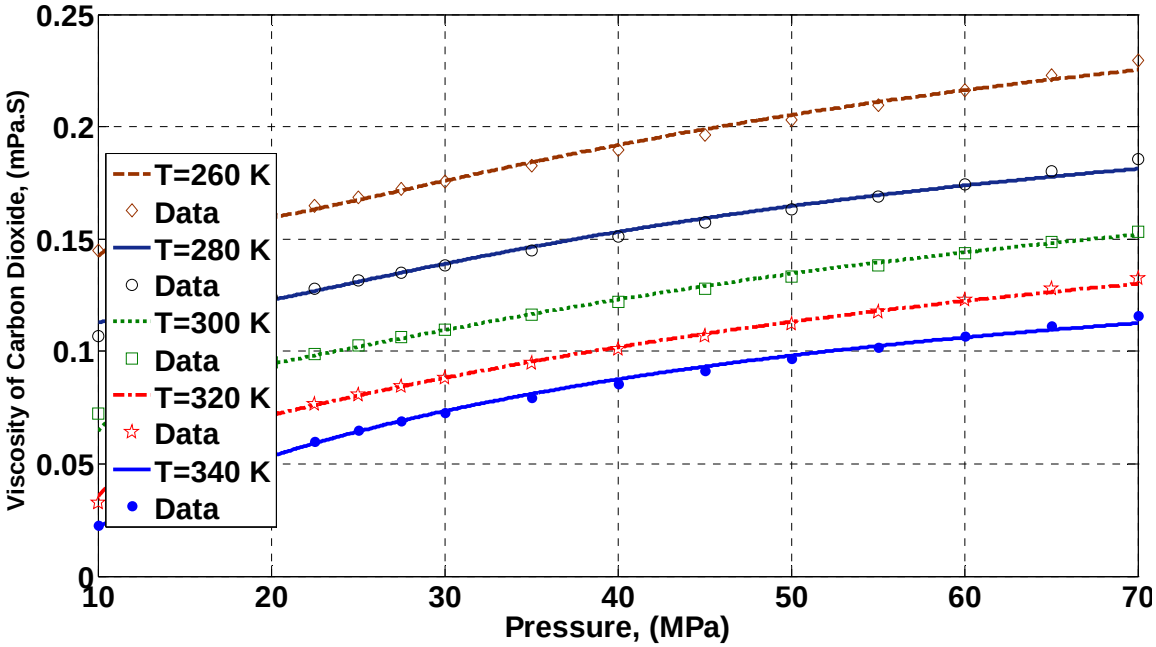

Figure 6.19: Comparison of correlation results with the data from Vesovic et al. (1990) for the prediction of CO_2 viscosity at temperature less than 340 K and pressure between 10 to 70 MPa.

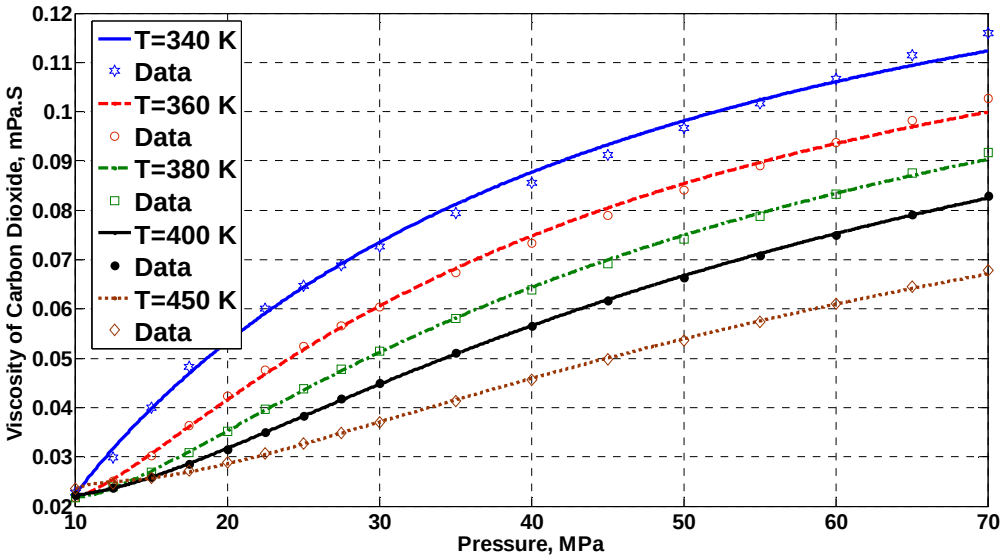

Figure 6.20: Comparison of correlation results with the data from Vesovic et al. (1990) for the prediction of CO_2 viscosity at temperature more than 340 K and pressure between 10 to 70 MPa

6.8 Saturated air water content at elevated pressures

In a compressed air system, condensed water vapor can have corrosive effects on metals and wash out protective lubricants from tools, equipments and pneumatic devices. To protect against such undesirable effects in a compressed air system, it is necessary to be able to predict the water content of air in order to design and apply the appropriate type of drying to be used in the system (Bahadori and Vuthaluru, 2010n). In this section, a simple predictive tool, which is easier than currently available models and involves a fewer number of parameters, requiring less complicated and shorter computations, is presented here for the prediction of water content of air as a function of temperature and relative humidity as well as for compressed saturated air as a function of pressure and temperature using an Arrhenius-type asymptotic exponential function. (Bahadori and Vuthaluru, 2010n).

The proposed method predicts the amount of air water content for temperatures up to 45°C, pressures up to 1400 kPa and relative humidity up to 100%. Designing a tool based on this methodology can be of immense practical value for engineers and scientists to have a quick check on the water content of atmospheric air and saturated compressed air at various conditions without opting for any experimental measurements (Bahadori and Vuthaluru, 2010n).

Figures 6.21 and 6.22 shows the predicted results from the proposed predictive tool for the water content of atmospheric air as a function of relative humidity and temperature with the data (IPS 1993, Perry, and Green 1997). It is evident from the figure that there is a good agreement between predicted values (for relative humidity up to 100% and temperatures up to 45°C) and the reliable data (Bahadori and Vuthaluru, 2010n).

Figures 6.21 and 6.22 shows that the temperature itself has a significant effect on the ability of air at a given pressure to hold moisture. The higher air temperature causes greater capacity to hold water vapor. Conversely, as the air temperature is lowered, the capacity to hold water vapor decreases which is measured in terms of relative humidity (Bahadori and Vuthaluru, 2010n). Figure 6.23 illustrates the predicted results from the proposed predictive tool for the water content of compressed saturated air as a function of pressure and temperature along with the reported data.

As shown in the figure, there is a good agreement between predicted values for pressures up to 1400 kPa (abs) and temperatures up to 45°C and the reliable data. It shows that pressure has a major effect on the vapor content in air. The capacity of air at a given temperature to hold moisture in vapor form decreases as the pressure increases (Bahadori and Mokhatab 2008a). Current efforts in this investigation are likely to pave the way for alleviating the problems associated with the calculations for air water contents which can be used by the process engineers and experts for monitoring the operational parameters on a regular basis (Bahadori and Vuthaluru, 2010n).

In brief, a novel and simple predictive tool was developed for the prediction of the water content of air as a function of temperature and relative humidity and compressed saturated air as a function of pressure and temperature using an Arrhenius-type asymptotic exponential function. The proposed method predicts the amount of water contents in air for temperatures up to 45°C, pressures up to 1400 kPa (abs) and relative humidities up to 100%. Estimations are found to be in excellent agreement with the reliable data in the literature (IPS 1993, Perry, and Green 1997).

The predictive tool described in this section is superior and reliable due to its accuracy and simple background, wherein the relevant coefficients can be retuned quickly if new and more accurate data become available in the future. Example shown clearly demonstrates the usefulness of the proposed method for practice engineers. Our efforts in this investigation will definitely pave the way for arriving at accurate estimations of water content of atmospheric and saturated compressed air which can assist engineers and scientists for the periodic monitoring of operational parameters (Bahadori and Vuthaluru, 2010n).

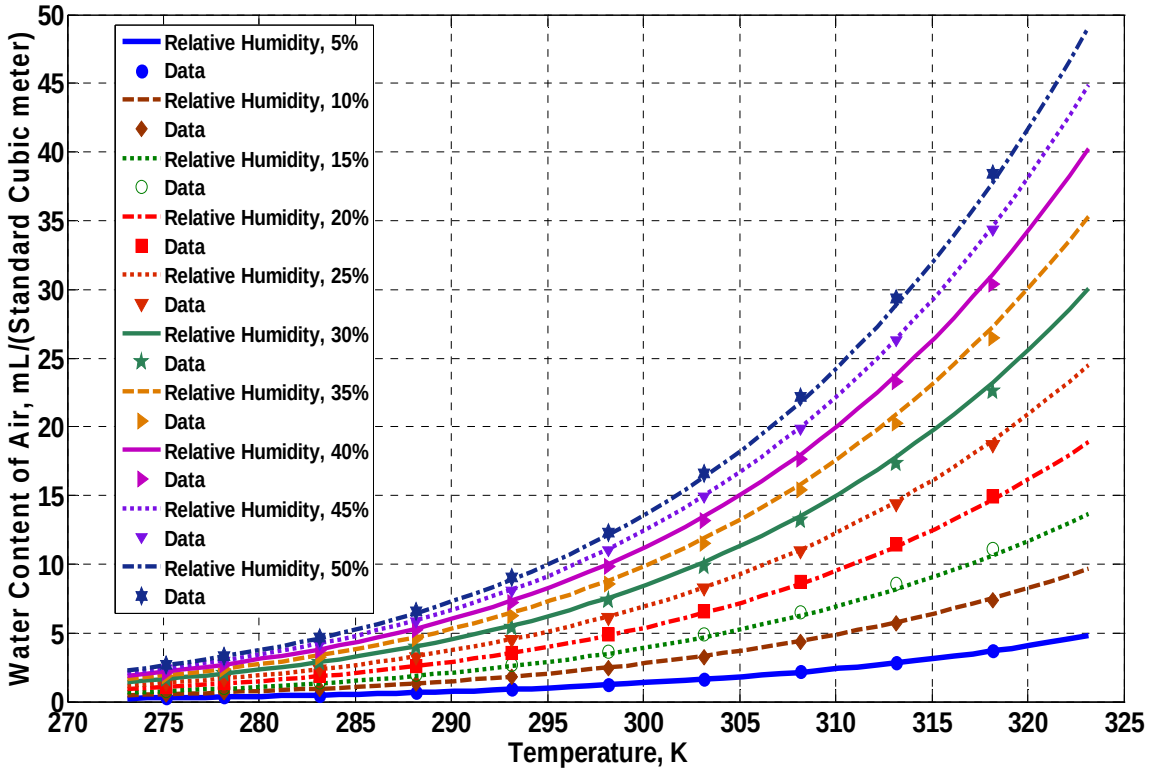

Figure 6.21: Air water content at atmospheric pressure as a function of relative humidity and temperature. Bahadori A. and Vuthaluru H. B, (2010n), *Chemical Engineering Research and Design*, in press (DOI: doi:10.1016/j.cherd.2010.05.008)

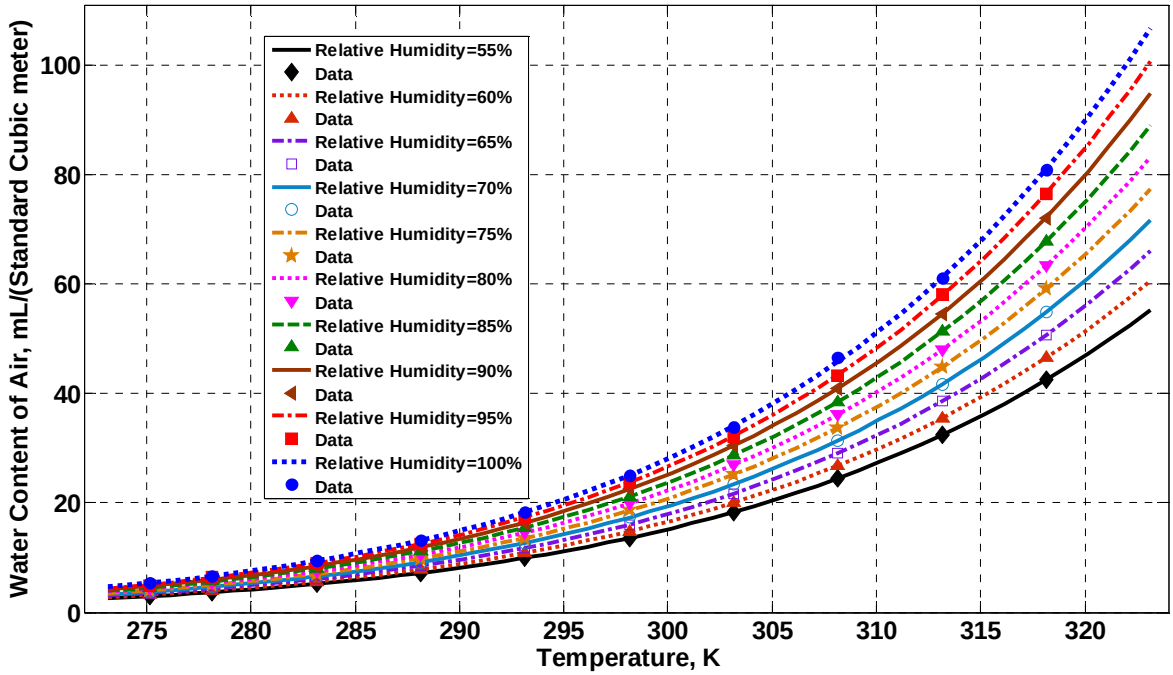

Figure 6.22: Air water content at atmospheric pressure as a function of relative humidity and temperature. Bahadori A. and Vuthaluru H. B, (2010n), *Chemical Engineering Research and Design*, in press (DOI: doi:10.1016/j.cherd.2010.05.008)

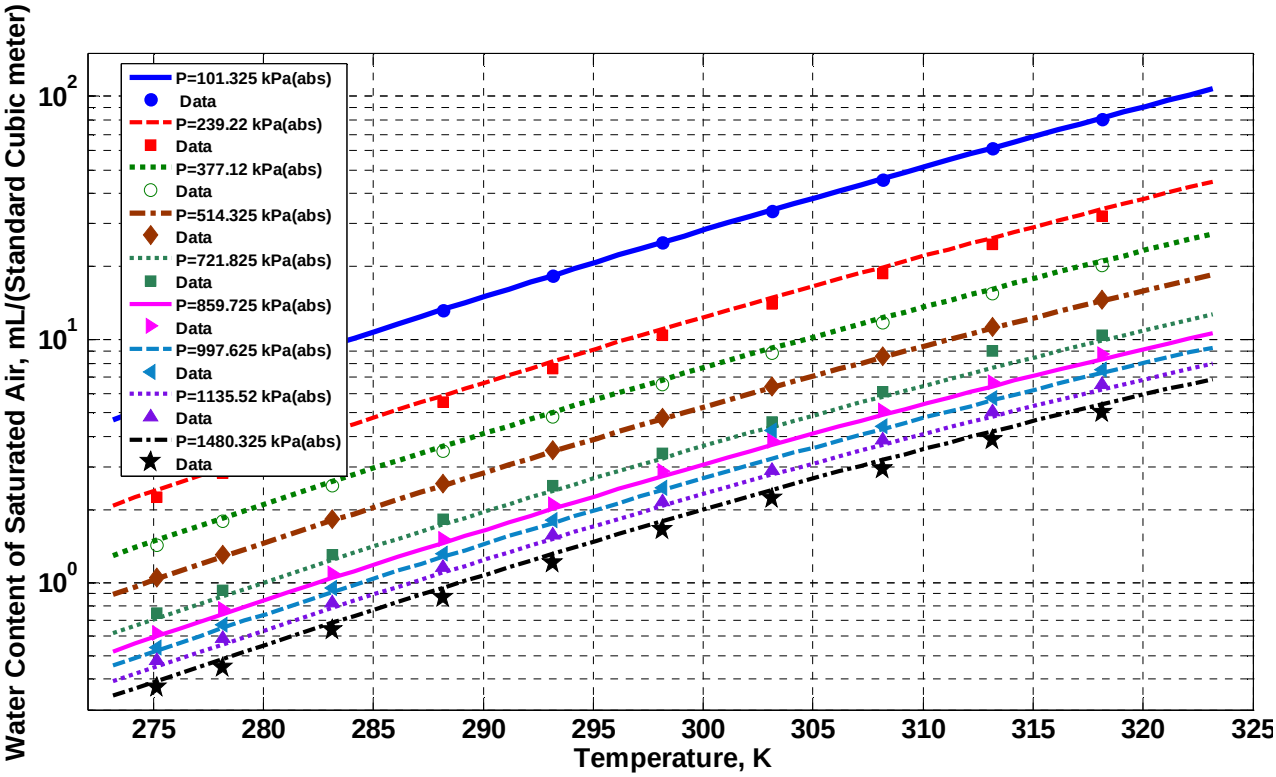

Figure 6.23: Saturated Air water content at elevated pressures. Bahadori A. and Vuthaluru H. B, (2010n), *Chemical Engineering Research and Design*, in press (DOI: doi:10.1016/j.cherd.2010.05.008)

6.9 Aqueous solubility and density of carbon dioxide

In this section, correlations for predicting density and the solubility of carbon dioxide in pure water as well as the aqueous sodium chloride solutions are developed, where using the generated interaction parameters, the solubility model is applied to correlate the carbon dioxide solubilities in aqueous solutions for temperatures between 300 to 400 K and pressures from 5 to 70 MPa. The correlation developed for predicting density of carbon dioxide accurately works for pressures between 2.5 and 70 MPa and temperatures between 293 K and 433 K (Bahadori et al 2009c).

The sequestration of anthropogenic carbon dioxide into geological formations has been considered as a potential method to mitigate climate change. Accurate evaluation of the capacity of a saline aquifer for CO_2 sequestration, and the fate of the injected fluids in sedimentary basins needs precise representation of brine and CO_2 PVT data (Hassanzadeh et al. 2008). There

are a large number of experimental equilibrium data on the CO2–brine system that have been used to tune the equations of state for CO2 and water under subsurface conditions. Accurate prediction of CO_2 solubility over a wide range of temperature, pressure and ionic strength (T–P–m) is important to the studies of the carbonate precipitation and to the tracing of the global carbon cycle (Butcher et al 1992). Several thermodynamic models are available to analyse the solubility of CO_2 in aqueous solutions of alkanolamines and to correlate the equilibrium CO2 loading (Harvey and Prausnitz, 1989; Li and Ngheim 1986; Zuo and Guo, 1991).

These models involve a large number of parameters and require more complicated and longer computations (Bahadori et al 2009c). Largely for environmental reasons, a great amount of work have been performed in order to determine the solubility of carbon dioxide in water at various temperatures. These solubility data have been compiled and correlated. In most cases, however, the thermodynamics models may not be sufficient if accurate predictions are needed. Therefore, there is an essential need to develop a correlation for accurate predicting aqueous solubility of carbon dioxide. Since accurate predicting carbon dioxide density is a key parameter in carbon dioxide sequestration. In this study, a simple correlation is also developed to predict density of CO_2 as a function of pressure and temperature. This correlation is helpful to realize the variation of carbon dioxide density in CO_2 sequestration process and also for enhanced oil recovery process (Bahadori et al, 2009). A table in appendix B presents the tuned coefficients used for determining the CO_2 solubilities for pure water as well as different sodium chloride (NaCl) solutions (Bahadori et al 2009c). Figure 6.24 compares results of the proposed correlation for predicting the solubility of CO_2 in pure water with the reported experimental data (Wiebe 1941).

Figures 6.25 and 6.27 also compare the results of the proposed correlation for predicting the solubility of CO_2 in 1, 2 and 4 molar solutions of sodium chloride with the reported data (Duan and Sun, 2003). As can be seen, there is a good agreement between the observed data and the model predictions. Figure 6.28 shows the results of simple proposed correlation to predict density of carbon dioxide for pressure range between 2.5 MPa to 70 MPa and temperature range between 293 K and 433 K. Results illustrate that the simple developed correlation has a good agreement with the reported data (Ahmed 2007). Figure 6.29 compares the results of proposed correlation for predicting the solubility of CO_2 in pure water and aqueous NaCl solutions. This study shows the solubility of CO_2 in aqueous NaCl solutions is more than pure water (Bahadori et al 2009c).

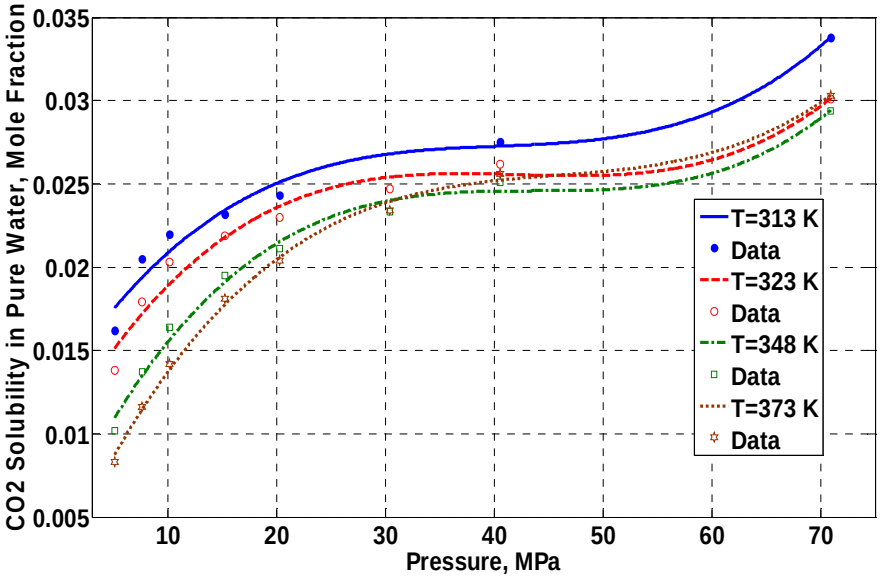

Figure 6.24 :Predicting CO2 solubility in pure water based on the proposed correlation Bahadori A., Vuthaluru H. B. and Mokhatab S. (2009c) *International Journal of Greenhouse Gas Control***.** (3), PP. 474–480

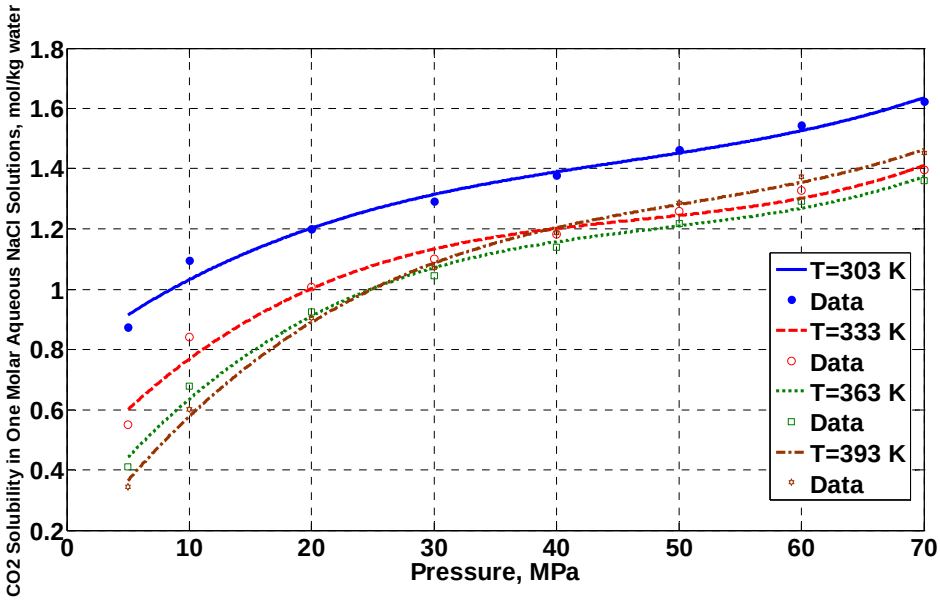

Figure 6.25: Predicting CO_2 solubility in one molar aqueous NaCl solution based on the proposed correlation. Bahadori A., Vuthaluru H. B. and Mokhatab S. (2009c) *International Journal of Greenhouse Gas Control***.** (3), PP. 474–480

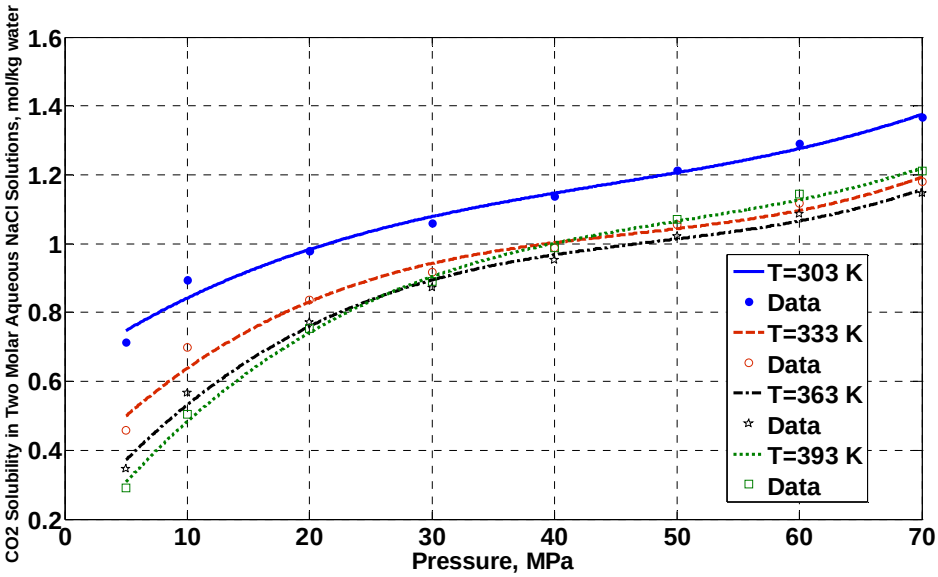

Figure 6.26: Predicting CO2 solubility in two molar aqueous NaCl solution based on the proposed correlation Bahadori A., Vuthaluru H. B. and Mokhatab S. (2009c) *International Journal of Greenhouse Gas Control***.** (3), PP. 474–480

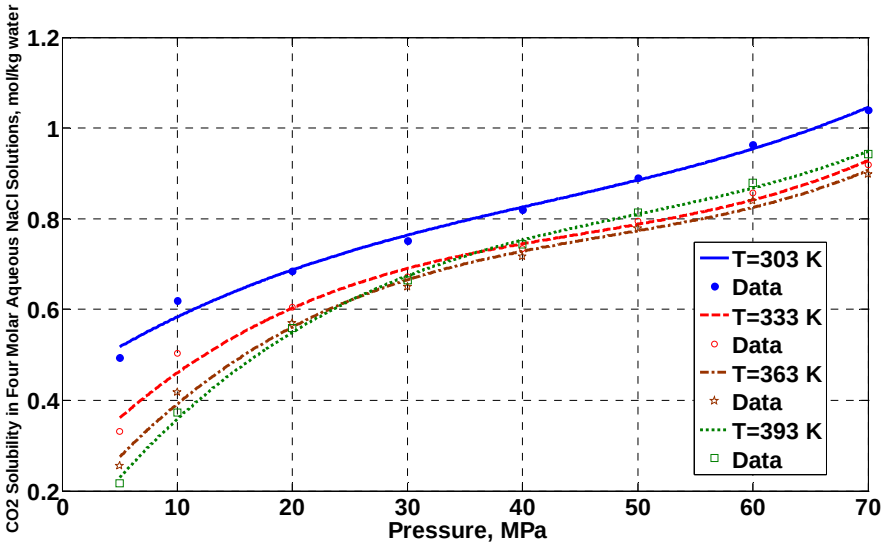

Figure 6.27: Predicting CO2 solubility in four molar aqueous NaCl solution based on the proposed correlation Bahadori A., Vuthaluru H. B. and Mokhatab S. (2009c) *International Journal of Greenhouse Gas Control* (3), PP. 474–480

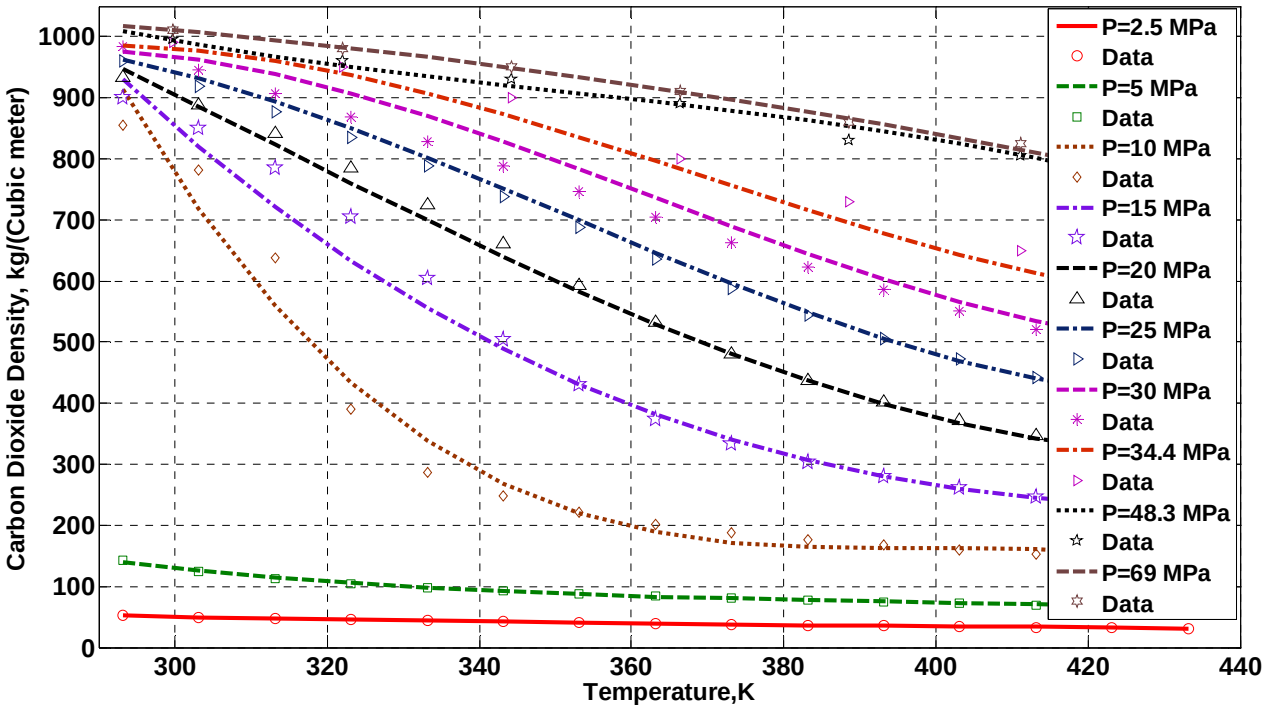

Figure 6.28: Predicting CO2 density based on the proposed correlation Bahadori A., Vuthaluru H. B. and Mokhatab S. (2009c) *International Journal of Greenhouse Gas Control* (3), PP. 474–480

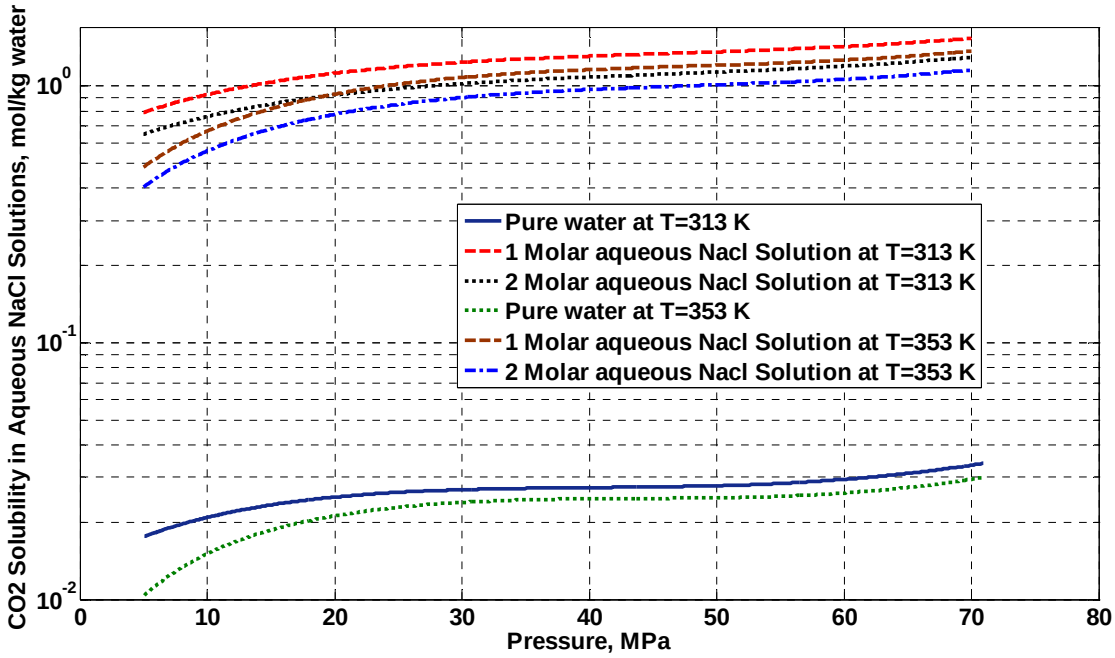

Figure 6.29: Predicting CO2 solubility in different molar aqueous NaCl solutions and temperatures based on the proposed correlation (Bahadori A., Vuthaluru H. B. and Mokhatab S. (2009c) *International Journal of Greenhouse Gas Control* (3), PP. 474–480)

Easy-to-use correlations have been developed to accurately predict the CO_2 density as well as the solubility of carbon dioxide in pure water and in aqueous NaCl solutions (Bahadori et al 2009c). The density correlation predicts density of carbon dioxide for pressure between 25 and 70 MPa and temperature between 293 K and 433 K. The solubility correlation is recommended for prediction of CO_2 solubility in the pure water and different aqueous solutions of NaCl for CO_2 pressures up to 70 MPa and temperatures less than 373 K and 393 K, respectively (Bahadori et al 2009c).

6.10 Thermal conductivity of hydrocarbons

Knowing thermal conductivity of hydrocarbons is an essential parameter in designing heat transfer equipments. The aim of this study is to develop a correlation for predicting thermal conductivity of liquid paraffin hydrocarbons, petroleum fractions and atmospheric natural hydrocarbon gases as a function of temperature and molecular weight or relative density.

The thermal conductivity is the important quantity of heat transmitted due to unit temperature gradient, under steady conditions in a direction normal to a surface of unit area. Heat transfer by conduction involves transfer of energy within a material without any motion of the material as a whole (Bahadori 2008b). From a process engineer's view point, utilizing various commercial software and using equations of state approaches to predict properties is convenient and easy-to-use, but such approaches do not work equally well for all properties. Accurate and reliable values result for some properties such as gas phase densities, volumes and Z-factors, while liquid volumes and densities are not so accurate but still as reliable as predictions using traditional methods. However experience show that equations of states are not suitable to predict thermal conductivities, viscosities, and surface tensions (Bahadori and Mokhatab 2008b; Bahadori 2008b).

For many simple organic liquids, the thermal conductivities are much more than those of the low-pressure gases at the same temperature (Reid, et al 1987). Pressure has a little effect on thermal conductivities of liquid; however, it will usually decrease by raising the temperature of the liquid. In the gas phase, the molecules are relatively free to move about transfer momentum and energy by a collisional mechanism. In the liquid, however, this hypothesis is not even roughly true (Bahadori and Mokhatab 2008b). The close proximity of molecules to one another emphasizes strongly the intermolecular forces of attraction.

There is little movement of the individual molecules, as evidenced by the low value of liquid diffusion coefficients, and often a liquid is modeled as a lattice with each molecule caged by its nearest neighbors (Reid, et al 1987). Energy and momentum are primarily exchanged by oscillations of molecules in the shared force fields surrounding each molecule (Bahadori and Mokhatab 2008b). To date, theory has not been successful in formulating useful and accurate expressions to calculate liquid thermal conductivities; approximate techniques must be employed for engineering applications (Reid, et al 1987).

In many instances the reported data are not believed to be particularly reliable and the estimation errors are in the same range as the experimental uncertainty. Thermal conductivity data is highly important in designing heat exchangers. The tuned coefficients used in these equations are given in Table B15. These tuned coefficients help to cover reported data in the temperature variation of -150°C to 300°C for liquid paraffin hydrocarbons, 0-200°C for natural/hydrocarbon gases, and liquid petroleum fractions (Bahadori and Mokhatab 2008b).

These coefficients can be retuned quickly by the proposed numerical methodology if more accurate experimental data are available in the future. Figure 6.30 illustrates the results of proposed correlation for predicting the thermal conductivity of natural gases as a function of temperature and molecular weight, comparing with some typical data from (Touloukian, et al 1970; Smith, et al 1960). As can be seen, the results of proposed correlation are accurate and acceptable (Bahadori and Mokhatab 2008b).
Figure 6.31 shows the results of proposed correlation for predicting the thermal conductivity of liquid petroleum fractions as a function of temperature and relative density (specific gravity), comparing with some typical data (Touloukian, et al 1970). As can be seen, the results of proposed correlation are in good agreement with the reported data. It also shows thermal conductivity increases for heavier petroleum fractions (Bahadori and Mokhatab 2008b).

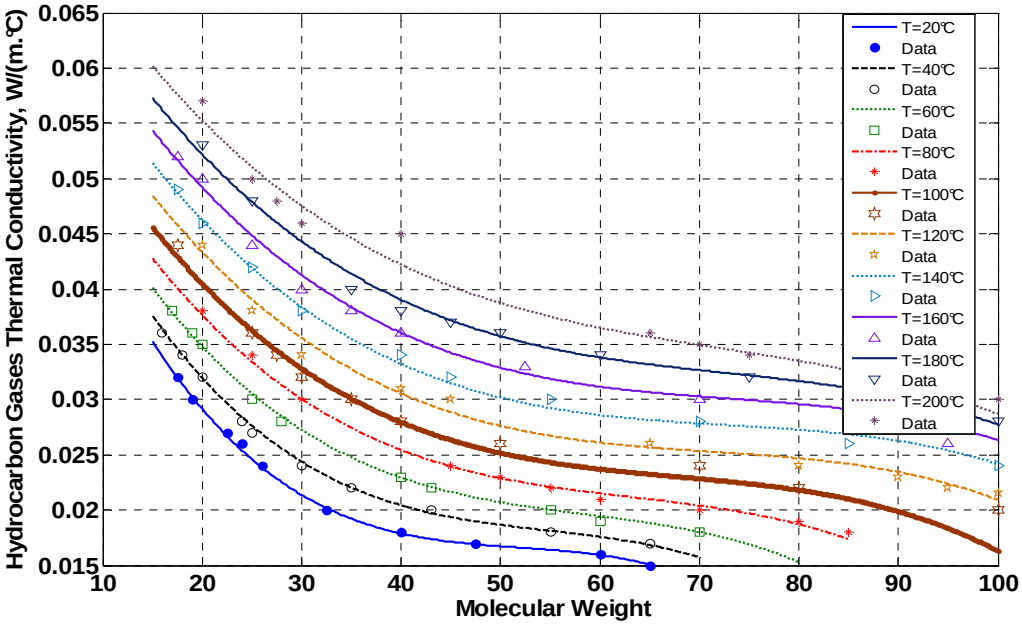

Figure 6.30: Predicting thermal conductivity of atmospheric natural hydrocarbon gases using new proposed correlation (Bahadori A. and Mokhatab S. (2008b) *Chemical Engineering*, 115, (13), pp. 52-54)

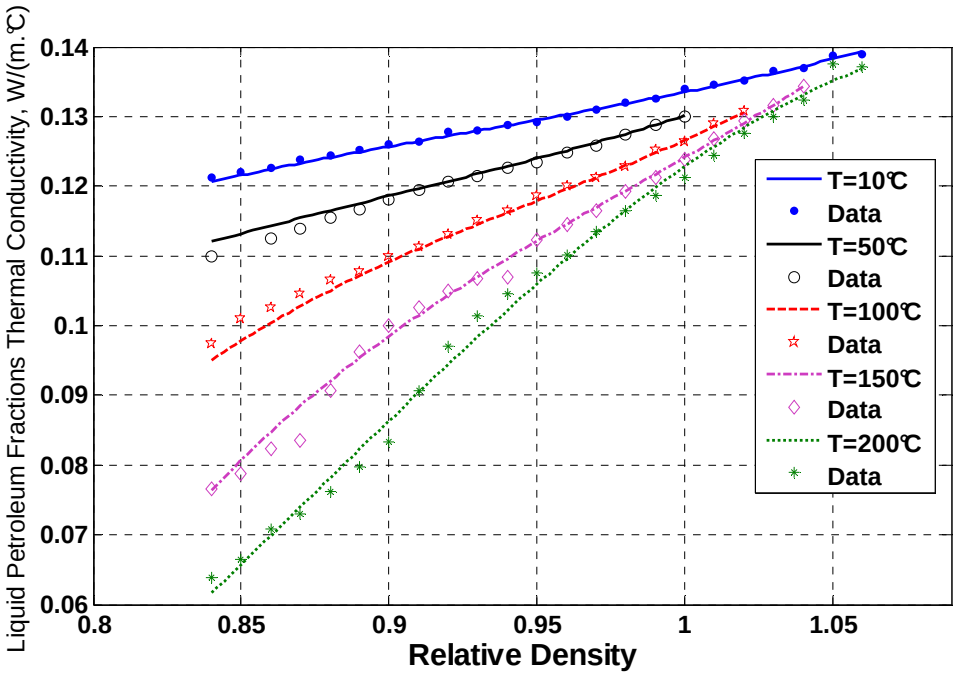

Figure 6.31: Predicting thermal conductivity of liquid petroleum fractions using new proposed correlation (Bahadori A. and Mokhatab S. (2008b) *Chemical Engineering*, 115, (13), pp. 52-54)

6.11 Water-hydrocarbon systems mutual solubility

Describing the mutual solubilities of hydrocarbons and water is very important in the energy industry. The presence of water in a hydrocarbon mixture can affect product's quality and damage the operation equipment due to corrosion and formation of gas hydrates (Bahadori et al 2008d). Tracing the concentration of hydrocarbons in aqueous media is also important for technical purposes like preventing oil spills and for ecological concerns such as predicting the fate of these organic pollutants in the environment. Over the last three decades a number of rigorous approaches to the description of the mutual solubilities of hydrocarbons and water have been attempted (Bahadori et al 2008d). However, there was no new model for a qualitative description of the mutual solubility of water and hydrocarbons for a broad range of systems, in a wide range of thermodynamic conditions. This part of thesis presents a correlation for an excellent prediction of water-hydrocarbon systems mutual solubility in a broad range of temperatures between 0 to 120 °C and heavy hydrocarbons between propane to Decan. The average absolute deviation from available reported data is 3%.

The knowledge of mutual solubility of liquid hydrocarbons in aqueous phase is important in a wide variety of applications in the oil and gas industry such as design and selection of operating conditions of oil/gas pipelines and production/processing facilities, storage of natural gas/sequestration of acid gases in underground caverns, produced water disposal and gas hydrate calculations (Bahadori et al 2008d). The knowledge of the phase equilibriums of aqueous mixtures with hydrocarbons is also important for environmental purposes since hydrocarbons, like other pollutants, must be removed from refinery wastewater streams and from sea or freshwaters when oil spills occur. For this purpose, knowing the solubility of hydrocarbons is required to describe the phase distribution through the removal process and also to assist in the design of separation equipment (Oliveira et al 2007).

Various thermodynamic models are available, which can calculate the phase equilibrium in water-hydrocarbon systems. However, all current thermodynamic models use difficult approaches to model the fluid phases. Considering this, there is a requirement to develop a correlation for a qualitative description of the mutual solubility of water and hydrocarbons for a broad range of systems in a wide range of thermodynamic conditions (Bahadori et al 2008d). The solubility of light alkanes (methane and ethane) in pure water has been studied extensively in the past decades. Figures 6.32 and 6.33 illustrate the solubility trends of C_3 to C_{10} components in water at different temperatures (Bahadori et al 2008d).

These graphs also show that light hydrocarbons such as propane are more soluble than heavy hydrocarbons such as decane in water and the solubility of hydrocarbon in water increases in higher temperatures. Figures 6.34 and 6.35 illustrate the solubility trends of water in different hydrocarbon components over a wide range of temperatures (Bahadori et al 2008d). These graphs also show that water is more soluble in light hydrocarbons comparing with the heavy hydrocarbon components. (Bahadori et al 2008d).

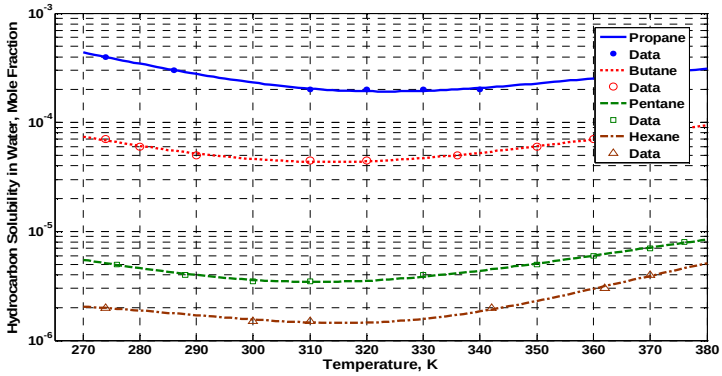

Figure 6.32: Predicting the aqueous solubility of C_3 to C_6 based on the new developed correlation (Bahadori A., Vuthaluru H.B., and Mokhatab S. and Tade M. O. (2008d), Chemical *Engineering & Technology*, 31, (12), pp. 1743-1747)

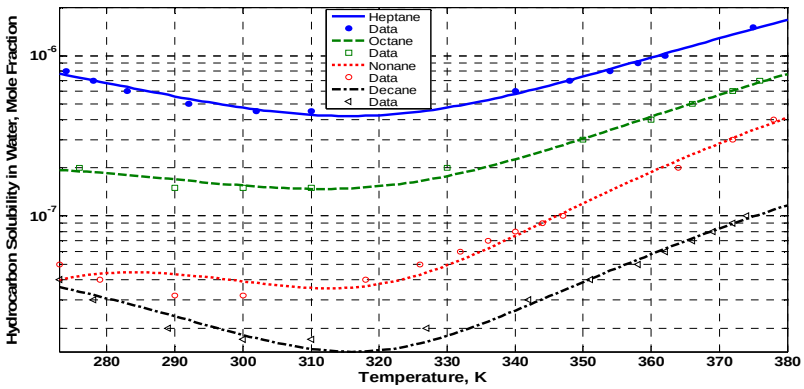

Figure 6.33: Predicting the aqueous solubility of C_6 to C_{10} based on the new developed correlation (Bahadori A., Vuthaluru H.B., and Mokhatab S. and Tade M. O. (2008d), *Chemical Engineering & Technology*, 31, (12), pp. 1743-1747)

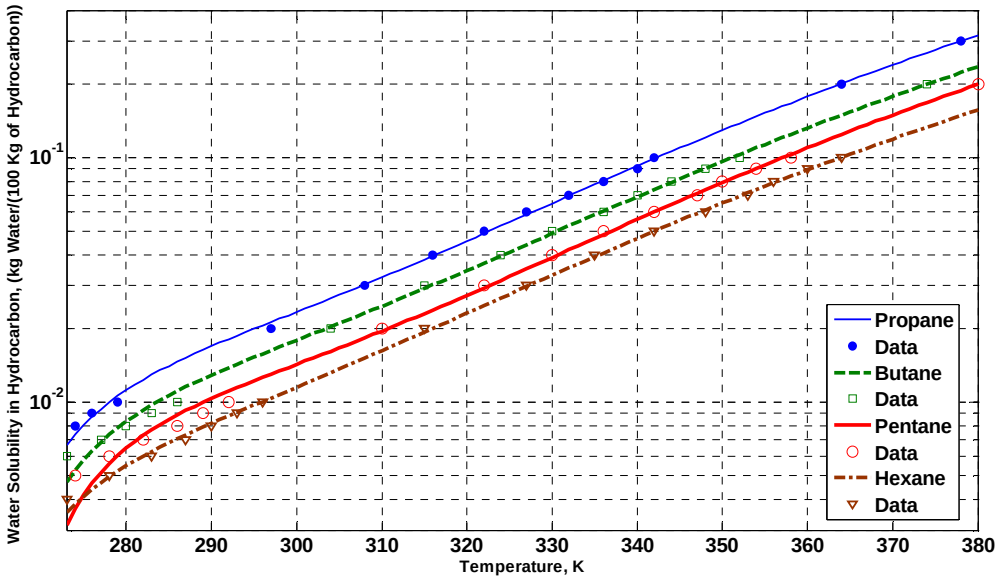

Figure 6.34: Predicting the solubility of water in C_3 to C_6 based on the new developed correlation (Bahadori A., Vuthaluru H.B., and Mokhatab S. and Tade M. O. (2008d), *Chemical Engineering & Technology*, 31, (12), pp. 1743-1747)

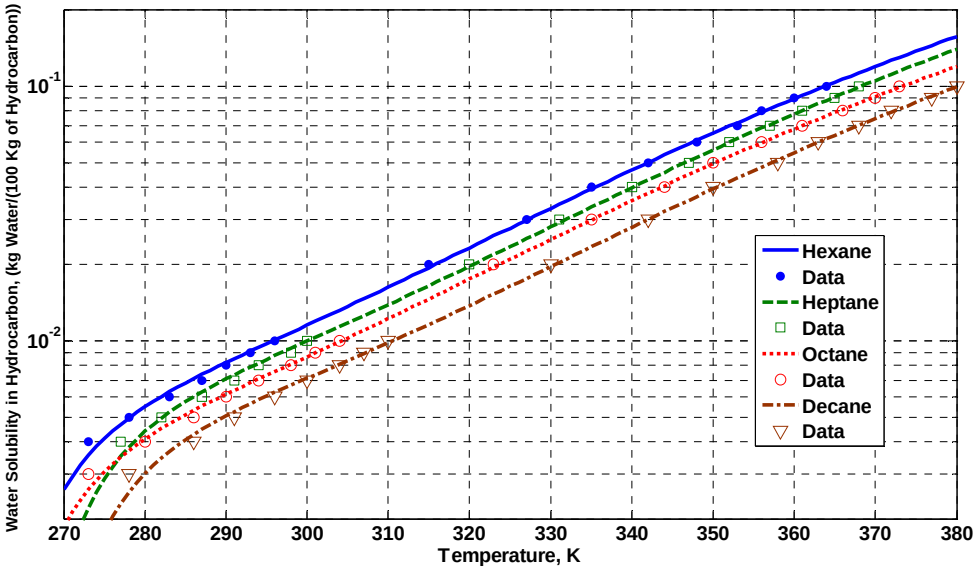

Figure 6.35: Predicting the solubility of water in C_6 to C_{10} based on the new developed correlation (Bahadori A., Vuthaluru H.B., and Mokhatab S. and Tade M. O. (2008d), *Chemical Engineering & Technology*, 31, (12), pp. 1743-1747)

6.12 Design of radiant and convective sections of direct fired heaters

Direct fired heaters are used considerably in the energy related industries and petroleum industries for heating crude oil in the petroleum refining and petrochemical sectors. The aim of the current study is to formulate new correlations to design the radiant and convective sections of direct fired heaters. The developed tools are easier than currently available models and involves a fewer number of parameters, requiring less complicated calculations and shorter computations.

Firstly, a simple correlation was developed to provide an accurate and rapid prediction of the absorbed heat in the radiant section of a fired heater, expressed as a fraction of the total net heat liberation, in terms of the average heat flux to the tubes, the arrangement of the tubes (circumferential), and the air to fuel mass ratio. Secondly, another simple correlation was developed to approximate external heat transfer coefficients for 75, 100, and 150 mm nominal pipe size (NPS) steel pipes arranged in staggered rows and surrounded by combustion gases. Finally, a simple correlation is presented to predict the gross thermal efficiency as a function of percent excess air and stack gas temperature. The proposed method can be of significant practical value for the engineers and scientists quickly check the design of radiant and convective sections of direct fired heater. In particular, mechanical and process engineers would find the proposed approach to be user-friendly involving no complex expressions with transparent and easy to understand calculations.

Figure 6.36 illustrates the results of proposed predictive tool for predicting the absorbed fraction of total heat liberation in the radiant section of a direct fired heater as a function of air to fuel mass ratio, kg/kg and the allowable heat flux to the tubes (W/m^2), comparing with some typical data (Gas Processors and Suppliers Association, 2004). As can be seen, the results of the new proposed predictive tool are accurate and acceptable. It also shows the emissivity of combustion gases decreases at higher air to fuel mass ratio, and increases for lower allowable heat flux to the tubes. Figure 6.37 shows the results of the proposed method to calculate the correcting coefficient "C" of the allowable heat flux to the tubes as a function pipes nominal size in meter.

Figures 6.38 and 6.39 shows the accuracy of predictive tool to estimate the percent gross thermal efficiency as a function of stack gas temperature and excess air percent in comparison with the reported data (Gas Processors and Suppliers Association, 2004). These graphs show excellent agreement between proposed predictive tool and reliable data in the literature. Figures

6.40 and 6.41 show external heat transfer coefficients for 75, 100 mm nominal pipe sizes (NPS) for steel pipes arranged in staggered rows and surrounded by combustion gases as a function of mass velocity and gas temperature. These graphs also demonstrate the excellent performance of the proposed predictive tool.

According to the authors' knowledge, there is no predictive tool in current literature to design radiant and convective sections of direct fired heaters. In view of this status, our efforts have been directed at formulating new predictive tool that can help engineers to design radiant and convective sections of direct fired heaters. This predictive tool is simple and unique expression which is non-existent in the literature.

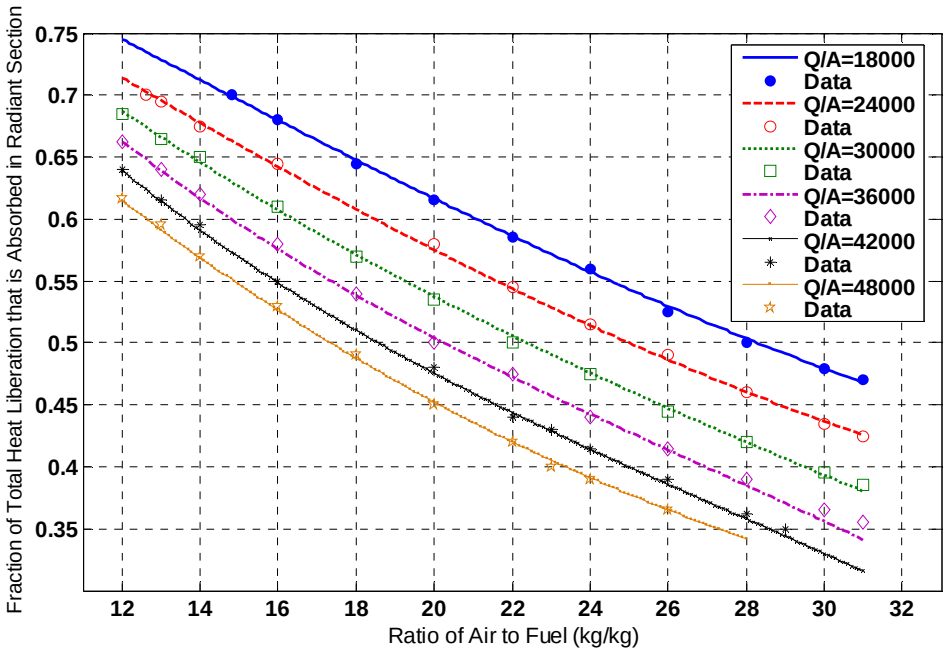

Figure 6.36: Prediction of absorbed fraction of total heat liberation in the radiant section of a direct fired heater as a function of air to fuel mass ratio, kg/kg and the allowable heat flux to the tubes (W/m^2) (Bahadori A. and Vuthaluru H. B, *Applied Energy*, (2010o) 87 2194–2202)

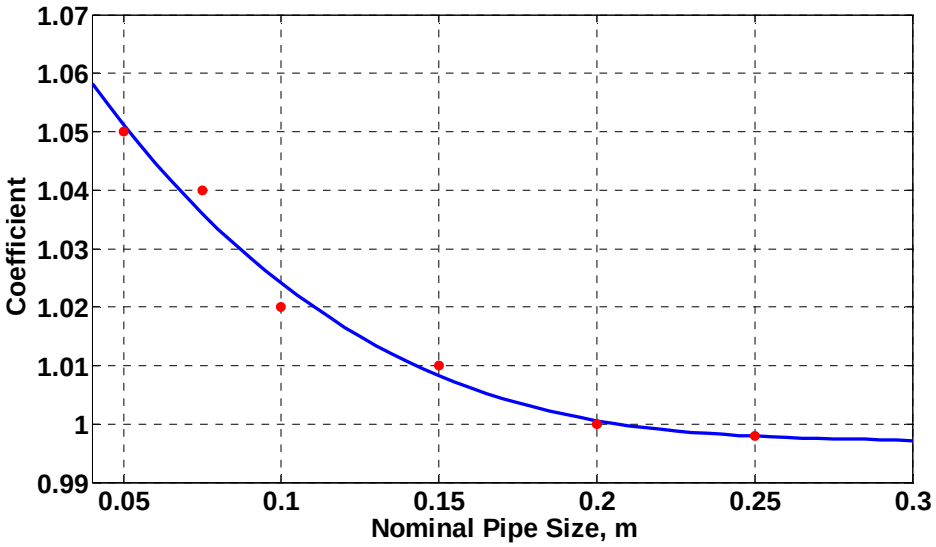

.

Figure 6.37: Results of the proposed method to calculate the correcting coefficient "C" of the allowable heat flux to the tubes as a function pipes nominal size. (Bahadori A. and Vuthaluru H. B, *Applied Energy*, (2010o) 87 2194–2202)

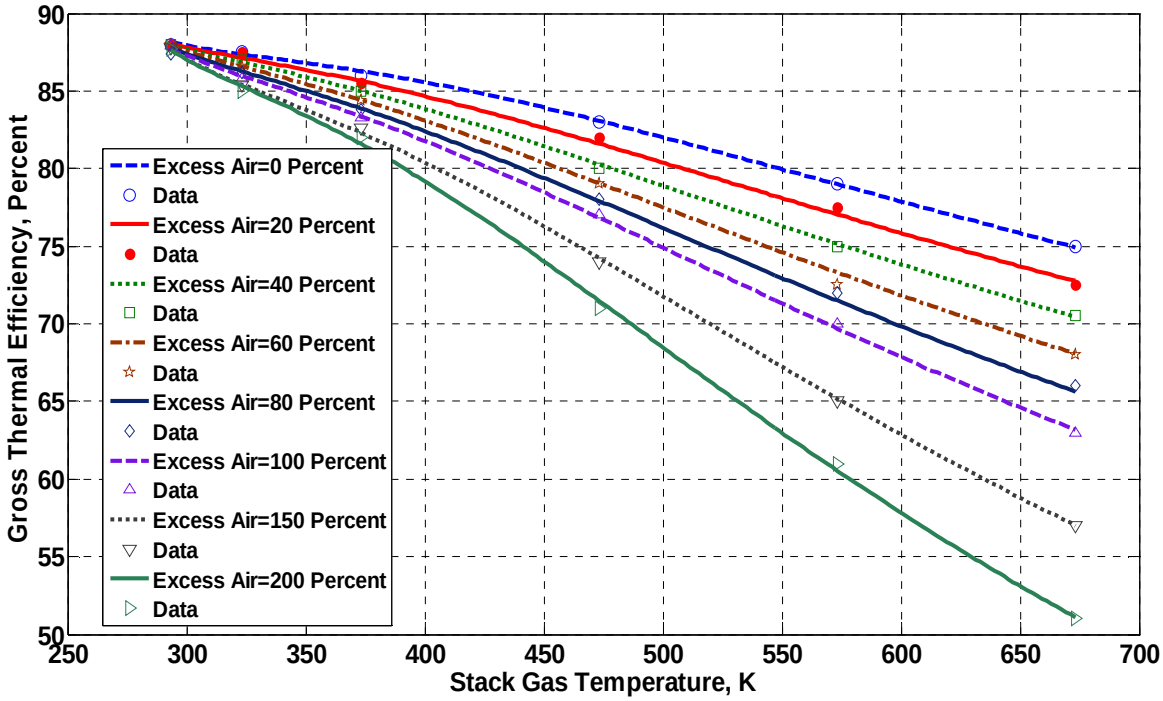

Figure 6.38: Gross thermal efficiency percent as a function of stack gas temperature and excess air percent for temperature less than 400°C (Bahadori A. and Vuthaluru H. B, *Applied Energy*, (2010o) 87, 2194–2202)

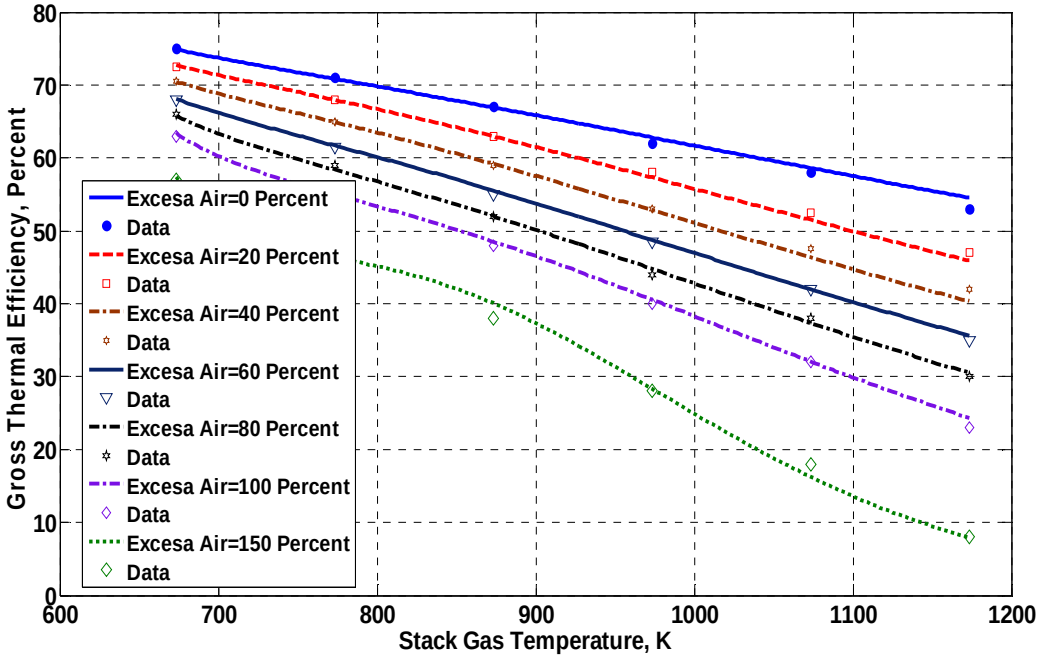

Figure 6.39: Percent gross thermal efficiency as a function of stack gas temperature and excess air percent for temperatures more than 673 K. (Bahadori A. and Vuthaluru H. B, *Applied Energy*, (2010o) 87 2194–2202)

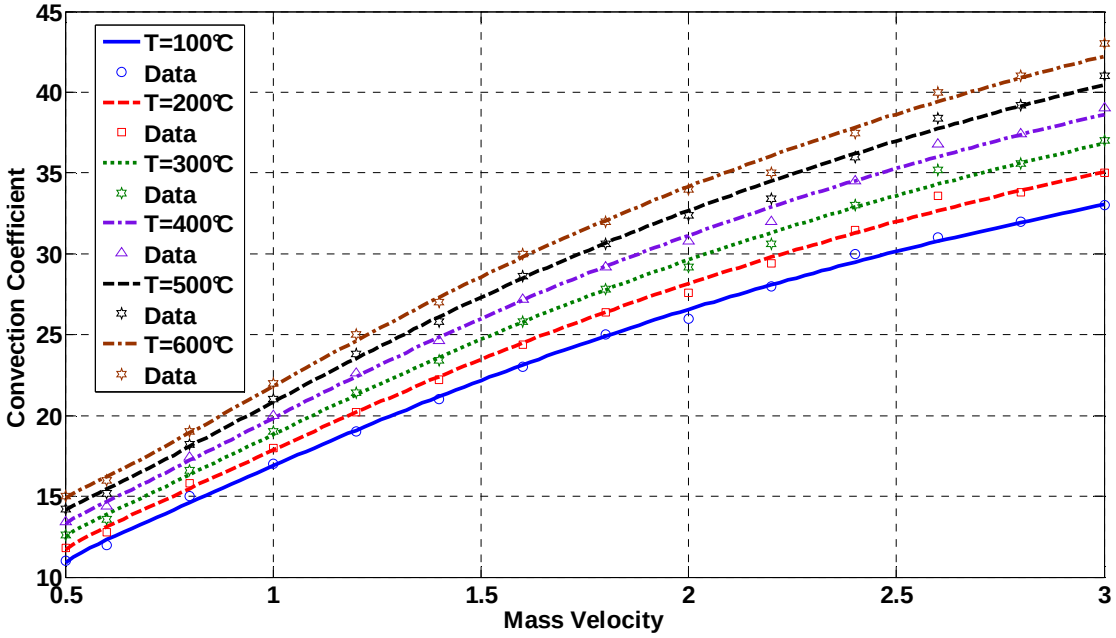

Figure 6.40: Prediction of convection heat transfer coefficient $(\frac{W}{m^2 °C})$ as a function of mass velocity $(\frac{kg}{m^2 S})$ and temperature for 89 mm OD steel pipe. (Bahadori A. and Vuthaluru H. B, *Applied Energy*, (2010o) 87 2194–2202)

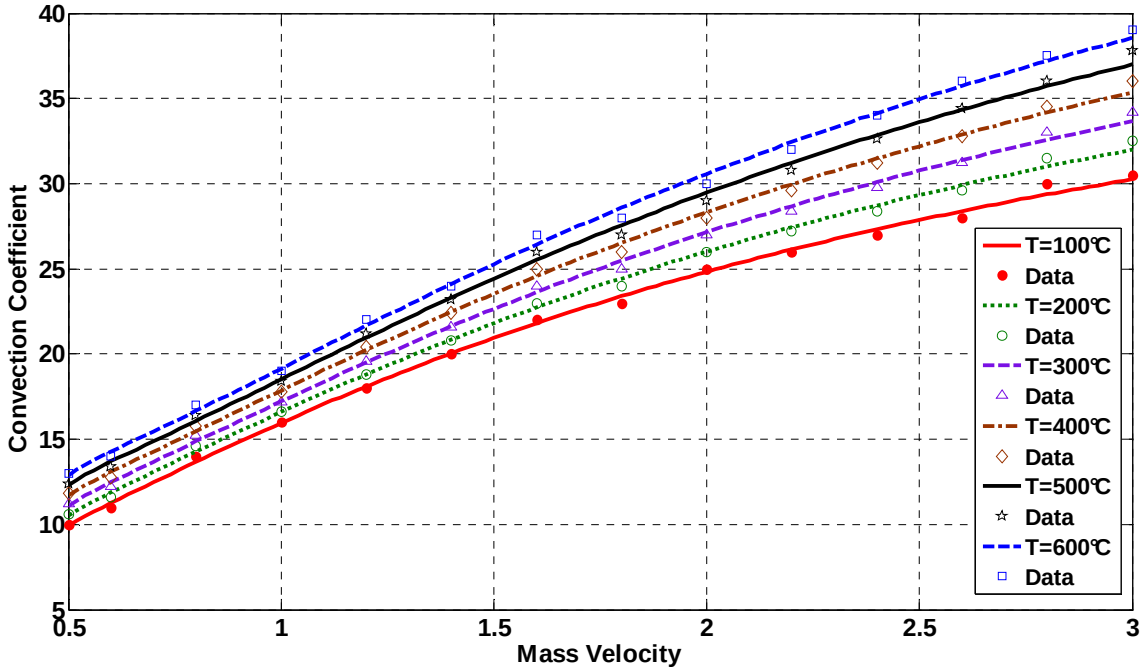

Figure 6.41: Prediction of convection heat transfer coefficient ($\frac{W}{m^2 °C}$) as a function of mass velocity ($\frac{kg}{m^2 S}$) and temperature for 114 mm OD (outside diameter) (Bahadori A. and Vuthaluru H. B, *Applied Energy*, (2010o) 87 2194–2202)

6.13 A method for estimation of absorption/stripping factors

Absorption and stripping are the unit operations which are widely used in the chemical processing industries. Many attempts have been made to define an average absorption factor method to short-cut the time consuming rigorous calculation procedures (Bahadori and Vuthaluru 2010p). The sole restriction of such a method is how well the average factor, as it is defined, will represent the absorption that actually occurs. The stripping operation is essentially the reverse of absorption and can be handled in a similar fashion. In this work, a simple predictive tool which is easier than existing approaches, less complicated with fewer computations is formulated to accurately predict the absorption efficiency as a function of absorption factor and number of absorber stages (Bahadori and Vuthaluru 2010p). The proposed predictive tool also can be used to determine the number of trays required for a given lean oil rate or to calculate recoveries with a given oil rate and tray count.

This method showed consistently accurate results for number of stages and absorption factors up to 20. This method is superior owing to its accuracy and clear numerical background, wherein the relevant coefficients can be retuned quickly for various cases (Bahadori and Vuthaluru 2010p). This proposed approach can be of immense practical value for the engineers and scientists to quickly check on absorption efficiency and estimating the trays required for a given lean oil rate or to calculate recoveries from a known oil rate and tray count at wide range of operating conditions without the necessity of any pilot plant set up and experimental runs. In particular, process engineers would find the proposed approach to be user friendly involving transparent calculations with no complex expressions (Bahadori and Vuthaluru 2010p).

This paper discusses the formulation of a predictive tool in a systematic manner to show the simplicity of the model and usefulness of such tools. Figure 6.42 shows the results of the proposed predictive tool in comparison with the reported data (GPSA Engineering Data book, 2004). It is clear that the proposed method yields results with good accuracy. Figure 6.43 illustrates the results of the proposed correlation for predicting absorption efficiency as a function of absorption factor and number of absorber stages. As can be seen from the figure, predicted values are reasonable for wide range of operating conditions.

Figures 6.42 and 6.43 show that when an oil rate declines with increasing number of trays and that beyond about eight theoretical trays little increase in efficiency is achieved. Since higher oil rates require more energy for heating, cooling and pumping, the optimum design is usually one that uses the minimum possible oil rate with a reasonable size absorber. The lowest molecular weight lean oil should be used. This will be fixed by oil vapor pressure and absorber operating temperature.

The predictive tool proposed in the present work is novel and unique expression which is non-existent in the literature. This is expected to benefit the oil and gas industries in making design amendments leading to informed decisions for the prediction of absorption/stripping efficiency for a given application in any process industry. Furthermore, the predictive tool described in the paper appears to be superior and reliable, wherein the relevant coefficients can be retuned quickly if more data are available in the future.

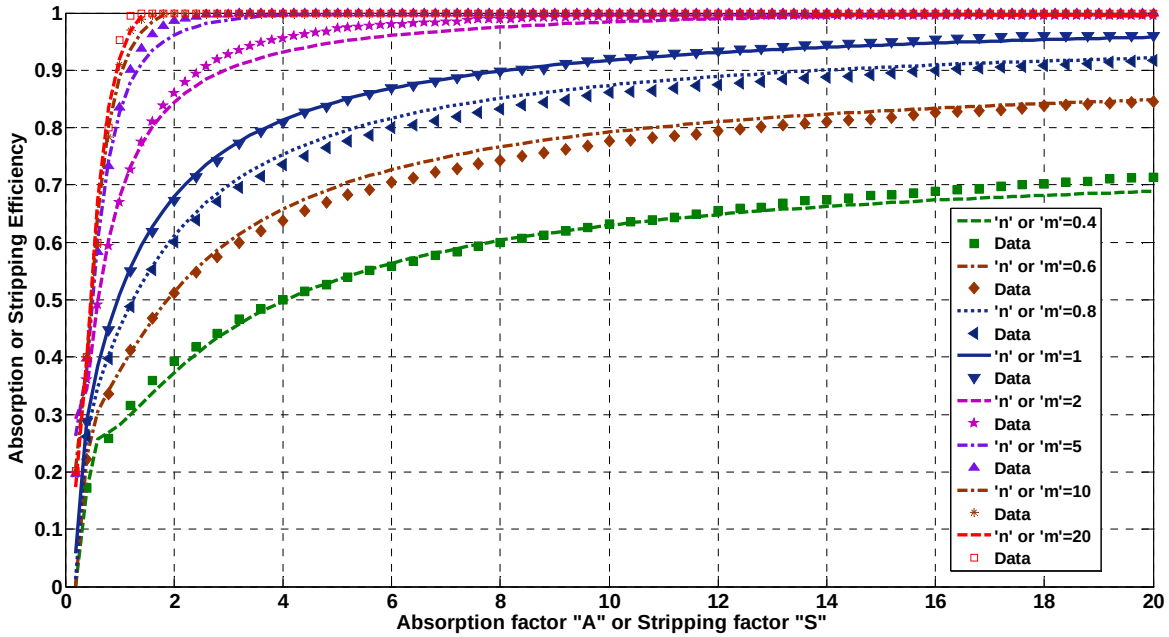

Figure 6.42: Prediction of absorption and stripping efficiency in comparison with data [(GPSA Engineering Data book, 2004), Kremser (1930) and Brown (1932)] Bahadori A. and Vuthaluru H. B, (2010p), *Computers & Chemical Engineering* 34, 1731-1736

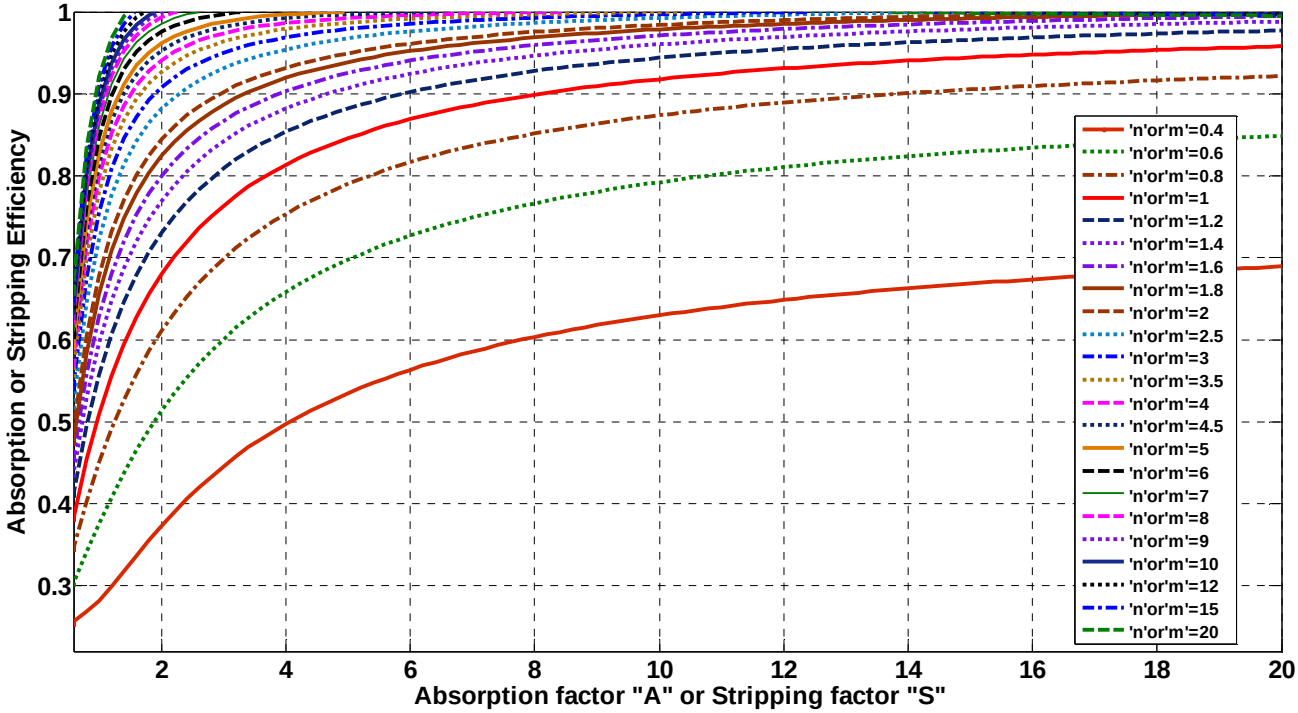

Figure 6.43: Performance of predictive tool in prediction of absorption and stripping efficiency, Bahadori A. and Vuthaluru H. B, (2010p) *Computers & Chemical Engineering* 34, 1731-1736

6.14 Estimation of maximum shell-side vapour velocities through heat exchangers

Shell-side vapour velocities through heat exchangers should be kept low to prevent erosion when moisture or suspended particles are present (Bahadori and Vuthaluru 2010q) In this work, new equations, which are easier than currently available models and involve a fewer number of parameters, requiring less complicated and shorter computations, are formulated to arrive at an appropriate prediction of maximum shell-side vapour velocities through heat exchangers for wide range of conditions as a function of molecular weight and pressure. The proposed fitted equations accurately estimate the maximum shell-side vapour velocities through heat exchangers for pressures up to 7500 kPa(abs), and molecular weights up to 400 (Bahadori and Vuthaluru 2010q). In order to reduce pressure drop, velocities must be well below the maximum values (Bahadori and Vuthaluru 2010q).

The fitted equations developed in this study can be of immense practical value for engineers and scientists to quickly check the maximum shell-side vapour velocities through heat exchangers at a wide range of conditions without opting for any experimental measurements (Bahadori and Vuthaluru 2010q). In particular, chemical and process engineers would find the simple equations to be user-friendly with transparent calculations involving no complex expressions. To date, there are no simple equations for an accurate and rapid estimation of maximum shell-side vapour velocities through heat exchangers. In view of this necessity, our efforts have been directed at formulating new tool that can help engineers and researchers. These fitted coefficients help to maximum shell-side vapour velocities through heat exchangers for vapor molecular weights up to 400 as well as pressures up to 7500 kPa (abs). The optimum tuned coefficients given in appendix B can be further retuned quickly according to proposed approach if more data are available in the future (Bahadori and Vuthaluru 2010q).

The proposed fitted equations in the present work are simple and unique expression which is non-existent in the literature. Furthermore, the selected exponential function to fit the equations leads to well-behaved (i.e. smooth and non-oscillatory) equations enabling fast and more accurate predictions. For nozzles, velocities can be 1.2 to 1.4 times values are calculated here. (Bahadori and Vuthaluru 2010q) Figure 6.44 shows the calculated results from the proposed fitted equations for the maximum shell-side vapor velocities through heat exchangers as a function of pressure and molecular weight with the reported data (Ludwig 1983 and Branan, 2005).

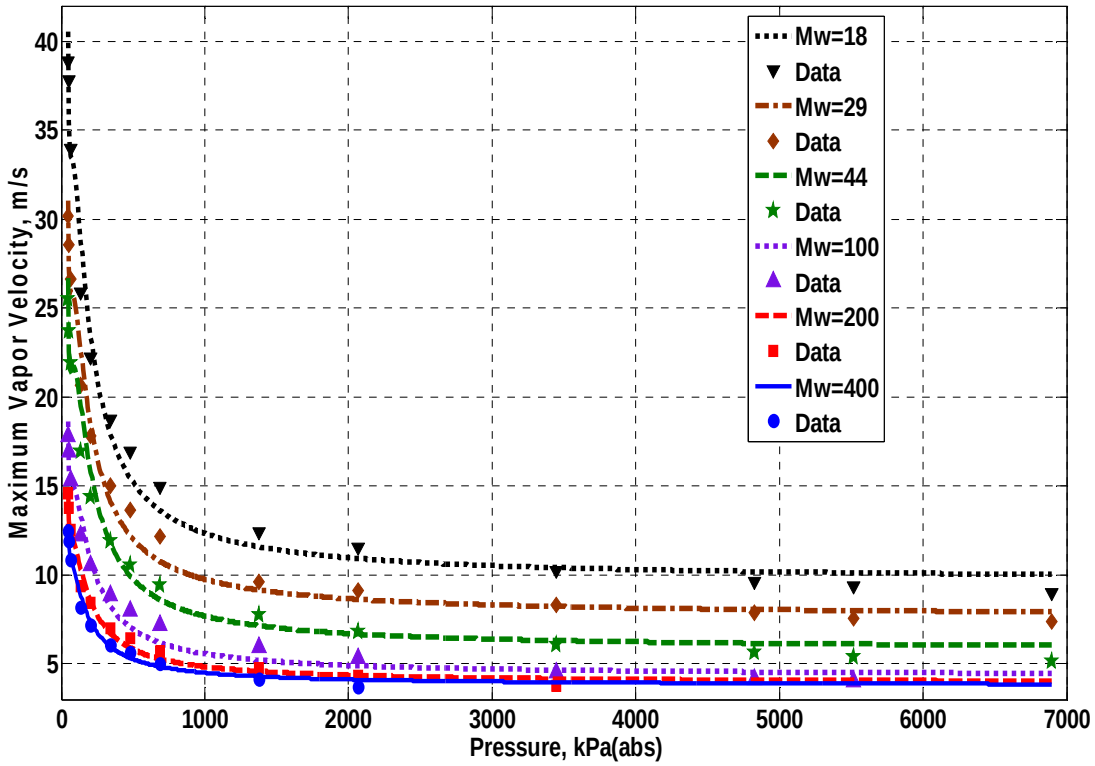

Figure 6.44: Maximum shell-side vapour velocities through heat exchangers as a function of molecular weight in comparison with the reported data (Ludwig 1983 and Branan, 2005) (Bahadori A. and Vuthaluru H. B, (2010q) Chemical Engineering Research and Design. doi:10.1016/j.cherd.2010.04.001)

6.15 Prediction of dissolved oxygen saturation concentrations in aquatic systems

A sufficient supply of dissolved oxygen (DO) is vital for life in higher organisms. In aquatic systems, oxygen regulates respiratory metabolism, mediates biogeochemical cycles, and is an integral component of water quality. In this section, a simple predictive tool for dissolved oxygen saturation concentrations in aquatic systems as a function of chloride concentration and temperature using a novel Arrhenius-type asymptotic exponential function has been formulated (Bahadori and Vuthaluru, 2010r). The proposed method predicts the amount of dissolved oxygen saturation concentrations for temperatures up to 50°C and chloride concentrations up to 25 gram per litre.

The tool developed in this study can be of significant engineering value for the engineers and scientists to quickly check on the oxygen saturation concentrations in aquatic systems at various conditions without opting for any experimental measurements. In particular, environmental science experts would find the proposed approach to be user-friendly with transparent calculations involving no complex expressions. A large number of textbooks cover the principles of water-quality modelling such as James (1993) and Chapra (1997), which include references to particular modelling tools. There is also a very large body of literature that describes individual models and processes (Cox, 2003, and Streat et al., 2008) (Bahadori and Vuthaluru, 2010r). The relationship between the mole fractions of the gas in a liquid is given by Henry's law; However, Henry's law does not consider the salinity parameter in the prediction of oxygen solubility in aquatic systems. In light of the above mentioned issues, there is an essential need to develop a practical reliable and easy-to-use method for practice engineers for the rapid prediction of dissolve oxygen saturation concentrations in aquatic systems.

Here it will be discussed the formulation of a simple predictive tool which can be of significant importance for the environmental science experts and engineers dealing with the aquatic systems. The predictive tool is of practical value for environmental issues in terms of assessing operational parameters by providing an advance indication of key variables which could potentially assist practice engineers to take appropriate remedial measures to monitor the quality of aquatic systems (Bahadori and Vuthaluru, 2010r).

These optimum tuned coefficients, reported in appendix B help to cover the oxygen saturation concentrations in aquatic systems (C_O) for temperatures up to 50°C as well as chloride concentrations up to 25 gram per liter. The optimum tuned coefficients given in appendix B can be retuned quickly according to proposed approach if more data are available in the future. The proposed novel tool in the present work is simple and unique expression which is non-existent in the literature. Furthermore, we have selected exponential function to develop the tool which is well-behaved (i.e. smooth and non-oscillatory) equations enabling fast and more accurate predictions.

Figure 6.45 shows the predicted results from the predictive tool for the oxygen saturation concentrations in aquatic systems (C_O) as a function of temperature along with the reported data (Droste 1997). It is evident from this figure that there is a good agreement between predicted values (for wide range of chloride concentrations (ψ) and temperatures) and the reliable data (Droste 1997). Figure 6.45 shows the oxygen saturation concentrations in aquatic

systems decreases at high temperature and high chloride concentrations. Figure 6.46 shows the performance of proposed correlation for wide range of conditions (Bahadori and Vuthaluru, 2010r). Current efforts in this investigation are likely to pave the way for handling the problems associated with the calculations for oxygen saturation concentrations in aquatic systems which can be used by the process engineers and environmental experts for monitoring the operational parameters on a regular basis (Bahadori and Vuthaluru, 2010r).

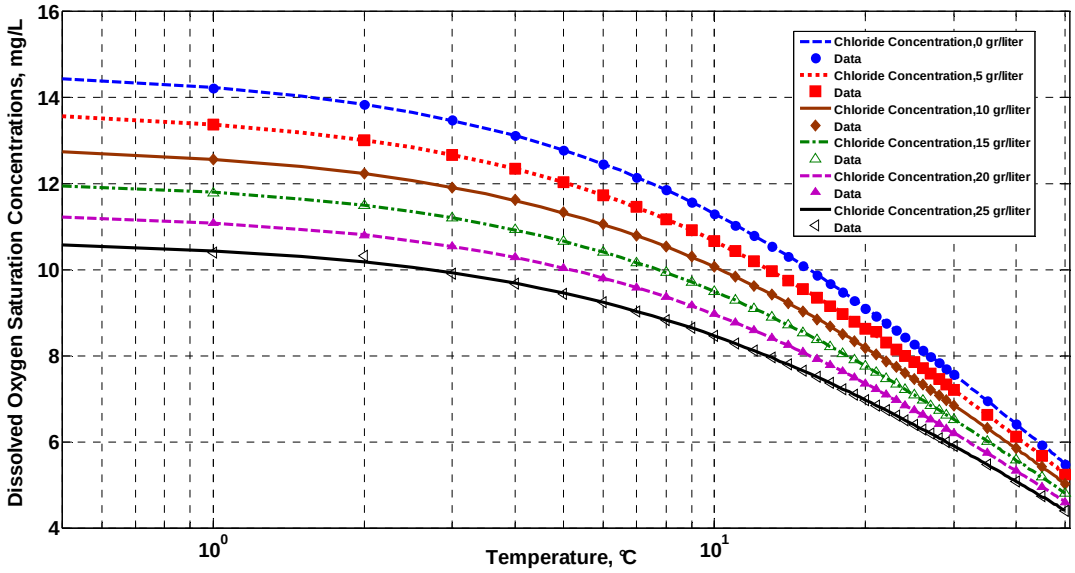

Figure 6.45: Oxygen saturation concentrations in aquatic systems as a function of chloride concentration and temperature with the reported data (American Public Health Association Standard method for the examination of water and wastewater, 1992 and Droste 1997) (Bahadori A. and Vuthaluru H. B, (2010r) *Process Safety and Environmental Protection* 88, pp. 335-340

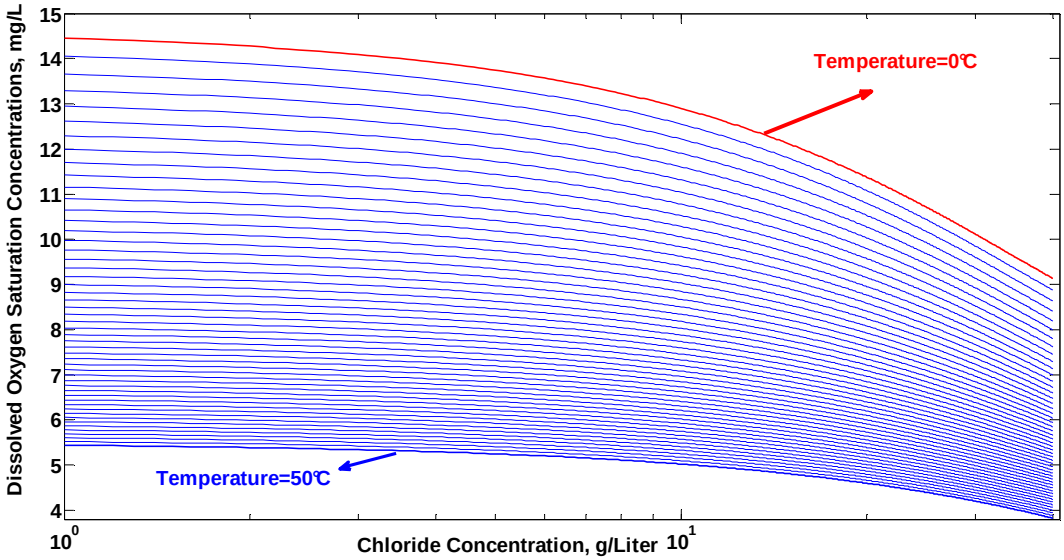

Figure 6.46: Performance of proposed predictive tool for prediction of the oxygen saturation concentrations in aquatic systems as a function of aqueous chloride concentrations and temperatures (Bahadori A. and Vuthaluru H. B, (2010r) *Process Safety and Environmental Protection* 88, pp. 335-340

6.16 Simple method for estimation of unsteady state conduction heat flow in slabs and spheres

When a solid is exposed to a hot gas or liquid, the resistance to heat transfer in the fluid is usually significant, as the surface temperature changes with time (Bahadori and Vuthaluru, 2010s). In this work, an attempt has been made to formulate a new method for one-dimensional heat flow with variable surface temperatures in slabs and spheres as a function of the Fourier number and the Biot number in order to arrive at the temperature distribution in the solid and the average solid temperature changes with time. The proposed correlation is simple to use, employing basic algebraic equations that can easily and quickly be solved using a spreadsheet. In addition, the estimates are quite accurate, as evidenced by the comparisons with literature data (McCabe et al 2005). The proposed tool appears to be superior owing to its accuracy and simple background, wherein the relevant coefficients can be retuned quickly if more data are available in the future. It is expected that our efforts in this investigation will pave the way for arriving at an accurate prediction of heat flow with variable surface temperature in slabs and spheres to get the temperature distribution in the solid and the average solid temperature change with time at various conditions (Bahadori and Vuthaluru, 2010s).

This investigation has definitely paved the way to accurate predict one-dimensional heat flow with variable surface temperature in slabs and spheres. In particular, mechanical and process engineers would find the proposed approach to be user-friendly involving no complex expressions with transparent calculations. The proposed method is superior owing to its accuracy and clear numerical background; wherein the relevant coefficients can be retuned quickly for various cases and if new data become available in the future.

Figure 6.47 illustrates the results of proposed method for predicting the average temperature change for slabs in comparison with some typical data obtained from the literature (McCabe et al 2005). Figure 6.48 shows the results of proposed method for predicting the average temperature change for spheres in comparison with some typical data (McCabe et al 2005) for wide range of conditions. As can be seen in figures 2 and 3, the results of the new proposed method are accurate and acceptable. Figures 6.49 and 6.50 show the excellent performance of proposed method in prediction of temperature distribution in the solid slab and sphere shape respectively and the average solid temperature change with time

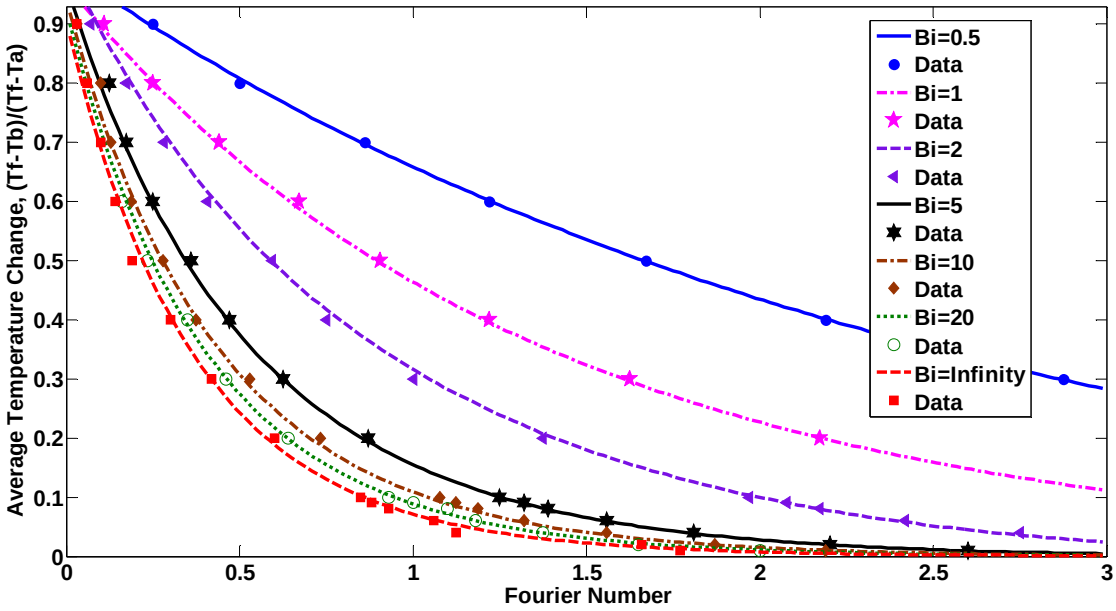

Figure 6.47: Prediction of the temperature distribution in the solid slab shape and the average solid temperature change with time (Bahadori A. and Vuthaluru H. B, (2010s), *International Journal of Heat and Mass Transfer*, 53, 4536-4542

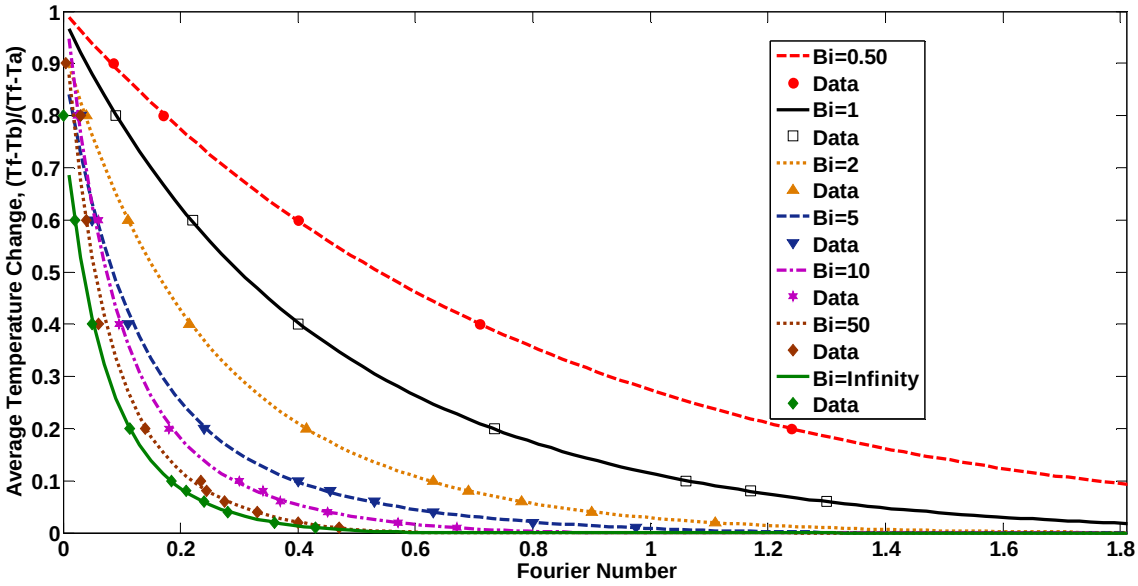

Figure 6.48: Prediction of the temperature distribution in the solid sphere shape and the average solid temperature change with time (Bahadori A. and Vuthaluru H. B, (2010s), *International Journal of Heat and Mass Transfer*, 53, 4536-4542

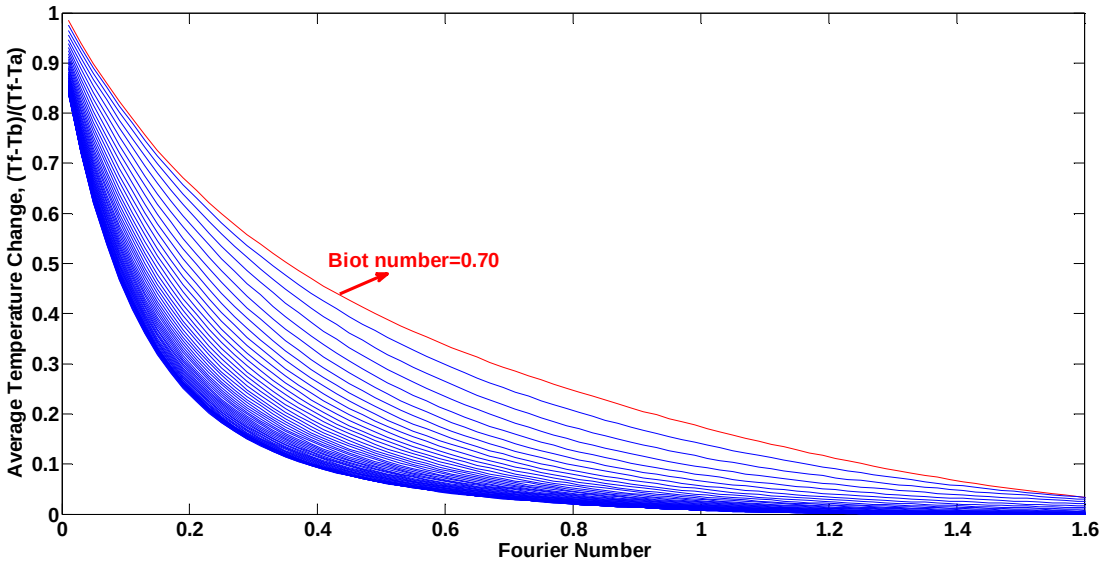

Figure 6.49: Performance of proposed tool for prediction of the temperature distribution in the solid slab shape and the average solid temperature change with time (Bahadori A. and Vuthaluru H. B, (2010s), *International Journal of Heat and Mass Transfer*, 53, 4536-4542

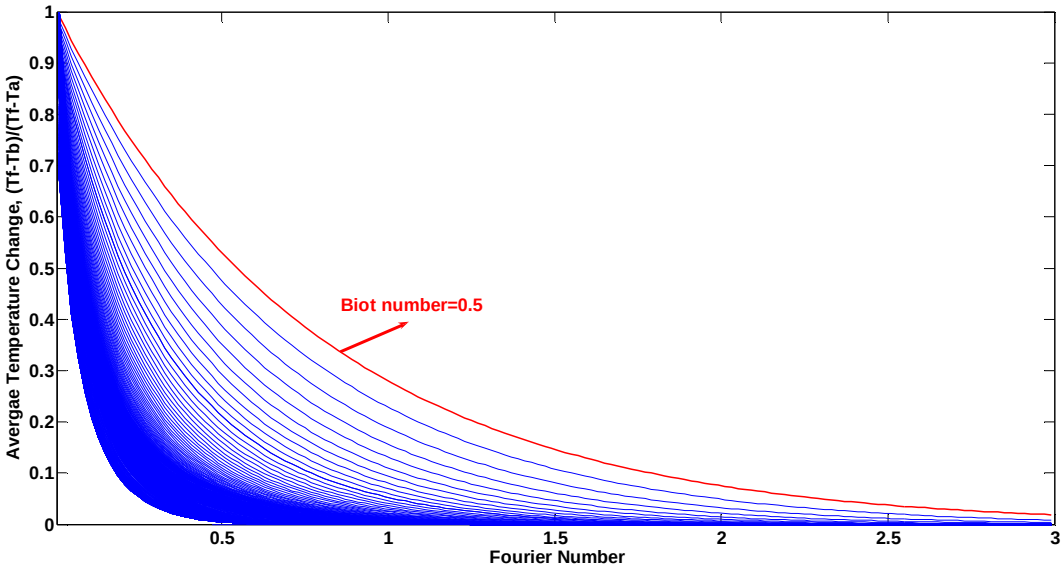

Figure 6.50: Performance of proposed tool for prediction of the temperature distribution in the solid sphere shape and the average solid temperature change with time (Bahadori A. and Vuthaluru H. B, (2010s), *International Journal of Heat and Mass Transfer*, 53, 4536-4542

6.17 Estimation of performance of steam turbines using a simple predictive tool

The objective of the steam turbine is to maximize the use of the available steam energy where the available steam energy is defined as the difference between the inlet and exhaust energies (enthalpies) for a 100% efficient constant entropy (i.e. isentropic) process (Bahadori and Vuthaluru, 2010t). There are numerous loss mechanisms which reduce the efficiency from isentropic process such as throttling losses, steam leakage, friction between the steam and the nozzles/buckets, bearing losses, etc. Efficiencies can range from a low of 40% for a low power single-stage turbine to a high approaching 90% for a large multistage, multi-valve turbine (Bahadori and Vuthaluru, 2010t). Most equipment driven by steam turbines are centrifugal machines where power varies as the cube of speed. Part load efficiency varies as a function of speed, flow, and the number of stages. By assuming power to vary as the cube of speed the turbine part load efficiency can be approximated as a percentage of the design efficiency (Bahadori and Vuthaluru, 2010s).

In this section, a simple predictive tool, which is easier than existing approaches, as it contains less complicated expressions with shorter computations, is presented for the rapid prediction of steam rate, turbine efficiency, and the inlet and exhaust nozzle diameters to determine the actual

steam rate (ASR) and total steam requirements for both multi-stage and single-stage turbines. The proposed method predicts the above mentioned parameters for inlet steam pressures up to 12000 kPa, turbine ratings up to 10000 kW as well as the exhaust air over inlet air ratios of up to 0.55 (Bahadori and Vuthaluru, 2010t).

Current methods are more complicated and need longer computations for rigorous investigation of the design and performance characteristics of hybrid system configurations consisting of gas turbine and steam turbine for power applications (Bahadori and Vuthaluru, 2010t). Moreover, when the mechanical equipments such as steam turbines are put into operation, their performance will degenerate with the increases in operation time. The levels of performance degeneration may vary with the working environment, mission, working character and maintenance of the equipment (Bahadori and Vuthaluru, 2010t). In addition, the high cost that companies incur in these days for energy consumption makes it necessary to develop a practical, reliable and easy-to-use method for power generating industries in terms of assessing operational parameters (Bahadori and Vuthaluru, 2010t).

In light of the above mentioned issues faced by the power generating industries, there is an essential need to develop a practical, reliable and easy-to-use method for practice engineers to estimate the steam rate, turbine efficiency and the inlet and exhaust nozzle diameters to determine the actual steam rate (ASR) and total steam requirements for both multi-stage and single-stage steam turbines (Bahadori and Vuthaluru, 2010t). This section discusses the formulation of a simple method which can be of significant importance for engineers dealing with steam turbines. The present approach is of practical significance for power generating industries in terms of assessing operational issues. In particular the proposed predictive tool gives an advance indication of key parameters which could potentially enable practice engineers to take appropriate measures so as to avoid operational problems with steam turbines in power generating industries (Bahadori and Vuthaluru, 2010t).

The optimum tuned coefficients given in appendix B can be retuned quickly according to this approach if more data become available in the future. To date, there is no predictive tool in literature for the rapid estimation of steam rate, turbine efficiency, and the inlet and exhaust nozzle diameters to determine the actual steam rate (ASR) and total steam requirements for both multi-stage and single-stage turbines. In view of this status, our efforts have been directed at formulating a predictive tool that can help engineers for rapid prediction of above mentioned parameters.

This predictive tool is simple and contains unique expression which is currently unavailable in the literature. In addition, we have selected exponential functions to develop the predictive tool, as these functions are smooth and well-behaved (i.e. smooth and non-oscillatory) equations which will allow for more accurate predictions (Bahadori and Vuthaluru, 2010t). Figure 6.51 shows the results of the proposed predictive tool for predicting the part load efficiency correction factor as a function of percent power multi-valve steam turbines and number of stages in comparison with reported data It is evident from this figure that there is a good agreement between predicted values and reported data in the literature. Figures 6.52 and 6.53 show the comparison between the percent power multi-valve condensing and non-Condensing steam turbines with the reported data (Bahadori and Vuthaluru, 2010t).

If the proposed approach is adopted in utilities on a periodic basis, significant savings can be assured with reduced maintenance and operational problems. Current efforts in this investigation pave the way to alleviate problems associated with the steam turbine inefficiencies by providing an accurate and rapid measure of various parameters which can be used by the engineers for monitoring the operational parameters. Figure 6.54 shows speed efficiency correction factor for condensing and non-condensing turbines. Figure 6.55 illustrates approximate steam rate calculations for single-stage application in comparison with data (Gas Processors and Suppliers Association, 2004). This method is robust and simple as it provides rapid prediction of steam rate, turbine efficiency, and the inlet and exhaust nozzle diameters to determine the actual steam rate (ASR) and total steam requirements for both multi-stage and single-stage turbines (Bahadori and Vuthaluru, 2010t). Unlike complex mathematical approaches, the proposed method is simple to use, employing basic algebraic equations that can easily and quickly be solved by a spreadsheet. The proposed method predicts the above mentioned parameters for inlet steam pressure up to 12000 kPa, turbine rating up to 10000 kW as well as the ratio of exhaust air over inlet air up to 0.55 (Bahadori and Vuthaluru, 2010s).

This tool also appears to be superior compared with other available methods because of its accuracy and simple background, wherein the relevant coefficients can be retuned if new and more accurate data are available in the future. This method can be of significant practical value for engineers to have a quick check on various parameters related to steam turbines at wide range of operating conditions. In particular, mechanical and utility practitioners dealing with steam turbines would find the proposed approach to be user friendly involving no complex expressions with transparent calculations (Bahadori and Vuthaluru, 2010t).

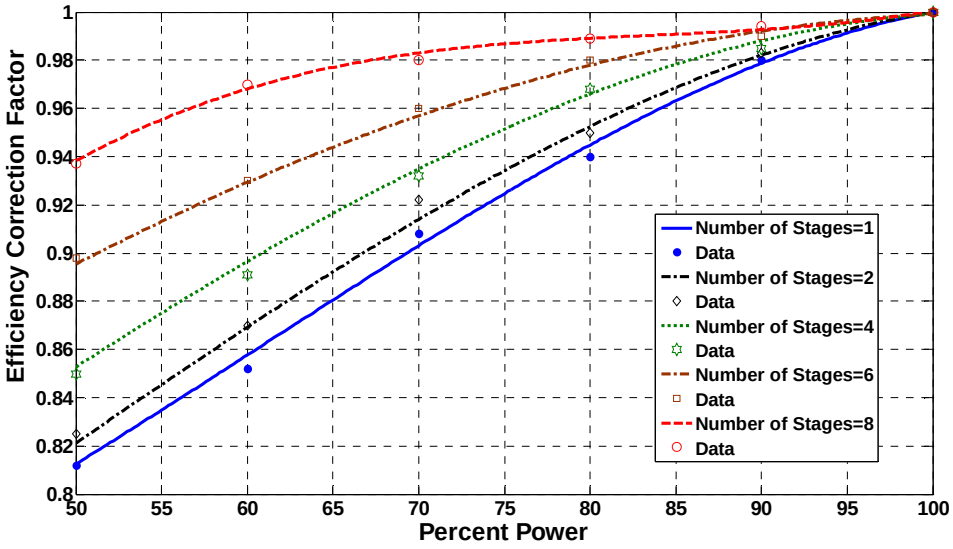

Figure 6.51: Part load efficiency correction factor vs. percent power multi-valve steam turbines and number of stages. (Bahadori A. and Vuthaluru H. B, (2010t) *Applied Thermal Engineering* 30 pp 1832-1838)

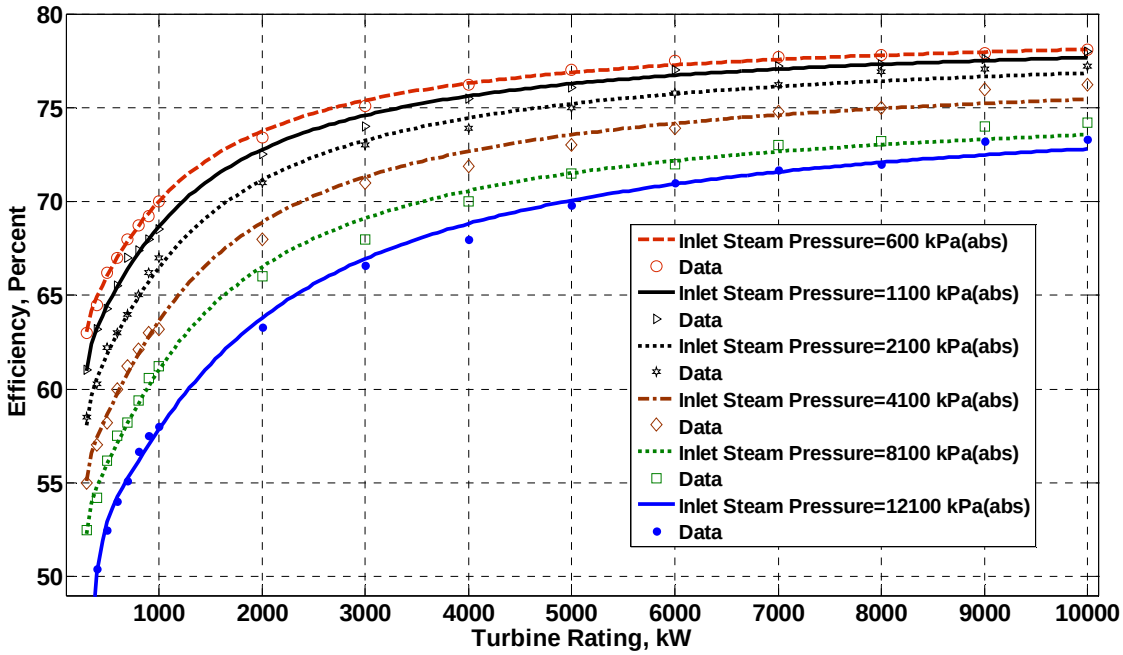

Figure 6.52: Basic efficiency of multi-valve, multi-stage condensing turbines as a function of inlet steam pressure and turbine rating in comparison with data (Bahadori A. and Vuthaluru H. B, (2010t) *Applied Thermal Engineering* 30 pp 1832-1838)

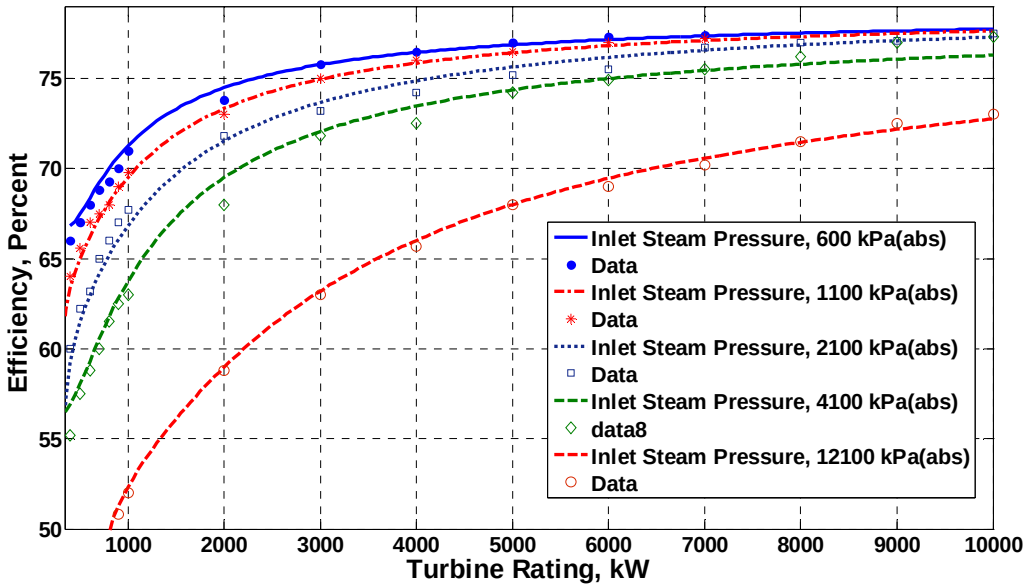

Figure 6.53: Basic efficiency of multi-valve, multi-stage non-condensing turbines as a function of inlet steam pressure and turbine rating in comparison with data (Bahadori A. and Vuthaluru H. B, (2010t) *Applied Thermal Engineering* 30 pp 1832-1838)

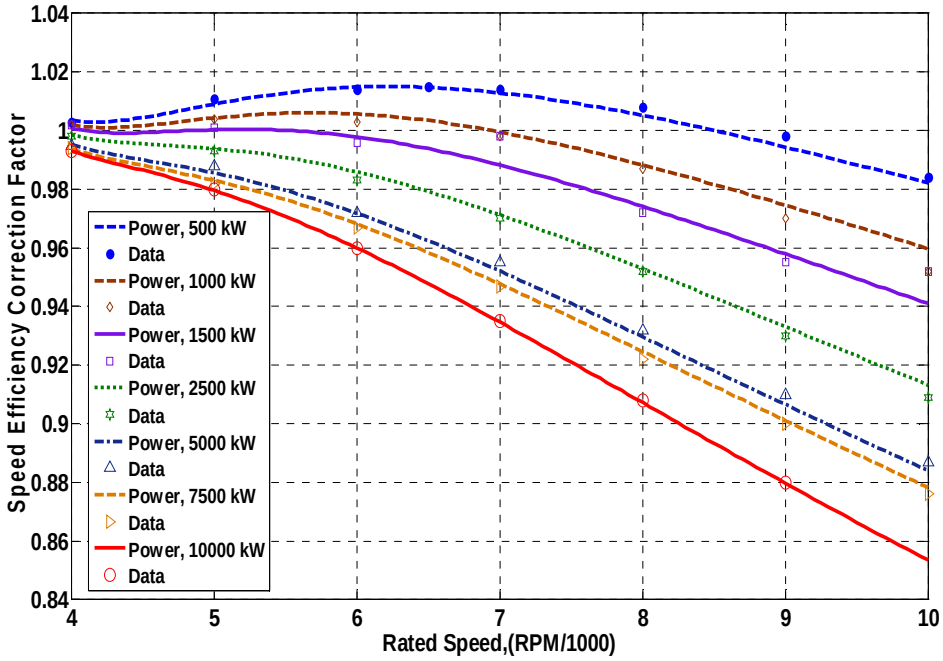

Figure 6.54: Speed efficiency correction factor for condensing and non-condensing turbines in comparison with data (Bahadori A. and Vuthaluru H. B, (2010t) *Applied Thermal Engineering* 30 pp 1832-1838)

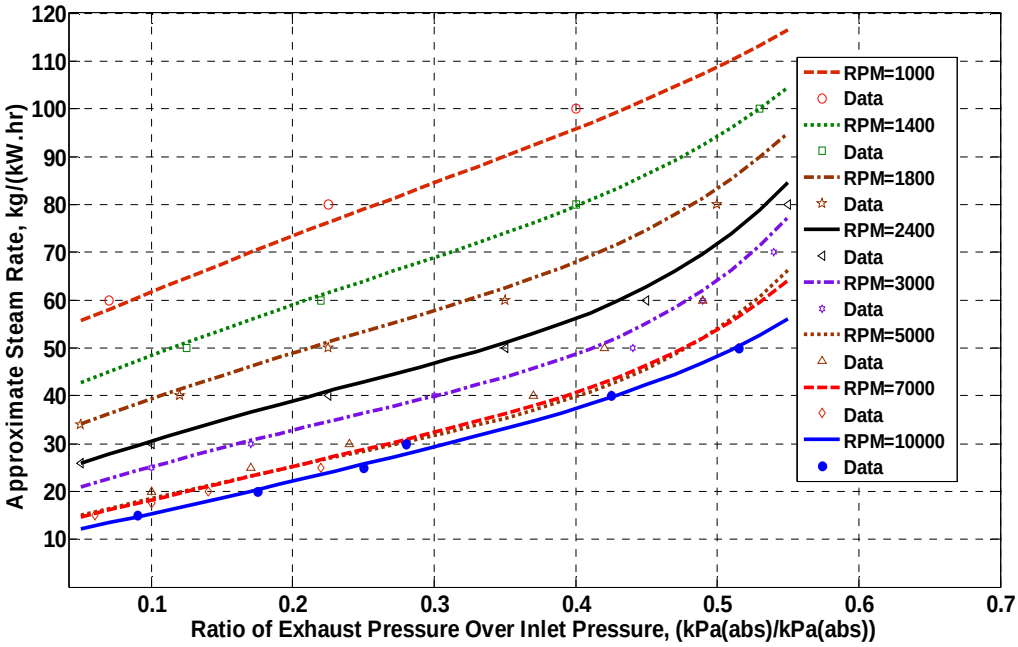

Figure 6.55: Approximate steam rate calculations for Single-Stage Application in comparison with data (GPSA 2004) (Bahadori A. and Vuthaluru H. B, (2010t) *Applied Thermal Engineering* 30 pp 1832-1838)

6.18 Compressed air transport properties

Compressed air energy storage is a way to store energy generated at one time for use at another time. At a utility scale, energy generated during periods of low energy demand can be released to meet higher demand periods. Also, compressed air is a commonly used utility across most manufacturing and processing industries because its production and handling are safe and easy. Compressed air systems are critical and play a pivotal role in the proper operation of many processing facilities since most of the instruments and controls depend on pressurized instrumentation air for operation. In this section, a simple predictive tool, which is easier than current available models involving a large number of parameters, requiring more complicated and longer computations, is presented here for the prediction of transport properties (namely thermal conductivity and viscosity) of compressed air at elevated pressures as a function of temperature and pressure using a simple Arrhenius-type function. The proposed correlation predicts the transport properties of air for temperature range between 260 to 1000 K, and pressures up to 1000 bar (100 MPa). Estimations are found to be accurate compared with the data in the literature with average absolute deviation being around 1.28 % and 0.68% for thermal conductivity and viscosity respectively (Bahadori 2011a).

Figure 6.56 shows the predicted results from the proposed predictive tool for thermal conductivity of compressed air as a function of temperature and pressure in comparison with the data [24]. It is evident from this figure that there is a good agreement between predicted values and the data. Figure 6.57 shows the performance of proposed predictive tool for the estimation of thermal conductivity of compressed air at elevated pressures. Figures 6.58 and 6.59 show the predicted results from the proposed predictive tool for viscosity of compressed air as a function of temperature and pressure in comparison with the data [24] for low and high pressures respectively. It is evident from the figure that there is also good agreement between predicted values and the reported data (Bahadori 2011a). Figure 6.60 illustrates the performance of proposed predictive tool for estimation of thermal conductivity of compressed air at elevated pressures.

Figures 6.61 and 6.62 are parity charts to show the accuracy of proposed predictive tool to calculate thermal conductivity and viscosity of compressed air at elevated pressures respectively. Current efforts in this investigation are likely to pave the way for alleviating the problems associated with the calculations for thermal conductivity and viscosity of compressed air which can be used by the process engineers and experts for calculating the engineering parameters on a regular basis (Bahadori 2011a).

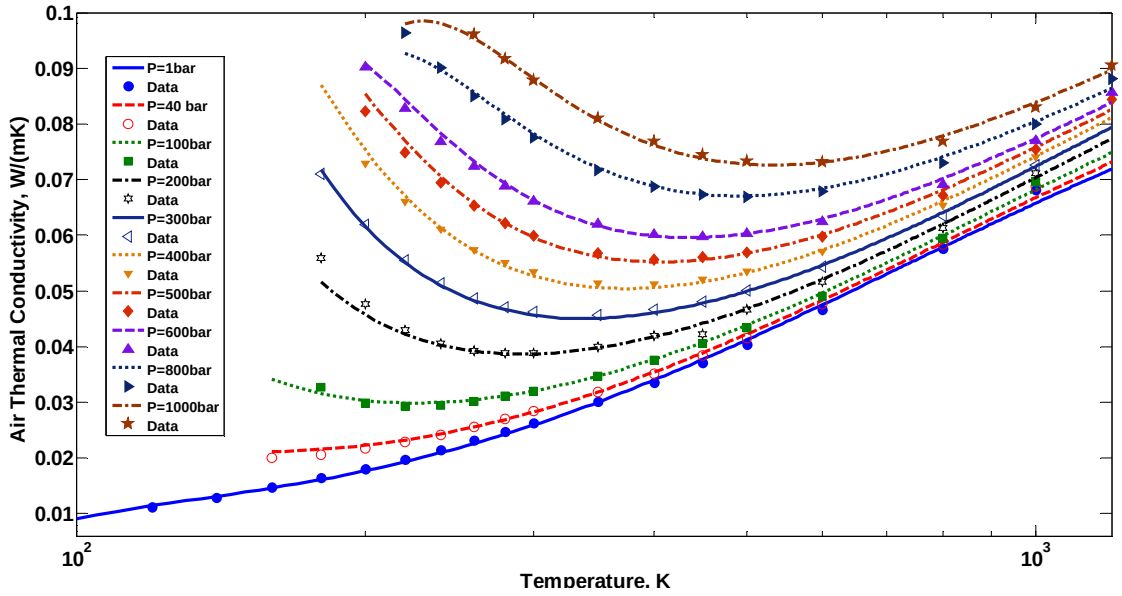

Figure 6.56: Thermal conductivity of compressed air in comparison with data (Perry and Green, 1997) (Bahadori, A., *Applied Energy*, in press, doi.org/10.1016/j.apenergy.2010.10.029)

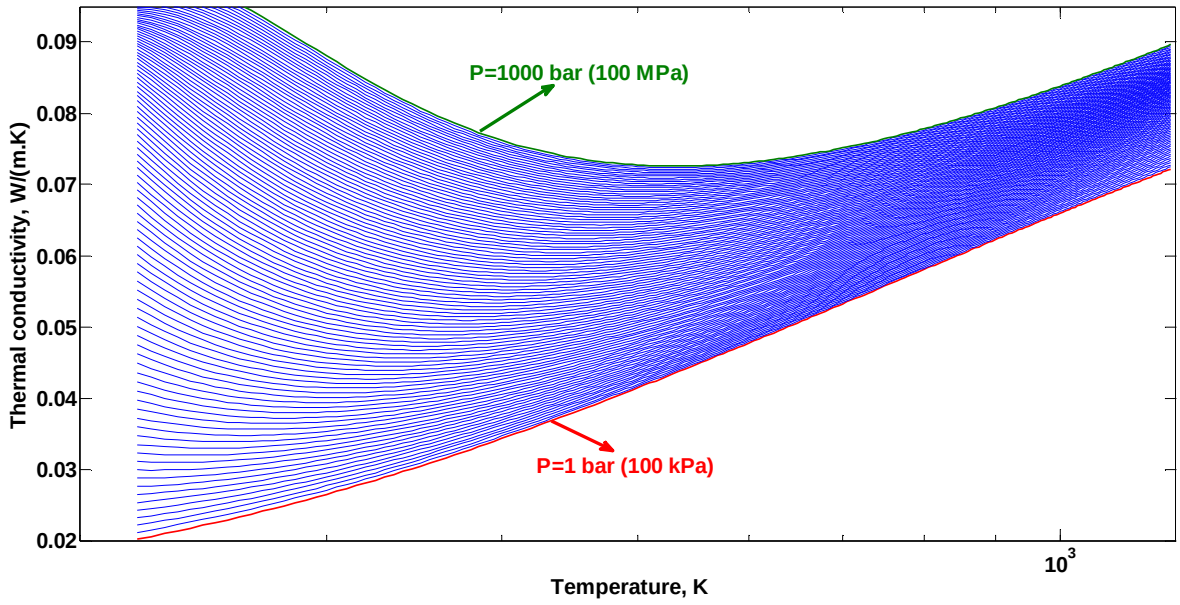

Figure 6.57: Performance of model for estimation thermal conductivity of compressed air (Bahadori, A., *Applied Energy*, in press, doi.org/10.1016/j.apenergy.2010.10.029)

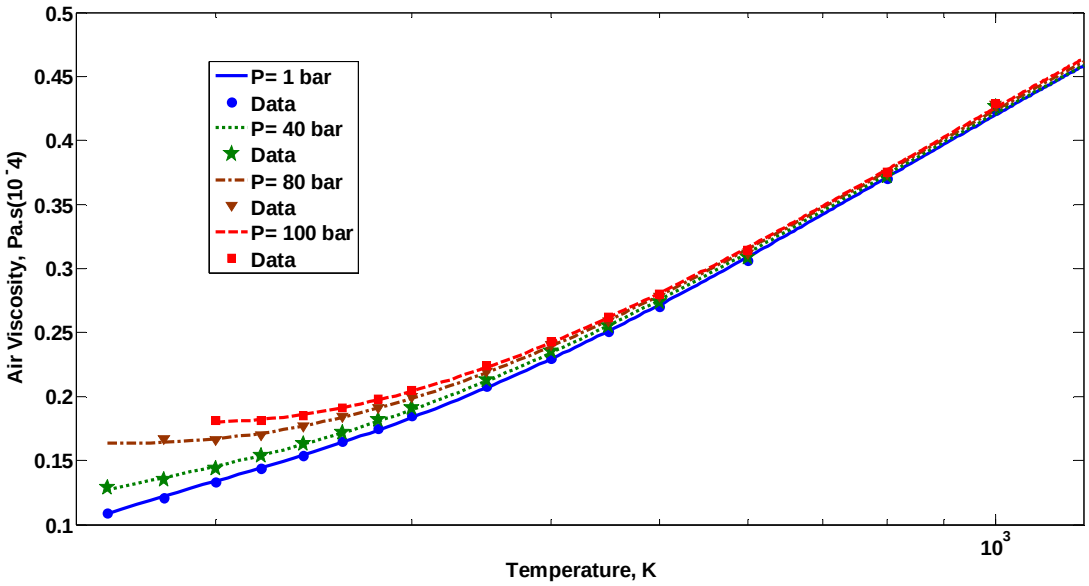

Figure 6.58: Viscosity of compressed air in comparison with data [24] for pressure less than 100 bar (Perry and Green, 1997) (Bahadori, A., *Applied Energy*, in press, doi.org/10.1016/j.apenergy.2010.10.029)

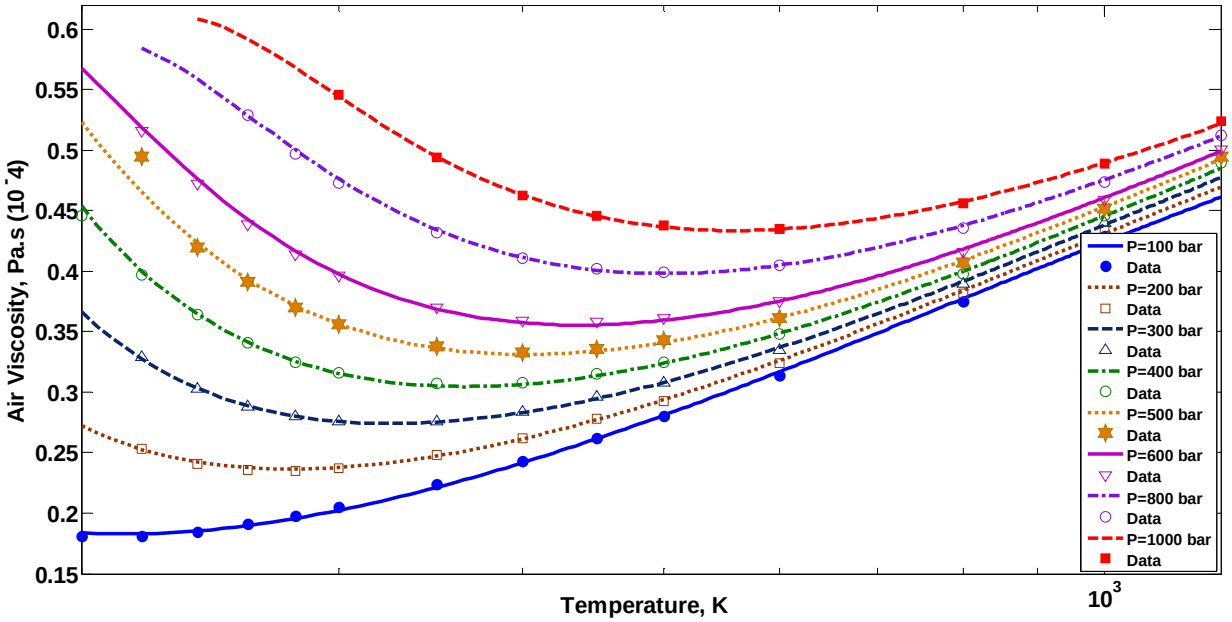

Figure 6.59: Viscosity of compressed air in comparison with data [24] for pressure greater than 100 bar (Perry and Green, 1997) (Bahadori, A., *Applied Energy*, in press, doi.org/10.1016/j.apenergy.2010.10.029)

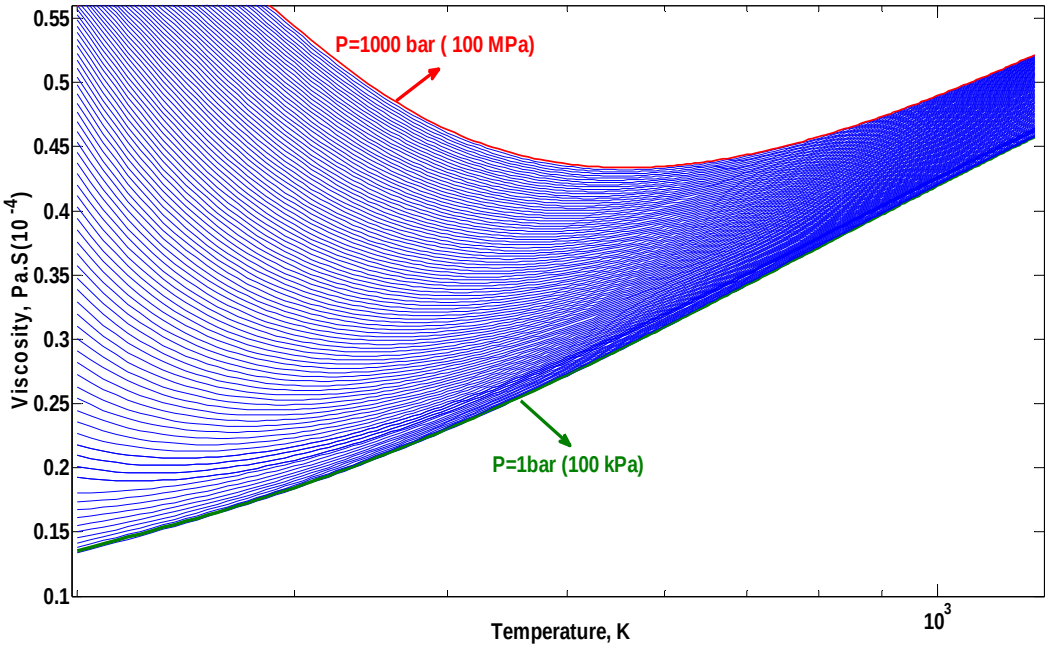

Figure 6.60: Performance of model for prediction of viscosity of compressed air, (Bahadori, A., *Applied Energy*, in press, doi.org/10.1016/j.apenergy.2010.10.029)

6.19 Compressed air specific heat ratio at elevated pressures

Over the years, considerable research effort has been expended towards evaluation of the thermophysical and transport properties of air for a wide range of temperatures. However, relatively limited attention was oriented towards investigation of air specific heat ratios at elevated pressures. This section shows simple predictive tool, which is easier than current available models, less complicated with fewer computations and is suitable for process engineers, is presented here for the prediction of specific heat ratio of air at elevated pressures as a function of temperature and pressure using a novel and theoretically based meaningful Arrhenius-type asymptotic exponential function combined with Vandermonde matrix (Bahadori and Vuthaluru, 2011a). The proposed method is superior owing to its accuracy and clear numerical background based on Vandermonde matrix, wherein the relevant coefficients can be retuned quickly if more data are available. The proposed correlation predicts the specific heat ratios of air for temperatures up to 1000 K, and pressures up to 1000 bar (100000 kPa). The tool developed in this study can be of immense practical value for the engineers and scientists to quickly check on the compressed air specific heat ratios at various conditions without opting for any experimental measurements. In particular, chemical and process engineers would find the approach to be user-friendly with transparent calculations involving no complex expressions (Bahadori and Vuthaluru, 2011a).

Figure 6.61 illustrates the specific heat ratios of air for temperature ranging between 200 to 1000 K and pressure in range of up to 100 bar. Figure 6.62 shows the specific heat ratios of air for temperatures ranging between 200 to 1000 K and pressures ranging between 100 bar to 1000 bar. Figures 6.63 and 6.64 shows the proposed method results and excellent performance in the prediction of specific heat ratios of air for wide range of conditions. Tables 3 illustrate the accuracy of proposed predictive tool for predicting the specific heat ratios of air in comparison with some reported data (Perry and Green 1997). According to the authors' knowledge, there are no new and theoretically meaningful predictive tools for the accurate estimation of specific heat ratios of air. In view of this necessity, our efforts have been directed at formulating a method that can help engineers and researchers. It is expected that our efforts in this investigation will lead the way for providing an accurate prediction of specific heat ratios of air at various conditions which can be used by engineers and scientists for monitoring the key parameters periodically. The proposed predictive tool works for temperatures in the range of 200 to 1000 K and pressure up to 1000 bar. The air specific heat ratios fall rapidly at low pressures because it is at very sensitive region.

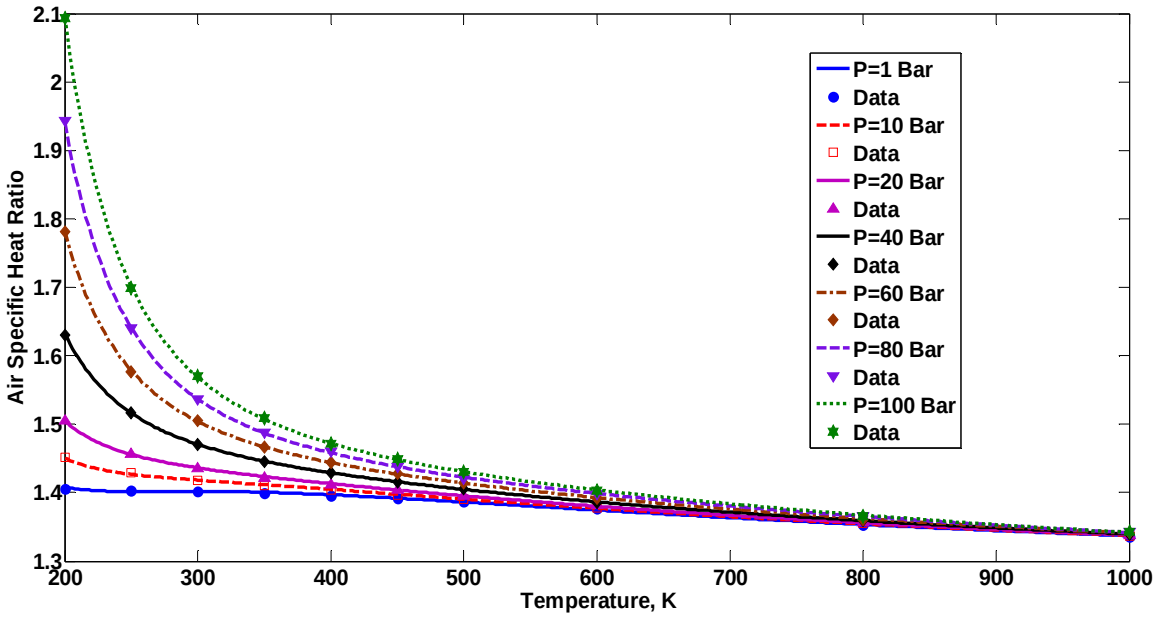

Figure 6.61: Air specific heat ratio as a function of pressure and temperature in comparison with the reported data (Perry and Green 1007) at elevated pressures (pressure less than 100 bar or 10000 kPa) Bahadori A. and Vuthaluru H. B. (2011a), *Energy Conversion and Management* 52, pp. 1526-1532.

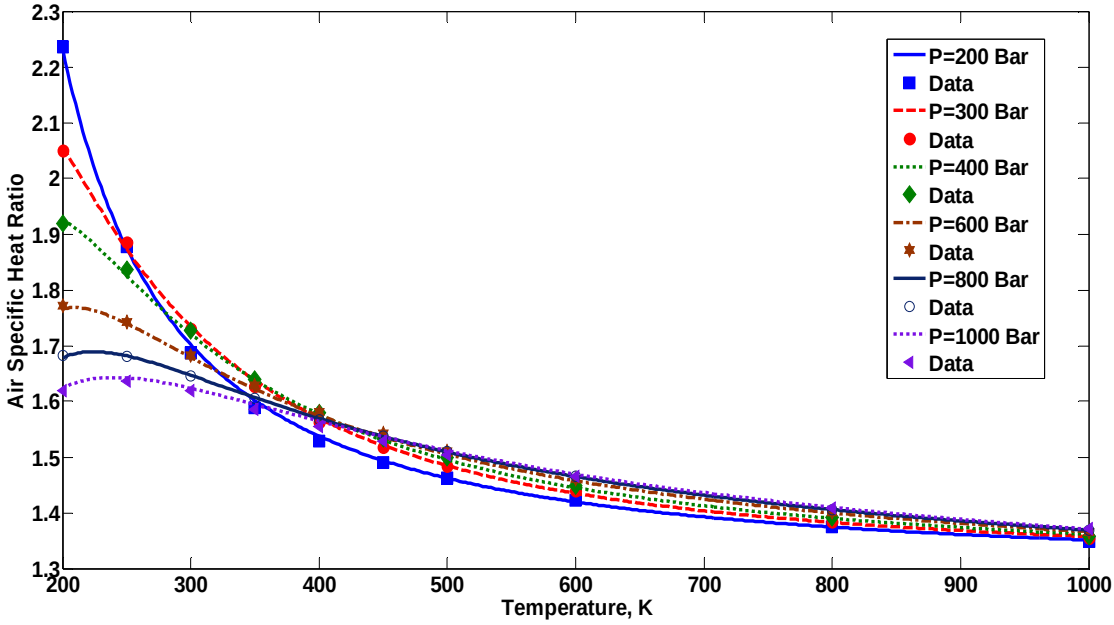

Figure 6.62: Air specific heat ratio as a function of pressure and temperature in comparison with the reported data (Perry and Green 1007) at low pressures (pressure more than 100 bar or 10000 kPa and up to 1000 bar or 100000 kPa) Bahadori A. and Vuthaluru H. B. (2011a), *Energy Conversion and Management* 52, pp. 1526-1532

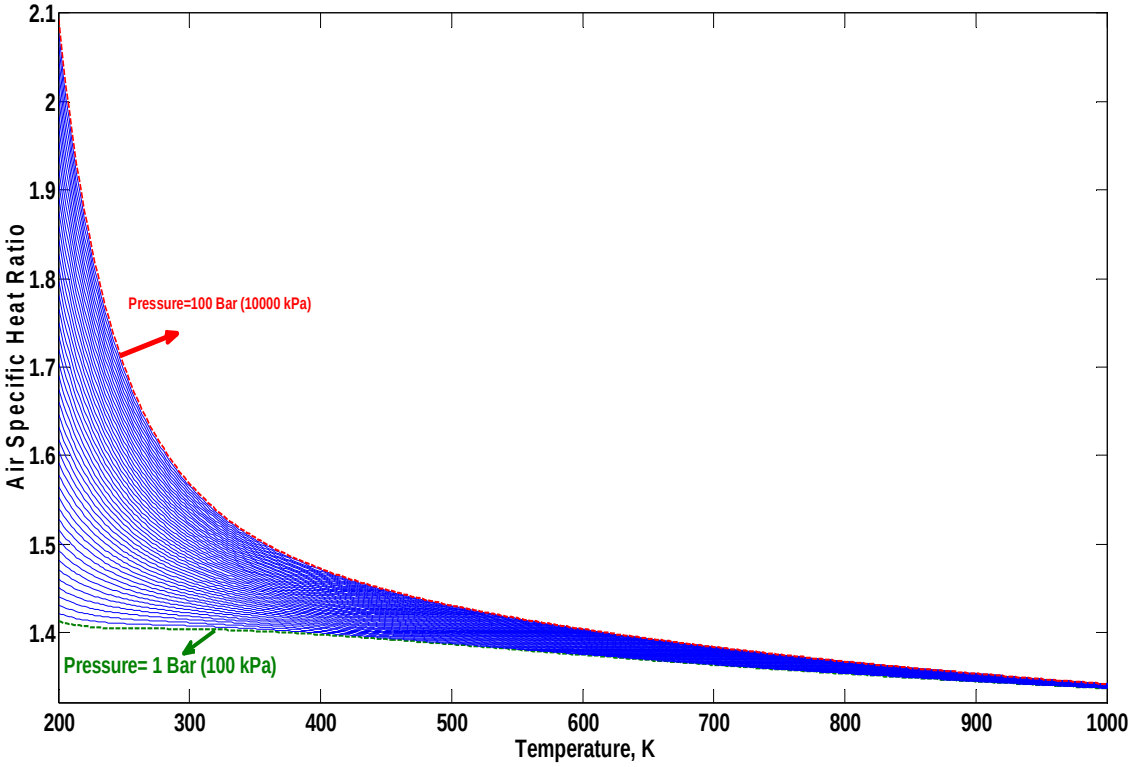

Figure 6.63: Performance of proposed predictive tool for calculating air specific heat ratio as a function of pressure and temperature at low pressures (pressure less than 100 bar or 10000 kPa) Bahadori A. and Vuthaluru H. B. (2011a), *Energy Conversion and Management* 52, pp. 1526-1532.

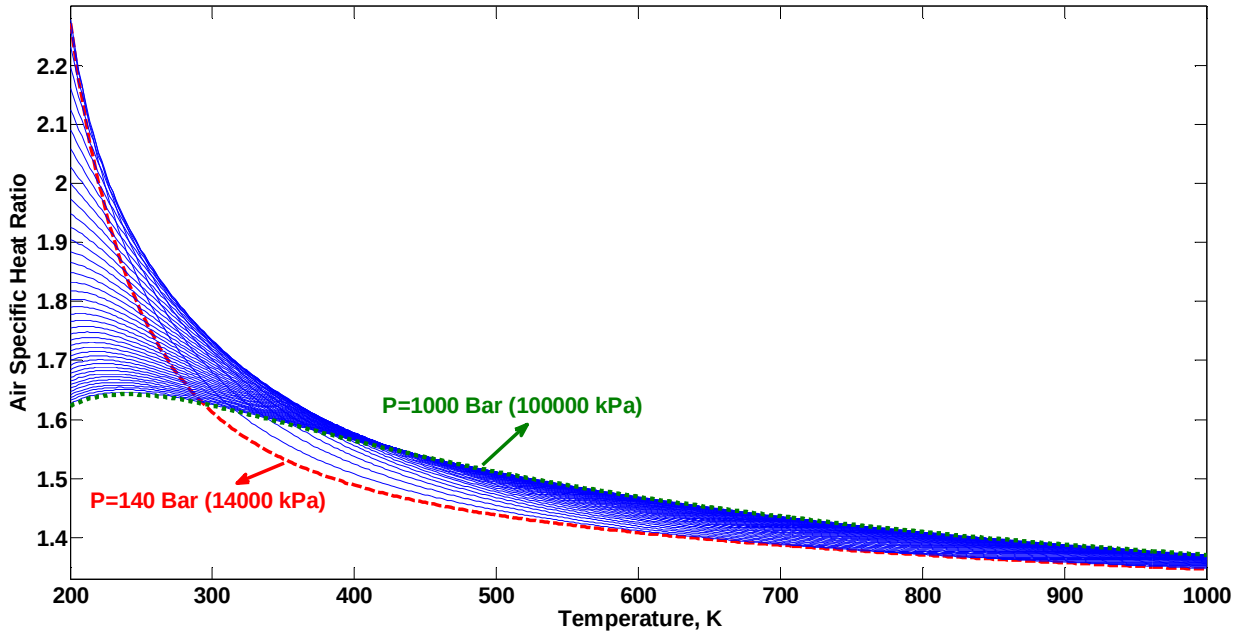

Figure 6.64: Performance of proposed predictive tool for calculating air specific heat ratio as a function of pressure and temperature at elevated pressures (pressure more than 100 bar or 10000 kPa) Bahadori A. and Vuthaluru H. B. (2011a), *Energy Conversion and Management* 52, pp. 1526-1532.

6.20 Prediction of saturated air dew point at elevated pressures

In a compressed air system condensed water vapor can have corrosive effects on metals and wash out protective lubricants from tools, equipments and pneumatic devices. To protect against such undesirable effects in a compressed air system, it is necessary to be able to predict the dew point temperature of atmospheric air and air dew point at elevated pressures in order to design and apply the appropriate type of drying to be used in the system. In this work, a simple predictive tool, which is easier than current available models involving a large number of parameters, requiring more complicated and longer computations, is presented here for the prediction of dew point of atmospheric moist air as a function of temperature and relative humidity and compressed saturated air dew point as a function of pressure and dew point of atmospheric moist air at given temperature using an Arrhenius-type asymptotic exponential function (Bahadori 2011b). The proposed method predicts the dew point of both atmospheric moist air and saturated compressed air for temperatures up to 50°C, pressure up to 1500 kPa and relative humidity up to 100%. Estimations are found to be in excellent agreement with the reliable data in the literature with average absolute deviation being around 0.15%. The tool developed in this study can be of immense practical value for the engineers and scientists to have a quick check on the dew point of atmospheric moist air and relative humidity and compressed saturated air dew point at various conditions without opting for any experimental measurements. In particular, engineers and scientists would find the approach to be user-friendly with transparent calculations involving no complex expressions.

Figures 6.65 and 6.66 shows the predicted results from the proposed predictive tool for the dew point of atmospheric moist air as a function of relative humidity and temperature with the reported data (Bahadori 2011b). It is evident from the figure that there is a good agreement between predicted values (for relative humidity up to 100% and temperatures up to 50°C) and the data. Figures 6.65 and 6.66 show temperature itself has a significant effect on the dew point of air at atmospheric pressure. The higher the air temperature the greater dew point of moisture at constant relative humidity percent. Figure 6.67 illustrates the

predicted results from the proposed predictive tool for the dew point of compressed saturated air as a function of pressure and dew point of moisture at atmospheric pressure with the reported data. It is evident from the figure that there is a good agreement between predicted values for pressures up to 1500 kPa(abs) and temperatures up to 50°C and the reliable data. This figure shows that pressure has a major effect on the dew point of saturated compressed air. Our efforts in this investigation will definitely pave the way for arriving at accurate estimations of dew point of atmospheric and saturated compressed air which can assist engineers and scientists with the periodic monitoring of operational parameters (Bahadori 2011b).

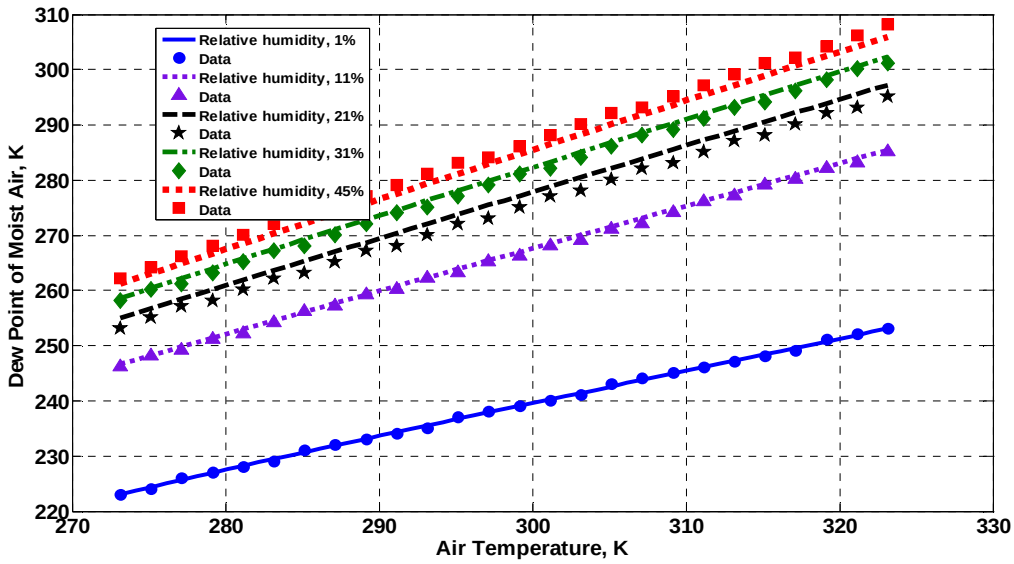

Figure 6.65: Dew point of atmospheric moist air as a function of relative humidity percent and temperature with the reported data for low relative humidity percent (< 50%) (Bahadori, A., *Chemical Engineering & Technology* (2011b), in press, doi.ceat.200900521)

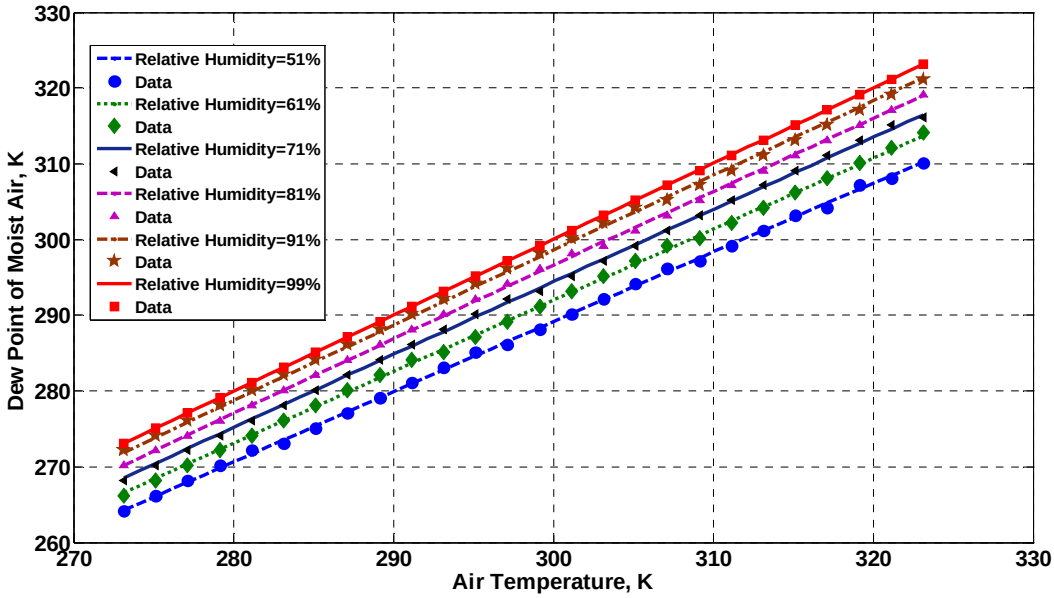

Figure 6.66: Dew point of atmospheric moist air as a function of relative humidity percent and temperature with the reported data for high relative humidity percent (> 50 %) (Bahadori, A., *Chemical Engineering & Technology* (2011b), in press, doi.ceat.200900521)

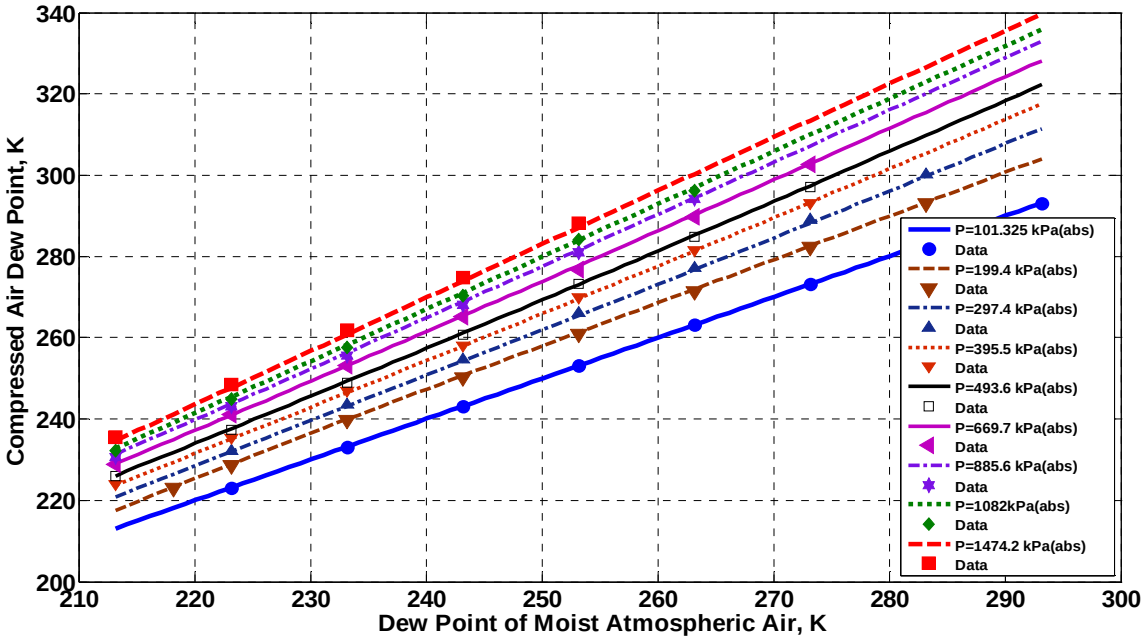

Figure 6.67: Dew point of saturated compressed air as a function of pressure and temperature with the reported data (Bahadori, A., *Chemical Engineering & Technology* (2011b), in press, doi.ceat.200900521)

6.21 Performance characteristics of cooling towers

Cooling towers are one of the most important and biggest heat and mass transfer devices that are in widespread use. They are commonly used in large cooling systems to reject the waste heat from the systems such as buildings to atmosphere via a water loop between two devices. In this work, a new predictive tool is presented to estimate performance characteristics of various types of cooling towers as a function of cold water temperature, wet bulb temperature and temperature difference range. Performance characteristics of various types of towers will vary with height, fill configuration, and flow arrangement (cross flow or counter flow). However, these factors have been taken into consideration in the present work while developing a predictive tool. The proposed predictive tool works well for cold water temperatures ranging between 15°C to 40°C and wet bulb temperatures ranging from 10 to 30°C. The study shows that the proposed method has a good agreement with the available reliable data in the literature. The proposed method is superior owing to its accuracy and clear numerical background based on Vandermonde matrix, wherein the relevant coefficients can be retuned quickly if more data are available.

Figure 6.68 shows the results of the proposed method for various cold water temperatures and wet bulb temperatures against the reported data in literature. Figure 6.69 demonstrates the results of the proposed method to predict the performance factor of cooling towers as a function of correction factors as well as temperature difference ranges at various conditions. It is clear that the proposed method yields results with good accuracy and reasonable predictions are achieved for wide range of conditions. This new approach can be of practical significance for engineers can have a quick check on the estimation of performance characteristics of various types of cooling tower options at various applications without the necessity of any lab- or pilot-scale units for testing purposes. In particular, mechanical and process engineers would find the approach to be user-friendly with transparent calculations involving no complex expressions.

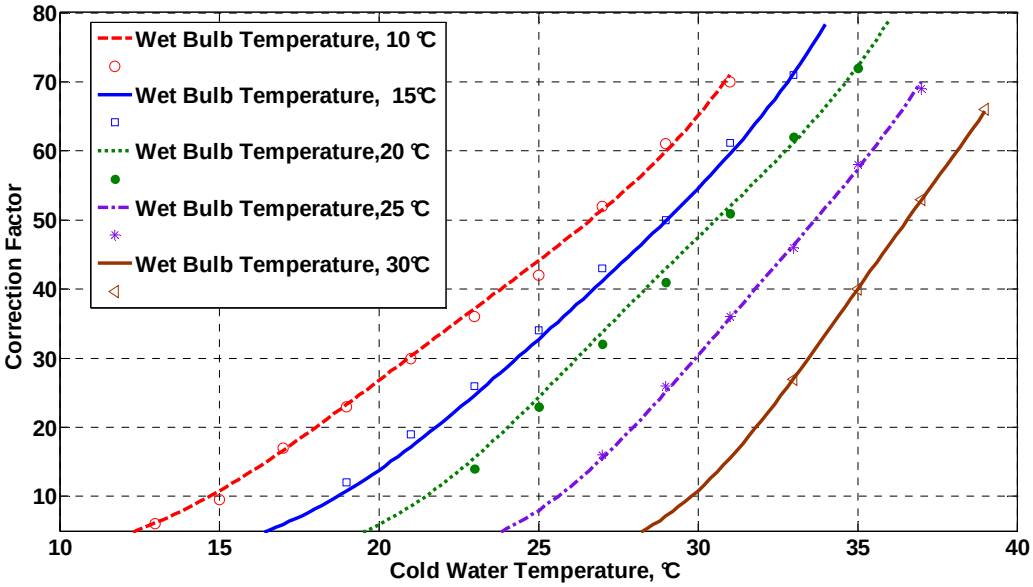

Figure 6.68: Comparison of predicted correction factor as a function of cold water temperature at various temperatures versus literature data (Bahadori (2011), in press, *Journal of the Energy Institute)*

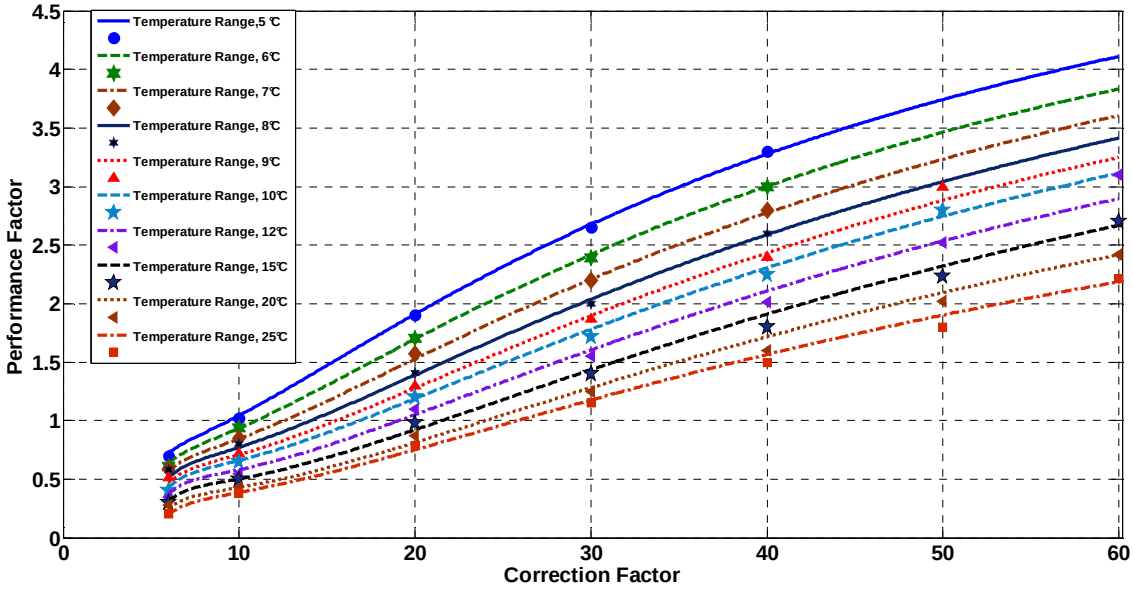

Figure 6.69: Comparison of predicted performance factor (P_F) of cooling towers as a function of correction factors and temperature difference ranges versus reported data (Bahadori (2011), in press, *Journal of the Energy Institute)*

6.22 Combustion flue gas acid dew point during heat recovery and efficiency gain

When cooling combustion flue gas for heat recovery and efficiency gain, the temperature must not be allowed to drop below the sulfur trioxide dew point. Below the SO_3 dew point, very corrosive sulfuric acid forms and leads to operational hazards on metal surfaces. In the present work, new predictive tool, which is easier than existing approaches, less complicated with fewer computations is formulated to arrive at an appropriate estimation of acid dew point during combustion flue gas cooling which depends on fuel type, sulfur content in fuel, and excess air levels. The resulting information can then be applied to estimate the acid dew point, for sulfur in various fuels up to 0.10 volume fraction in gas (0.10 mass fraction in liquid), excess air fractions up to 0.25, and elemental concentrations of carbon up to 3. The proposed predictive tool shows a very good agreement with the reported data. This approach can be of immense practical value for engineers and scientists for a quick estimation of acid dew point during combustion flue gas cooling for heat recovery and efficiency gain for wide range of operating conditions without the necessity of any pilot plant setup and tedious experimental trials. In particular, process and combustion engineers would find the tool to be user friendly involving transparent calculations with no complex expressions for their applications. Figure 6.70 shows the performance of proposed predictive tool for the estimation of calculating elemental concentrations of carbon correction factor (F1) as a function sulfur in fuel concentration mass fraction for liquid fuel (volume fraction for gaseous fuels) and elemental concentration of carbon in comparison with literature reported data. As can be seen, the results presented in Figure 6.71 shows good agreement with reported data suggesting that the proposed correlation is accurate, reliable and acceptable. Figures 6.71 and 6.72 show the proposed predictive tool's performance for the estimation of acid dew point temperature of combustion gas as a function of excess air fraction and elemental concentrations of carbon respectively. Figure 6.73 illustrates the performance of predictive tool for calculating the elemental concentrations of carbon correction factor (F1).

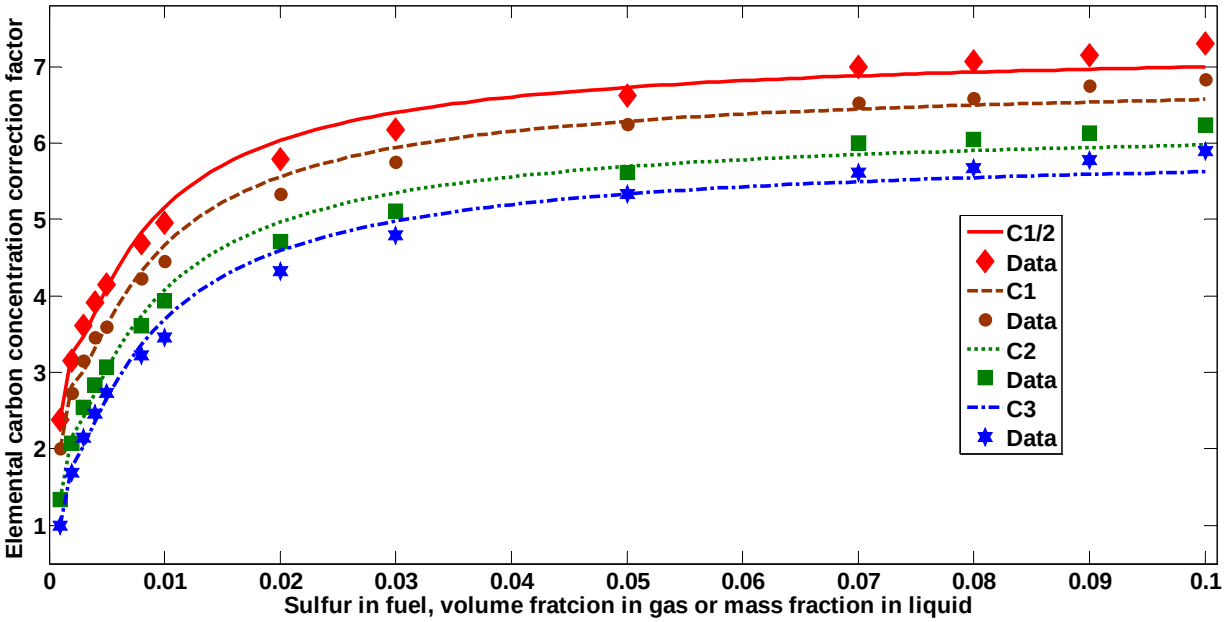

Figure 6.70: Performance of developed predictive tool for calculating the elemental concentrations of carbon correction factor (F1) in comparison with reported data [15]

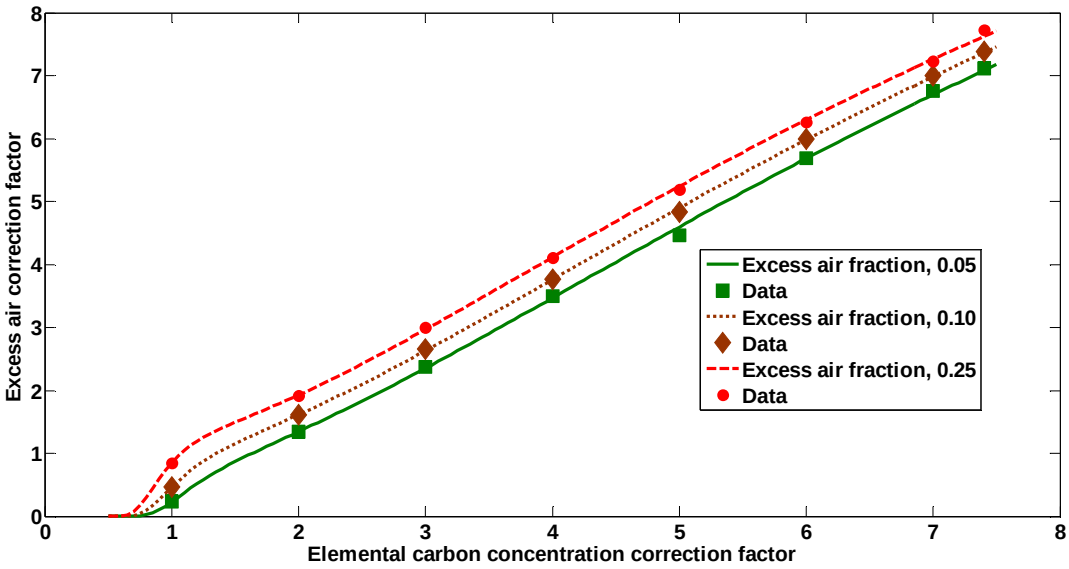

Figure 6.71: Performance of developed predictive tool for the elemental concentrations of carbon correction factor (F2) in comparison with reported data [15]

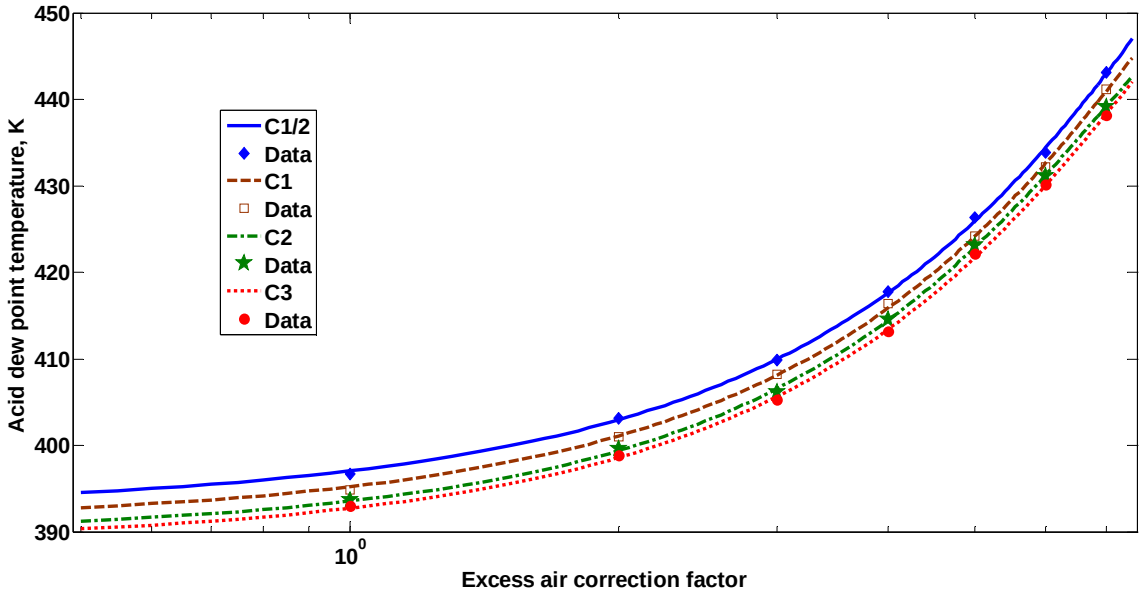

Figure 6.72: Performance of developed predictive tool for calculating acid dew point of acid dew point cooling combustion flue gas in comparison with reported data [15]

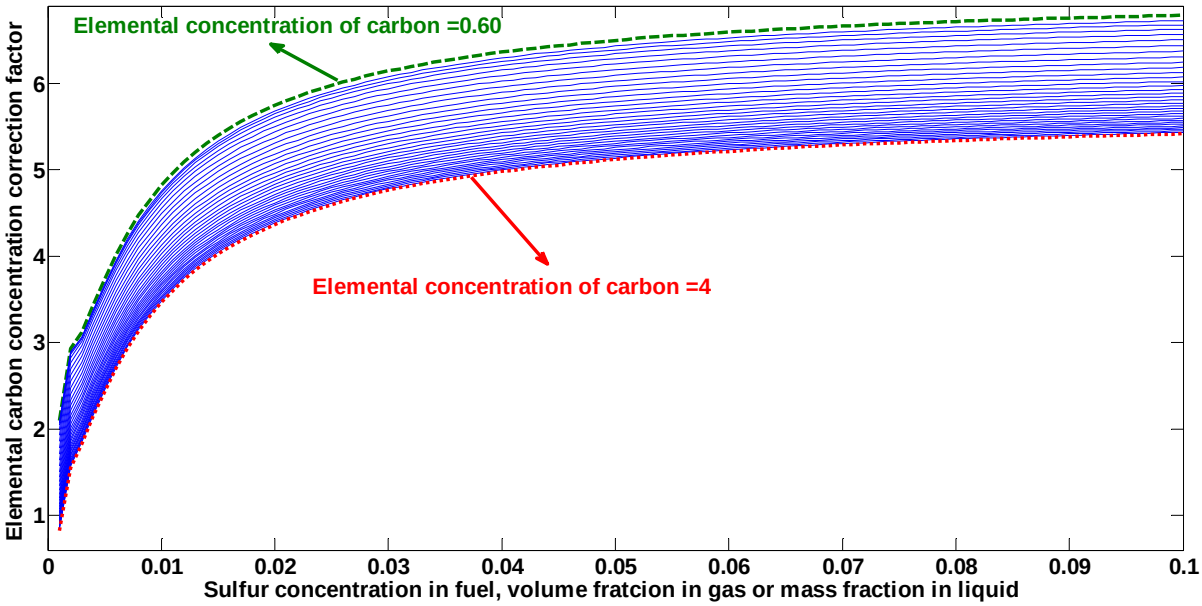

Figure 6.73: Performance of developed predictive tool for calculating the elemental concentrations of carbon correction factor (F1)

CHAPTER 7

Overall summary and typical case studies for potential benefits to various processing plants industries

Cost-benefit analysis is a term that refers both to the process involves, whether explicitly or implicitly, weighing the total expected costs against the total expected benefits of one or more actions in order to choose the best or most profitable option (Ascott, 2006). Benefits and costs are often expressed in money terms, and are adjusted for the time value for money, so that all flows of benefits and flows of project costs over time (which tend to occur at different points in time) are expressed on a common basis in terms of their present value. During cost–benefit analysis, monetary values may also be assigned to less tangible effects to the various risks that could contribute to partial or total project failure, such as loss of reputation, market penetration, or long-term enterprise strategy alignments (Folland et al 2007). PreTOG software has been developed using Matlab and based on Vandermonde-based methodology. Figures 7.1 to 7.4 illustrate various features of PreTOG software.

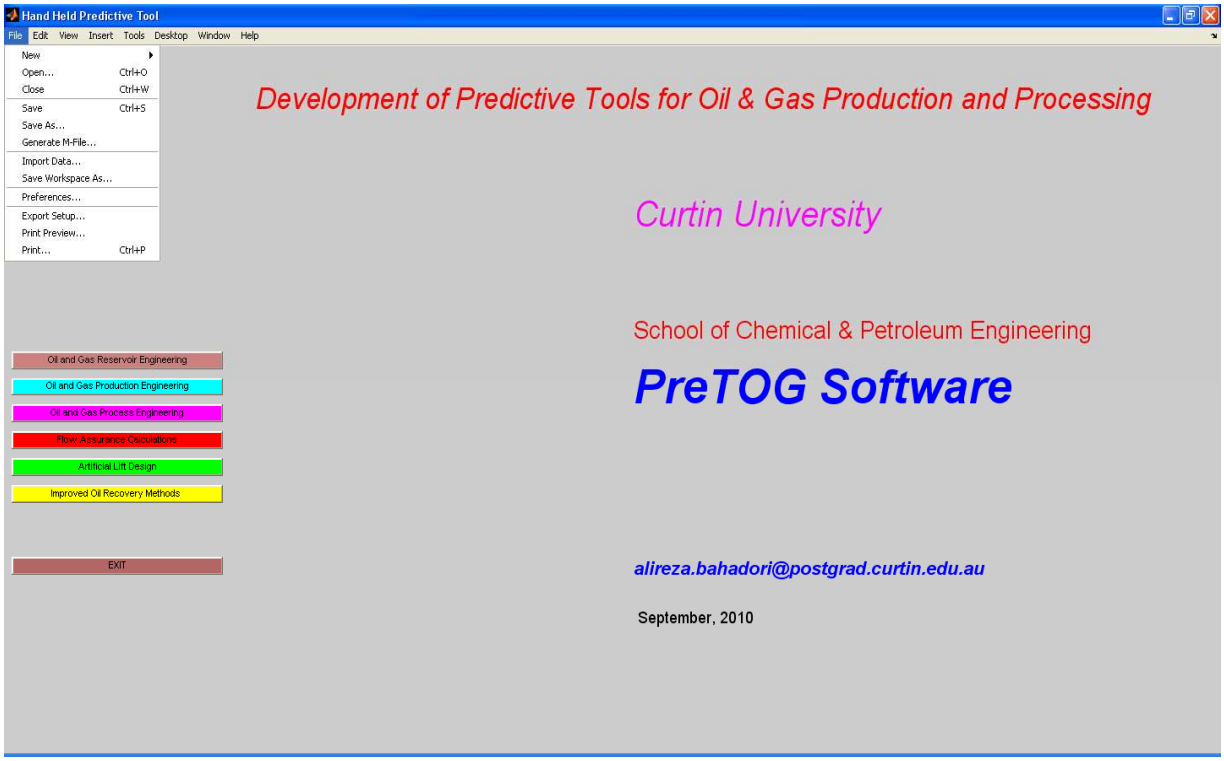

Figure 7.1 the vision for development of PreTOG software

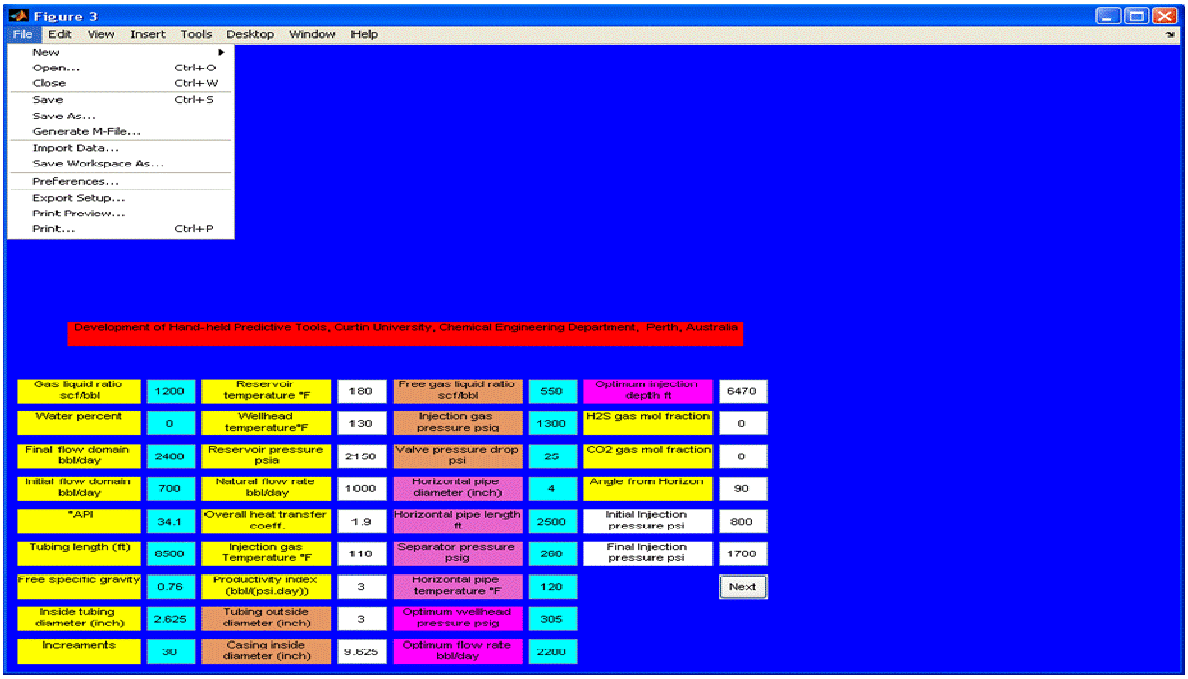

Figure 7.2, Typical input data for PreTOG software

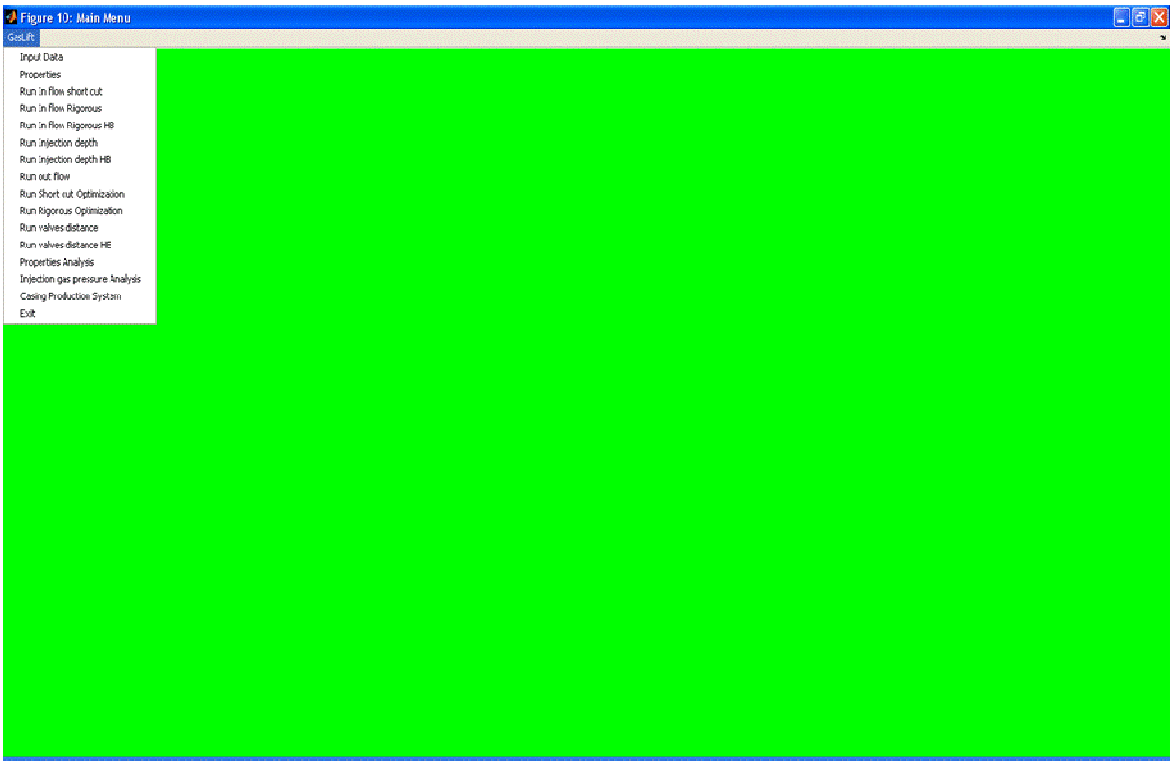

Figure 7.3. Selection of various engineering parameters in PreTOG software

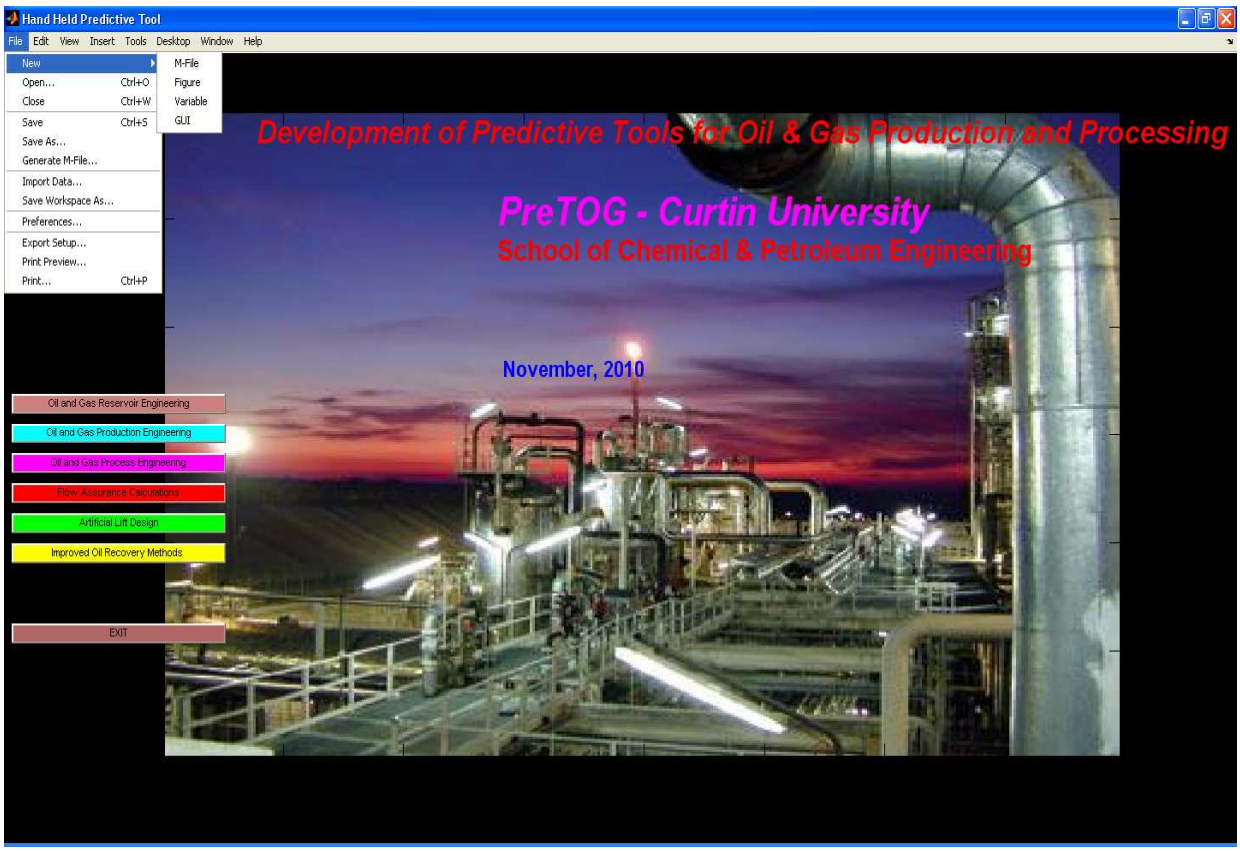

Figure 7.4. PreTOG software for engineering design and calculations

7.1 Case 1: Prediction of methanol loss in vapor phase during gas hydrate inhibition

This is a classic case study showing how the information evolving out of a predictive tool can be used to understand and predict the vaporization loss of methanol during natural gas hydrate inhibition. According to these calculations 2843 $ per day is the cost of vaporized methanol which is calculated by this proposed predictive tool for 2.83×10^{6} standard cubic meter per day of natural gas leaves an offshore platform. Gas hydrate formation in natural gas and NGL systems can block pipelines, equipment, and instruments, restricting or interrupting flow leading to safety hazards to production/transportation systems and to substantial economic risks (Bahadori and Vuthaluru, 2009g).

The amount of hydrate inhibitor to be injected must not only must be sufficient to prevent freezing of the inhibitor water phase, but also must be sufficient to provide for the equilibrium vapor phase content of the inhibitor. The vapor pressure of methanol has to

be high enough so that significant quantities will vaporize. Therefore to estimate methanol vaporization losses, it is necessary to develop a new predictive tool. The proposed correlation predicts the methanol vaporization loss for temperature between -16 and 16°C (Bahadori and Vuthaluru, 2010h).

Methanol is the most commonly used hydrate inhibitor in subsea petroleum industries, gas treatment and processing, pipelines and wells (Elgibaly and Elkamel, 2009, and Lundstrøm et al, 2006) with worldwide usage of several million dollars per year (Bruinsma et al., 2004). Because of its high volatility, methanol is lost in the vapor phase. Often when applying methanol as an inhibitor, there is a significant expense associated with the cost of "lost" methanol. Owing to lower surface tension and viscosity of methanol, however, it makes it possible to have an effective separation from the gas phase at cryogenic conditions and usually the most preferred inhibitor (GPSA, 2004).

In addition, one of the primary factors in the selection process is related with recovery, regeneration and reinjection possibilities of the spent material. Usually methanol is not regenerated due to its intermittent application (mainly during start-up or shutdown). However, when it is injected continuously, as is often observed in gas systems then it is sometimes regenerated. However, losses to the vapor phase can be prohibitive, in which case operators select monoethylene glycol (GPSA, 2004). The amount of inhibitor required to treat the water phase including the amount of inhibitor lost to the vapor phase and the amount that is soluble in the hydrocarbon liquid, equals the total amount required. Considering the above issues, there is an essential need for developing an accurate and theoretically meaningful predictive tool to represent aqueous methanol solution vapor pressure and methanol vaporization loss. In addition developing the new predictive tools to minimize the complex and time-consuming calculation steps are an essential need. It is apparent that a mathematically compact, simple and reasonably accurate equations that containing fewer tuned coefficients, would be preferable for computationally intensive simulations (Bahadori et al., 2008a,b and Bahadori and Vuthaluru 2010a,b) In fact, the development of practical correlations by a small modification to the well-known Vogel-Tammann-Fulcher (VTF) (Vogel, 1921, Tammann, G., Hesse, 1926, Flucher, 1926) and Arrhenius (1889) equations was the primary motivation of the present paper, which, nevertheless, yielded correlations with accuracy comparable to that of the existing rigorous simulations. This study discusses the formulation of a novel and simple predictive tool which can be of significant importance for process engineers.

Equation 7.1 illustrates methanol vaporization loss definition which is methanol vapor composition to the methanol liquid composition. Equation 7.2 is an Arrhenius-type function to correlate methanol vaporization loss as a function of temperature, wherein the relevant coefficients are correlated as a function of pressure in kPa (Equations 7.3-7.6).

$$L_M = \frac{\dfrac{\text{kg Methanol}}{\text{Thousand Standard m}^3\text{ Gas}}}{\text{Mass\% methanol in water phase}} \tag{7.1}$$

$$\ln(L_M) = a + \frac{b}{T} + \frac{c}{T^2} + \frac{d}{T^3} \tag{7.2}$$

Where:

$$\text{a} = A_1 + \frac{B_1}{P} + \frac{C_1}{P^2} + \frac{D_1}{P^3} \tag{7.3}$$

$$\text{b} = A_2 + \frac{B_2}{P} + \frac{C_2}{P^2} + \frac{D_2}{P^3} \tag{7.4}$$

$$\text{c} = A_3 + \frac{B_3}{P} + \frac{C_3}{P^2} + \frac{D_3}{P^3} \tag{7.5}$$

$$\text{d} = A_4 + \frac{B_4}{P} + \frac{C_4}{P^2} + \frac{D_4}{P^3} \tag{7.6}$$

The proposed novel tools present in this thesis are simple and has unique formulations non-existent in the literature. Furthermore, the selected exponential function to develop the tool leads to well-behaved (i.e. smooth and non-oscillatory) equations enabling fast and more accurate predictions.

Table 7.1 presents a summary of accuracies with the proposed predictive tools in terms of average absolute deviation percent with reliable data (GPSA, 2004). It shows the proposed correlation has an average absolute deviation percent less than 1.1% which are considered to be very small deviation from reliable data. Sample calculations shown below which clearly demonstrates the simplicity of the proposed tool and the benefits associated with such estimations.

7.1.1 Given Data for case study #1:

As an example, 2.83×10^{6} standard cubic meter per day of natural gas leaves an offshore platform at 38°C and 8300 kPa (abs). The gas comes onshore at 4°C and 6200 kPa (abs). The hydrate temperature of the gas is 18°C. Methanol mass percent in liquid phase is 27.5%. Calculate the amount of vaporized methanol. Consider the cost of methanol 3$ per kg.

7.1.2 Solution for case study #1:

x=0.275 mass fraction of methanol

T=277.15 K

For vapor pressure of aqueous methanol solution, we use tuned coefficients reported in table 7.1:

a= $-3.4124821400054\times10^{3}$

b= $2.8663831990333\times10^{6}$

c= $-8.004219677314\times10^{8}$

d= $7.437011549752\times10^{10}$

L_M = 16.4291

Losses=16.4291×10^{-6} $(kg/m^3)/(Wt\%\ Methanol)$

Daily vaporization losses=$16.4291\times10^{-6}(2.83\times10^{6})(27.5)$=1281 kg/day.

This is a classic example showing how the information evolving out of this simple tool can be used to understand and predict the vaporization loss of methanol.

1281 kg/day (3 $/kg) =2843 $/day is the cost of vaporized methanol which is calculated by this proposed predictive tool.

Table 7.1: Comparison of predicted results of methanol vaporization loss in comparison with the reliable data.

Pressure, kPa	Temperature, K	Reported methanol vaporization loss $\frac{\frac{kg\,Methanol}{Thousand\,Standard\,m^3\,Gas}}{Mass\%\,methanol\,in\,water\,phase}$ (GPSA 2004)	Calculated methanol vaporization loss $L_M = \frac{\frac{kg\,Methanol}{Thousand\,Standard\,m^3\,Gas}}{Mass\%\,methanol\,in\,water\,phase}$	Percent absolute deviation
2000	261.15	11	10.91	0.76
2000	277.15	32.7	32.21	1.47
3000	269.15	15.9	15.22	4.22
3000	281.15	31.2	31.60	1.29
4000	271.15	14.6	14.63	0.26
4000	283.15	29.8	30.23	1.27
5000	273.15	14.6	14.40	1.35
5000	285.15	29.3	28.59	2.41
6000	275.15	14.8	14.60	1.29
6000	287.15	29.2	29.21	0.06
7000	277.15	27.8	27.60	0.70
8000	279.15	16.8	16.97	1.03
9000	283.15	20.9	20.75	0.69
10000	285.15	22.2	22.23	0.16
20000	279.15	13.7	13.69	0.007
20000	289.15	23	22.95	0.21
Average absolute deviation percent (AADP)				1.07%

7.2 Case 2: Prediction of methanol loss in condensate liquid phase during gas hydrate inhibition.

Equations 7.7 represents the proposed governing equation in which four coefficients are used (equations 7-8 to 7-11) to correlate the methanol solubilities in liquid hydrocarbon phase (ω) in mole fraction as a function of temperature (T) for a given methanol mass fraction in aqueous phase where the relevant coefficients have been reported in appendix B:

$$\ln(\omega) = a + \frac{b}{T} + \frac{c}{T^2} + \frac{d}{T^3} \tag{7.7}$$

Where:

$$\mathrm{a} = A_1 + B_1\psi + C_1\psi^2 + D_1\psi^3 \tag{7.8}$$

$$b = A_2 + B_2\psi + C_2\psi^2 + D_2\psi^3 \tag{7.9}$$

$$\mathrm{c} = A_3 + B_3\psi + C_3\psi^2 + D_3\psi^3 \tag{7.10}$$

$$\mathrm{c} = A_4 + B_4\psi + C_4\psi^2 + D_4\psi^3 \tag{7.11}$$

These optimum tuned coefficients help to cover the temperatures in the range of 240 to 320 K and methanol concentrations up to 0.70 mass fraction in water phase. The optimum tuned coefficients given in appendix B can be further retuned quickly according to proposed approach if more data are available in the future. Figures 7.5 and 7.6 show the proposed numerical method results and excellent performance in the prediction of methanol solubility in hydrocarbon liquid phase in gas hydrate inhibition for wide range of conditions. It shows high temperatures and more injected methanol in water phase cause more solubility of methanol in liquid phase (Bahadori and Vuthaluru 2010f).

Table 7.2 illustrates the accuracy of proposed correlation for predicting the solubility of methanol in paraffinic hydrocarbons in comparison with some reported data (GPSA 2004). The accuracy of correlation in terms of average absolute deviations is 2.12%. To date,

there is no predictive tool for an accurate estimation of methanol loss in liquid hydrocarbon phase (ω) in mole fraction. In view of this necessity, our efforts have been directed at formulating a method that can help engineers and researchers. It is expected that with this investigation, this study will lead the way for arriving at an accurate prediction of methanol loss in liquid hydrocarbon phase (ω) in mole fraction at various conditions which can be used by engineers and scientists for monitoring the key parameters periodically. The case study is given below to illustrate the simplicity associated with the use of proposed predictive tool for rapid estimation of methanol loss in condensate liquid phase (Bahadori and Vuthaluru 2010f).

7.2.1 Case study:

2.83×10^{6} Sm^3/day of natural gas leaves an offshore platform at 38°C and 8300 kPa(abs) (Water content 850 mg/Sm^3). The gas comes onshore at 4°C and 6200 kPa (abs) (Water content 152 mg/Sm^3). The hydrate temperature of the gas is 18°C. Associated condensate production is 56 m^3/ (million standard m^3). The condensate has a density of 778 kg/ m^3 and a molecular mass of 140. The required methanol inhibitor concentration in water phase to avoid hydrate formation is 27.5%. Calculate the mass rate of inhibitor in water phase and the amount of methanol loss in hydrocarbon liquid phase. Consider the cost of methanol 3$ per kg (Bahadori and Vuthaluru 2010f).

7.2.2 Solution:

1. Given data:

   Win = 850 mg/ Sm^3.

   Wout=152mg/Sm^3

   ΔW =698 mg/Sm^3

   Water condensed = (2.83×10^{6}) (698) =1975 $\times10^{6}$ mg/day = 1975 kg/day

2. Calculate mass rate of inhibitor in water phase:

$$m_i = \frac{0.275(1975)}{1-0.275} = 749 \text{ kg/day}$$

3. Estimate losses to hydrocarbon liquid phase from proposed method at 4°C and 27.5 wt% MeOH:

a= $9.136448034367\times10^{1}$

b= $-8.869793699719\times10^{4}$

c=$2.8126995933983\times10^{7}$

d= $-3.0722013379\times10^{9}$

The solubility of methanol in hydrocarbon phase is estimated to be around 0.0011 or 0.11 mol%.

$$\left(\frac{2.83\times10^{6}\,Sm^{3}}{day}\right)\left(\frac{56m^{3}}{10^{6}\,Sm^{3}}\right)\left(\frac{778kg}{m^{3}}\right)\left(\frac{1kgmole}{140kg}\right) = 881 \text{ kgmol/day.}$$

Kgmol methanol=881(0.0011) = 0.97 moles/day.

Kg methanol = (0.96) (32) =30.72 kg/day.

The methanol in the condensate phase can be recovered by downstream water washing.

Cost per month= (3$/kg) (30.72 kg/day)(30 day/month)=2765 $ per month.

Table 7.2 Comparison of calculated solubility of methanol in hydrocarbons with reported data (Bahadori and Vuthaluru 2010f)

Temperature (°C)	Methanol mass fraction	Calculated solubility of methanol in hydrocarbons (mole fraction)	Reported methanol in hydrocarbons, mole fraction (GPSA 2004)	Absolute Deviation (Percent)
12	0.20	0.00099	0.001	1
30	0.20	0.00294	0.003	2
50	0.20	0.006	0.006	0
21	0.35	0.0044	0.004	1
47	0.35	0.01035	0.01	3.5
-10	0.60	0.00295	0.003	1.6
2	0.60	0.00514	0.005	2.8
43	0.60	0.02034	0.02	1.7
-40	0.70	0.0021	0.002	5
0	0.70	0.0073	0.0071	2.8
50	0.70	0.0265	0.027	1.9
Average absolute deviation, percent				2.1

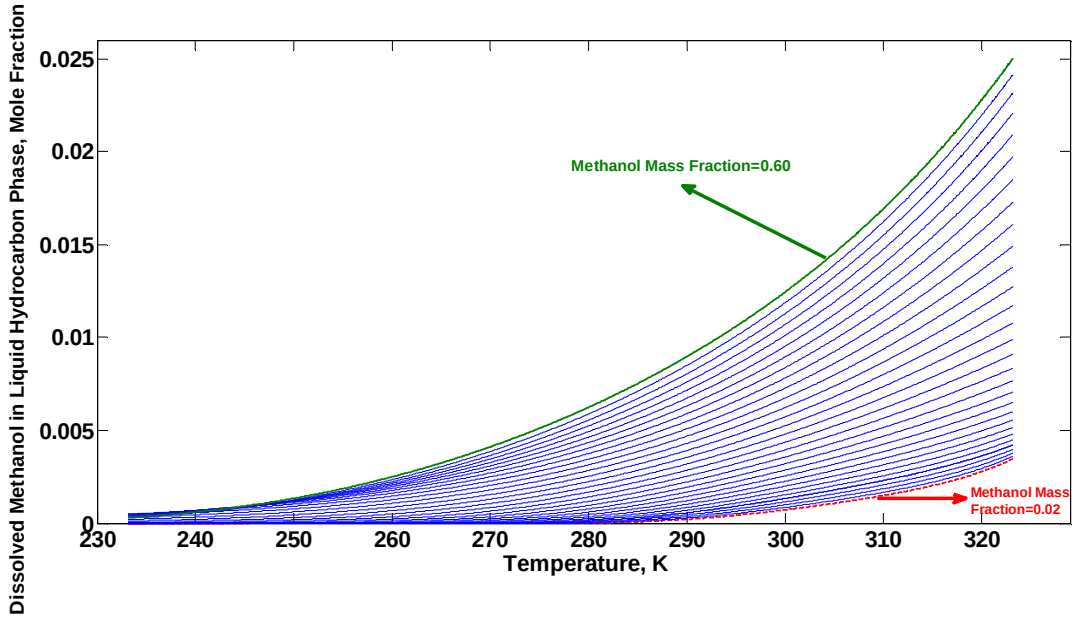

Figure 7.5: Performance of proposed predictive tool for prediction of solubility of methanol in hydrocarbon condensate phase

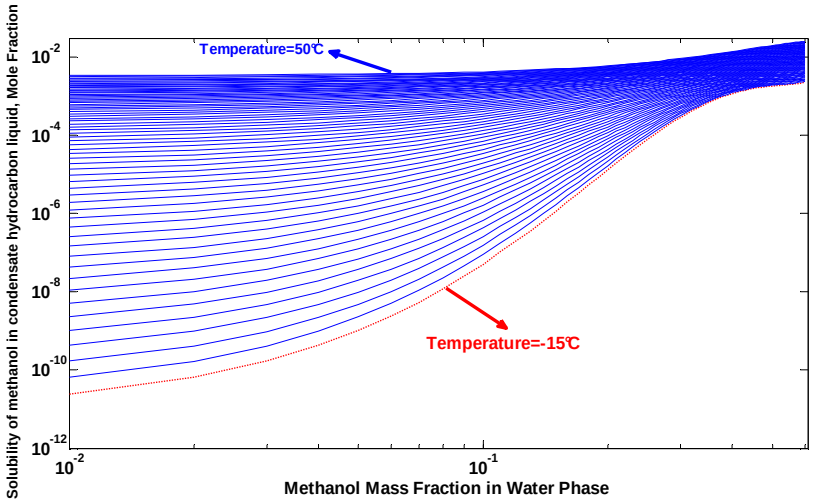

Figure 7.6: Performance of proposed predictive tool for prediction of solubility of methanol in hydrocarbon condensate phase in the other view point.

With reliable predictions of methanol losses to vapour and condensate phases it is possible to perform an effective economic evaluation of the impact of these losses to a producing company. By using the example above to determine quantitative values for methanol losses, and comparing these values to production rates the economic impact could be understood.

7.3 Estimation of potential savings from reducing unburned combustible losses in coal-fired systems

A potentially significant loss emanates from the combustion of coal fuels is usually called as the unburned carbon loss. All coal-fired steam generators and coal-fired vessels inherently suffer from efficiency debit attributable to unburnt carbon. The aim of this study is to develop a predictive tool which will be easier than existing approaches, less complicated with fewer computations and suitable for engineers to determine the approximate potential savings resulting from reducing unburned coal fuel loss (Bahadori and Vuthaluru 2010u). The proposed method determines the benefits of reducing the combustible losses in terms of annual fuel savings for coal-fired units as a function of percent combustibles in ash, achievable percent combustibles in ash, unit design heat output and average fuel cost. Results show that the proposed predictive tool has a very good agreement with the reported data with average absolute deviation percent being around 1.77%. The developed tool can be of immense practical value for the utility engineers to have a quick check on the benefits of reducing the combustible losses in

terms of annual fuel savings for a coal-fired unit for wide range of operating conditions without the necessity of any pilot plant set up and experimental/plant trials.

The increasing demand for thermal and electric energy in many branches of industry and municipal management accounts for a drastic diminishing of fossil fuel resources (Lawrence et al 2009). Although renewable energy sources are gaining increasing attention, about 90% of the total energy output worldwide is from the combustion of fossil fuels (Lawrence et al 2009) and coal will continue to play a major role in meeting the global demand for energy (Bilgen.and Kaygusuz 2008). Unfortunately, hydrocarbon combustion has a major impact on the global environment due to emission of CO_2, which is a greenhouse gas, and results in temperature rise, drought, flood, hunger, and eventually economic chaos (Ram and Masto, 2010). Excessive exploitation of natural deposits also causes degradation of the environment and the diminishing of plant-life on our planet (Arora et al 2006). Therefore, techniques to gain less achievable percent combustible in ash and the least amount of pollutant emissions are necessary, and this goal can be reached through the control of combustion processes or adjustment of the fuels applied (Jou et al 2008). Coal-fired power plants have a significant affect on the environment due to their large energy currents and the different mass flows of various substances that come in and out of the plant (Oman et al, 2002). The effects are even greater when there is a mine in the vicinity of the power plant that supplies the coal (Oman et al, 2002).

A potentially significant loss from the combustion of coal fuels is the loss of unburned carbon. All coal-fired steam generators and coal-fired vessels inherently suffer an efficiency debit attributable to unburned carbon (Turner and Doty 2007). Several items are general symptoms that are suspected to be causing a high unburnt carbon loss from the combustion of coal. It is probable that pulverized coal-fired installations suffer from an inordinately high unburned carbon loss when any of the following conditions are experienced (Turner and Doty 2007; Bahadori and Vuthaluru, 2010u):

- A change in the raw-fuel quality from the original design basis.
- Deterioration of the fuel burners, burner throats, or burner swirl plates or impellers.
- Increased frequency of soot blowing to maintain heat transfer surface cleanliness.
- Noted increase in stack gas opacity.
- Sluggish operation of combustion controls of antiquated design.
- Uneven flame patterns characterized by a particularly bright spot in one sector of the flame and a quite dark spot in another.

- CO formation as determined from a flue-gas analysis.
- Frequent smoking observed in the combustion zone.
- Increases in refuse quantities in collection devices.
- Lack of continued maintenance and/or replacement of critical pulverized internals and classifier assembly.
- High incidence of coal “hang-up” in the distribution piping to the burners.
- Frequent manipulation of the air/coal primary and secondary air registers.

In view of the above mentioned issues, it is necessary to develop an accurate and simple method which is easier than existing approaches less complicated with fewer computations for predicting the approximate potential financial savings resulting from reduction of unburnt coal fuel loss. The unburnt fuel is generally collected with the ash in either the boiler ash hopper(s) or in various collection devices. The quantity of ash collected at various locations is dependent and unique to the system design. The balance of ash and unburned fuel is either collected in flue-gas cleanup devices or discharged to the atmosphere (Turner and Doty 2007). This work discusses the formulation of such predictive tool in a systematic manner along with sample example to show the simplicity of the model and usefulness of such tool.

7.3.1 Methodology to Develop Predictive Tool

The required data to develop this predictive tool includes combustible losses in terms of annual fuel savings for coal-fired units as a function of percent combustible in ash, achievable percent combustible in ash, unit design heat output and average fuel cost. In order to take into account, the unit design heat output and average fuel cost into the model, two correction factors F1 and F2 are introduced. In this work, the combustible losses in terms of annual fuel savings for coal-fired units are predicted rapidly by proposing a simple tool (Bahadori and Vuthaluru 2010u).

In this study, F1 and F2 are parameters to connect unit heat output and the average fuel cost to annual fuel saving, achievable percent combustible in ash and percent combustible in ash. The development of predictive tool contains three individual steps. The first step, unit heat output correction factor (F1) is correlated as a function of percent combustible in ash (X) and achievable percent combustible in ash (Y). In the second step the average fuel cost correction factor (F2) is correlated as a function of design unit heat output (Q) and correction factor (F1). Then annual fuel savings (η) is correlated as a function of average fuel cost (ε) and correction factor F2 (Bahadori and Vuthaluru 2010u).

In order to clarify the details of methodology to develop the predictive tool using Vandermonde matrix, the first step is explained (Bahadori and Vuthaluru 2010u).

Unit heat output correction factors (F1) are correlated as a function of percent combustible in ash (X) for different achievable percent combustible in ash (Y). Then, the calculated coefficients for these polynomials are correlated as a function of achievable percent combustible values in ash (Y). The derived polynomials are applied to calculate new coefficients for equation (7.12) to predict the unit heat output correction factors (F1). Table 7.3 shows the tuned coefficients for equations (7.13) to (7.16) for unit heat output correction factors (F1) as a function of percent combustible in ash (X) for different achievable percent combustible in ash (Y) according to the reliable data (Turner and Doty 2007).
In brief, the following steps are repeated to tune the correlation's coefficients using Matlab (2008) software (Bahadori and Vuthaluru 2010u).

4. Correlate unit heat output correction factors (F1) as a function of percent combustible in ash (X) for a given achievable percent combustible in ash (Y).
5. Repeat step 1 for other achievable percent combustible in ash (Y).

6. Correlate corresponding polynomial coefficients, which are obtained in previous steps versus achievable percent combustible in ash (Y), a = f(Y), b = f(Y), c = f(Y), d = f(Y) [see equations (7.13)-(7.16)].

Equation 7.12 represents the proposed governing equation in which four coefficients to be used to correlate the design unit heat output correction factors (F1) as a function of percent combustible in ash for a given achievable percent combustible value in ash where the relevant coefficients have been reported in Table 7.3.

$$\ln(\text{F1}) = \text{a} + b(X) + c(X)^2 + d(X)^3 \quad (7.12)$$

Where:

$$a = A_1 + B_1 Y + C_1 Y^2 + D_1 Y^3 \quad (7.13)$$

$$b = A_2 + B_2 Y + C_2 Y^2 + D_2 Y^3 \quad (7.14)$$

$$c = A_3 + B_3 Y + C_3 Y^2 + D_3 Y^3 \quad (7.15)$$

$$d = A_4 + B_4 Y + C_4 Y^2 + D_4 Y^3 \quad (7.16)$$

These optimum tuned coefficients (A, B, C and D) help to cover the data reported in the literature (Turner and Doty 2007).

The above-mentioned procedure is applied to correlate average fuel cost correction factor (F2) as a function of design unit heat output (Q) and correction factor (F1). The relevant tuned coefficients have been reported in Table 7.4. The governing equations are equations 7.17-7.21 (Bahadori and Vuthaluru 2010u).

$$\ln(\text{F2}) = \text{a} + b(F1) + c(F1)^2 + d(F1)^3 \quad (7.17)$$

Where:

$$a = A_1 + B_1 Q + C_1 Q^2 + D_1 Q^3 \quad (7.18)$$

$$b = A_2 + B_2 Q + C_2 Q^2 + D_2 Q^3 \quad (7.19)$$

$$c = A_3 + B_3 Q + C_3 Q^2 + D_3 Q^3 \quad (7.20)$$

$$d = A_4 + B_4 Q + C_4 Q^2 + D_4 Q^3 \quad (7.21)$$

The above-mentioned methodology is applied for the third step, to correlate annual fuel savings (η) as a function of average fuel cost (ε) and F2 correction factor. The relevant tuned coefficients are reported in Table 7.5. The governing equations are equations 7.22-26 (Bahadori and Vuthaluru 2010u).

$$\ln(\eta) = \mathrm{a} + b(F2) + c(F2)^2 + d(F2)^3 \quad (7.22)$$

Where:

$$a = A_1 + B_1 \varepsilon + C_1 \varepsilon^2 + D_1 \varepsilon^3 \quad (7.23)$$

$$b = A_2 + B_2 \varepsilon + C_2 \varepsilon^2 + D_2 \varepsilon^3 \quad (7.24)$$

$$c = A_3 + B_3 \varepsilon + C_3 \varepsilon^2 + D_3 \varepsilon^3 \quad (7.25)$$

$$d = A_4 + B_4 \varepsilon + C_4 \varepsilon^2 + D_4 \varepsilon^3 \quad (7.26)$$

The annual fuel savings are based on 8,760 hr/yr. For an operating factor other than the method basis, it is necessary to apply a correction factor to the method's results. Annual fuel savings are corrected to actual operating conditions (Bahadori and Vuthaluru 2010u).

Actual Savings $ = (predictive value) x [(operating heat output)/(design heat output)] x [(actual annual operating hours)/(8,760 hr/yr)].

Actual Savings $ = (η) x [(operating heat output)/(Q)] x [(actual annual operating hours)/(8,760 hr/yr)]

(7.27)

According to the authors' knowledge, there is no predictive tool for an accurate and rapid determination of the benefits of reducing the combustible losses in terms of annual fuel savings for coal-fired units as a function of percent combustible in ash, achievable percent

combustible value in ash, unit design heat out put and average fuel cost. In view of this necessity, our efforts were directed at formulating a method that will be of values for engineers and researchers. This predictive tool can be used to determine the approximate energy savings resulting from reducing unburned coal fuel loss (Bahadori and Vuthaluru 2010u).

The unburned fuel is generally collected with the ash in either the boiler ash hopper(s) or in various collection devices. The quantity of ash collected at various locations is dependent and unique to the system design. The boiler manufacturer will generally specify the proportion of ash normally collected in various ash hoppers furnished on the boiler proper. The balance of ash and unburned fuel is either collected in flue-gas cleanup devices or discharged to the atmosphere. A weighted average of total percentage combustibles in the ash must be computed to use this method (Turner and Doty 2007).

7.3.2 Figure 7.7 shows the performance of the proposed predictive tool for estimating the design unit heat output correction factor (F1) as a function of percent combustible in ash and achievable percent combustible in ash and in comparison with data in the literature [14]. As can be seen from Figure 1, the results show striking resemblance with the reported data. The proposed tool is accurate, reliable and acceptable.

Figures 7.8 and 7.9 show the proposed predictive tool's performance for the estimation of the average fuel cost correction factor (F2) as a function of, design unit heat output and correction factor (F1) in comparison with data (Turner and Doty 2007). Figures 7.8 and 7.9 show the proposed predictive tool can provide reliable and smooth results for wide range of conditions. Figures 7.10 and 7.11 show the predicted benefits of reducing the combustible losses in terms of annual fuel savings for coal-fired units as a function of F2 correction factor and average fuel cost in comparison with data (Turner and Doty 2007). Figure 7.8 shows the excellent performance of proposed predictive tool. Table 7.6 shows that the proposed predictive tool has a very good agreement with the reported data (Turner and Doty 2007) where the average absolute deviation percent is 1.77 %.

Our efforts in this investigation will pave the way for arriving at an accurate prediction of benefits of reducing the combustible losses in terms of annual fuel savings for coal-fired units as a function of percent combustible in ash, achievable percent combustible in ash, unit design heat out put and average fuel cost at various conditions which can be used by engineers and scientists for monitoring the operational parameters periodically (Bahadori and Vuthaluru 2010u).

The predictive tool proposed in this section is simple and unique expression which is absent in the literature. If the unit heat output or average fuel cost exceeds the limit of proposed method, use half the particular value and double the savings obtained from step 3 of method (correlating annual fuel savings with average fuel cost).
The annual fuel savings are based on 8,760 hr/yr. For an operating factor other than the method basis, apply a correction factor to method results. The application of the method assumes operating at, or close to, optimum excess air values. A typical example is given below to illustrate the simplicity associated with the use of proposed predictive tool for rapid estimating benefits of reducing the combustible losses in terms of annual fuel savings for coal-fired units (Bahadori and Vuthaluru 2010u).

7.3.3 Example:

Determine the benefits of reducing the combustible losses for a coal-fired steam generator having a maximum continuous rating of 65801 kgs/hr at an operating pressure of 1548.8 kPa(abs) and a temperature of 246.1°C at the desuperheater outlet, feedwater is supplied at 121.1°C

Available Data:

Average boiler load 65801 kg/hr
Superheater pressure 1548.8 kPa(abs)
Superheater temperature 246.1°C
Fuel type Coal
Measured flue gas oxygen 3.5%
Operating combustibles in ash 40%
Obtainable combustibles in ash 5%
Yearly operating time 8500 hr/yr
Design unit heat output 43.96 MW
Average unit heat output 37.806 MW
Average fuel cost US$1.582/GJ

7.3.3.1 Solution:

Step A:

Calculator F1 coefficient to consider the effects of percent combustible in ash and achievable percent combustible value in ash.

a=-1.3816952672

b= $2.6574093854\times10^{-1}$

c=$-6.1116957535\times10^{-3}$

d= 5.560494238×10^{-5}

F1=2.065475132×10^{1}

Step B:

Consider design unit output in calculations:

a= 1.500345968

b= 1.844816229×10^{-1}

c= $-4.921665457\times10^{-3}$

d= $5.1736743308\times10^{-5}$

F2= 3.913362681×10^{1}

Step C:

Consider average fuel cost in calculations

a= 2.743464882

b= $1.5572663379\times10^{-1}$

c= $-3.608982845\times10^{-3}$

d= $3.3257583098\times10^{-5}$

Annual fuel saving (in1000 US$) = 201.10437

Annual fuel savings will be: US$ 201104.

Annual fuel savings corrected to actual operating conditions:

Savings US$ = (predictive value) x [(operating heat output)/(design heat output)] x [(actual annual operating hours)/(8,760 hr/yr)]= (US$201,104/yr) x [(37.806 MW)/(43.96 MW)] [(8,500 hr/yr)/(8,760 hr/yr)]= 167,818 /yr. (from equation 7.27).

The calculated result has good agreement with reported data (Turner and Doty 2007) which is 175200, where the average absolute deviation percent is less than 4.5%.

A new predictive tool has been formulated for predicting the approximate potential savings resulting from reducing unburnt coal fuel loss. The proposed method presented here, determines the benefits of reducing the combustible losses in terms of annual fuel savings for coal-fired units as a function of percent combustible in ash, achievable percent combustible in ash, unit design heat out put and average fuel cost.

In this study, the benefits of reducing the combustible losses in terms of annual fuel savings for coal-fired units are calculated for design unit heat output up to 120 MW , average fuel cost up to 7 US$ per GJ and percent combustible in ash up to 50% (Bahadori and Vuthaluru 2010u).

The proposed tool is easier than existing approaches less complicated with fewer computations and suitable for combustion and process engineers. Unlike complex mathematical approaches for estimating potential savings resulting from reducing unburnt coal fuel loss, the proposed predictive tool is new and would be of immense value for combustion engineers especially those dealing with boiler and furnace operations and design.

Additionally, the level of mathematical formulations associated with the estimation of combustion efficiencies can be easily handled by a combustion engineer without any in-depth mathematical abilities. An example shown for the benefit of engineers clearly demonstrates the usefulness of the proposed tools. Furthermore, the estimations are quite accurate as evidenced from the comparisons with literature data (with average absolute deviations being around 1.77 %) and would help in attempting design and operations modifications with less time (Bahadori and Vuthaluru 2010u).

Table-7.3. Tuned coefficients in equations 7-13 to 7-17 for estimating the F1 correction factor as a function of percent combustible in ash and achievable percent combustible in ash (Bahadori and Vuthaluru 2010u)

Coefficient	Value
A_1	2.9237
B_1	-1.1794
C_1	7.4556×10^{-2}
D_1	-2.1787×10^{-3}
A_2	-6.8212×10^{-2}
B_2	9.3269×10^{-2}
C_2	-6.0976×10^{-3}
D_2	1.6037×10^{-4}
A_3	3.2952×10^{-3}
B_3	-2.6897×10^{-3}
C_3	1.8437×10^{-4}
D_3	-4.5429×10^{-6}
A_4	-3.4060×10^{-5}
B_4	2.6232×10^{-5}
C_4	-1.8858×10^{-6}
D_4	4.5214×10^{-8}

Table 7.4: Tuned coefficients for equations 7.18-7.21 estimating the F2 correction factor as a function of design unit heat output and F1 correction factor (Bahadori and Vuthaluru 2010u)

Coefficient	Unit heat output less than 30 MW/hr	Unit heat output more than 30 MW/hr
A_1	1.2367	1.802417
B_1	-1.8742×10^{-1}	-3.0371×10^{-2}
C_1	1.2322×10^{-2}	6.7628×10^{-4}
D_1	-1.9682×10^{-4}	-3.2234×10^{-6}
A_2	-1.3903×10^{-1}	-9.3940×10^{-2}
B_2	4.5225×10^{-2}	1.2497×10^{-2}
C_2	-2.1264×10^{-3}	-1.7352×10^{-4}
D_2	3.1322×10^{-5}	7.5781×10^{-7}
A_3	5.3406×10^{-3}	8.1904×10^{-3}
B_3	-1.3067×10^{-3}	-6.1183×10^{-4}
C_3	5.8022×10^{-5}	8.8911×10^{-6}
D_3	-8.0525×10^{-7}	-3.9995×10^{-8}
A_4	-5.3162×10^{-5}	-1.3218×10^{-4}
B_4	1.2018×10^{-5}	8.7897×10^{-6}
C_4	-4.9505×10^{-7}	-1.3111×10^{-7}
D_4	6.2723×10^{-9}	5.9910×10^{-10}

Table 7.5: Tuned coefficients for equations 7.23 to 7.26 to estimate the annual fuel savings (in 1000 $) as a function of average fuel cost and F2 correction factor (Bahadori and Vuthaluru 2010u)

Coefficient	Unit heat output less than 2 US $ per GJ	Unit heat output more than 2US $ per GJ and up to 6.4 $ per GJ
A_1	2.1162	2.0064
B_1	-1.4835	6.2654×10^{-1}
C_1	2.0750	-9.6004×10^{-2}
D_1	-5.6061×10^{-1}	6.8178×10^{-3}
A_2	-6.4006×10^{-2}	1.0652×10^{-1}
B_2	6.5013×10^{-1}	3.3755×10^{-2}
C_2	-5.2062×10^{-1}	-3.3735×10^{-3}
D_2	1.2482×10^{-1}	1.0134×10^{-5}
A_3	7.8664	-1.8634×10^{-3}
B_3	-3.5092×10^{-2}	-1.1609×10^{-3}
C_3	2.8353×10^{-2}	9.8477×10^{-5}
D_3	-6.7998×10^{-3}	2.0491×10^{-6}
A_4	-1.2254×10^{-4}	1.6964×10^{-5}
B_4	4.8131×10^{-4}	9.7302×10^{-6}
C_4	-3.8994×10^{-4}	-4.6467×10^{-8}
D_4	9.3527×10^{-5}	-1.3030×10^{-7}

Table 7.6: Accuracy of developed predictive tool for estimating the F1 correction factor as a function of percent combustible in ash and achievable percent combustible in ash in comparison with data (Bahadori and Vuthaluru 2010u)

Combustible in ash, percent	**Achievable percent combustible in ash, percent**	**Reported F1 factor value [14]**	**Calculated F1 factor value**	**Absolute deviation percent**
10	5	2	2.	2.5
20	5	7	6.9	1.2
30	5	13.1	13.3	1.3
50	5	35.2	35.7	1.4
15	10	2	2.08	4
30	10	11	11.1	1.7
40	10	19	18.3	3.2
45	10	24.3	23.6	2.7
50	10	32.6	33.2	2.0
20	15	2.67	2.7	1.8
30	15	9	9.1	2.1
40	15	17.3	17.0	1.7
45	15	22.2	21.8	1.6
50	15	29.	29.3	0.9
25	20	3	3.0	0.6
35	20	10	10.2	2.8
40	20	15	14.8	1.2
45	20	20	19.9	0.1
50	20	27.	27.1	0.1
Average absolute deviation percent (AADP)				1.7 %

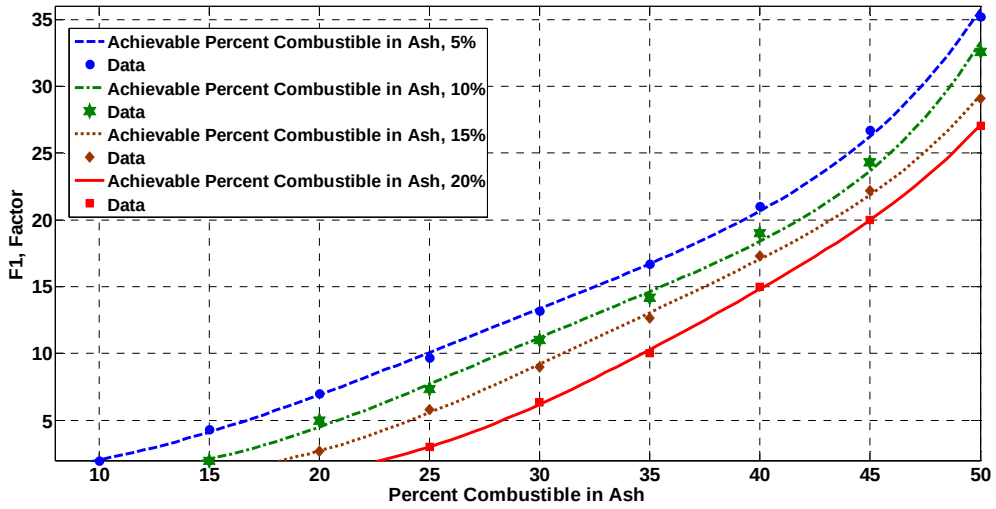

Figure 7.7: Performance of developed predictive tool for estimating the F1 correction factor as a function of percent combustible in ash and achievable percent combustible in ash in comparison with data, Bahadori A. and Vuthaluru H. B (2010u), *Applied Energy* 87, 3792-3799

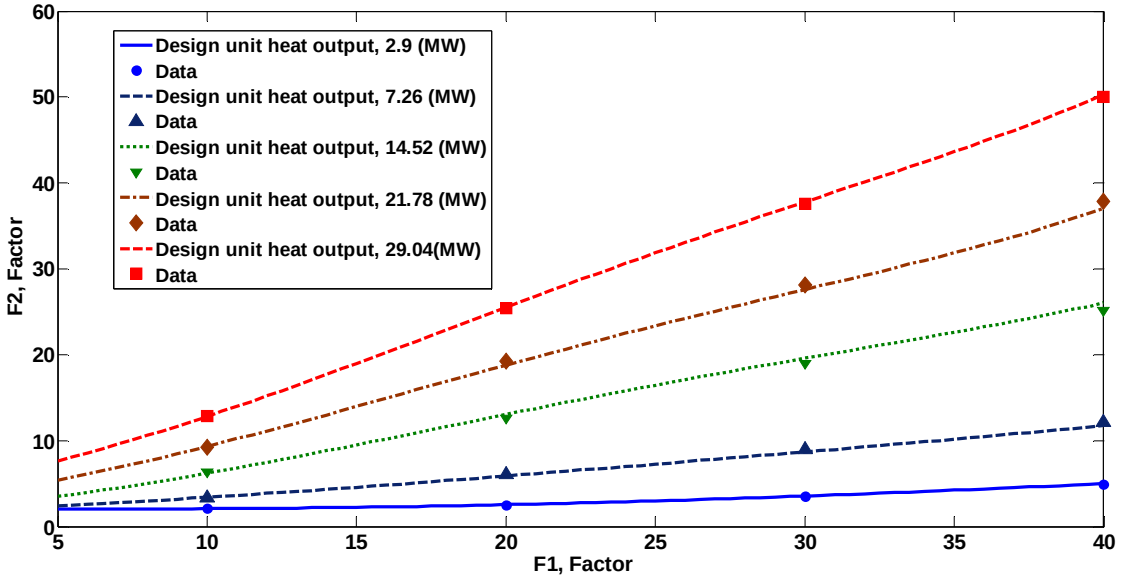

Figure 7.8: Performance of developed predictive tool for estimating the F2 correction factor as a function of design unit heat output and F1 correction factor in comparison with data for design unit heat output less than 29 MW, Bahadori A. and Vuthaluru H. B (2010u), *Applied Energy* 87, 3792-3799

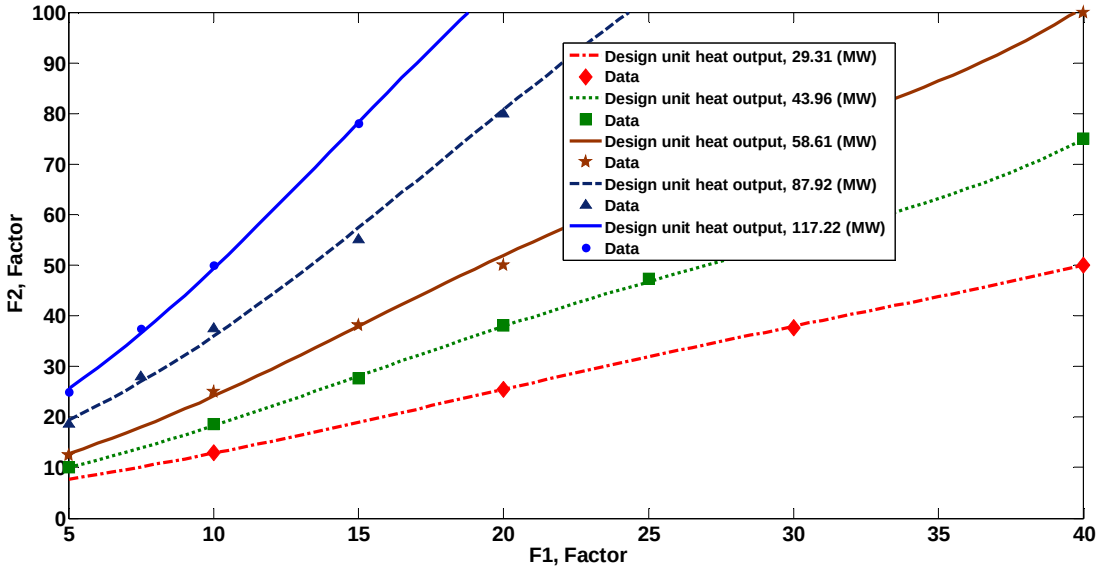

Figure 7.9: Performance of developed predictive tool for estimating the F2 correction factor as a function of design unit heat output and F1 correction factor in comparison with data for design unit heat output between 29 MW and 118 MW, Bahadori A. and Vuthaluru H. B (2010u), *Applied Energy* 87, 3792-3799

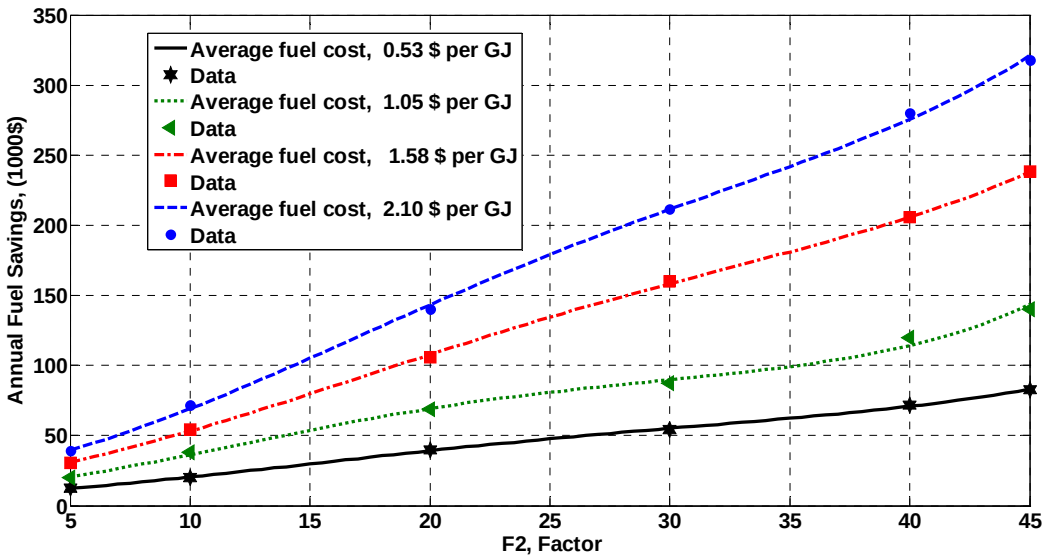

Figure 7.10: Performance of developed predictive tool for estimating the annual fuel savings (in 1000 $) as a function of average fuel cost and F2 correction factor in comparison with data for average fuel cost less than 2.1 US$ per GJ, Bahadori A. and Vuthaluru H. B (2010u), *Applied Energy* 87, 3792-3799

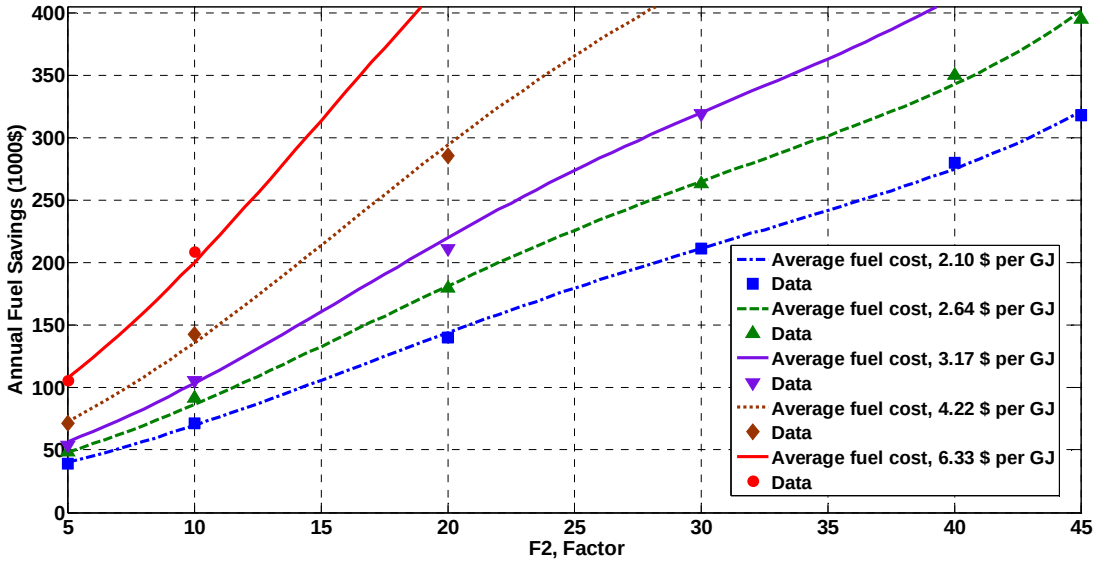

Figure 7.11: Performance of developed predictive tool for estimating the annual fuel savings (in 1000 $) as a function of average fuel cost and F2 correction factor in comparison with data] for average fuel cost less than between 2.1 US$ and 6.3 US$ per GJ, Bahadori A. and Vuthaluru H. B (2010u), *Applied Energy* 87, 3792-3799

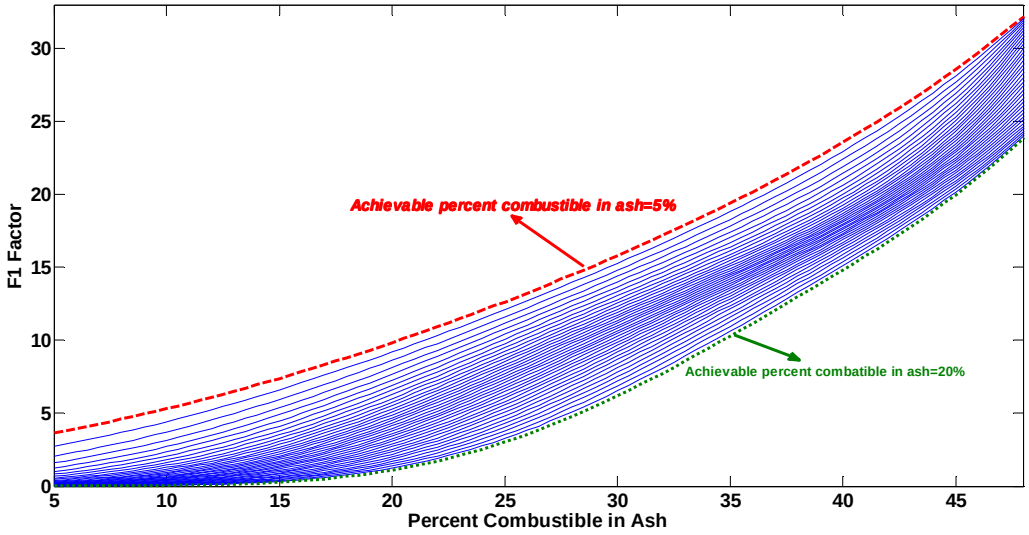

Figure 7.12: Performance of developed predictive tool for estimating the F1 correction factor as a function of percent combustible in ash and achievable percent combustible in ash, Bahadori A. and Vuthaluru H. B (2010u), *Applied Energy* 87, 3792-3799

7.4 Estimation of recoverable heat from blowdown systems during steam generation

During the generation of steam, most water impurities are not evaporated with the steam and builds up in the boiler water. The concentration of the impurities is usually regulated by the adjustment of the continuous blowdown valve, which controls the amount of water (and concentrated impurities) purged from the steam drum (Bahadori and Vuthaluru

2010v). Since a certain amount of continuous blowdown must be maintained for satisfactory boiler performance, a significant quantity of heat is removed from the boiler. It is necessary to provide a new method to calculate the total amount of heat that is recoverable using this system. In this section, a new predictive tool, which is easier than existing approaches, less complicated with fewer computations and with the minimum complex and time-consuming calculation steps, is formulated to arrive at an accurate estimation of the percent of blowdown that is flashed to steam as a function of flash drum pressure and operating boiler drum pressure followed by the calculation of the amount of heat recoverable from the condensate. Since all of the heat in the flashed steam is recoverable, the total percent of heat recoverable from the flash tank and heat-exchanger system is calculated in the final step (Bahadori and Vuthaluru 2010v).

Boilers and other fired systems are the most significant energy consumers (Turner and Doty, 2007). In a boiler system, the analysis can become more complex. Energy input comes from the following: condensate return, make-up water, combustion air, fuel, and few others depending on the complexity of the system (Bujak, 2009). Energy output departs via steam, blowdown, exhausts gases, shell/surface losses, possibly ash, and other discharges depending on the complexity of the system (Niu and Wong, 1998). For analysing complex systems, the mass and energy balance equations can be used simultaneously with solving multiple equations with multiple unknowns. During the generation of steam, most water impurities are not evaporated with steam and thus concentrate in the boiler water (Bhambre et al 2007). The concentration of impurities is usually regulated by the adjustment of continuous blowdown valve, which controls the amount of water (and concentrated impurities) purged from the steam drum (Figure 7.13). When the amount of blowdown is not properly established and/or maintained, either of the following may occur (Turner and Doty, 2007): If too little blowdown occurs, sludge deposits and results in carryover. If too much blowdown occurs, excessive hot water is removed, resulting in increased boiler fuel requirements, boiler feedwater requirements, and boiler chemical requirements. The continuous blowdown from any steam-generating equipment has the potential for energy savings whether it is a fired boiler or waste-heat-steam generator (Turner and Doty, 2007). Since a certain amount of continuous blowdown must be maintained for satisfactory boiler performance, a significant quantity of heat is removed from the boiler.

A large fraction of heat in the blowdown is recoverable by using a two-stage heat-recovery system as shown in Figure 7.13 before discharging to the sewer. In this system, blowdown lines from each boiler discharge into a common flash tank. The flashed steam may be tied

into an existing header, used directly by process, or used in the deaerator. The remaining hot water may be used to preheat makeup water to the deaerator or preheat other process streams. The following procedure may be used to calculate the total amount of heat that is recoverable using this system (Turner and Doty, 2007).

Many publications present physical modelling of boilers and they have shown that physical modelling is difficult and complicated, such as using artificial neural network and mathematical modelling of a steam boiler room to research thermal efficiency (Bahadori and Vuthaluru 2010v).

In view of the above mentioned issues, it is necessary to develop an accurate and simple method which is easier than existing approaches less complicated with fewer computations for predicting the total amount of heat that is recoverable using blowdown system. The results of the proposed predictive tool can be used in follow-up calculations to determine relative operating efficiency and to establish energy conservation benefits for steam generation using blowdown system. The paper discusses the formulation of such a predictive tool in a systematic manner along with sample example to show the simplicity of the model and usefulness of such tools (Bahadori and Vuthaluru 2010v).

7.4.1 Methodology to develop predictive tool

The required data to develop the predictive tool includes the percent of blowdown that is flashed to steam as a function of flash drum pressure and operating boiler drum pressure. In this work, the percent of blowdown that is flashed to steam is predicted rapidly by proposing a simple tool. The following methodology has been applied to develop the simple tool (Bahadori and Vuthaluru 2010v).

Firstly, the percentages of blowdown that is flashed to steam are correlated as a function of operating boiler drum pressure (P_b) in kPa(abs) for different flash drum pressures (P_{FD}) in kPa(abs) (Equation 7.28). Then, the calculated coefficients for these polynomials are correlated as a function of flash drum pressures (P_{FD}) (Bahadori and Vuthaluru 2010v). The derived polynomials (equations 7.29-7.32) calculate the new coefficients "a","b","c"and "d" as a function of flash drum pressures (P_{FD}) for equation (7.28) to predict, the percent of blowdown that is flashed to steam. Table 7.7 shows the tuned coefficients for equations (7.29) to (7.32) for the percent of blowdown that is flashed to steam in the design of boilers with blowdown systems according to reliable data available in the literature (Turner and Doty, 2007).

In brief, the following steps are repeated to tune the correlation's coefficients.

- Correlate the percent of blowdown that is flashed to steam as a function of operating boiler drum pressure (P_b) in kPa for a given flash drum pressures (P_{FD}).
- Repeat step 1 for other flash drum pressures (P_{FD}).
- Correlate corresponding polynomial coefficients, which are obtained in previous steps versus flash drum pressures, so a = f(P_{FD}), b = f(P_{FD}), c = f(P_{FD}), d = f(P_{FD}) [see equations (7.29)-(7.32)].

So, equation 7.28 represents the proposed governing equation in which four coefficients are used to correlate the percent of blowdown that is flashed to steam as a function of operating boiler drum pressure (P_b) in kPa for different flash drum pressures (P_{FD}) in kPa where the relevant coefficients have been reported in Table 7.7.

$$S = a + bP_b + cP_b^2 + dP_b^3 \tag{7.28}$$

Where:

$$a = A_1 + B_1P_{FD} + C_1P_{FD}^2 + D_1P_{FD}^3 \tag{7.29}$$

$$b = A_2 + B_2P_{FD} + C_2P_{FD}^2 + D_2P_{FD}^3 \tag{7.30}$$

$$c = A_3 + B_3P_{FD} + C_3P_{FD}^2 + D_3P_{FD}^3 \tag{7.31}$$

$$d = A_4 + B_4P_{FD} + C_4P_{FD}^2 + D_4P_{FD}^3 \tag{7.32}$$

These optimum tuned coefficients (A, B, C and D) help to cover the data pertinent to the percent of blowdown that is flashed to steam available in the literature (Turner and Doty, 2007).

In order to obtain the amount of heat recoverable from the condensate, the enthalpy of liquid leaving the flash tank at the flash tank pressure and enthalpy of liquid leaving the heat exchanger are calculated.

$$H_{TK} = 153.25 \ln(P_{FD}) - 300.24 \quad (7.33)$$

$$H_{EX} = 4.3501T - 1186.4 \quad (7.34)$$

Here, H_{TK} is the enthalpy of liquid leaving the flash tank (kJ/kg) and H_{EX} is the enthalpy of liquid leaving the heat exchanger (kJ/kg).

The following procedure may be used to calculate the total amount of heat that is recoverable using blowdown system:

1- Determine percent of blowdown that is flashed to steam.

Then condensate percent (C_p) will be:

$$C_p = 100 - S \quad (7.35)$$

2- Calculate enthalpy of liquid leaving the flash tank.

3- Calculate enthalpy of liquid leaving the heat exchanger for planning purposes, a 16.67°C to 22.22°C approach temperature (condensate discharge to makeup water temperature) may be used.

4- Calculate the percent of heat recoverable from the condensate (Q_C) using:

$$Q_C = [(H_{TK} - H_{EX}) / H_{TK}] \times C_p \quad (7.36)$$

5- Since all of the heat in the flashed steam is recoverable, the total percent of heat recoverable (Q) from the flash tank and heat-exchanger system will be:

$$Q = Q_C + S \quad (7.37)$$

Figure 7.14 shows the proposed the performance of the predictive tool for the estimation of the percent of blowdown that is flashed to steam as a function of flash drum pressure and operating boiler drum pressure and is compared with data reported in the literature (Turner and Doty, 2007). As can be seen, the results in figure 3 show good agreement with the reported data and the proposed new correlation is accurate, reliable and acceptable.

Figure 7.15 shows the performance of proposed predictive tool for the estimation of percent of blowdown that is flashed to steam as a function of flash drum pressure and operating boiler drum pressure (Bahadori and Vuthaluru 2010v).

Figures 7.16 and 7.17 show the predicted the enthalpy of liquid leaving the flash tank at the flash tank pressure and enthalpy of liquid leaving the heat exchanger as a function of flash drum pressure (kPa(abs)) and blowdown heat exchanger rejection temperature (K) in comparison with the reported data (Turner and Doty, 2007). Results presented in Table 7.8 shows that the proposed predictive tool has a very good agreement with the reported data (Turner and Doty, 2007).

The predictive tool proposed in this study is simple and contains an unique expression which currently unavailable in literature. Typical examples are given below to illustrate the simplicity associated with the use of proposed predictive tool for rapid estimation of the total amount of heat that is recoverable using blowdown system. In particular, process and combustion engineers would find the proposed approach to be user friendly involving transparent calculations with no complex expressions for their applications to the design and operation of blowdown heat recovery system for steam generation in boilers (Bahadori and Vuthaluru 2010v).

7.4.2 Example 1:

To further illustrate the predictive tool capabilities, lets consider the following example:

Determine the percent of heat recoverable percent (Q) from a 1153 kPa(abs) boiler blowdown waste stream, if the stream is sent to a 253 kPa(abs) flash tank and heat exchanger.

Available Data:

1- Boiler drum pressure 1153 kPa(abs)
   Flash tank pressure 253 kPa(abs)
   Makeup water temperature 21.11°C
   Assume a 16.66°C approach temperature between condensate discharge and makeup water temperature.

7.4.3 Calculation and Analysis for example 1:

According to equations (1-5) determine flash % with a boiler drum pressure of 1153 kPa(abs) and a flash tank pressure of 253 kPa(abs) , and then calculate the steam percentage (Flash %):

a= -1.153248810

b=$1.5157891426 \times 10^{-2}$

c=$-3.492536720 \times 10^{-6}$

d= $3.446464646 \times 10^{-10}$

S=12.06%

2- Determine condensate percent (C_p):

C_p = 100 – S

C_p = 100 - 12.06

C_p = 87.94%

3- Determine H_{TK} at a flash tank pressure of 253 kPa(abs) and calculate the enthalpy of the drum water (H_{TK}) to be 547.75 kJ/kg.

4- Determine H_{EX} :

Assuming a 16.66°C approach temperature between condensate discharge and makeup water temperature, the temperature of the blowdown discharge is equal to the makeup water temperature plus the approach temperature which equals:

T=21.11+16.66=37.77 °C which after conversion to K will be 310.92 K

Entering blowdown heat exchanger rejection temperature of 310.92 K into equation 7, the enthalpy of the blowdown discharge water can be estimated to be 166.13 kJ/kg.

Calculate the percent of heat recoverable from the condensate (Q_C):

So, Q_C = [(547.75 kJ/kg - 166.13 kJ/kg)/547.75 kJ/kg](87.94/100) =0.612

Q_C = 61.2%

Determine total percent of heat recoverable (Q) from the flash tank and heat-exchanger system is:

Q = Q_C + S

Q = 61.2+ 12.06=73.26%

Therefore, approximately 73.7% of the heat energy can be recovered using this blowdown heat recovery method (Bahadori and Vuthaluru 2010v).

7.4.4 Example 2:

Determine the percent of heat recoverable percent (Q) from a 1000 kPa(abs) boiler blowdown waste stream, if the stream is sent to a 100 kPa(abs) flash tank and heat exchanger (Bahadori and Vuthaluru 2010v).

Available Data:

Boiler drum pressure 1000 kPa(abs)

Flash tank pressure 100 kPa(abs)

Makeup water temperature 20°C

Assume a 16 °C approach temperature between condensate discharge and makeup water temperature.

Calculation and Analysis for example 2:

1- According to equations (7.28-7.33) determine flash % with a boiler drum pressure of 1153 kPa(abs) and a flash tank pressure of 253 kPa(abs) , calculate the steam percentage (Flash %) :

a= 3.44647611

b=1.434533644×10^{-2}

c=$-3.337197885\times10^{-6}$

d= 3.392194×10^{-10}

S=14.79%

2- Determine condensate percent (C_p):

C_p = 100 – S

C_p = 100 – 14.79

C_p = 85.21%

3- Determine H_{TK} at a flash tank pressure of 100 kPa(abs) and calculate the enthalpy of the drum water (H_{TK}) to be 405.5 kJ/kg.

4- Determine H_{EX}

Assuming a 16.66°C approach temperature between condensate discharge and makeup water temperature, the temperature of the blowdown discharge is equal to the makeup water temperature plus the approach temperature which equals:

T=20+17=37 °C which after conversion to K will be 310.15 K

Entering equation 7 with a blowdown heat exchanger rejection temperature of 310.15 K and calculate the enthalpy of the blowdown discharge water to be 162.78 kJ/kg.

Calculate the percent of heat recoverable from the condensate (Q_C):

So, Q_C = [(405.5 kJ/kg – 162.78 kJ/kg)/405.5 kJ/kg] (85.21/100) =0.51

Q_C = 51%

Determine total percent of heat recoverable (Q) from the flash tank and heat-exchanger system is:

$Q = Q_C + S$

Q = 51+ 14.79=65.79%

Therefore, approximately 65.79% of the heat energy can be recovered using this blowdown heat recovery method.

This new predictive tool is easier than existing approaches, because it is less complicated, with fewer computations and minimizes the complex and time-consuming calculation steps, to arrive at an appropriate estimation of the percent of blowdown that is flashed to steam as a function of flash drum pressure and operating boiler drum pressure (Bahadori and Vuthaluru 2010v). Then the enthalpy of liquid leaving the flash tank at the flash tank pressure and enthalpy of liquid leaving the heat exchanger are calculated in order to obtain the amount of heat recoverable from the condensate. Since all of the heat in the flashed steam is recoverable, so in the final step the total percent of heat recoverable from the flash tank and heat-exchanger system is calculated (Bahadori and Vuthaluru 2010v).

Unlike complex mathematical approaches for estimating the total amount of heat that is recoverable in boilers using blowdown system, the proposed predictive tool is new and would be of immense assistance for combustion engineers especially those dealing with boiler operations and design. Additionally, the level of mathematical formulations associated with the estimation of combustion efficiencies can be easily handled by a combustion engineer without any in-depth mathematical abilities. The example shown will benefit to engineers as it clearly demonstrates the usefulness of the proposed tools. Furthermore, the estimations are quite accurate as evidenced from the comparisons with literature data (with average absolute deviations being around 2%) and would help in attempting design and operations modifications with less time (Bahadori and Vuthaluru 2010v). The proposed method is superior due to its accuracy and clear numerical background, wherein the relevant coefficients can be retuned quickly for various cases.

Table 7.7: Tuned coefficients for equations 7.29 to 7.32 (Bahadori and Vuthaluru 2010v)

Coefficient	Value
A_1	7.7923673
B_1	-4.8262233×10^{-2}
C_1	4.9873209×10^{-5}
D_1	-1.8400016×10^{-8}
A_2	1.3073383×10^{-2}
B_2	1.5964326×10^{-5}
C_2	-3.3981625×10^{-8}
D_2	1.5336398×10^{-11}
A_3	-2.9941415×10^{-6}
B_3	-4.5266157×10^{-9}
C_3	1.14973954×10^{-11}
D_3	-5.3686723×10^{-15}
A_4	3.1198635×10^{-10}
B_4	3.8327763×10^{-13}
C_4	-1.1655781×10^{-15}
D_4	5.6108885×10^{-19}

Table 7.8: Accuracy of developed predictive tool for calculating the percent of blowdown that is flashed to steam as a function of flash drum pressure and operating boiler drum pressure (Bahadori and Vuthaluru 2010v)

Flash drum pressure	Operating boiler drum pressure	Steam percent, reported data	Steam percent, calculated values	Absolute deviation percent
0	55.9	10	9.63	3.70
0	226.47	20	19.59	2.05
0	579.41	30	29.49	1.70
5	153	15	15.03	0.20
5	435.29	25	25.02	0.08
5	641.2	30	30.44	1.46
15	329.4	20	20.55	2.75
15	505.9	25	24.98	0.08
15	725	30	31.91	6.36
25	129.41	10	9.95	0.50
25	379.41	20	20.41	2.05
25	575	25	25.15	0.60
50	191.2	10	9.96	0.40
50	308.82	15	14.96	0.27
50	491.2	20	19.97	0.15
75	149	5	4.93	1.40
75	247	10	9.87	1.30
75	379.4	15	14.61	2.60
100	295	10	9.70	3.0
100	450	15	14.72	1.87
100	650	20	19.79	1.05
125	218	5	4.78	4.4
125	725	20	20.14	0.70
150	150	0	0.11	1
150	564.7	15	15.19	1.27
150	775	20	19.87	0.65
200	200	0	0	0
200	662	15	14.95	0.33
200	850	20	20.14	0.70
Average absolute deviation percent (AADP)				1.47%

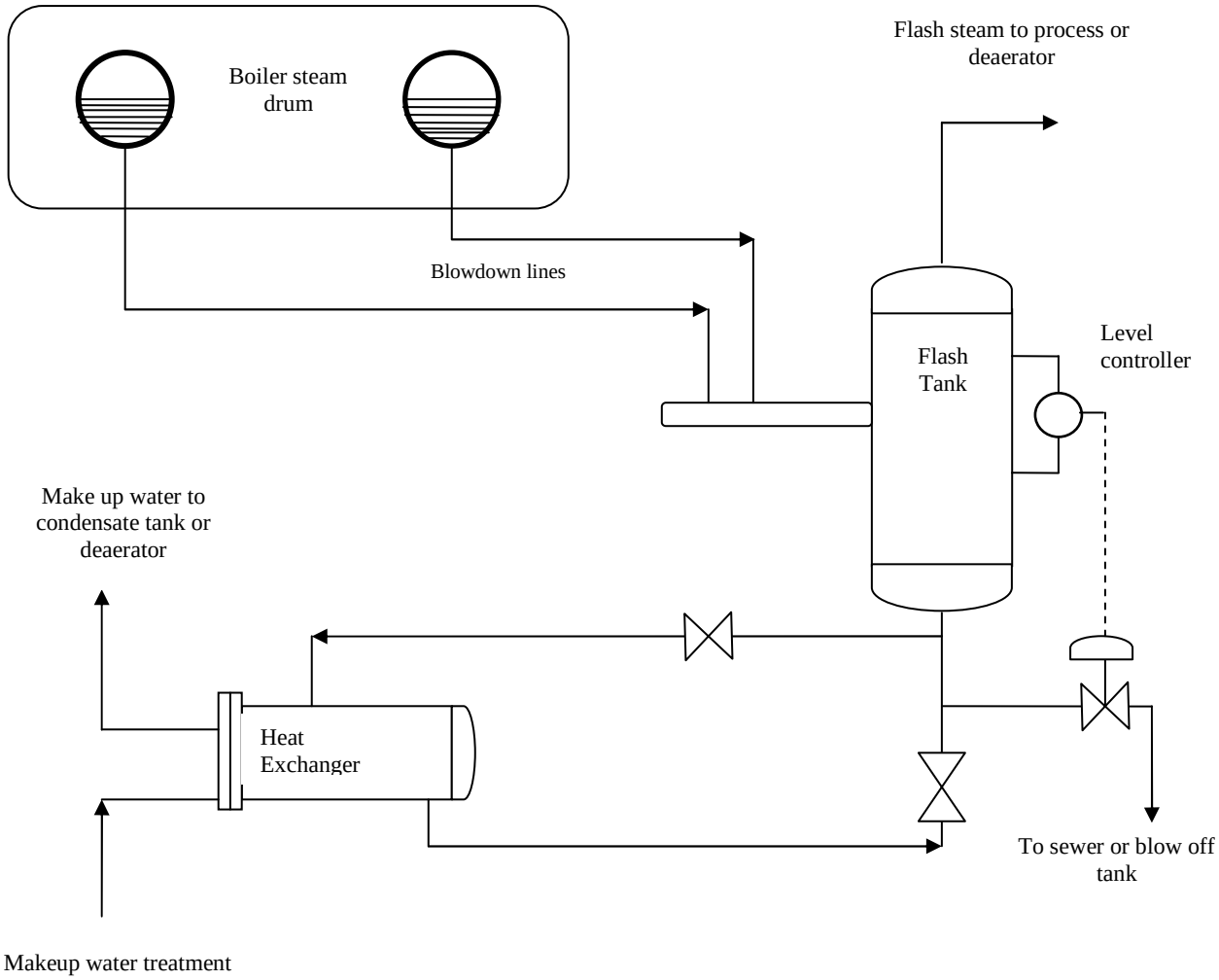

Figure 7.13: Typical two-stage blowdown heat-recovery system (Bahadori A. and Vuthaluru H. B (2010v) *Energy*, 35, 3501-3507)

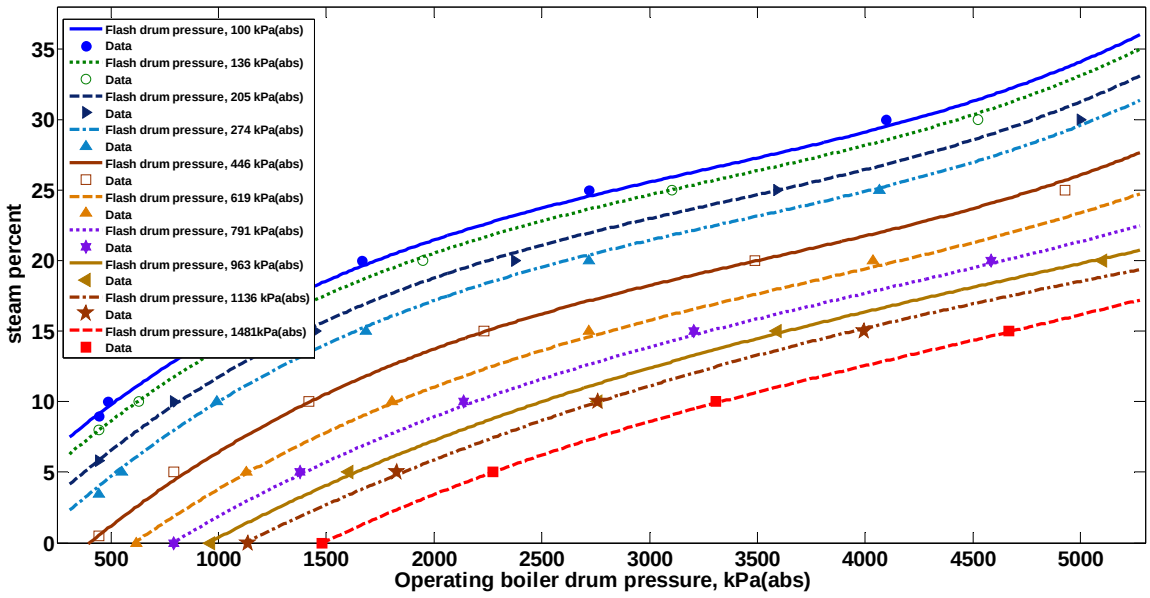

Figure 7.14: Performance of predictive tool for the estimation of percent of blowdown that is flashed to steam as a function of flash drum pressure and operating boiler drum pressure in comparison with data (Bahadori A. and Vuthaluru H. B (2010v) *Energy* ,35, 3501-3507)

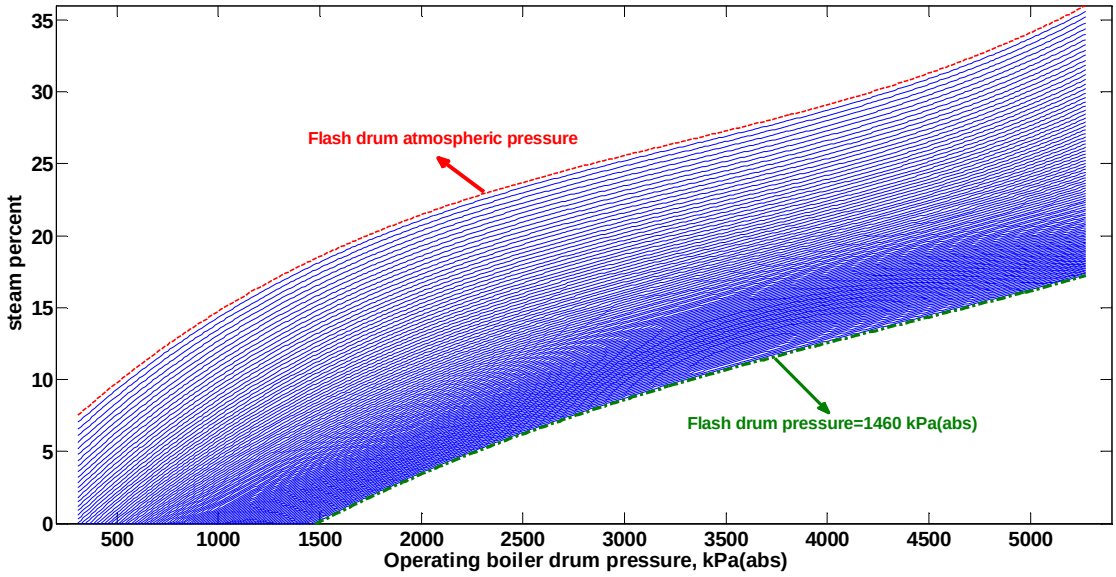

Figure 7.15: Performance of predictive tool for the estimation of percent of blowdown that is flashed to steam as a function of flash drum pressure and operating boiler drum for wide range of conditions (Bahadori A. and Vuthaluru H. B (2010v) *Energy* ,35, 3501-3507)

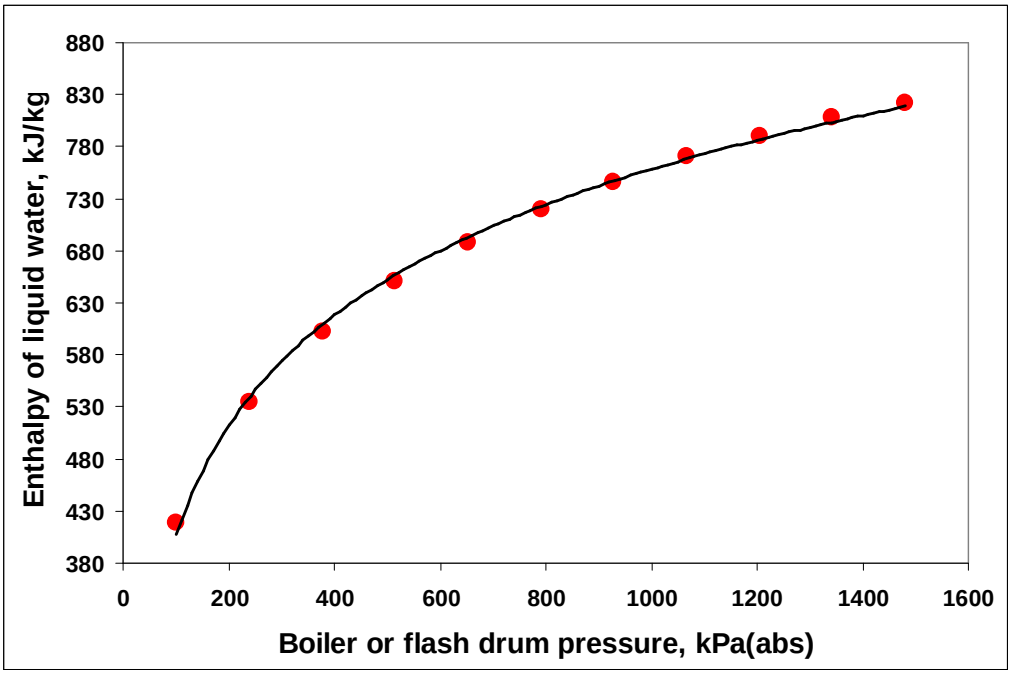

Figure 7.16: Predicted the enthalpy of liquid leaving the flash tank at the flash tank pressure and enthalpy of liquid leaving the heat exchanger as a function of flash drum pressure (kPa(abs)) in comparison with data (Bahadori A. and Vuthaluru H. B (2010v) *Energy* ,35, 3501-3507)

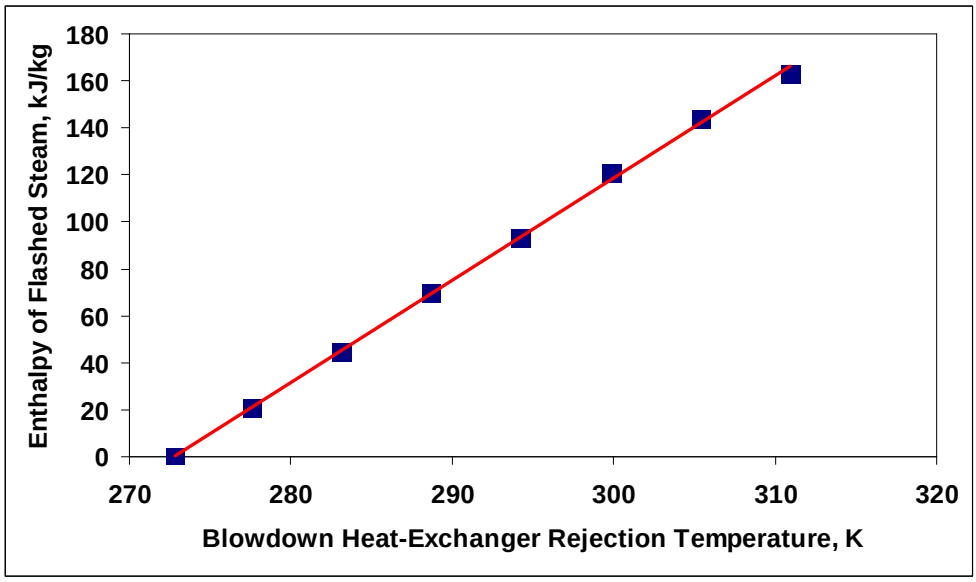

Figure 7.17: Predicted enthalpy of liquid leaving the heat exchanger as a function of blow down heat exchanger rejection temperature (K) in comparison with data (Bahadori A. and Vuthaluru H. B (2010v) *Energy*, 35, 3501-3507)

7.5 Estimation of energy conservation benefits in excess air controlled gas-fired systems

The most significant energy consumers in energy related industries are boilers and other gas-fired systems. Combustion efficiency term commonly used for boilers and other fired systems and the information on either carbon dioxide (CO_2) or oxygen (O_2) in the exhaust gas can be used. The aim of this study is to develop a new predictive tool which is easier than existing approaches contains less complicated with fewer computations and suitable for combustion engineers for predicting the natural gas combustion efficiency as a function of excess air fraction and stack temperature rise (the difference between the flue gas temperature and the combustion air inlet temperature).

The results of proposed predictive tool can be used in follow-up calculations to determine relative operating efficiency and to establish energy conservation benefits for an excess-air control program. Results show that the proposed predictive tool has a very good agreement with the reported data where the average absolute deviation percent is 0.1%. It should be noted that these calculations are based on assuming complete natural gas combustion at atmospheric pressure and the level of unburned combustibles is considered

negligible. The proposed method is superior owing to its accuracy and clear numerical background, wherein the relevant coefficients can be retuned quickly for various cases.

This proposed approach can be of immense practical value for the engineers and scientists to have a quick check on natural gas combustion efficiencies for wide range of operating conditions without the necessity of any pilot plant set up and experimental trials. In particular, process and combustion engineers would find the proposed approach to be user friendly involving transparent calculations with no complex expressions for their applications to the design and operation of natural gas-fired systems such as furnaces and boilers. Today about 90% of the total energy output worldwide is from the combustion of fossil fuels (Xu et al 2005). Unfortunately, hydrocarbon combustion has a major impact on the global environment due to emission of CO_2, which is a greenhouse gas, and a huge contributor to climate change, temperature rise, drought, flood, hunger, and eventually economic chaos.

Furthermore, the emission of NO_x, SO_x, polycyclic aromatic hydrocarbons (PAHs), CO, and particles leads to air pollution, acid rain, and health hazards (Miller, and Srivastava 2000). Nevertheless, the demand for fossil fuel continues to rise globally (Barroso et al 2005). Therefore, techniques to achieve better combustion efficiency and the least amount of pollutant emissions are necessary, and this goal can be reached through the control of combustion processes or adjustment of the fuels applied. It is an assertion well established by researchers and engineers related to the industrial boiler field that excess air is a control variable affecting thermal efficiency and the operating reliability of boilers (Bahadori and Vuthaluru 2010w). The increase in the value of the excess of air in the furnace leads to a reduction in the adiabatic flame temperature, and might prompt an increase in the heat transfer coefficients for all the convective equipments, causing a reduction in the flue gas temperature.

As the excess air ratio goes up, the O_2 concentration in the main combustion area also increases, resulting in the rise of the flame temperature in the boiler. This leads to a drop of the temperature in the boiler radiation area and eventually affects the boiler efficiency (Bahadori and Vuthaluru 2010w). A boiler should always be supplied with more combustion air than is theoretically required, in order to ensure complete combustion and safe operation. If the air rate is too low, there will be a rapid build up of carbon monoxide in the flue gas and, in extreme cases, smoke will be produced (i.e. unburned carbon particles) (Bahadori and Vuthaluru 2010w). At the same time, boiler efficiency is very dependent on the excess air rate. Excess air should be kept at the lowest practical level to

reduce the quantity of unneeded air that is heated and exhausted at the stack temperature (Bahadori and Vuthaluru 2010w).

The amount of excess air (or O_2) in the flue gas and the stack temperature rise above the inlet air temperature are significant in defining the efficiency of the combustion process. Excess oxygen (O_2) measured in the exhaust stack is the most typical method of controlling the air-to-fuel ratio. Careful attention to furnace operation is required to ensure an optimum level of performance. To accomplish optimal control over avoidable losses, the continuous measurement of the excess air is a necessity (Bahadori and Vuthaluru 2010w).

Fossil-fuel-fired steam generators, process fired heaters/furnaces, duct heaters, and separately fired superheaters may benefit from an excess-air-control program. Specialized process equipment, such as rotary kilns, and fired calciners, can also benefit from an air control program (Bahadori and Vuthaluru 2010w). In view of the above mentioned issues, it is necessary to develop an accurate and simple method which will be easier than existing approaches less complicated with fewer computations for predicting the natural gas combustion efficiency as a function of, excess air fraction and stack temperature rise. The results of the proposed predictive tool can be used in follow-up calculations to determine the relative operating efficiency and to establish energy conservation benefits for an excess-air control program. This paper discusses the formulation of such predictive tool in a systematic manner along with sample example to show the simplicity of the model and usefulness of such tools.

7.5.1 Methodology to Develop Predictive Tool

The required data to develop this predictive tool includes natural gas combustion efficiency fraction (E) as a function of, excess air fraction (X) and stack temperature rise (ΔT) in °C. In this work, the the natural gas combustion efficiencies (E) are predicted rapidly by proposing a simple tool. The following methodology has been applied to develop this simple tool (Bahadori and Vuthaluru 2010w).

Firstly, natural gas combustion efficiencies (E) are correlated as a function of stack temperature rise (ΔT) for different excess air fractions (X). Then, the calculated coefficients for these polynomials are correlated as a function of excess air fractions (X). The derived polynomials are applied to calculate new coefficients for the equation (7.38) to predict, natural gas combustion efficiencies for the design of fired systems. Table 1

shows the tuned coefficients for equations (7.39) to (7.42) for natural gas combustion efficiencies in the design of natural gas-fires systems according to the available data (Bahadori and Vuthaluru 2010w).

In brief, as performed in previous efforts the following sections are repeated to tune the correlation's coefficients (Bahadori and Vuthaluru 2010w):

7. Correlate the natural gas combustion efficiencies (E) as a function of stack temperature rise or ΔT in °C for a given excess air fraction (X).
8. Repeat step 1 for other excess air fraction (X).
9. Correlate corresponding polynomial coefficients, which are obtained in previous steps versus excess air fraction (X), a = f(X), b = f(X), c = f(X), d = f(X) [see equations (7.39)-(7.42)].

Therefore the equation 7.38 represents the proposed governing equation in which four coefficients are used to correlate natural gas combustion efficiencies (E) stack temperature rise (ΔT) in °C for a given excess air fraction (X) where the relevant coefficients have been reported in Table 7.9.

$$\mathrm{E} = \mathrm{a} + b(\Delta T) + c(\Delta T)^2 + d(\Delta T)^3 \quad (7.38)$$

Where:

$$a = A_1 + B_1 X + C_1 X^2 + D_1 X^3 \quad (7.39$$

$$b = A_2 + B_2 X + C_2 X^2 + D_2 X^3 \quad (7.40)$$

$$c = A_3 + B_3 X + C_3 X^2 + D_3 X^3 \quad (7.41)$$

$$d = A_4 + B_4 X + C_4 X^2 + D_4 X^3 \quad (7.42)$$

These optimum tuned coefficients (A, B, C and D) help to cover the natural gas combustion efficiencies (E) data reported in literature (Bahadori and Vuthaluru 2010w).

The amount of excess air (or O_2) in the flue gas and the stack temperature rise above the inlet air temperature are significant in defining the efficiency of the combustion process.

Excess oxygen (O_2) measured in the exhaust stack is the most typical method of controlling the air-to-fuel ratio (Bahadori and Vuthaluru 2010w).

In order to correlate excess air fraction as a function of oxygen mole fraction in the flue gas (Y_o), the equation 7.43 has been developed based on the data reported in the literature (Bahadori and Vuthaluru 2010w).

$$X= 56.519Y_o^2 + 2.2766Y_o + 0.0159 \quad (7.43)$$

In order to justify the development of equation (7.43), it should be emphasised that the combustion efficiency is similar to the heat loss method, but only the heat losses due to the exhaust gases are considered (Bahadori and Vuthaluru 2010w). Combustion efficiency can be measured in the field by analyzing the products of combustion the exhaust gases. Typically measuring either carbon dioxide (CO_2) or oxygen (O_2) in the exhaust gas can be used to determine the combustion efficiency as long as there is excess air (Bahadori and Vuthaluru 2010w).

Realistically, however, it is impossible to obtain the perfect mixture of air and fuel to achieve complete combustion without some amount of excess air (Bahadori and Vuthaluru 2010w). As excess air is reduced toward the fuel rich side, incomplete combustion begins to occur resulting in the formation of carbon monoxide, carbon, smoke and in extreme cases, raw unburned fuel (Bahadori and Vuthaluru 2010w).

The amount of carbon dioxide, percent by volume, in the exhaust gas reaches a maximum with no excess air stoichiometric conditions. While carbon dioxide can be used as a measure of complete combustion, it can not be used to optimally control the air-to-fuel ratio in a fired system (Bahadori and Vuthaluru 2010w). A drop in the level of carbon dioxide would not be sufficient to inform the control system if it were operating in a condition of excess air or insufficient air (Bahadori and Vuthaluru 2010w). However, measuring oxygen in the exhaust gases is a direct measure of the amount of excess air. For these reasons, measuring oxygen in the exhaust gas is a more common and preferred method of controlling the air-to-fuel ratio in a fired system.

Figure 7.18 shows proposed predictive tool's performance for the estimation of natural gas combustion efficiency as a function of the excess air fraction and stack temperature rise in comparison with reported data in the literature (Bahadori and Vuthaluru 2010w).

As can be seen, the results in figure 7.18 show good agreement with the reported data, illustrating that the proposed correlation is accurate, reliable and acceptable.

Figures 7.19 and 7.20 show the proposed predictive tool provides reliable and smooth results for wide range of conditions. Figure 7.21 shows the predicted excess air fraction as a function of flue gas oxygen fraction in comparison with reported data (Turner 2005). Table 7.10 shows that the proposed predictive tool has a very good agreement with the reported data where the average absolute deviation percent is 0.1%.

In this study our efforts have been directed at formulating a method which will assist engineers and researchers. It is expected that our efforts in this investigation will pave the way for arriving at an accurate prediction of energy conservation benefits in excess air controlled gas-fired systems at various conditions which can be used by engineers and scientists for monitoring the key parameters periodically. A typical example is given below to illustrate the simplicity associated with the use of proposed predictive tool for rapid estimating natural gas combustion efficiency.

7.5.2 Example:

For illustration purposes, let's consider the following example (Bahadori and Vuthaluru 2010w):

Determine the potential energy savings associated with reducing the amount of excess air to an optimum level for a natural gas-fired steam boiler.

Operating Data are:

Current energy consumption 116061000 MJ/yr
Boiler rated capacity 600 boiler horsepower
Operating hours 8,500 hr/yr
Current stack gas analysis 9% Oxygen (by volume, dry)
Minimal CO reading
Combustion air inlet temperature 26.7°C (299.82 K)
Exhaust gas stack temperature 304.4°C (577.6K)
Proposed operating condition 2% Oxygen (by volume, dry)

Solution:

Step 1: Determine the current stack temperature rise (STR).

STR = (exhaust stack temperature) – (combustion air temperature)

STR = 577.6 K – 299.82 K = 277.8°C

Enter the equation 9 with an oxygen mole fraction of 0.09 :

Excess air to be approximately 66%.

$X= 56.519Y_o^2 + 2.2766Y_o + 0.0159$

$X= 56.519\ (0.09)^2 + 2.2766(0.09) + 0.0159$

X=0.6786 (Excess air fraction to be approximately 67.86%).

For a stack temperature rise of 277.8°C calculate the current combustion efficiency fraction:

$a= -1.1353975223\times10^{-1}$

$b= -5.2185187749\times10^{-4}$

$c= -4.8836104024\times10^{-7}$

$d= 5.3528037326\times10^{-10}$

Thus, the natural gas combustion efficiency will be 0.7612 or E= 0.7612

Step 2: Determine the proposed boiler combustion efficiency using the same equations for the proposed combustion efficiency assuming the same stack temperature operating condition.

$a= -1.0883373154\times10^{-1}$

$b= -2.9799718134\times10^{-4}$

$c= -2.5360699913\times10^{-7}$

$d= 2.8903807586\times10^{-10}$

The proposed combustion efficiency will be 0.82006 or E= 0.82006

Step 3:Determine the fuel savings.

e) Percent fuel savings = [(new efficiency) – (old efficiency)]/(new efficiency)
   Percent fuel savings = [(0.82006) – (0.7612)]/(0.82006)
   Fuel savings fraction= 0.0718 or 7.18%

f) Fuel savings = (current fuel consumption) (percent fuel savings)
   Fuel savings = (116061000 MJ/yr) (0.0718)
   Fuel savings = 8333180 MJ/yr

The calculated combustion efficiency will be 82.006%.

Note: in many cases reducing the amount of excess air will tend to reduce the exhaust stack temperature, resulting in an even more efficient combustion.
In this work, a new predictive tool is formulated for predicting the natural gas combustion efficiency as a function of increasing excess air fraction and stack temperature. This tool is easier than existing approaches less complicated with fewer computations and suitable for combustion and process engineers.

The results of the proposed predictive tool can be used in follow-up calculations to determine relative operating efficiency and to establish energy conservation benefits for an excess-air control program. Unlike complex mathematical approaches for estimating natural gas combustion efficiency, the proposed predictive tool is new and would be of immense help for combustion engineers especially those dealing with boiler and furnace operations and design. Additionally, the level of mathematical formulations associated with the estimation of combustion efficiencies can be easily handled by a combustion engineer without any in-depth mathematical abilities. The example is shown for the benefit of engineers to clearly demonstrate the usefulness of the proposed tools. Furthermore, the estimations are quite accurate as evidenced from the comparisons with literature data (with average absolute deviations being around 0.1%) and would help in attempting design and operations modifications with less time.

Table 7.9: Tuned coefficients for equations 7.39 to 7.42

Coefficient	Values of the optimum tuned coefficients
A_1	-1.0898×10^{-1}
B_1	8.9774×10^{-3}
C_1	-7.9590×10^{-2}
D_1	8.3206×10^{-2}
A_2	-2.8107×10^{-4}
B_2	-8.8879×10^{-4}
C_2	2.1773×10^{-3}
D_2	-2.0490×10^{-3}
A_3	-3.2183×10^{-7}
B_3	3.7051×10^{-6}
C_3	-1.4949×10^{-5}
D_3	1.3451×10^{-5}
A_4	4.2503×10^{-10}
B_4	-7.3486×10^{-9}
C_4	2.7938×10^{-8}
D_4	-2.4859×10^{-8}

Table 7.10: Accuracy of developed predictive tool the natural gas combustion efficiency as a function of, excess air fraction and stack temperature rise

Excess Air, Fraction	**Stack Temperature Rise, °C**	**Reported Combustion Efficiency, Fraction** (Turner 2005)	**Calculated Combustion Efficiency, Fraction**	**Absolute deviation percent**
0	65.5	0.88	0.8792	0.09
0	204.4	0.84	0.8384	0.19
0	371.1	0.789	0.7898	0.10
0.2	93.3	0.864	0.8636	0.05
0.2	232.2	0.814	0.8144	0.05
0.2	315.5	0.784	0.7841	0.01
0.2	371.1	0.764	0.76338	0.08
0.4	65.5	0.867	0.8678	0.09
0.4	176.6	0.82	0.8216	0.19
0.4	232.2	0.7995	0.798	0.19
0.4	343.3	0.751	0.7514	0.05
0.6	93.3	0.8495	0.8497	0.02
0.6	204.4	0.796	0.7953	0.09
0.6	315.5	0.742	0.7417	0.04
0.6	371.1	0.717	0.7167	0.04
0.8	65.5	0.8595	0.8582	0.15
0.8	121.1	0.828	0.8272	0.1
0.8	260	0.75	0.7509	0.12
0.8	315.5	0.72	0.72049	0.07
0.8	371.1	0.69	0.6898	0.03
1	65.5	0.8525	0.8541	0.19
1	121.1	0.819	0.8173	0.21
1	148.8	0.8005	0.8006	0.01
1	204.4	0.769	0.7684	0.08
1	232.2	0.751	0.7522	0.16
1	315.5	0.7	0.6989	0.16
1	371.1	0.655	0.6572	0.34
Average absolute deviation percent (AADP)				0.10

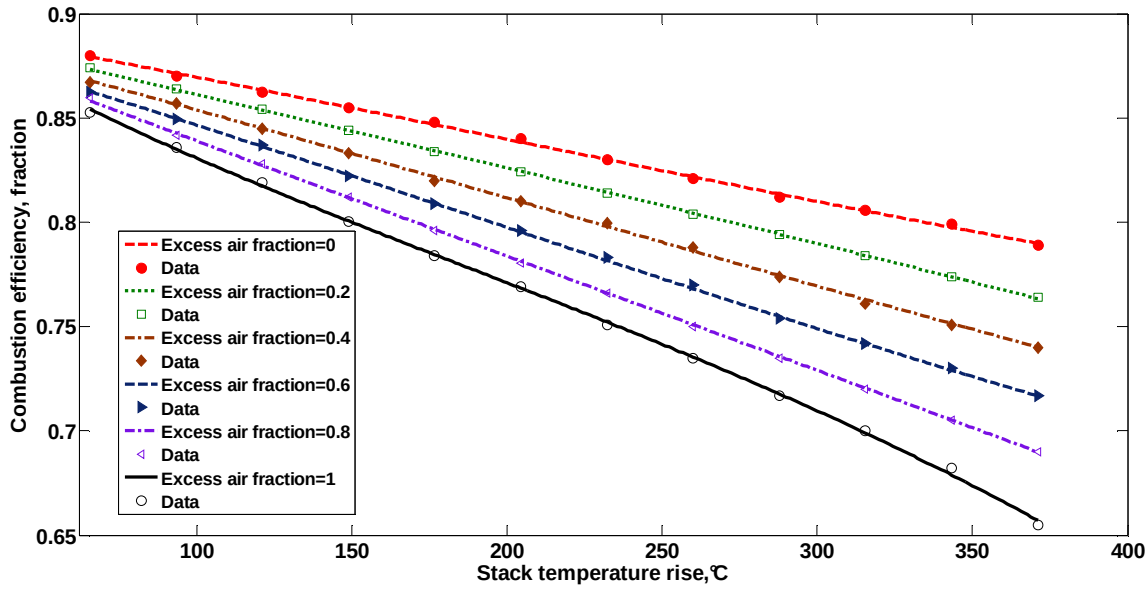

Figure 7.18: Developed predictive tool's performance for estimating the natural gas combustion efficiency as a function of, excess air fraction and stack temperature rise in comparison with data, Bahadori A. and Vuthaluru H. B (2010w) *Fuel Processing Technology,* 91, 1198-1203

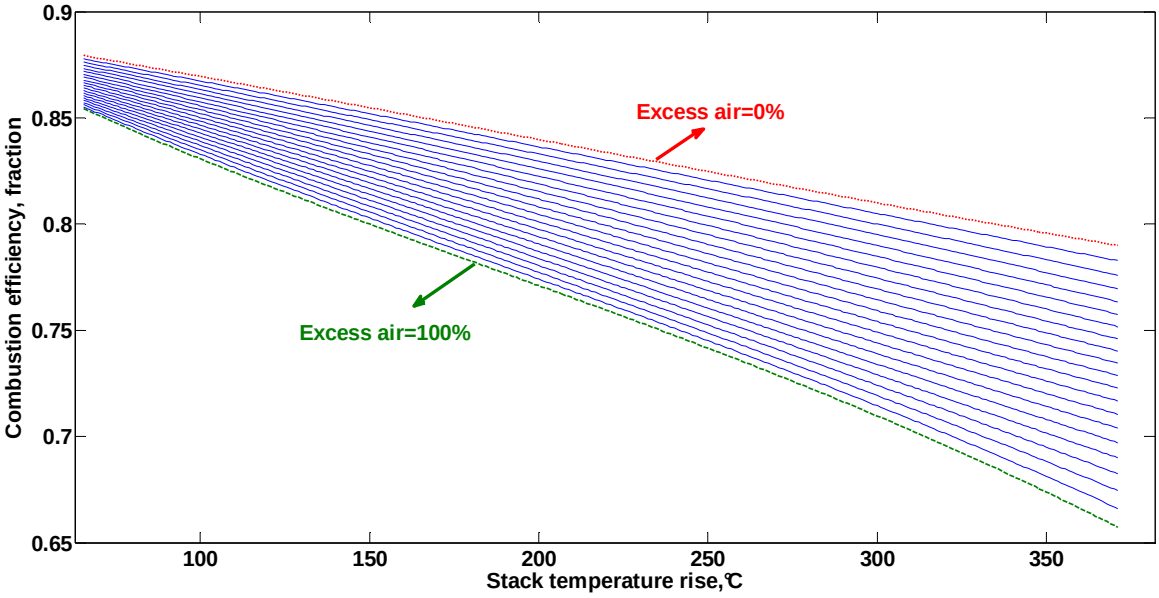

Figure 7.19: Proposed predictive tool's performance for the estimation of natural gas combustion efficiency as a function of, excess air fraction and stack temperature rise, Bahadori A. and Vuthaluru H. B (2010w) *Fuel Processing Technology*. 91, 1198-1203

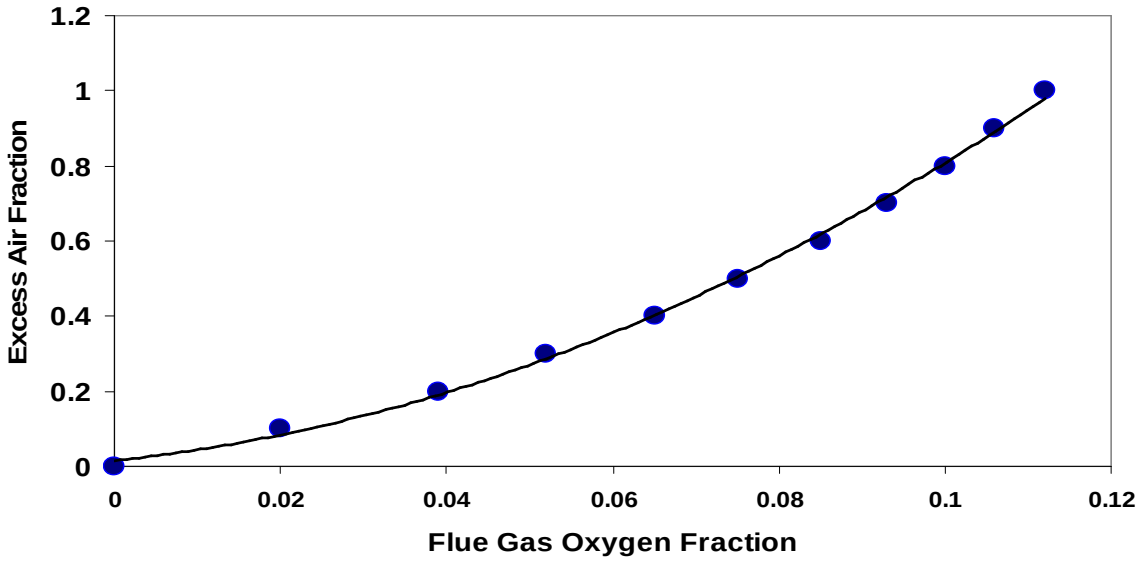

Figure 7.20: Prediction of excess air fraction as a function of flue gas oxygen fraction in comparison with data (Bahadori A. and Vuthaluru H. B (2010w) *Fuel Processing Technology*, 91, 1198-1203.

7.6 Prediction of Salinity of Salty Crude Oil

Production of wet crude due to the raise in oil-water contact in many oil fields has been a growing field problem and it has affected the quality of crudes. In almost all cases, the salt is found dissolved in the water that is dispersed in the crude oil and its separation is not an easy task because desalting is considered as a critical operation due to the importance of meeting the specifications of the acceptable quantities of salt and water in the treated oil. For these reasons, measurements of salt and water content in crude oils are very important in all oil industry operations including crude oil production, processing, and transportation and refining. In this part of thesis, an attempt has been made to formulate a method for accurate and rapid estimation of crude oil salinity as a function of brine quantity that remains in the oil, its salinity (in vol% of sodium chloride concentration) and temperature using an Arrhenius-type asymptotic exponential function and Vandermonde matrix. The proposed method predicts the Salinity of Salty Crude Oil for temperatures up to 373 K and sodium chloride concentrations up to 250,000 ppm (25%

by volume). Estimations from the proposed correlation are found to be in excellent agreement with the reported data in the literature with average absolute deviation being 0.3%. In this part of thesis both Partial least squares (PLS) and Principal Component Analysis (PCA) methods are applied to predict the salt content of crude oil.

7.6.1. Methodology for the development of novel predictive tool

The primary purpose of the present study is to accurately correlate the density of aqueous sodium chloride solution (ρ) data in the temperature range of 0 °C to 100 °C by a simple predictive tool. This is accomplished here by a small modification of the Vogel-Tammann-Fulcher (VTF) equation (Vogel, H. 1921, Tammann, and Hesse, 1926 and Fulcher, 1925). This is important, because such an accurate and mathematically simple correlation of the salt content in crude oil (C_S) as a function of density of remnant water (ρ), concentration of sodium chloride in volume fraction (ψ) and basic and sediments percent (W_R) is required frequently for the engineering calculations to avoid the additional computational burden of complicated density correlations.

7.6.2 Vandermonde matrix

Vandermonde matrix is a matrix with the terms of a geometric progression in each row, i.e., an $m \times n$ matrix (Fulton and Harris, 1991) and α is matrix elements in equation (7.44).

$$V = \begin{bmatrix} 1 & \alpha_1 & \alpha_1^2 & \dots & \alpha_1^{n-1} \\ 1 & \alpha_2 & \alpha_2^2 & \dots & \alpha_2^{n-1} \\ 1 & \alpha_3 & \alpha_3^2 & \dots & \alpha_3^{n-1} \\ \vdots & \vdots & \vdots & \ddots & \vdots \\ 1 & \alpha_m & \alpha_m^2 & \dots & \alpha_m^{n-1} \end{bmatrix} \tag{7.44}$$

Or

$$V_{i,j} = \alpha_i^{j-1} \tag{7.45}$$

for all indices *i* and *j*. The determinant of a square Vandermonde matrix (where *m*=*n*) can be expressed as (Fulton and Harris, 1991):

$$\det(V) = \prod_{1 \le i < j \le n} (\alpha_j - \alpha_i) \tag{7.46}$$

The Vandermonde matrix *evaluates* a polynomial at a set of points; formally, it transforms *coefficients* of a polynomial $a_0 + a_1 x + a_2 x^2 + \ldots + a_{n-1} x^{n-1}$ to the *values* the polynomial takes at the point's α_i. The non-vanishing of the Vandermonde determinant for distinct points α_i shows that, for distinct points, the map from coefficients to values at those points is a one-to-one correspondence, and thus that the polynomial interpolation problem is solvable with unique solution; this result is called the unisolvence theorem (Horn, and Johnson, 1991).

They are thus useful in polynomial interpolation, since solving the system of linear equations $Vu = y$ for u with V an $m \times n$ Vandermonde matrix is equivalent to finding the coefficients u_j of the polynomial(s) (Horn, and Johnson, 1991).

$$P(x) = \sum_{j=0}^{n-1} u_j x^j \tag{7.47}$$

of degree $\le n-1$ which has (have) the property:

$$P(\alpha_i) = y_i \quad \text{for i=1,...,m.} \tag{7.48}$$

The Vandermonde matrix can easily be inverted in terms of Lagrange basis polynomials: each *column* is the coefficients of the Lagrange basis polynomial, with terms in increasing order going down. The resulting solution to the interpolation problem is called the Lagrange polynomial (Horn, and Johnson, 1991).

The VTF equation is an asymptotic exponential function that is given in the following general form (Civan 2007, 2008):

$$\ln f = \ln(f_c) - \frac{E}{R(T - T_C)} \qquad (7.49)$$

In equation 7.49, f is a properly defined temperature-dependent parameter, the units for which are determined individually for a certain property; fc is a pre-exponential coefficient, having the same unit of the property of interest; T and T_c are the actual temperature and the characteristic-limit temperature, respectively (both given in degrees Kelvin); E is referenced as the activation energy of the process causing parameter variation (given in units of J/kmol); and R is the universal gas constant (R) 8.314 J/(kmol K)). Monkos (2003) proposed a least-squares method for unique determination of its parameters fc, E, and Tc. A special case of the Vogel-Tammann-Fulcher (VTF) equation (Vogel, H. 1921, Tammann and Hesse, 1926 and Fulcher, 1925) equation for Tc = 0 is the well-known Arrhenius (1889) equation (Civan 2007, 2008).

For the purpose of present application which involves the temperature-density correlation of liquid water, the VTF equation has been modified in the following form by adding a second-order and third terms term and also Tc

$$\ln f = \ln f_c + \frac{b}{T - T_C} + \frac{c}{(T - T_C)^2} + \frac{d}{(T - T_C)^2} \qquad (7.50)$$

In equation 7.51, T_c has been considered zero to convert equation 7.50 to the well-known Arrhenius equation type. (see equation 7.51)

$$\ln f = \ln f_c + \frac{b}{T} + \frac{c}{T^2} + \frac{d}{T^3} \qquad (7.51)$$

The required data to develop this correlation includes the reported data (Abdel-Aal et al., 2003) for the density of aqueous sodium chloride solution (ρ) as a function of aqueous salt solution concentration (ψ) in volume fraction and temperature (T) in K. Equation 7.52 converts volumetric ppm to volume fraction. The following methodology has been applied to develop this correlation.

Firstly, density of aqueous salt solution is correlated as a function of temperature for several concentrations of aqueous salt solution. Then, the calculated coefficients for these

polynomials are correlated as a function of aqueous salt solution concentration. The derived polynomials are applied to calculate new coefficients for equation (7.53) to predict the density of aqueous salt solution.

In brief, the following steps are repeated to tune the correlation's coefficients (Bahadori and Vuthaluru 2009, 2010).

10. Correlate the density of aqueous salt solution as a function of temperature (T) for a given aqueous salt solution concentration.
11. Repeat step 1 for other aqueous salt solution concentrations.
12. Correlate corresponding polynomial coefficients, which were obtained for different temperature versus aqueous salt solution concentrations, a = f (T), b = f (T), c = f (T), d = f (T) [see equations (7.54)-(7.57)].

Equation 7.53 represents the proposed governing equation in which four coefficients are used to correlate the density of aqueous salt solution as a function of temperature and aqueous salt solution concentration.

$$\psi = \frac{S}{10^6} \tag{7.52}$$

$$\ln(\rho) = a + \frac{b}{T} + \frac{c}{T^2} + \frac{d}{T^3} \tag{7.53}$$

Where:

$$\mathrm{a} = A_1 + \frac{B_1}{\psi} + \frac{C_1}{\psi^2} + \frac{D_1}{\psi^3} \tag{7.54}$$

$$\mathrm{b} = \mathrm{A}_2 + \frac{B_2}{\psi} + \frac{C_2}{\psi^2} + \frac{D_2}{\psi^3} \tag{7.55}$$

$$\mathrm{c} = \mathrm{A}_3 + \frac{B_3}{\psi} + \frac{C_3}{\psi^2} + \frac{D_3}{\psi^3} \tag{7.56}$$

$$\mathrm{d} = A_4 + \frac{B_4}{\psi} + \frac{C_4}{\psi^2} + \frac{D_4}{\psi^3} \tag{7.57}$$

These optimum tuned coefficients help to cover the density of aqueous salty solution for temperatures up to 373.15 K (100°C) as well as aqueous salt solution concentrations up to 0.25 volume fraction.

Equation 7.58 predicts salt content in crude oil (C_S) as a function of density of remnant water (ρ), concentration of sodium chloride in volume fraction (ψ) and basic and sediments percent (W_R).

$$C_s = 997.1698\rho\left(\frac{1000W_R}{100-W_R}\right)\left(\frac{S}{10^6}\right) \qquad (7.58)$$

To date, there is no correlation exists in the literature for rapid estimation of density of aqueous salty solutions. Given this status, our efforts directed at formulating a predictive tool can assist engineers for rapid prediction of density of aqueous salty solution as a function of aqueous salt solution concentration (ψ) and temperature. The proposed novel tool in the present work is simple and unique expression which is non-existent in the literature. Furthermore, we have selected exponential function to develop the tool which is well-behaved (i.e. smooth and non-oscillatory) equations enabling fast and more accurate predictions.

Table 7.11. Comparison of predicted results with the reported data (Abdel-Aal et al., 2003)

T, °C	Sodium chloride concentration. (Volume Percent)	Reported density of aqueous sodium chloride solution g/cm^3	Calculated density of sodium chloride solution g/cm^3	Percent absolute deviation
0	1	1.00747	1.007505	0.0035
0	12	1.09244	1.088417	0.368
10	2	1.01442	1.0147927	0.0367
10	16	1.12056	1.12412	0.318
25	4	1.0253	1.0228192	0.242
25	20	1.14533	1.15239	0.616
40	8	1.04798	1.053893	0.564
40	24	1.16971	1.17766	0.679
60	12	1.0667	1.062858	0.36
60	26	1.1747	1.18046	0.4903
80	1	0.9785	0.978384	0.012
80	16	1.0842	1.08661	0.222
100	2	0.9719	0.9724218	0537
100	20	1.1017	1.1013217	0.0343
Average Absolute Deviation Percent (AADP)				0.3202%

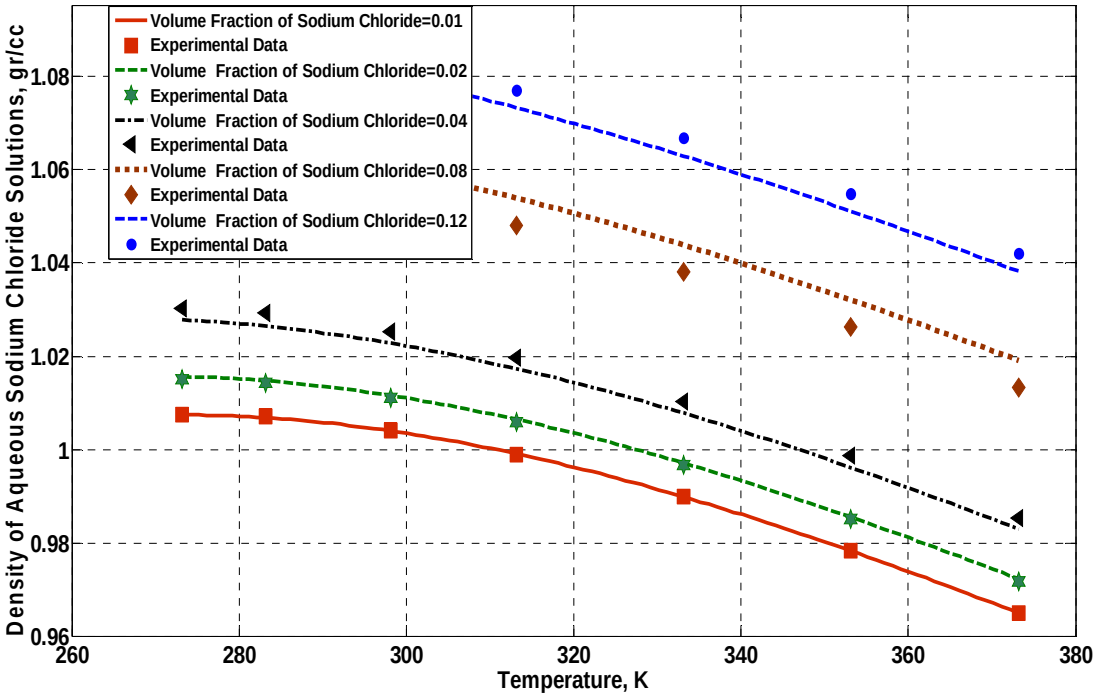

Figure 7.21. Comparison of predicted density of aqueous sodium chloride solutions (less than 0.12 volume fraction of sodium chloride) against literature reported data (Abdel-Aal et al., 2003).

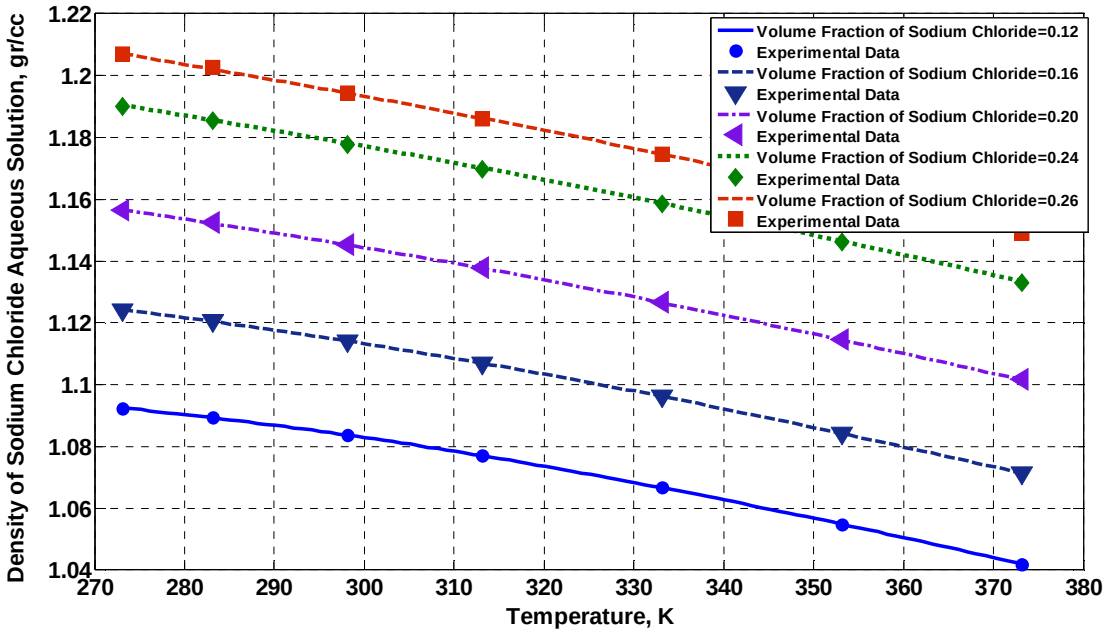

Figure 7.22. Comparison of predicted density of aqueous sodium chloride solutions (more than 0.12 volume fraction of sodium chloride) against literature reported data (Abdel-Aal et al., 2003)

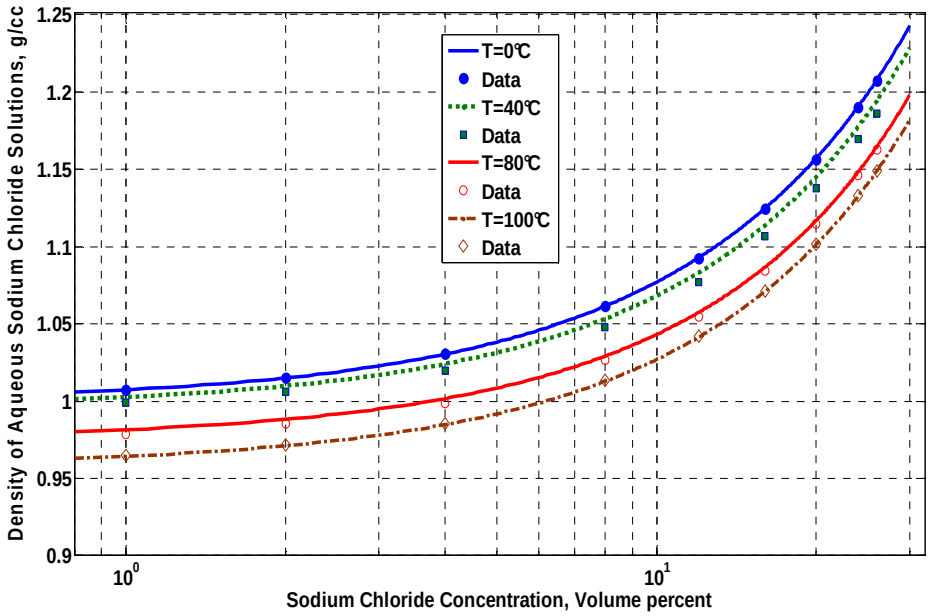

Figure 7.23. Comparison of predicted density of aqueous sodium chloride solutions against literature reported data (Abdel-Aal et al., 2003)

7.6.3 Principal component analysis (PCA)

The principal component analysis (PCA) is a multivariate statistical method that selects a small number of components to account for the variance of original multi-response. The technique procedure is described as follows (Horn, and Johnson, 1991):

1. The original multi-response array:

$$x_i(j), \quad i = 1, 2, \ldots, m; \quad j = 1, 2, \ldots, n \tag{7.59}$$

$$X = \begin{bmatrix} x_1(1) & x_1(2) & \cdots & \cdots & x_1(n) \\ x_2(1) & x_2(2) & \cdots & \cdots & x_2(n) \\ \vdots & \vdots & \cdots & \cdots & \vdots \\ \vdots & \vdots & \cdots & \cdots & \vdots \\ x_m(1) & x_m(2) & \cdots & \cdots & x_m(n) \end{bmatrix} \tag{7.60}$$

where *m* is the number of test trial and *n* is the number of the response.

2. Normalizing the response

The response is normalized using the following formula to get rid of the difference between units.

$$x_i^*(j) = \frac{x_i(j) - x_i(j)^-}{x_i(j)^+ - x_i(j)^-} \tag{7.61}$$

$$X^* = \begin{bmatrix} x_1^*(1) & x_1^*(2) & \cdots & \cdots & x_1^*(n) \\ x_2^*(1) & x_2^*(2) & \cdots & \cdots & x_2^*(n) \\ \vdots & \vdots & \cdots & \cdots & \vdots \\ \vdots & \vdots & \cdots & \cdots & \vdots \\ x_m^*(1) & x_m^*(2) & \cdots & \cdots & x_m^*(n) \end{bmatrix} \tag{7.62}$$

Where *xi** (*j*) is the normalized response, *x*i (*j*) +is the maximum of *x*i (*j*), and *x*i (*j*)− is the minimum of *x*i(*j*).

3. Correlation coefficient array The correlation coefficient array of the normalized response array is evaluated as follows (Horn, and Johnson, 1991):

$$R_{jl} = \left(\frac{\mathrm{Cov}(x_i^*(j), x_i^*(l))}{\sigma_{x_i^*(j)} \times \sigma_{x_i^*(l)}} \right), \tag{7.63}$$

$$j = 1, 2, \ldots, n; \quad l = 1, 2, \ldots, n \tag{7.64}$$

where Cov(*x*i* (*j*), *x*i* (*l*)): The covariance of sequences *x*i* (*j*) and *xi* (*l*); *σx* i* (*l*): The standard deviation of sequence *x i* (*l*) (Horn, and Johnson, 1991).

4. Determining the eigenvalues and eigenvectors. The eigenvalues and eigenvectors are determined from the correlation coefficient array,

$$(R - \lambda_k I_m) V_{ik} = 0 \tag{7.65}$$

$$\text{where } \lambda_k\text{: eigenvalues, } \sum_{k=1}^{n} \lambda_k = n, \quad k = 1, 2, \ldots, n; \tag{7.66}$$

$V_{ik} = [a_{k1} a_{k2} \ldots a_{kn}]^T$ eigenvectors corresponding to the eigenvalue λk.

5. Evaluating the principal components. We have the following uncorrelated principal components:

$$Y_{mk} = \sum_{i=1}^{n} X_m^*(i) \cdot V_{ik} \tag{7.67}$$

The principal components are created in order of decreasing variance, and therefore the first principal component, *Ym*1, accounts for most variance in the data. In fact the components with an eigenvalue greater than one are chosen to replace the original responses for further analysis.

6. Evaluating the coefficient of determination(Chin, 1998; Fornell and Bookstein, 1982).

$$C_k = \frac{\lambda_k}{n}, \quad k = 1, 2, \ldots, n \tag{7.68}$$

The coefficient of determination, *Ck*, represents the weight of the principle component, *Ymk in equation 7.67*(Chin, 1998; Fornell and Bookstein, 1982)..

The PCA method was integrated in this study to deal with multi-response problems. First, the multiresponse array, in which the elements were the water saline density of each response, was normalized using Equations (7.61 and 7.62). The results are listed in Table 7.12. Then, the correlation coefficient matrix was evaluated from the normalized response array. Table 7.13 lists the eigenvalues, which were determined using Equations (7.63-7.67). There are two of four eigenvalues larger than one. The eigenvector that corresponded to the largest eigenvalue 1.712 was [−0.62, −0.87, 0.56, 1.00]. The other eigenvectors were [0.79, 0.66, 1.00, 0.51], [1.00, −0.64, −0.57, 0.38], and [−0.32, 0.85, −0.82, 1.00], that corresponded to the eigenvalues 1.412, 0.615, and 0.215, respectively. The four elements of the eigenvector are the weights of the four responses.

The first principal component was the sum of the products of the water saline densities of four responses multiplied by the elements of the eigenvector, which corresponded to the largest eigenvalue. The other principal components were obtained in the same way. The results are all listed in Tables 7.12 and 713.

.

Table 7.12. The principal components of four quality responses

Data number	Normalized Multi-response Array				Principal component			
	Density, g/cm^3	Density (PCA), g/cm^3	ψ	ψ (PCA)	First	Second	Third	Fourth
1	1.00747	1.006	1	1.00747	-0.568	1.652	0.241	1.195
2	1.09244	1.0892	12	11.09244	-0.384	1.968	0.611	0.812
3	1.01442	1.0134	2	1.91442	-0.220	0.455	-0.243	0.665
4	1.12056	1.1102	16	15.12056	0.453	1.564	0.012	0.612
5	1.0253	1.0125	4	3.0253	-1.188	1.402	0.452	0.282
6	1.14533	1.1225	20	19.14533	0.653	1.035	0.152	0.732
7	1.04798	1.0358	8	7.04798	-0.432	1.665	0.542	0.925
8	1.16971	1.1524	24	23.16971	0.469	1.032	1.001	0.611
9	1.00747	1.0068	12	11.0667	-1.345	1.452	0.158	0.511

Table 7.13 Eigenvalues for the principal components

Principal	Eigenvalue
First	1.712
Second	1.412
Third	0.615
Fourth	0.215

In previous published studies (Chin, 1998; Fornell and Bookstein, 1982) only the first principal component has been chosen to represent the original responses since one eigenvalue has been larger than one.

However, this is no longer relevant to the majority of cases in today's complex crude oil processing. In this study, two of four eigenvalues were greater than one. Thus, comparing different optimal process factor/level combinations, as determined by extracting different number of principal components, is a major concern. To integrate more than one principal component to a comprehensive index, another approach based on the coefficient of determination was used.

Since the coefficient of determination represents the weight of the principle component, the comprehensive index was obtained from the sum of the products of the principle component multiplied by the coefficient of determination(Chin, 1998; Fornell and Bookstein, 1982). The results are listed in Table 7.14.

Table 7.14 The comprehensive index that obtained by extracting different number of principal components

Data number	Comprehensive index		
	First principal component	First + second principal components	Fourth principal components
1	-0.582	0.335	0.439
2	-0.385	0.532	0.679
3	-0.221	0.069	0.068
4	0.464	1.119	1.152
5	-1.195	-0.011	0.077
6	0.659	0.650	0.0716
7	-0432	0.415	0.545
8	0.525	0.571	0.761
9	-1.365	-0.068	-0.013

In addition, the contribution of each factor to salt of content of crude oil can be evaluated using the analysis of variance (ANOVA). Four salty crude oil properties, i.e. water cut percent and saline water density in different temperatures and salt volume fractions, were separately selected to be

the target quality in this study (A-D factors). In addition, the contribution of each factor to the crude oil salt content can be evaluated using the analysis of variance (ANOVA).

A minimum standard salt content of crude oil is normally required in most industry cases. Therefore, the smaller and better methodology of salt content calculation was employed for the calculation of crude oil salt content. The various properties of the several data are listed in Table 7.15. The response table of saline water density of the water cut percent coefficient was calculated, as shown in Table 7.15. The saline water density of factors A–D is maximum at A1, B3, C1 and D3, respectively. As a result, the factor/level combination A1 B3 C1 D3 was recommended. The results of ANOVA for the saline water density are also shown in Table 7.15. It can be seen that the contribution of saline water density to the salt content of crude oil was the largest.

The temperature (factor B) was an important factor to the salt content of crude oil as well. In such a case, an engineering judgment that refers to past experience is the only real guarantee of correct decision making in the crude oil salt content calculations.

Table 7.15. The response table and ANOVA crude oil salt content calculations

Factor	Levels			Degree of freedom	Sum of square	Mean square	F value	Contribution
	1	2	3					
A	1265.2 (1.162)	1255.2 (0.916)	1215.2 (0.206)	2	2.452	2.225	1.002	0.02
B	1227.5 (0.211)	1193.1 (0.412)	1319.1 (1.018)	2	2.543	3.265	5.577	41.4
C	1276.2 (0.68)	1204.2 (0.345)	1257.1 (1.225)	2	3.865	2.412	1.898	8
D	1245.2 (0.352)	1255.5 (0.935)	1280.2 (1.031)	2	2.895	2.442	1.977	8.7
Total				8	5.023	-	-	-
Error				2	2.452	2.225	-	-

Note: Values enclosed in parentheses represent standard deviation.

7.6.4 Partial least squares regression modelling

Partial least squares (PLS) regression, a multivariate calibration technique aims to find the relationship between a set of predictor (independent) data, X (m×n), and a set of responses (dependent), Y (m×l). Here, n and l are the independent and dependent variables, respectively, and m is the observation vectors. However, it differs from the multiple linear regression technique (MLR) mainly that PLS is able to give stable predictions even when X contains highly correlated variables. Both the linear and non-linear PLS regression methods were applied here.

Detailed description of PLS method and its algorithms could be found elsewhere (Kaspar and Ray, 1993 and Kourti, 2002). however, in brief, it can be expressed as a
bilinear decomposition of both X and Y as (Shaw, 2003);

$$X = \boldsymbol{TW}^T + E_X \tag{7.69}$$

$$Y = \boldsymbol{UQ}^T + E_Y \tag{7.70}$$

such that the scores in X and the scores of the yet unexplained part of Y have maximum covariance. Here, T and W, and U and Q are X and Y PLS scores and loadings (weights) vectors, respectively; EX and EY are the X and Y residuals, respectively. The decomposition models of X and Y and the expression relating these models through regression constitute the linear PLS regression model.

In case of one Y-variable, y, the model (PLS1) can be expressed as a regression equation (y=Xb+E), where b is the regression coefficient (Shaw, 2003). The PLS model performed in two stages, uses a set of calibration (training) samples to construct the model, which is employed to compute a set of regression coefficients (bPLS).

These coefficients are then used to make prediction of the dependent variable (ynew) in new (test) experimental set as;

$$y_{\text{new}} = X_{\text{new}} \cdot \boldsymbol{b}_{\text{PLS}} + E \tag{7.71}$$

Here, the bPLS vector is derived from the model parameters. Here, we have used the linear PLS1 model to analyse our data set (Kaspar and Ray, 1993 and Kourti, 2002).

Consider a data set representing the "normal" operating conditions of a process. The objective of linear PLS is to project the data down onto a number of latent variables, say tj and uj (j=1,. . ., A), where A is the number of the latent variables, and then to develop a regression model between tj and uj:

$$\mathbf{u}_j = b_j \mathbf{t}_j + \mathbf{e}_j \qquad j = 1, \ldots, A \tag{7.72}$$

Where ej is a vector of errors and bj is an unknown parameter estimated by b j. The latent variables are computed by tj =Xjwj and uj =Yjqj, where both wj and qj have unit length and are determined by maximizing the covariance between tj and uj. Letting uj=bjtj be the prediction of uj, the matrices X and Y can be decomposed as the sum of the following outer products:

$$\mathbf{X} = \sum_{j=1}^{A} \mathbf{t}_j \mathbf{p}_j^{\mathrm{T}} + \mathbf{E} \text{ and } \mathbf{Y} = \sum_{j=1}^{A} \hat{\mathbf{u}}_j \mathbf{q}_j^{\mathrm{T}} + \mathbf{F} \qquad (7.73)$$

Where E and F are the residuals of X and Y after extracting the first A pairs of latent variables. In PLS regression, each pair of latent variables, tj and uj (j=1,.... A) is sequentially extracted through an iterative procedure (Kaspar and Ray, 1993 and Kourti, 2002).

The only issue remaining to be addressed is how to determine the number of latent variables, A.

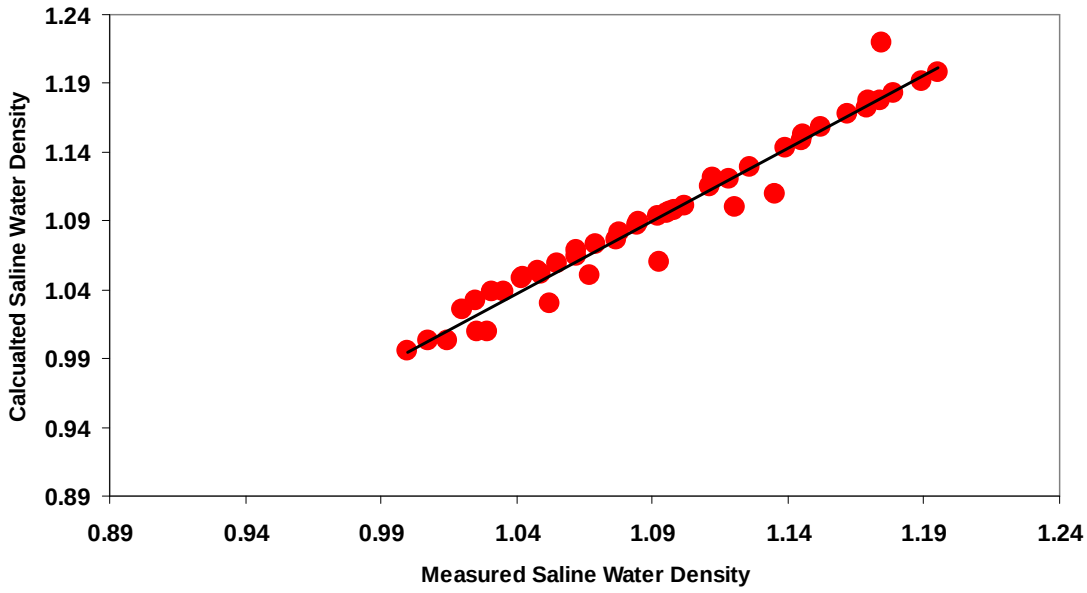

Figure 7.24 Measured values versus calculated values for saline water density

Figure 7.24 shows measured versus calculated values for saline water density calculations using PLS. Further, the residuals versus Ymodel (model predicted values of the salt content of ctude oil and density of saline water) plots (calibration and prediction sets) for the linear PLS1 are shown in Figures 7.25 and 7.26 Residuals versus Ymodel plots can be more informative regarding model fitting to a data set. If the residuals appear to behave randomly (low correlation), it suggests that the model fits the data well. On the other hand, if non-random distribution is evident in the residuals, the model does not fit the data adequately.

Figures 7.25 and 7.26show random pattern in distribution of the residuals with a very low correlation (R2**) between the Ymodel and residual values (hence, suggests that the PLS1 model fits appropriately to all the data points).

Although, in terms of various model performance criteria parameters considered here, the linear PLS1 model fitted well to the experimental data set and yielded satisfactory results suggesting for its suitability for predicting the salt content of crude oil taking all the four different process

variables in to consideration simultaneously, since, it is a bilinear method and the salty crude oil variables may have some degree of nonlinear relationships, we attempted to treat the salty crude oil data set using the non-linear modeling approaches and make a comparative study. Figure 7.28 shows the range of saline water densitY which has been considered in this study as a function of temperature for PLS analysis to predict crude oil salt content.

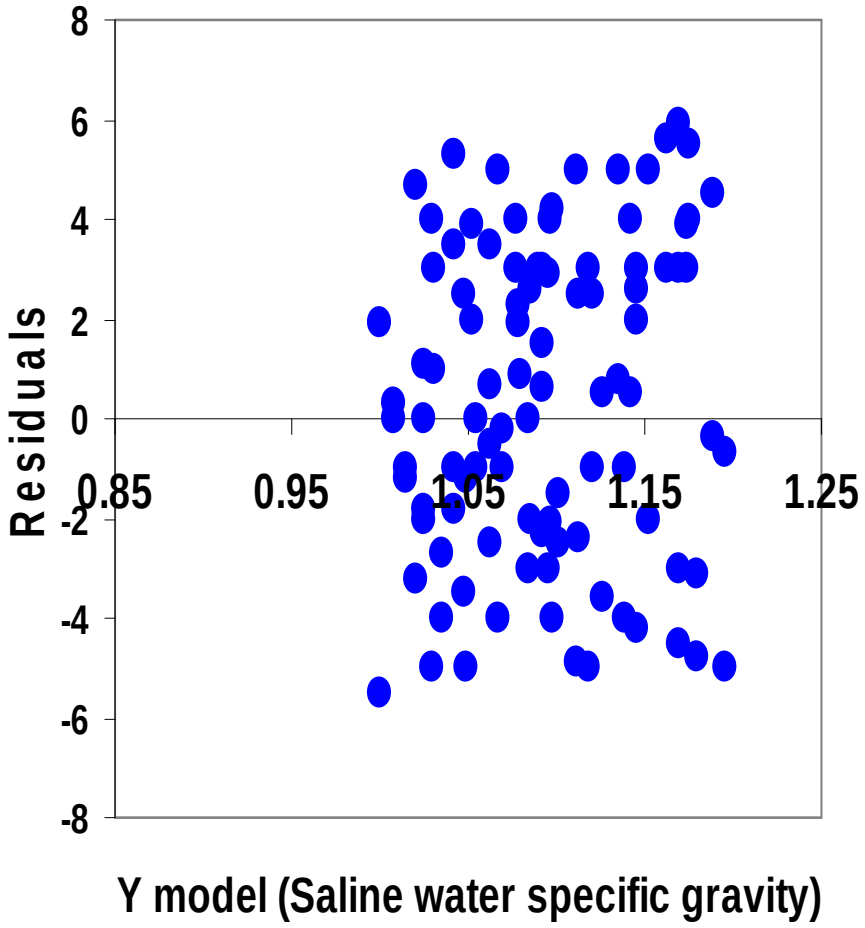

Figure 7.25: Residuals results for saline water specific gravity calculations

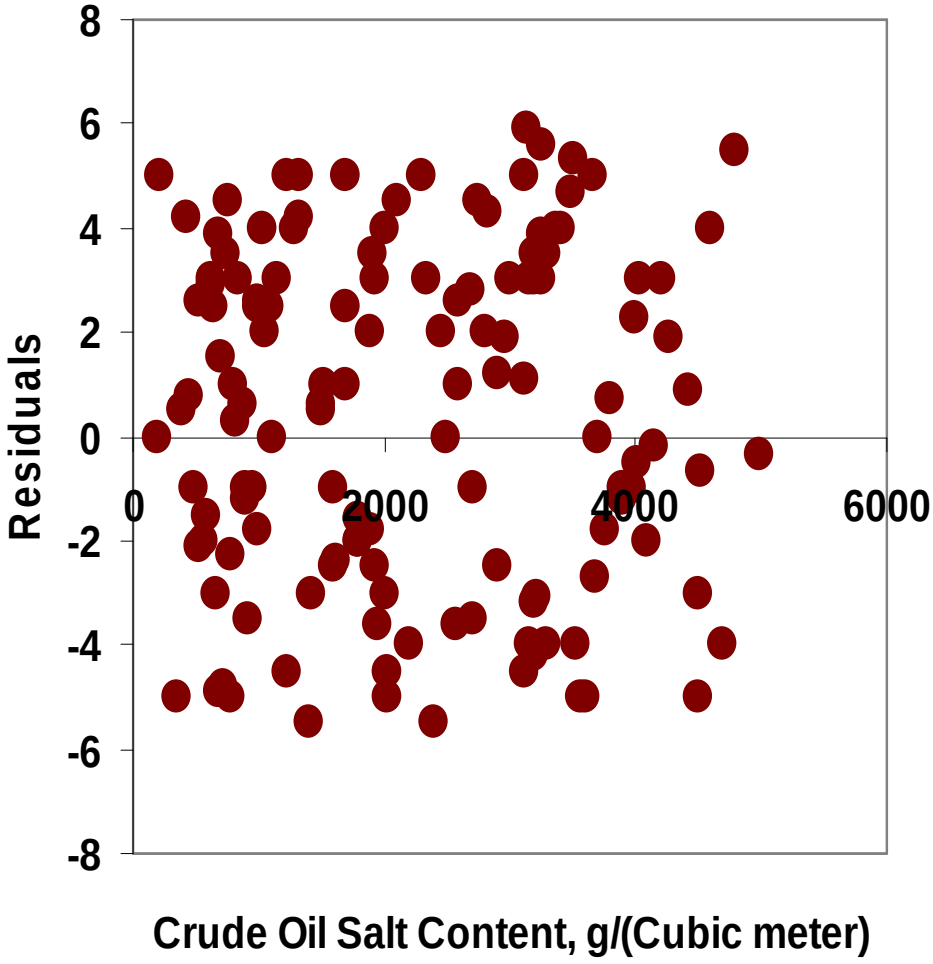

Figure 7.26: Residuals results for crude oil salt content calculations

7.6.5. Conclusion

In this case studies three different methods have been evaluated to predict density of saline water and salt content of crude oil. Figure 7.28 shows the new developed predictive tool has less deviation than partial least squares (PLS) and principal component analysis (PCA) in terms of accuracy where the average errors percent for new method, PLS and PCA are 0.4%, 1.5% and 2% respectively.

Figure 7.29 clearly shows the proposed method has better performance in predicting saline water density in comparison with PCA and PLS methods. The great advantage of the new proposed methodology and PreTOG software in compare with PLS and PCA, is that there is no need to have any iterations or loops in calculations. Therefore PreTOG software converges quickly and provides the results with minimum computation time.

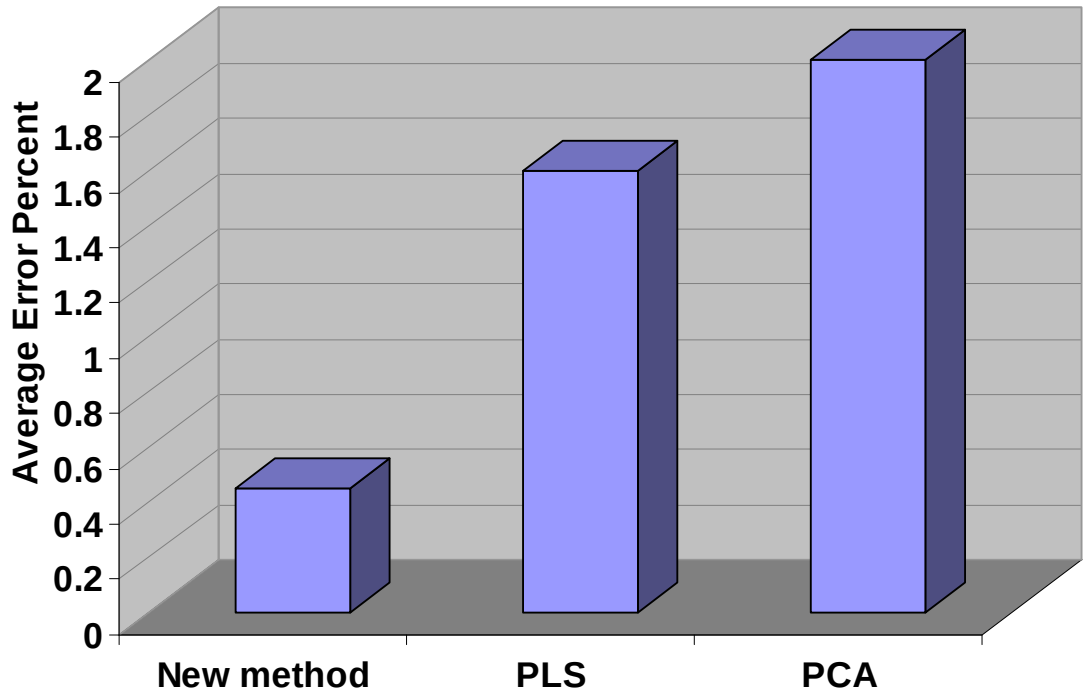

Figure 7.27 Accuracy of different methods to predict the salt content of crude oil

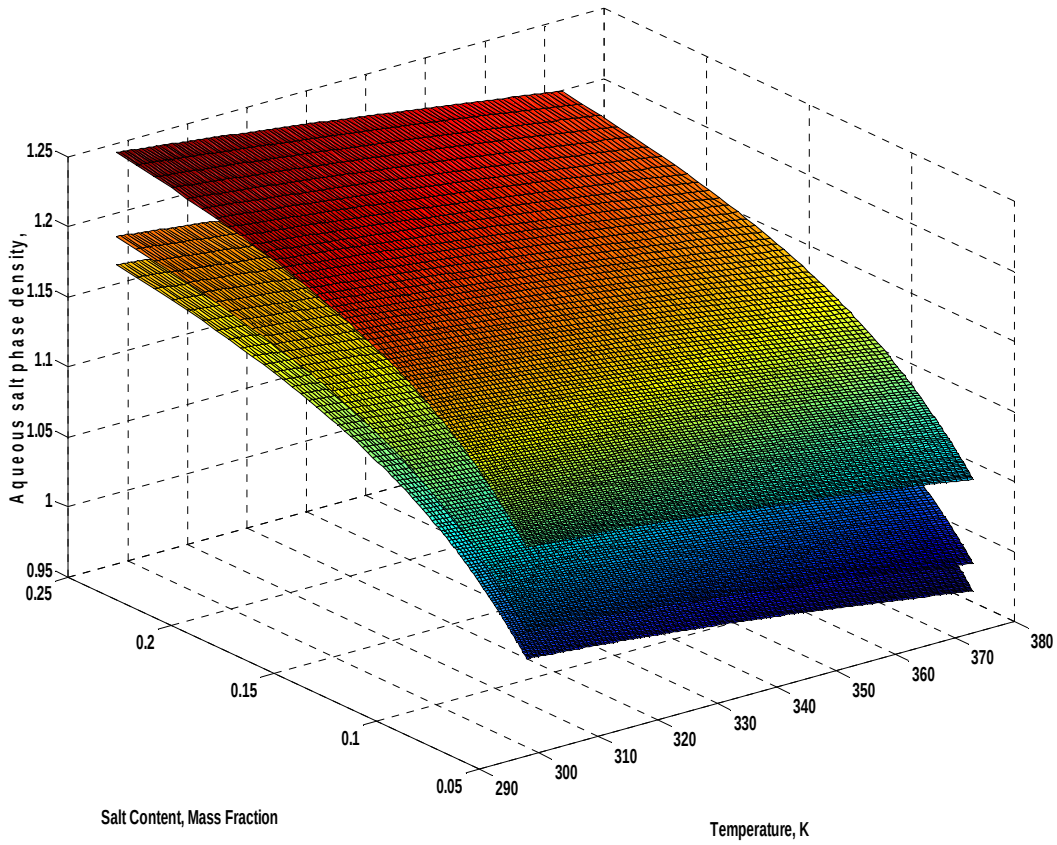

Figure 7.28: Different models results for prediction of the density of saline water

CHAPTER 8

Conclusion and Recommendations

The aim of this dissertation was the development of novel and easy-to-use methods to minimize the complex and time-consuming calculation steps for selected process engineering parameters. Most simulations require simultaneous iterative solutions of many nonlinear and highly coupled sets of equations, and it is because that a mathematically compact, simple and reasonably accurate equations, as proposed in this thesis, would be preferable to current computationally intensive simulations. In fact, the development of engineering correlations by a modification to the well-known (Vogel, 1921; Tammann and Hesse, 1926; Fulcher, 1925) equation was the primary motivation of this research, which nevertheless, yielded predictive tools with accuracy comparable to that of the existing rigorous simulations. Following the development of predictive tools, experimental works were undertaken to measure the density and viscosity, of ethylene glycol and water, diethylene glycol and water, and triethylene glycol and water mixtures at temperatures ranging from 290 K to 440 K and concentrations ranging from 20 mol % glycol to 100 mol % glycol. The data were correlated using a novel Arrhenius-type equation based predictive tool and a thermodynamical method (the generalized corresponding states principle (GCSP)).

This chapter summarizes the main findings made during this research as well as concludes with recommendations for future work to further apply the developed concept for creation of predictive tools for other process engineering parameters:

- The first part of this thesis addressed the current status of research in this field such as introduction to oil and gas industries, parameters of interest to oil and gas engineers, current remedial practices and existing gaps, possible improvement options, experimental and thermodynamical modeling for validation.

- The other part of this dissertation work introduced the formulation of simple-to-use approach for development of predictive tools, parameter prediction, formulation of generic algorithm, selection of appropriate variables for developing the predictive tools and the Generalized Corresponding States Principle (GCSP), thermodynamical model applications for prediction of density and viscosity of aqueous glycol solutions.

- The next section of this dissertation work covered the measurement of density and viscosity of aqueous glycol solutions in a wide temperature range for validation of proposed predictive tool and the modeling the results using the Generalized Corresponding States Principle (GCSP) thermodynamical model.

- The following section of this thesis addressed the development of several predictive tools for various oil and gas processing, parameters, testing and validation for many engineering applications. Currently several models are available to predict various design parameters in the oil and gas processing industries. However, the calculations may require rigorous computer solutions for some particular applications. Therefore, developing novel easy-to-use methods to minimize the complex and time-consuming calculation steps were an essential requirement. The selected predictive tools have been developed and published in several refereed international journals during my candidacy.

- The next part of thesis presents the development of the predictive tools, testing and validation for other typical process engineering parameters (apart the oil and gas area). All developed predictive tools have been peer-reviewed and published in several refereed international journals during my PhD candidacy. The thesis discusses the formulation of such predictive tools in a systematic manner to show the simplicity of the model and usefulness of predictive tools.

- In the next section of the thesis some typical case studies have been presented for the overall summary and potential benefits to oil and gas processing industries using the typical developed predictive tools. These classic case studies showed how the information evolving out of the developed predictive tools can be used to understand and predict the various oil, gas and process engineering.

- The final part of this dissertation will provide conclusions and some recommendations for the future works.

8.1 Recommendations for future works

Clearly, the possible applications for this method are very diverse and require accurate and reliable data for the model to be generated. Many of the produced works have found usage internationally from industries that have not had convenient, accurate and simple techniques to determine key process quantities. However, the primary reason why such predictive tools are so valuable is the ease of use relative to other methods available.

Sometimes conventional methods typically are not easy-to-use for the purposes of practical importance with most simulations requiring iterative solutions of non-linear equations. Other situations may require experimental trials, expensive operational testing, or other time consuming and economically straining methods. For this reason, predictive models are a very promising tool becoming increasingly widespread in the literature and industry.

Some recommendations to further improve this methodology are given below:

- Currently, there is little data available on some engineering parameters. For example for prediction of transport properties of carbon dioxide. My effort is concerned at present with pure CO_2 whereas it is likely that real CO_2 pipeline systems will be transporting CO_2 along with small amounts of incondensable impurities such as nitrogen, argon and oxygen. At present there is limited data available on physical properties of such mixtures although these mixtures will be predicted by commercial physical property routines. It would be useful in the future work to test this correlation method for such mixtures.

- In part of this dissertation work, a simple predictive tool was developed for the prediction of transport properties (namely thermal conductivity and viscosity) of compressed air at elevated pressures and high temperatures using a novel and simple-to-use Arrhenius-type asymptotic exponential function. The proposed correlation predicts the transport properties (namely thermal conductivity and viscosity) of compressed air for temperature range between 260 and 1000 K, and pressures up to 1000 bar. It would be useful in the follow-up studies to test this correlation method for humidified air at elevated pressures and high temperatures in the future.

- In another section of this research, an attempt has been made to formulate a novel and simple-to-use method which is easier than existing approaches, less complicated and with fewer computations for one-dimensional heat flow with variable surface temperature in

slabs and spheres as a function of Fourier number and Biot number in order to arrive at the temperature distribution in the solid and the average solid temperature change with time. The work was concerned at present with one-dimensional heat flow with variable surface temperature in slabs and spheres. It would be useful to extend to two- and three-dimensional configurations in future studies.

- The proposed method in this research is superior due to its accuracy and clear numerical background based on Vandermonde matrix, wherein the relevant coefficients can be retuned quickly if more data are available. Therefore, it would be useful to keep the developed predictive tool updated by readjusting the tuned coefficients or development of new predictive tools using this methodology.

- Determining various process parameters with the model is an extremely straight-forward process requiring little computational time. The accomplishment of this goal should make it sufficiently simple for engineers to use without extensive calculation time requiring anything more than a simple calculator. In conclusion then, a final comment may be made that the research outcome was a success, yielding a highly accurate and intuitive mathematical tool able to calculate many oil, gas and process engineering parameters for wide range of conditions. These recommendations, particularly the testing of other more data sources, would be highly valuable to further validation of method. As the accuracy of the model has already proven, all that is required to improve the potential for industry-wide use is for a greater scope of works to be modelled for, as well as development of a 'backward' calculation tool which would be the next logical step for improving this model.

References

Abdel-Aala, H. K. Aggour M. and Fahim M. A., (2003) Petroleum and gas field processing, Marcel Dekker, N.Y., USA.

Ahmed, T.,(2007) "Hydrocarbon phase behavior", Gulf Publishing Company, Austin, TX, USA.

Ameripour S. and Barrufet, M. A. (2009), Improved correlations predict hydrate formation pressures or temperatures with or without inhibitors, *Journal of Canadian Petroleum Technology*, 78 (5) pp. 45-50.

Andrews, M.J. and Master, B.I., (2005) Three-dimensional modelling of a helixchanger heat exchanger using CFD, *Heat Transfer Engineering*, 26(6), pp. 22–31.

Arnold, K., and Stewart, M., (1999) "Surface production operations, Vol. 1: Design of Gas-Handling Systems and Facilities", 2nd Edition, Gulf Professional Publishing, Houston, TX, USA.

Arora, V. Jha, U., Bandhopadhyay P. and Kumar, S.,(2006) An investigation of the relationship between raw coal characteristics and effluent quality of Kedla and Rajrappa Washeries, Jharkhand, India, *Journal of Environmental Management*, 26, pp.392-404.

Arrhenius, S. (1889) Uber die reactions ges chwindigkeit der inversion von rohrzucker durch saeuren. *Z. Phys. Chem*., 4, pp. 226-248.

Ascott, E. (2006) Benefit cost analysis of wonder world drive overpass in san marcos, Texas. Applied Research, Project. Texas State University, USA.

Assael, M.J., Trusler, J.P.M., and Tsolakis, T.F., Imperial College Press, London, UK (1996).

Bahadori, A (2011a) Prediction of compressed air transport properties at elevated pressures and high temperatures using simple method, *Applied Energy*, in press, doi.org/10.1016/j.apenergy.2010.10.029

Bahadori, A (2011b) Prediction of saturated air dew point at elevated pressures using simple Arrhenius-type function, *Chemical Engineering & Technology*, in press, doi: ceat.200900521.

Bahadori A. (2011C) A simple method for the estimation of performance characteristics of cooling towers, accepted for publication in *Journal of the Energy Institute.*

Bahadori, A. (2009a) Minimize vaporization and displacement losses from storage containers" *Hydrocarbon Processing*, 88(6) pp.83-84.

Bahadori, A. (2009b) Estimation of hydrate inhibitor loss in hydrocarbon liquid phase, *Petroleum Science & Technology* (27) pp. 943–951.

Bahadori A. (2009c), Predicting storage pressure of gasoline in uninsulated tanks, *Journal of the Energy Institute.* 82(1), p. 61.

Bahadori A., (2009d), Estimating water-adsorption isotherms, *Hydrocarbon Processing*, 88(1) pp. 55-56.

Bahadori, A. (2008a) Correlation accurately predicts hydrate forming pressure of pure components, *Journal of Canadian Petroleum Technology***,** 47 (2) pp.13-16.

Bahadori A. (2008b) New correlation accurately predicts thermal conductivity of liquid paraffin hydrocarbons, *Journal of the Energy Institute* 81(1) pp. 59-61.

Bahadori, A. (2007a) Model accurately predicts HC solubility in methanol, *Oil & Gas Journal* 105 (33) pp. 40-42.

Bahadori, A. (2007b) New numerical model for light alkanes solubility in triethylene glycol, *Korean Journal of Chemical Engineering*, 24 (3), pp.418-425.

Bahadori, A. (2007c) A numerical approach for multicomponent vapor solid equilibrium calculations in gas hydrate formation, *Journal of Natural Gas Chemistry* 16 (1) pp. 16-21.

Bahadori, A. (2007d) New model predicts solubility in glycols, *Oil & Gas Journal* 105 (8) pp. 50-55.

Bahadori A. and Mokhatab S.(2007a) Predicting the true vapour pressure of LPG and natural gasoline", *Hydrocarbon Processing*, 86 (10) pp. 123-124.

Bahadori A. and Mokhatab S. (2008a) Predicting water content of compressed air, *Chemical Engineering*, 115, (9), pp. 56-57.

Bahadori A. and Mokhatab S. (2008b) Estimating thermal conductivity of hydrocarbons, *Chemical Engineering*, 115, (13), pp. 52-54.

Bahadori A. and Mokhatab S. (2009a) Simple methodology predicts optimum pressures of multistage separators, *Petroleum Science & Technology* 27 (03) pp. 315-324.

Bahadori A. and Mokhatab S. (2009b) Correlation rapidly estimates pure hydrocarbons' surface tension, *Journal of the Energy Institute* 82 (2), pp.118-119.

Bahadori A. and Vuthaluru H. B. (2008a), Simplified method for calculating hydrocarbons solubilities in hydrate inhibitors, *Chemical Engineering and Technology* 31 (9), pp. 1369-1375**.**

Bahadori A. and Vuthaluru H. B. (2009a) Rapid estimation of equilibrium water dew Point of natural gas in TEG dehydration systems, *Journal of Natural Gas Science & Engineering* 1(3), pp. 68-71.

Bahadori A. and Vuthaluru H. B. (2009b) Predicting emissivity of combustion gases, *Chemical Engineering Progress*, 105 (6), pp.38-41.

Bahadori A. and Vuthaluru H. B. (2009c) Prediction of bulk modulus and volumetric expansion coefficient of water for leak tightness test of pipelines, *International Journal of Pressure Vessels and Piping* (86), pp. 550–554.

Bahadori A. and Vuthaluru H. B. (2009d), A numerical method for prediction of transport properties of carbon dioxide, SPE Asia Pacific Health, Safety, Security and Environment Conference and Exhibition (APHSSEC) 4-6 August Jakarta, Indonesia, Society of Petroleum Engineers paper, SPE paper122859.

Bahadori A. and Vuthaluru H. B. (2009e) A simple method for accurate prediction of temperature drops in natural gas production systems, Society of Petroleum Engineers**,** SPE/EAGE Reservoir Characterization and Simulation Conference held in Abu Dhabi, UAE, 19–21 October, SPE paper 125510.

Bahadori, A. and Vuthaluru H. B. (2009f) New method accurately predicts carbon dioxide equilibrium adsorption isotherms *International Journal of Greenhouse Gas Control* (3), pp 768-772.

Bahadori, A. and Vuthaluru H. B. (2009g) A novel correlation for estimation of hydrate forming condition of natural gases, *Journal of Natural Gas Chemistry*, 18(4), pp. 453-457.

Bahadori, A. and Vuthaluru H. B. (2009h) Simple methodology for sizing of absorbers for teg gas dehydration systems, *Energy* 34, pp 1910–1916.

Bahadori, A. and Vuthaluru H. B. (2009i) Explicit numerical method for prediction of transport properties of aqueous glycol solutions, *Journal of the Energy Institute* 82 (4), pp. 218-222.

Bahadori A. and Vuthaluru H. B. (2010a) Estimation of displacement losses from storage containers using a simple method, *Journal of Loss Prevention in the Process Industries*, 23, pp 367-372

Bahadori A. and Vuthaluru H. B. (2010b) Prediction of silica carry-over and solubility in steam of boilers using simple correlation" *Applied Thermal Engineering* 30, pp 250-253.

Bahadori A. and Vuthaluru H. B. (2010c)" Novel predictive tool for accurate estimation of packed column size" *Journal of Natural Gas Chemistry*, 19(2), pp. 146-150.

Bahadori A. and Vuthaluru H. B. (2010d)" A simple method for the estimation of thermal insulation thickness" *Applied Energy*, 87, pp 613–619.

Bahadori A. and Vuthaluru H. B. (2010e) A Simple correlation for estimation of economic thickness of thermal insulation for process piping and Equipment" *Applied Thermal Engineering* 30, pp 254–259.

Bahadori A. and Vuthaluru H. B. (2010f) Predictive tool for the estimation of methanol loss in condensate phase during gas hydrate inhibition" *Energy & Fuels*, 24, pp 2999–3002.

Bahadori A. and Vuthaluru H. B. (2010g) "A method for estimation of densities and vapour pressures of aqueous methanol solutions" *OIL GAS European Magazine*, 36(2), pp 84-88.

Bahadori A. and Vuthaluru H. B. (2010h) Prediction of methanol loss in vapor phase during gas hydrate inhibition using Arrhenius-type functions" *Journal of Loss Prevention in the Process Industries*, 23(3), pp. 379-384

Bahadori A., Vuthaluru H. B. and Jalili, J. (2010i) Novel approach for an accurate estimation of the saturated water content of sour natural gases, 2010 Society of Petroleum Engineers (SPE) International Oil & Gas Conference & Exhibition in China, (IOGCEC) 8-10 June 2010, Beijing, China. (SPE paper # 130135).

Bahadori A. and Vuthaluru H. B, (2010j) Estimation of salinity of salty crude oil using Arrhenius-type asymptotic exponential function and Vandermonde matrix, in press, *SPE Projects Facilities and Construction Journal.*

Bahadori A. and Vuthaluru H. B, (2010k), Accurate prediction of molten sulfur viscosity" *Petroleum Technology Quarterly* 15(1) pp.13-14.

Bahadori A. and Vuthaluru H. B, (2010L), Simple equations to correlate theoretical stages and operating reflux in fractionators, *Energy***,** 35, pp.1439–1446.

Bahadori A. and Vuthaluru H. B, (2010m), "Predictive tools for the estimation of downcomer velocity and vapor capacity factor in fractionators, *Applied Energy* 87, pp 2615-2620.

Bahadori A. and Vuthaluru H. B, (2010n), Estimation of saturated air water content at elevated pressures using simple predictive tool, *Chemical Engineering Research and Design*, in press, (DOI: doi:10.1016/j.cherd.2010.05.008).

Bahadori A. and Vuthaluru H. B, (2010o), Novel predictive tools for design of radiant and convective sections of direct fired heaters, *Applied Energy* 87, pp 2194–2202.

Bahadori A. and Vuthaluru H. B, (2010p)" A new method for prediction of absorption/stripping factors, *Computers & Chemical Engineering* 34, 1731-1736.

Bahadori A. and Vuthaluru H. B, (2010q) "Estimation of maximum shell-side vapour velocities through heat exchangers" *Chemical Engineering Research and Design*, 88, 1588-1592.

Bahadori A. and Vuthaluru H. B, (2010r)" Simple Arrhenius-type function accurately predicts dissolved oxygen saturation concentrations in aquatic systems," *Process Safety and Environmental Protection*, 88, 335-340

Bahadori A. and Vuthaluru H. B, (2010s) Simple Method for Estimation of Unsteady State Conduction Heat Flow with Variable Surface Temperature in Slabs and Spheres, *International Journal of Heat and Mass Transfer*, 53 (2010) 4536–4542

Bahadori A. and Vuthaluru H. B, (2010t) Estimation of performance of steam turbines using a simple predictive tool, *Applied Thermal Engineering* 30, pp 1832-1838.

Bahadori A. and Vuthaluru H. B (2010u), Estimation of potential savings from reducing unburned combustible losses in coal-fired systems, *Applied Energy*, 87, 3792-3799.

Bahadori A. and Vuthaluru H. B (2010v) A method for estimation of recoverable heat from blowdown systems during steam generation, *Energy*, 35, pp 3501-3507.

Bahadori A. and Vuthaluru H. B (2010w) Estimation of energy conservation benefits in excess air controlled gas-fired systems, *Fuel Processing Technology*, 91, 1198-1203

Bahadori A. and Vuthaluru H. B. (2011a), Estimation of air specific heat ratio at elevated pressures using simple predictive tool, *Energy Conversion and Management* 52, pp. 1526-1532.

Bahadori A., Vuthaluru H. B. and Mokhatab S. (2009a)" Method accurately predicts water content of natural gases, *Journal of Energy Sources, Part A: Recovery, Utilization, and Environmental Effects*,31 (9) pp. 754 – 760.

Bahadori A., Vuthaluru H. B. and Mokhatab S. (2009b)" " Rapid estimation of water content of sour natural gases, *Journal of the Japan Petroleum Institute*, 52(5) pp. 270-274.

Bahadori A., Vuthaluru H. B. and Mokhatab S. (2009c)" New correlations predict aqueous solubility and density of carbon dioxide" *International Journal of Greenhouse Gas Control*, (3), pp 474–480

Bahadori A., Vuthaluru H. B. and Mokhatab S. (2009d))" Simple correlation accurately predicts aqueous solubility of light alkanes" *Journal of Energy Sources, Part A: Recovery, Utilization, and Environmental Effects* 31:(9), pp 761—766.

Bahadori A., Vuthaluru H.B., and Mokhatab S. and Tade M. O. (2008a) "Predicting hydrate forming pressure of pure alkanes in the presence of inhibitors" , *Journal of Natural Gas Chemistry*, 17(3), pp. 249-255.

Bahadori A., Vuthaluru H. B. and Mokhatab S. (2008a), "Optimizing separators pressures in the multistage crude oil production unit " *Asia-Pacific Journal of Chemical Engineering*, 3, (4) pp. 380-386,

Bahadori A., Vuthaluru H. B. and Mokhatab S. (2008b) Estimating methanol vaporization loss and its solubility in hydrocarbon liquid phase" *OIL GAS European Magazine* 34, (3), pp. 149-151.

Bahadori A., Vuthaluru H. B. and Mokhatab S. (2008c) Analysing solubility of acid gas and light alkanes in triethylene glycol" *Journal of Natural Gas Chemistry* 17(1) pp. 51-58.

Bahadori A., Vuthaluru H.B., and Mokhatab S. and Tade M. O. (2008d), Predicting water-hydrocarbon systems mutual solubility" *Chemical Engineering & Technology*, 31, (12), pp. 1743-1747.

Bair, E., Hastie, T., Paul, D., & Tibshirani, R. (2006). Prediction by supervised principal components. *Journal of the American Statistical Association*, 101, 119–137.

Barroso, J. Barreras, F. Ballester, J. (2004) Behavior of a high-capacity steam boiler using heavy fuel oil Part I. High-temperature corrosion, *Fuel Processing Technology* 86, 89–105.

Bebar, L. Kermes, V. Stehlik, P. Canek, J. Oral, J. (2002) Low NOx burners prediction of emissions concentration based on design, measurements and modelling, *Waste Management* 22, 443–451.

Beggs, H. D., and Robinson, J. R. (1975). Estimating the viscosity of crude oil systems, *Journal of Petroleum Technology*, 27(9):1140–1141.

Bejan A., (1993), *Heat Transfer*, John Wiley and Sons, New York, USA.

Bejan A., (2000) *Shape and structure, from engineering to nature*, Cambridge University Press, Cambridge, UK.

Berends, K. (2007)Engineering and construction projects for oil and gas processing facilities: Contracting, uncertainty and the economics of information, *Energy Policy* 35, pp. 4260-4270.

Bhambre, K., Mitra, S.K. and Gaitunde, U.N. (2007) Modeling of a coal-fired natural circulation boiler, Trans *ASME J Energy Res Tech*, 129, pp.159–67

Bilgen S.and Kaygusuz, K. (2008) The calculation of the chemical exergies of coal-based fuels by using the higher heating values, *Applied Energy*, 85(8), pp.776-785

Bohne, D.; Fischer, S.; Obermeier, E. (1984), Thermal conductivity, density, viscosity, and prandtl numbers of ethylene glycol +water mixtures. Ber. Bunsen-Ges. *Phys. Chem*., 88, pp.739-742.

Branan C. 2005 "Rules of thumb for chemical engineers" Gulf Professional Publishing, MA, USA.

Bruinsma D. F., M. Desens J.T, Notz, P.K. and Sloan, E.D. (2004), A novel experimental technique for measuring methanol partitioning between aqueous and hydrocarbon phases at pressures up to 69 MPa, *Fluid Phase Equilibria* 222–223 , pp.311–315.

Bucklin, R.W., and Schendel, R.L., (1985) "Comparison of physical solvents used for gas processing", from Acid and Sour Gas Treating Processes, Stephen, S. Newman, ed., Gulf Publishing Company, Houston, TX.

Bujak, J. (2009) Optimal control of energy losses in multi-boiler steam systems, *Energy*, 34: pp.1260-70.

Butcher, S.S., Charlson, R.J., Orians, G.H., and Wolfe, G.V., (1992) Global biogeochemical cycles, Academic Press, London, UK.

Butterworth, D., (2002), Design of shell-and-tube heat exchangers when the fouling depends on local temperature and velocity *Applied Thermal Engineering*, 22: 789–801.

Callister, W.D. Jr. (2000), Materials science and engineering—an introduction (fifth ed.), Wiley, New York, p. 871.

Carroll J. J. (2002)"The water content of acid gas and sour gas from 100° to 220°F and pressures to 10,000 Psia" Presented at the 81st Annual GPA Convention March 11-13, Dallas, Texas, USA.

Chang J. I. and Lin C. C. (2006)" A study of storage tank accidents", *Journal of Loss Prevention in the Process Industries* 19 (1) 51-59.

Chapra S. C. (1997) Surface water-quality modeling. McGraw-Hill International editions, USA.

Chen, C.J., Woo, H.J., and Robinson, D.B., (1988) "The solubility of methanol or glycol in water-hydrocarbon systems." GPA Research Report RR-117, Gas Processors Association, OK ,USA.

Chin, W.W. (1998). Issues and opinion on structural equation modeling. MIS Quarterly, 22(1), vii–xvi.

Civan, F., (2005). Applicability of the Vogel–Tammann–Fulcher type asymptotic exponential functions for ice, hydrates, and polystyrene latex. *Journal of Colloid and Interface Science* 285, 429–432.

Civan, F. (2007) Critical Modification to the Vogel-Tammann-Fulcher equation for temperature effect on the density of water, *Ind. Eng. Chem. Res*., 46, 5810-5814.

Civan, F, (2008a) A correlation for thermal conductivity of liquid n-alkanes based on the Vogel–Tammann–Fulcher–Hesse equation, *Chemical Engineering Science*, 63 (24), 5883-5886

Civan, F. (2008b). Use exponential functions to correlate temperature dependence. *Chemical Engineering Progress* 104 (7), 46–52.

Civan, F. (2008c). Correlation of permeability loss by thermally-induced compaction due to Grain expansion. *Petrophysics Journal* 49 (4), 351–361.

Civan, F. and Weers, J.J., (2001). Laboratory and theoretical evaluation of corrosion-inhibiting emulsions. *SPE Production and Facilities*, 16(4), 260–266

Cowan. J. C.; Weintritt, D. J. (1976) Water-Formed Scale Deposits, Knovel Publishing Co. USA.

Cox, B.A., (2003) A review of currently available in-stream water-quality models and their applicability for simulating dissolved oxygen in lowland rivers, *The Science of the Total Environment*, 314 –316, :335–377

Darakchiev R. and Dodev, C. (2002) Gas flow distribution in packed columns, *Chem. Engineering and Processing*, 41, p. 385.

Droste R. L. (1997) "Theory and practice of water and wastewater treatment" John Wiley & Sons, NY, USA.

Duan, Z. Sun R., (2003) “An improved model calculating CO2 solubility in pure water and aqueous NaCl solutions from 273 to 533 K and from 0 to 200 MPa”, Chemical *Geology* 193, pp.257– 271.

El-Banbi, A. H. and McCain, W.D(2000a)” Producing rich-gas-condensate reservoirs—case history and comparison between compositional and modified black-oil approaches” Paper SPE 58988 presented at the 2000 SPE International Petroleum Conference and Exhibition in Mexico, , Villahermosa, Mexico, 1-3 February 2000.

El-Banbi, A. H. and McCain, W.D., (2000b)“Investigation of well productivity in gas-condensate reservoirs” Paper SPE 59773 presented at the 2000 SPE/CERI Gas Technology Symposium, Calgary, Alberta, Canada, 3-5 April, 2000.

Elgibaly A. and Elkamel, A. (1999), Optimal hydrate inhibition policies with the aid of neural networks, *Energy & Fuels*, 13, pp.105-113.

Epps, R., (1994) “Use of selexol solvent for hydrocarbon dewpoint control and dehydration of natural gas”, Proceedings of the Laurance Reid Gas Conditioning Conference, Norman, OK.

Esteban, A., Hernandez, V., and Lunsford, K., (2000) “Exploit the benefits of methanol”, Proceedings of the 79th Gas Processors Association Annual Convention, Atlanta, GA, USA.

Fang, Q. Wang, H. Wei, Y. Lei, L. Duan, X. Zhou, H., (2010) Numerical simulations of the slagging characteristics in a down-fired, pulverized-coal boiler furnace, *Fuel Processing Technology* 91, pp.88–96.

Farris, C.B., (1983) Unusual design factors for supercritical CO_2 pipelines. *Energy Progress*. 3 (3), 150–158.

Fevang, O. and Whitson C. H. (1995) “Modeling Gas Condensate Deliverability” Paper SPE 30714 presented at the SPE Annual Technical Conference and Exhibition, Dallas, Texas, 22-25 October.

Flyvbjerg, B., N. Bruzelius, and W. Rothengatter, (2003), Megaprojects and Risk: An Anatomy of Ambition (Cambridge University Press) UK.

Flyvbjerg, B. Skamris-Holm, M. K. and Buhl, S. L., 2005 "How (In)accurate Are Demand Forecasts in Public Works Projects? The Case of Transportation." *Journal of the American Planning Association*, 71 (2), pp.131-146.

Folland, S., Goodman A. C. and Stano. M. (2007), The Economics of Heath and Health Care. Fifth ed. Pearson Prentice Hall: New Jersey, pg 83, 84.

Fornell, C., & Bookstein, F.L. (1982). Two structural equation models: LISREL and PLS applied to consumer exit-voice theory. *Journal of Marketing Research*, 19(4), 440–452.

Frankel, M. (2000)“ Piping Handbook- Chapter C17 Fuel Gas Distribution Piping Systems” 7th edition, edited by Nayyar, Mohindar, McGraw-Hill, USA,.

Fulcher, G. S. (1925) Analysis of Recent Data of the Viscosity of Glasses. *J. Am. Ceram. Soc*., 8, pp.339-355.

Fulton, W., Harris, J. (1991) Representation theory. A first course, Graduate Texts in Mathematics, Readings in Mathematics, 129, New York: Springer-Verlag, USA.

Gandhidasan, A. Al-Farayedhi, A., Al-Mubarak, A. A (2001) Dehydration of natural gas using solid desiccants, *Energy* 26**,** pp. 855–868.

Geankoplis, C. J., Transport processes and unit operations - Third Edition Prentice Hall. Englewood Cliffs, NJ. USA, 1993.

Geladi, P., and Esbensen, K. (1991). Regression on multivariate images: Principal component regression for modeling, prediction and visual diagnostic tools. *Journal of Chemometrics*, 5, 111.

Glasø, Ø. (1980). Generalized pressure–volume–temperature correlations, *Journal of Petroleum Technology*, 32(5) pp.785–795.

GPSA Data book (2004), Gas processors and suppliers association data book, 12th Edition, OK, USA.

Gray J.C. (1976) "How temperature affects pipeline hydrostatic testing", *Pipeline and Gas Journal*, August, (203), pp. 26-30.

Harvey, A.H., Prausnitz, J.M., 1989 "Thermodynamics of high-pressure aqueous systems containing gases and salts", *AIChE Journal*, 35, 4, pp.635– 644.

Hassanzadeh, H., Pooladi-Darvish, M., Elsharkawy, A.M., Keith, D.W., and Leonenko, Y., (2008) "Predicting PVT data for CO2–brine mixtures for black-oil simulation of CO2 geological storage", International Journa l of Greenhouse Gas Control, 2, 65 – 77.

Herskowitz, M. and Gottlieb, M. (1984), Vapor-liquid equilibrium in aqueous solutions of various glycols and polyethylene glycols *J. Chem. Eng. Data*, , 29. P.173.

Horn, R. A. and Johnson C. R. (1991) Topics in matrix analysis, Cambridge University Press. Section 6.1.

Hottel, H. C., in Heat transmission (W. H.McAdams, Ed.), Chap. 4, p. 83-85, 3rd ed., McGraw-Hill, 1954.

Iranian Petroleum Standard (IPS)(1993) Report No. IPS-E-PR-330, National Iranian Oil Company, January, Ahwaz, Iran.

Iranian Petroleum Standard (IPS)(1996)"Engineering standard for thermal insulations"1st edition, Report IPS-E-TP-700, National Iranian Oil Company, January, Ahwaz, Iran.

James A. (1993), An introduction to water quality modelling. 2nd ed..Wiley, USA.

Jou, C. G. Lee, C. Tsai, C. and Wang, H. P.,(2008) Reduction of energy cost and CO2 emission for the boilers in a full-scale refinery plant by adding waste hydrogen-rich fuel gas, *Energy & Fuels*, 22 pp.564–569.

Jou, F.Y., Otto, F.D., and Mather, A.E., (1994) “Solubility of methane in glycols at elevated pressures”, *Canadian Journal of Chemical Engineering,* 72, pp. 130-133.

W. Kaewboonsonga, V.I. Kuprianov, N. Chovichien, (2006) Minimizing fuel and environmental costs for a variable-load power plant (co-)firing fuel oil and natural gas: Part 1. Modelling of gaseous emissions from boiler units, *Fuel Processing Technology* 87, pp.1085–1094

Kadleca, P., Gabrys, B., & Strandt, S. (2009). Data-driven soft sensors in the process Industry, *Computers & Chemical Engineering*, 33, pp.795–814.

Kalyon M. and Sahin, A. Z. “Application of optimal control theory in pipe insulation”, *Numerical Heat Transfer, Part A*, 41: (2002) pp.391- 402.

Kapale, U.C. and Chand, S., (2006) Modeling for shell-side pressure drop for liquid flow in shell-and-tube heat exchanger. *Int J. Heat Mass Transfer*, 49: 601–610.

Karimi A., Abdi M.A. (2009) Selective dehydration of high-pressure natural gas using supersonic nozzles, *Chemical Engineering & Processing*, pp., 48**,** pp. 560–568.

Kaspar, M. H., and Ray, W. H. (1993). Partial least squares modelling as successive singular value decompositions. *Computers & Chemical Engineering*, 17(10), pp.985–989.

Katz D L,(1945) Prediction of conditions for hydrate formation in natural gases, Trans AIME: 160 : 140.

Kister, H. Z. (1992) "Distillation design," McGraw-Hill, USA.

Kohl, A. L.; Nielsen, R. B. (1997) Gas purification, 5th Edition, Elsevier, Amsterdam, The Netherland.

Kourti, T. (2002) Process analysis and abnormal situation detection: From theory to practice, *Control Systems Magazine, IEEE*, 22(5), pp.10–25.

Kubiak, J., García-Gutiérrez S, A. and Urquiza G. B. (2002) The diagnosis of turbine component degradation - case histories” *Applied Thermal Engineering* 22 , pp. 1955–1963.

Lawrence, B. Annamalai , K.. Sweetenand J M Heflin K.,(2009) Cofiring coal and dairy biomass in a 29 kW_t furnace *Applied Energy* 86(11) pp.2359-2372

Lederhos, J.P., Longs, J.P., Sum, A., Christiansen, R.l., and Sloan, E.D. (1996) Effective kinetic inhibitors for natural gas hydrates, *Chemical Engineering Science*, 51, (8), pp.1221-1229.

Lee, C.C. and Dar L. S., Handbook of Environmental Engineering Calculations, McGraw-Hill, USA, 2000.

Lee, H.; Hong, W. H. (1990), Excess Volumes of Binary and Ternary Mixtures of Water, Methanol, and Ethylene Glycol. *J. Chem. Eng. Data* 35, 371-374.

Lee, B. I and Kesler, M. O. (1975) A Generalized Thermodynamic Correlation Based on Three-Parameter Corresponding States, *AIChE Journal*, 1975, 27, 510.

Letsou, A.; Stiel, L. I. (1973), Viscosity of Saturated Nonpolar Liquids at Elevated Pressures *AIChE Journal*, 79, 409.

Li, H.D. and Kottke, V., (1998a), Effect of the leakage on pressure drop and local heat transfer in shell- and tube heat exchangers for staggered tube arrangement. *Int J Heat Mass Transfer*, 41(2) pp. 425–433.

Li, H.D. and Kottke, V., (1998b), Visualization and determination of local heat transfer coefficients in shell-and-tube heat exchangers for staggered tube arrangement by mass transfer measurements. *Exp Therm Fluid Sci*, 17(3) pp. 210–216.

Li, Y., Ngheim, L.X., 1986 "Phase Equilibria of Oil, Gas and Water/Brine Mixtures from a Cubic Equation of State and Henry's Law", *Canadian Journal of Chemical Engineering*, 64, pp.486– 496.

Lobo, W. E. and Evans, J. F., (1939) *AIChE Trans*., 35, 743.

Jou, C.G. Lee, C. Tsai, C. Wang, H.P. (2008) Reduction of energy cost and CO2 emission for the boilers in a full-scale refinery plant by adding waste hydrogen-rich fuel gas, *Energy & Fuels*, 22, 564–569.

Lukacs, J., and Robinson, D.B., (1963) "Water content of sour hydrocarbon systems", *SPE Journal*, 3, pp.293-297.

Lundstrøm C., Michelsen M. L., Kontogeorgis, G. M., Pedersen, K. S. and Sørensen, H., (2006) , Comparison of the SRK and CPA equations of state for physical properties of water and methanol, *Fluid Phase Equilibria* 247, pp.149–157.

Ludwig, E. E., (1983) Applied process design for chemical and petrochemical plants, 2nd Ed., Gulf Publishing Co.

Makogon, Y.F., (1997) Hydrates of natural gas", PennWell Publishing Company, Tulsa, OK, USA.

Maroto-Valer, M.M. Song, C. and Soong, Y. (2002), Environmental challenges and greenhouse gas control for fossil fuel utilization in the 21st century, Kluwer Academic/Plenum Publishers, New York, USA.

Master, B.I., Chunangad, K.S., Boxma, A.J., Kral, D. and Stehlik, P., (2006), Most frequently used heat exchangers from pioneering research to worldwide applications. *Heat Transfer Engineering*, 27(6) pp. 4–11.

MATLAB software(2008), Version 7.6.0.324, The MathWorks, Inc, MA, USA.

McCabe, W. L., Smith J. C. and Harriot, P., (2005) Unit operations of chemical engineering, 7th edition, McGraw Hill, NY, USA.

McKetta, J.J., and Wehe, A.H., (1958), Use this chart for water content of natural gases *Petroleum Refiner (Hydrocarbon Processing)*, 37, 8, 153.

Miller, C.A. Srivastava, R.K. (2000) The combustion of Orimulsion and its generation of air pollutants, *Progress Energy Combustion* 26 pp.131–160.

Minkkinen, A., Larue, J., Patel, S., and Levier, J.F., (1992) Methanol gas-treating scheme offers economics, versatility, *Oil & Gas Journal*, 90**,** pp**.** 65-72.

Mofarahi, M. , Khojasteh, Y. Khaledi H., Farahnak, A. (2008) Design of CO2 absorption plant for recovery of CO2 from flue gases of gas turbine, *Energy* 33 pp.1311– 1319.

Mohammadzadeh, S. and Zahedi,G. (2008), A new vapor pressure equation for pure substances, *Korean J. Chem. Eng*., 25(6) pp. 1514-1517.

Mokhatab, S., Poe, W.A., and Speight, J.G., (2006) “Handbook of natural gas transmission & processing”, Gulf Professional Publishing, Burlington, MA, USA.

Mokhatab, S., and Wilkens, R.J., and Leontaritis, K.J, (2007), A Review of Strategies for Solving Gas-Hydrate Problems in Subsea Pipelines, *Energy Sources: Part A*, 29, 1, pp.39-45.

Motiee, M. (1991), Estimate possibility of hydrates, *Hydrocarbon Processing*, **71** (7), 98.

Nasrifar, K., Moshfeghian, M., and Maddox, R.N, Prediction of equilibrium conditions for gas hydrate formation in the mixtures of both electrolytes and alcohol, *Fluid Phase Equilibria*, 146, 1–2, 1–13 (1998).

Ng HJ, Robinson DB (1985) Hydrate formation in systems containing methane, ethane, propane, carbon dioxide or hydrogen sulfide in the presence of methanol. *Fluid Phase Equilibria*, 21, pp.145-155.

Nino, J. C. Lanagan M.T. and Randall, C.A., (2001) Dielectric relaxation in Bi_2O_3-ZnO-Nb_2O_5 cubic pyrochlore, *J. Appl. Phys.* 89 (8), pp. 4512–4516.

Niu, Z. and Wong, K.V., (1998) Adaptive simulation of boiler unit performance, *Energy Conversion and Management* 39 pp.1383–94.

Obermeier, E.; Fischer, S.; Bohne, D (1985) Thermal conductivity, density, viscosity, and prandtl numbers of di- and triethylene glycol +water mixtures. Ber. Bunsen-Ges. *Phys. Chem*., 89, pp. 805-809.

Oliveira, M.B., Coutinho, J.A.P., Queimada, A.J.(2007) Mutual solubilities of hydrocarbons and water with the CPA EoS. *Fluid Phase Equilibria* , 258, pp.58-66.

Oman , J. Dejanovi B. and. Tuma, M., (2002) Solutions to the problem of waste deposition at a coal-fired power plant, *Waste Management*, 22 (6) pp.617-623.

Ozdemir, E., (2004) Energy conservation opportunities with a variable speed controller in a boiler house, *Applied Thermal Engineering* 24, pp.981–993.

Pakseresht, S., Kazemeini M., Akbarnejad, M. M.(2002), Equilibrium isotherms for CO, CO2, CH4 and C2H4 on the 5A molecular sieve by a simple volumetric apparatus, Separation and Purification Technology 28, 53–60.

Papatzacos, P., Herring, T. U., Martinsen, R., and Skjaeveland, S. M., (1989), Cone breakthrough time for horizontal wells, SPE Paper 19822, presented at the 64th SPE Annual Conference and Exhibition, San Antonio, TX, Oct. 8–11.

Papatzacos, P., Herring, T.R., Martinsen, R., Skjaeveland, S.M., (1991) Cone breakthrough time for horizontal wells, SPE Reservoir Engineering, 6, (3) 311-318.

Parrish, W.R. , Won, K.W. and Baltatu, M.E., (1986) paper presented at the 65th GPA Annual Convention, San Antonio, TX, USA

Pavlík, Z. and Cerny R. (2009) Hygrothermal performance study of an innovative interior thermal insulation system, *Appl. Thermal Eng.* 29, 1941–1946.

Pedenaud, P., Goulay C. , Pottier, F., Garnier, O. and Gauthier B (2006) Silica-scale inhibition for steam generation in OTSG boilers, SPE Production & Operations 21, pp. 26-32.

Perry, R. E. and Green, D. W. (1997) Perry's Chemical engineers' handbook, 7th edition, Mc-Graw-Hill, USA.

Pitzer, K. S.; Lippman, D. A.; Curl, R. F.; Huggins, C. M.; Peterson, D. E., (1955) The volumetric and thermodynamic properties of fluids. 11. Compressibility factor, vapor pressure and entropy of vaporization *J. Am. Chem. Soc*., 77, 3433.

Poling, B. E., Prausnitz, J. M. and O'Connell, J. P. (2001), The properties of gases and liquids, fifth ed., McGraw-Hill.

Ponce-Ortega, J.M., Serna-Gonzalez, M., Salcedo-Estrada, L.I. and Jimenez-Gutierrez, A., (2006), Minimum-investment design of multiple shell and tube heat exchangers using a MINLP, formulation. *Trans IChemE, Part A, Chem Eng Res Des*,

84(A10) pp. 905–910.

Ram L. C. and Masto, R. E. (2010), An appraisal of the potential use of fly ash for reclaiming coal mine spoil, *Journal of Environmental Management*, 91(3) pp.603-617.

Reid, R.C., Prausnitz, J.M., and Poling, B.E.,(1987) "The properties of gases and liquids", 4th Edition, McGraw-Hill, New York, NY.

Reynolds, J. P.; Jeris, J. S.; Theodore, L. (2002) "Handbook of chemical and environmental engineering calculations ", John Wiley & Sons, NY, USA.

Riddick, J. A.; Bunger, W. B.; Sakano, T. K. (1986), Organic solvent physical properties and methods of purification, 4th ed.; Wiley: New York, USA.

Rodriguez, C. and Smith, R., (2007) Optimization of operating conditions for mitigating fouling in heat exchanger networks. *Trans IChemE, Part A, Chem Eng Res Des*, 85(A6): 839–851.

Rosman, A., Water equilibrium in the dehydration of natural gas with triethylene glycol, *Trans. AIME*, 255, (1973) p. 297.

Ross, M. J. and Toczylkin, L.S. (1992), Hydrate dissociation pressures for methane or ethane in the presence of aqueous solutions of triethylene glycol, *Journal of Chemical Engineering Data*, 37, 488.

Rowley, R. L.; Wilding, W. V.; Oscarson, J. L.; Zundel, N. A.; Marshall, T. L.; Daubert, T. E.; Danner, R. P. (2002) DIPPR Data, Compilation of pure compound properties; design institute for physical properties (DIPPR), American Institute of Chemical Engineers: New York.

R.S. Sastri and K.K. Rao, 1999 A new temperature-thermal conductivity relationship for predicting saturated liquid thermal conductivity, *Chemical Engineering Journal* **74** (3), pp. 161–169

Shaw P. J.A, Multivariate statistics for the environmental sciences, (2003) Hodder-Arnold

Siriwardane R. V., Shen M. S.,. Fisher E. P, and Poston J. A., (2001), Adsorption of CO_2 on Molecular Sieves and Activated Carbon, *Energy & Fuels*, 15 (2), 279-284.

Sklet, S., (2006) Hydrocarbon releases on oil and gas production platforms: Release scenarios and safety barriers, *Journal of Loss Prevention in the Process Industries*, 19, pp. 481-493.

Sloan, E.D (1998), Clathrate Hydrates of Natural Gases 2nd Edition, Marcel Dekker Inc, New York, NY, USA.

Smith, R., (2005). Chemical process design (John Wiley & Sons, Ltd, UK).

Smith, W.J.S., Durbin, L.D., and Koboyashi, R., (1960) "Thermal conductivity of light hydrocarbon and methane-propane mixtures at low pressures", *J. Chem. Eng. Data*, 5, 3.

Streat, M., Hellgardt, K. and Newton, N.L.R., (2008) hydrous ferric oxide as an adsorbent in water treatment: Part 2. Adsorption studies, *Process Safety and Environmental Protection*, 86 (1):11-20

Sun T. and Teja A. S., (2003) Density, viscosity, and thermal conductivity of aqueous ethylene, diethylene, and triethylene glycol mixtures between 290 K and
450 K *Journal of Chemical and Engineering Data*, 48, 198-202.

Tammann, G.; Hesse, W. Die abha¨ngigkeit der viskosita¨t von der temperature bei unterku¨hlten flu¨ssigkeiten. *Z. Anorg. Allg. Chem*. 1926,156, pp.245-257.

Taplin H. R. Jr., Combustion Efficiency Tables, Fairmont Press, Lilburn, GA, USA, 1991.

Teja, A. S. (1980) A corresponding states equation for saturated liquid densities, applications to LNG, *AlChE J*., 26, pp.337-345.

Teja, A. S., Rice, P. (1981), General corresponding states method for the viscosities of liquid mixtures. *Ind. Eng. Chem. Fundam*. 20, pp.77-81.

Teja, A. S.; Rice, P. (1981) The measurement and prediction on the viscosities of some binary liquid mixtures containing n-hexane, *Chemical Engineering Science*. 36, pp.7-10.

Teja, A. S.; Rice, P. (1981) A generalized corresponding states method for the prediction of the thermal conductivity of liquids and liquid mixtures. *Chemical Engineering Science*, 36, 417-422.

Teja, A. S.; Rice, P. (1982) The prediction of the thermal conductivity of binary aqueous mixtures, *Chemical Engineering Science*., 37, 788-790.

Touloukian, Y.S., Liley, P.E., and Saxena, S.C., (1970)Thermal Conductivity of Nonmetallic Liquids and Gases", Thermophysical Properties of Matter, 3, IFI/Plenum, New York, NY.

Tsierkezos, N. G.; Molinou, I. E. (1998),Thermodynamic Properties of Water + Ethylene Glycol at 283.15, 293.15, 303.15, and 313.15 K. *J. Chem. Eng. Data*, 43, 989-993.

Turner, W. C., Doty, S. (2007), Energy management handbook, , 6th edition. Fairmont press, GA, USA.

Twu, C. H., Tassoneb, V., Simb, W. D. and Watansiri, S. (2005) , Advanced equation of state method for modeling TEG–water for glycol gas dehydration , *Fluid Phase Equilibria*, 228, pp. 213–221.

Velasco, S., Román, F.L., White, J.A. and Mulero, A., (2008) A predictive vapor-pressure equation, *The Journal of Chemical Thermodynamics*, 40 (5) pp. 789-797.

Vandeginste V., Piessens K. (2008) "Pipeline design for a least-cost router application for CO_2 transport in the CO_2 sequestration cycle", *International Journal o f Greenhouse Gas Control* 2, pp. 571 – 581.

Vesovic V., Wakeham W. A., Olchowy G. A., Sengers J. V.,. Watson J. T. R and Millat J., (1990) "The transport properties of carbon dioxide" *Journal of Physical Chemistry Ref. Data*, 19, pp. 763-808.

Vogel, H. 1921, Das temperature-abha¨ngigketsgesetz der viskosita¨t von flu¨ssigkeiten. Phys. Z., 22, pp. 645-646.

Wagner, J., Research Report 169, (1999) GPSA Engineering Data Book Revitalization and Maintenance, Gas Processors Suppliers Association, Tulsa, OK, USA.

Wagner, W.; Pruss, A. (2002) The IAPWS formulation 1995 for the thermodynamic properties of ordinary water substance for general and scientific use. *J. Phys. Chem. Ref. Data*, 31, 387-535.

Wang, Q., Chen, Q., Chen, G. and Zeng, M., (2009), Numerical investigation on combined multiple shell-pass shell-and-tube heat exchanger with continuous helical baffles. *Int J Heat Mass Transfer*, 52 pp. 1214–1222.

Wang, L.K., Chin, G.J., Han, G.H., Guo, X.O., Guo, T.M. (2003), Experimental study on the solubility of natural gas components in water with or without hydrate inhibitor *Fluid Phase Equilibria*, 207, 143–154.

Warne, K., Prasad, G., Rezvani, S., &Maguire, L. (2004). Statistical and computational intelligence techniques for inferential model development: A comparative evaluation and a novel proposition for fusion. *Engineering Applications of Artificial Intelligence*, 17(8), 871–885.

Wiebe, R., (1941) "The binary system carbon dioxide–water under pressure", *Chem. Rev.* 21, 475–481.

Wold, S., Ruhe,A. Wold H., and Dunn W.J. (1984) "The collinearity problem in linear regression. the partial least squares (PLS) approach to generalized inverses." *SIAM J. Sci. Stat. Comp.*, 5:735-743.

Won, K.W., (1994) paper presented at the 73rd GPA Annual Convention, New Orleans, LA, USA

Worley, S. (1967), Proceedings Gas Conditioning Conference, Univ. of Oklahoma, Norman, OK, USA.

Xiang, H.W. (2001)Vapor pressures from a corresponding-states principle for a wide range of polar molecular substances , *International Journal of Thermophysics*, 22(3), pp. 919-932.

Xu X., Song C., Andresen J. M., Miller B. G., Scaroni A.W. (2002), Novel Polyethylenimine-Modified Mesoporous Molecular Sieve of MCM-41 Type as High-Capacity Adsorbent for CO_2 Capture" *Energy and Fuels* 16, 1463.

Xu, X. Song C., Miller, B.G. Scaroni, A.W., (2005) Adsorption separation of carbon dioxide from flue gas of natural gas-fired boiler by a novel nanoporous "molecular basket" adsorbent, *Fuel Processing Technology* 86 pp. 1457–1472.

Yang, W. Blasiak, W., (2005) Mathematical modelling of NO emissions from high temperature air combustion with nitrous oxide mechanism, *Fuel Processing Technology* 86, pp.943–957.

Yokoyama, C., Wakana, S., Kaminishi, G.I., and Takahashi, S., (1988) "Vapour-liquid equilibria in the methane-diethylene glycol-water system at 298.15 and 323.15 K", *J. Chem. Eng. Data*, 33, pp. 274-276.

Zhang F., Zhang R.and Kang, S. (2003) Estimating temperature effects on water flow in variably saturated soils using activation energy *Soil Sci. Soc. Am. J.* 67 (5), pp. 1327–1333.

Zheng, D.Q., Ma, W.M., Wei, R., and Guo, T.M., (1999) "Solubility study of methane, carbon dioxide and nitrogen in ethylene glycol at elevated temperatures and pressures", *Fluid Phase Equilibria*, 155, pp. 277-286.

Zuo, Y., and Guo, T.M., (1991) “Extension of the Patel–Teja equation of state to the prediction of the solubility of natural gas in formation water”, *Chemical Engineering Science*, 46, 12, pp. 3251– 3258.